



Insert Running Workflow Large

GRAYSCALE NAME:

---

HARDCOPY NAME:

1989017489

---

NASA Contractor Report 4111

# Design Considerations of Manipulator and Feel System Characteristics in Roll Tracking

Donald E. Johnston and Bimal L. Aponso

*Systems Technology, Inc.*

*Hawthorne, California*

Prepared for

Ames Research Center

Dryden Flight Research Facility

under Contract NAS2-12221



National Aeronautics  
and Space Administration

Scientific and Technical  
Information Division

1988

## **FOREWORD**

This research was accomplished at Systems Technology, Inc., Hawthorne, CA, under Contract NAS2-12221 for the NASA Ames Research Center, Dryden Flight Research Facility. The NASA Contract Technical Manager was Mr. D. T. Berry. Mr. D. T. McRuer was the STI Technical Director and D. E. Johnston was the Principal Investigator. The experimental setup, operation, and data reduction was accomplished by Mr. B. L. Aponso. Other staff members who contributed in the experiments were Messrs. R. H. Hoh, J. R. Hogue, and R. E. Magdaleno. The control sticks and force loader system were furnished by the McFadden Systems, Inc.

## TABLE OF CONTENTS

	<u>Page</u>
I. INTRODUCTION.....	1
II. BACKGROUND.....	5
A. Some Simple Pilot/Vehicle Considerations.....	6
B. The Neuromuscular System Model.....	10
C. Limb Actuation/Feel System Interface.....	16
III. EXPERIMENT GOALS AND SETUP.....	21
A. Experiment Setup.....	21
B. Disturbance (Target) Input Function.....	24
C. Protocol.....	25
IV. DISPLACEMENT SIDESTICK AND FEEL SYSTEM.....	27
A. Influence on Pilot's Neuromuscular System Mode.....	27
B. Influence on Closed-Loop Tracking Performance.....	37
C. Influence on Pilot Rating.....	41
D. Addition of 2nd Order Command Filter Lag.....	47
E. Summary.....	52
V. CENTER STICK WITH DISPLACEMENT VS FORCE SENSING.....	55
A. Configurations Investigated.....	55
B. Force vs Displacement Sensing.....	59
C. Influence of Dynamic Lag Location.....	64
D. Influence of Cumulative Effective Time Delay.....	67
E. Summary.....	71
VI. PILOT DYNAMIC MODEL WITH FORCE VS DISPLACEMENT CENTER STICK.....	73
A. High Order Dynamic Model.....	74
B. Crossover Model Approach.....	84
C. Roll Ratchet Potential.....	88
VII. CONCLUSIONS AND RECOMMENDATIONS.....	89
REFERENCES.....	93



## TABLE OF CONTENTS (Continued)

	<u>Page</u>
APPENDIX A.....	95
APPENDIX B.....	102
APPENDIX C.....	104

## LIST OF FIGURES

	<u>Page</u>
1. Roll Ratchet During Banking Maneuver.....	1
2. General Compensatory Control Situation and Basic Human Operator Subsystems.....	7
3. Ideal Crossover Model.....	9
4. Closed-Loop Neuromuscular System Model Fit to $Y_p$ for Pressure and Free-Moving Manipulator ( $Y_c = 1/s$ ) <sup>p</sup> from Ref. 2.....	11
5. Example Describing Function Showing High Frequency Peak (Taken from Gordon-Smith, Ref. 12).....	12
6. Neuromuscular Subsystems for Free-Moving and Pressure Manipulators and Central Equalization for Rate Dynamics.....	13
7. Bode and Root Locus for Spindle Feedback (Some Effects of Joint Sensor Feedback Shown) (Ref. 2).....	15
8. Bode Amplitude Ratio Plot for Neuromuscular System Contribution to Roll Ratchet Potential.....	16
9. Pilot Closed-Loop Limb Actuation With Feel System Dynamics.....	18
10. Closed-Loop Limb/Manipulator System with Force Sensing.....	19
11. Experimental Setup.....	22
12. Display Format.....	22
13. Definition of Flying Qualities Levels.....	26
14. Example Bode Plot With K/S Fit to Obtain $\Delta AR$ .....	29

## LIST OF FIGURES (Continued)

		<u>Page</u>
15.	Amplitude Deviation From $Y_c$ Asymptote Due to Neuromuscular Mode.....	30
16.	Influence of Feel Gradient and Effective Time Delay on Neuromuscular Mode Peaking With Stick Displacement Sensing.....	31
17.	Comparison of Neuromuscular Peaking With Displacement vs Force Sensing.....	34
18.	Typical Describing Function Plots for Displacement vs Force Sensing.....	35
19.	Roll Ratchet Tendency With Variation of Roll Lag and Command Gain; Displacement vs Force Sensing.....	36
20.	Roll Tracking Crossover vs Command Gain With Displacement Sensing.....	38
21.	Roll Tracking Crossover vs Command Gain With Force and Displacement Sensing.....	39
22.	Relationship Between Tracking Performance and Loop Closure Parameters.....	41
23.	Variation of CHPR With Position Sensing Command Gain and Feel Gradient.....	42
24.	Control Force-Response Gains, Up-and-Away Flight (Ref. 16).....	43
25.	Comparison of CHPR vs Command Gain for Flight and Lab With Feel Gradient 1.2 - 1.3 lb/deg.....	45
26.	Comparison of CHPR vs Command Gain for Flight and Lab With Feel Gradient 0.65 - 0.7 lb/deg.....	46
27.	Effective Controlled Element Dynamics for 2nd Order Command Filter Experiment with Sidestick.....	48
28.	Influence of Effective Time Delay and Command Gain on CHPR (0.65 lb/deg Sidestick).....	49
29.	Influence of Effective Time Delay and Command Gain on Roll Tracking Performance (0.65 lb/deg Sidestick).....	51

## LIST OF FIGURES (Continued)

		<u>Page</u>
30.	Command Gain Normalized Tracking Performance Measures Variation With Effective Time Delay (0.65 lb/deg Sidestick).....	51
31.	Command Gain Normalized CHPR Variation With Effective Time Delay (0.65 lb/deg Sidestick).....	53
32.	Comparison of CHPR With MIL-F-8785C Effective Time Delay Criteria (0.65 lb/deg Sidestick).....	53
33.	Effective Controlled Element Configurations Employed -- Roll Tracking With Center Stick.....	57
34.	Roll Acceleration Time Response to Step Stick Force.....	58
35.	Influence of Feel and Filter Dynamics on Tracking Bandwidth With Center Stick Displacement and Force Sensing.....	60
36.	Influence of Command Gain on Tracking Bandwidth (Center Stick).....	61
37.	Influence of Feel and Filter Dynamics on Tracking Performance With Center Stick Displacement and Force Sensing.....	62
38.	Influence of Feel and Filter Dynamics on CHPR With Center Stick Displacement and Force Sensing.....	63
39.	Influence of Dynamic Lag Location on Tracking Bandwidth (Center Stick).....	64
40.	Influence of Dynamic Lag Location on Tracking Error (Center Stick).....	65
41.	Influence of Dynamic Lag Location on CHPR (Center Stick).....	66
42.	RMS Tracking Error vs Effective Time Delay, Subject A (Center Stick).....	68
43.	RMS Tracking Error vs Effective Time Delay, Subject B (Center Stick).....	68
44.	CHPR Variation With Effective Time Delay and Command Gain (Center Stick).....	69

## LIST OF FIGURES (Concluded)

	<u>Page</u>
45. Comparison of CHPR with MIL-F-8785C Effective Time Delay Criteria (4 lb/in Center Stick).....	70
46. Example Root Locus of the Limb/Manipulator Positional Loop Closure.....	74
47. Dynamic Model Match to Describing Function Data, Force Sensing Center Stick, Subject A, $\omega_{FS} = 26$ , $\omega_{CF} = 14$ .....	76
48. Dynamic Model Match to Describing Function Data, Force Sensing Center Stick, Subject A, $\omega_{FS} = 14$ , $\omega_{CF} = 26$ .....	77
49. Dynamic Model Match to Describing Function Data, Displacement Sensing Center Stick, Subject A, $\omega_{FS} = 14$ , $\omega_{CF} = 26$ .....	78
50. Dynamic Model Match to Describing Function Data, Displacement Sensing Center Stick, Subject A, $\omega_{FS} = 26$ , $\omega_{CF} = 14$ .....	79
51. Pilot Generation of Lead With Displacement Sensing Center Stick, Subject A, $\omega_{FS} = 14$ , $\omega_{CF} = 26$ .....	80
52. Pilot Generation of Lead With Displacement Sensing Center Stick, Subject B, $\omega_{FS} = 14$ , $\omega_{CF} = 26$ .....	81
53. Effective Controlled Element Time Delay Summation for Crossover Model.....	85
A-1. Sidestick Tracking Station Set-Up.....	96
A-2. Small Displacement (Stiff) Sidestick Calibration.....	97
A-3. Large Displacement (Medium) Sidestick Calibration.....	98
A-4. Very Large Displacement (Soft) Sidestick Calibration.....	99
A-5. Center-Stick Calibration.....	100
A-6. Force Sensing Electrical Signal Breakout Calibration.....	101
B-1. Roll Analog Simulation.....	103

## LIST OF TABLES

	<u>Page</u>
1. Stick/Feel System Configurations.....	23
2. Roll Tracking Forcing Function.....	24
3. Configurations Fitted With High Order Models.....	75
C-1. Closed-Loop Tracking Measures, Center-Stick.....	107
C-2. Closed-Loop Tracking Measures, Side-Stick.....	111

## LIST OF SYMBOLS

A	Analog
ADI	Attitude Director Indicator
CHPR	Cooper Harper Pilot Rating
CRT	Cathode Ray Tube
D	Digital; Displacement
DFA	Describing Function Analyzer
DFRF	Dryden Flight Research Facility
dB	Decibel, $20 \log_{10}()$ for Amplitude Ratio; $10 \log_{10}()$ for Power
e	System Error
F	Roll Stick Force
$G_m$	Combined Muscle-Manipulator Dynamics
GM	Gain Margin
H	Feedback Loop Dynamic Transfer Functions
i	Forcing Function Input
K	System Gain
$K_c$	Controlled Element Gain; Command/Force Gradient
$K_{FS}$	Feel System Force/Displacement Gradient
m	Closed-Loop System Output
ms	Millisecond
n	Number of Runs
NM/L	Neuromuscular and Limb System
P	Roll Rate; First Order Inverse Time Constant of Transfer Function Denominator
PIO	Pilot Induced Oscillations
RMS (rms)	Root Mean Square

## LIST OF SYMBOLS (Continued)

$s$	Laplace Transform Variable
$t$	Time
$T$	First-Order Time Constant
$X$	Internal Muscle Length
$Y$	Forward Loop Transfer Function Particularized by Subscript
$Z$	First Order Inverse Time Constant of Transfer Function Numerator
$\alpha$	Alpha Motor Neuron
$\delta$	Stick or Control Surface Command
$\Delta R$	Neuromuscular Peak Amplitude Ratio Departure from $Y_p Y_c$ Bode Asymptote
$\zeta$	Damping Ratio Terms
$\sigma$	Standard Deviation
$\sigma_e$	Task RMS Error
$\tau$	Time Delay
$\phi$	Roll Response Angle
$\phi_M$	Phase Margin
$\omega$	Angular Frequency Term
$\omega_c$	Closed-Loop Bandwidth (Crossover of the 0 dB Gain Line with the K/s Amplitude Ratio Plot)
$\omega_c \sigma_e$	Product of Crossover Frequency and RMS Error (Performance Measure)
$\omega_u$	Frequency at Which System Becomes Unstable ( $\phi = 180^\circ$ )
$\chi$	Angle
$\#$	Unit of Pound Force

## LIST OF SYMBOLS (Concluded)

### Subscripts

a	Muscle Actuation Open-Loop Elements
c	Controlled Element; Command; Crossover
CF	Command Filter
e	Error;
FS	Feel System
i	Input or Forcing Function
j	Joint Receptor
N or NM	Neuromuscular System Closed-Loop Dynamic Mode
p	Pilot
r or R	Roll Mode
sp	Muscle Spindle
$\phi$	Roll Angle



## SECTION I

### INTRODUCTION

Almost every new aircraft with fly-by-wire or command augmentation in the roll axis has encountered either Pilot Induced Oscillations (PIO) or roll ratchet (or both) in early flight phases. PIO has typically been associated with high gain, neutrally stable closed-loop pilot-vehicle control oscillations with a frequency of about 1/2 Hz (3 rad/sec). The "roll ratchet" has been somewhat more obscure and idiosyncratic, appearing most often in rapid rolling maneuvers. Ratchet frequencies are typically 2-3 Hz (12-19 rad/sec). Figure 1 illustrates this seldom recorded phenomenon. The frequency alone indicates that the PIO and ratchet situations are different phenomena, yet both clearly involve the closed-loop pilot/vehicle system.

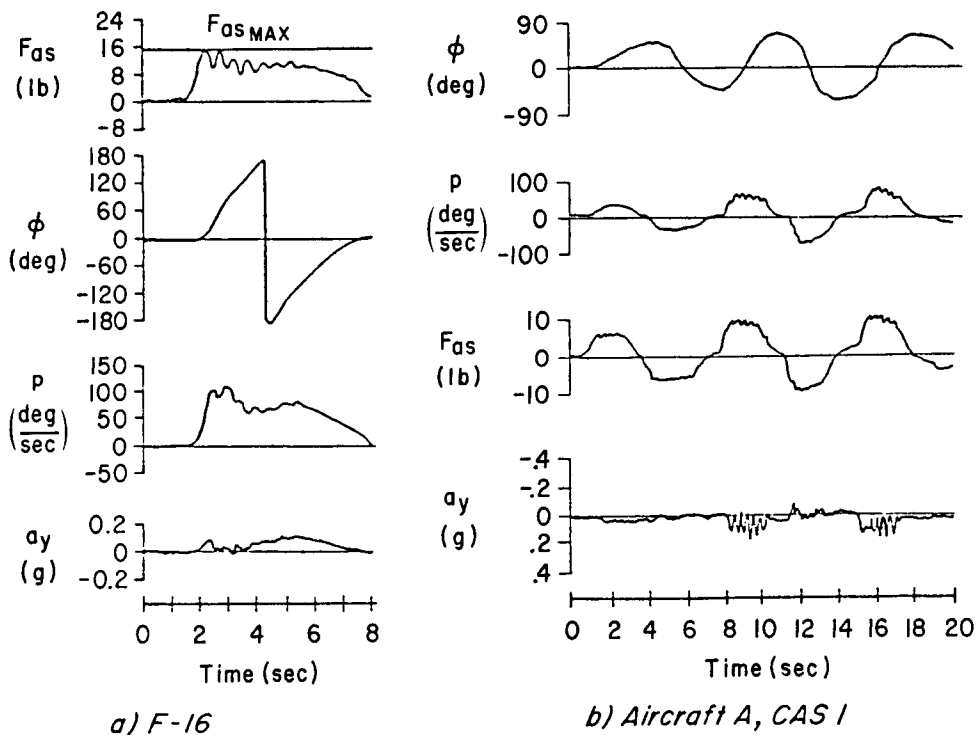


Figure 1. Roll Ratchet During Banking Maneuver

From the earliest studies on the interaction between the human pilot's neuromuscular system and aircraft control devices (e.g., Refs. 1 and 2) the presence of a neuromuscular system limb manipulator dynamic resonance peak at 14-19 rad/sec has been well known. In Ref. 3 the neuromuscular system characteristics are cited as "exceptionally important and critically limiting in such matters as

- control precision where limited by the pilot's neuromuscular system dynamics.
- effects of control system nonlinearities, including their connections with control system sensitivity requirements."

Reference 4 and other summaries place great stress on the importance of considering these characteristics even though this frequency range of major activity may be well above the bandwidth associated with the "usual" control task.

It is becoming more and more apparent that modern, high performance, high gain, command response flight control system bandwidths may be encroaching on the neurological system. Advances in flight control system fly-by-wire technology permit new manipulation devices, for example force sensing sticks, at the pilot output/effective-vehicle interface. These have thus far been generally successful in application, but have introduced or enlarged some pilot-vehicle flying qualities problems. Particular problems include:

- high roll control sensitivity and PIO's in precision maneuvering;
- roll ratchet or jerkyness in otherwise steady rolling maneuvers;
- sensitivity to the way the pilot grips the stick or to location of his hand/arm support;
- effective time delay associated with stick filters, with attendant increase in pilot remnant;
- biodynamic interactions, e.g., hand/arm stick bobweight effects.

Attempts to alleviate these effects have involved adjustments in stick force gradients, filtering, and sensitivity. These have included introduction of various nonlinear elements such as command gain reduction as a function of pilot input amplitude or frequency (Ref. 5), filter time constant changes with sense of input (increase or decrease) (Ref. 6), and different force gradient for right and left roll commands (Ref. 6). These adjustments have generally involved complex ad hoc empirical modifications in the course of the aircraft development. Much of this has been accomplished in flight test with correspondingly large cost.

Other modifications have included reverting from stick force sensing to displacement sensing (Ref. 7) to take advantage of the natural filtering of the associated mechanical systems. This approach may involve increased complexity in the manipulator and feel package due to the necessary pivots, detents, springs, dash pots, etc., but the dynamic lag of the quasi-linear elements can be compensated for by reducing other intentional forward path filter elements. Furthermore, recent flight experience (Refs. 8, 9) has suggested that the pilot may not be as sensitive to this feel system lag contribution as he is to other downstream lags from electronic filters, computational delays, etc. This has led to some controversy (Ref. 9) concerning intent and interpretation of the response time delay criteria of the current flying qualities specification (Ref. 10) and is discussed in the next section.

Thus there is a need to revisit and expand the earlier neuromuscular system experimentation with a focus on now practical flight control system configurations in order to quantify possible interactions between these and the neuromuscular system. The result should provide manipulator/flight control system design guides and criteria to minimize roll control problems. A first step was taken in the Ref. 11 investigation of side-stick force sensing and the interaction with the neuromuscular system. The experimental program with results documented herein was taken to further satisfy these goals.

In the section which follows, a fairly broad and simplified view of some pertinent manual control considerations are presented as background for the experiment. These include the pilot/controlled-element

crossover model and the basic human operator subsystems of particular interest (arm neuromuscular subsystem model, limb/manipulator and feel system interaction, etc.). This sets the stage for definition of experiment setup and goals which is presented in Section III.

The experiment encompassed some 48 manipulator/filter/aircraft configurations involving 320 runs by two subjects. Key findings are summarized in Sections IV through VI. Section IV concentrates on the displacement side-stick experiment results and compares these with the Ref. 11 force sidestick results. Attention is focused on control bandwidth, excitement (peaking) of the neuromuscular mode, feel force/displacement gradient effects, time delay effects, etc. Section V is devoted to experiments with a center-stick in which force vs displacement sensing, feel system lag, and command prefilter lag influences on tracking performance and pilot preference are investigated. Results in these two sections are summarized in numerous plots which are intended to serve as guides in the design of future control systems.

Section VI concentrates on extraction of dynamic models for the pilot and closed-loop arm/manipulator/feel system from the describing function data obtained in the Section V experiments. Parameters suitable for detailed models and for the simple crossover model are derived.

Section VII summarizes the findings and conclusions. Details concerning the manipulators, feel gradients, etc. along with run logs and data summaries are presented in the several Appendixes.

## SECTION II

### BACKGROUND

In the preceding Ref. 11 study a fixed-base simulation was performed to identify and quantify interactions between the pilot's hand/arm neuromuscular subsystem and various effective controlled element aspects representative of typical modern fighter aircraft high-response, roll-rate-command control system mechanizations. In particular:

- force-sensing side-stick type manipulator
- command augmentation prefiltering
- flight control system effective time delay

The simulation results provided insight to high frequency PIO (roll ratchet), low frequency PIO, and roll-to-right control and handling problems previously observed in experimental and production fly-by-wire control systems. The simulation configurations encompassed and/or duplicated several actual flight situations, reproduced control problems observed in flight, and validated the concept that the high frequency nuisance mode known as "roll ratchet" can derive from the pilot's own neuromuscular subsystem. The results demonstrated that roll ratchet tendency, difficult to detect in fixed-base simulation display or time traces, is readily apparent from application of frequency response spectral analysis techniques to the experimental data with adjustment for the pilot's motion sensing neurological apparatus. Results show that force-sensing sidestick manipulator force/displacement/command gradients, command prefilters, and flight control system time delays, need to be carefully tuned to minimize neuromuscular mode amplitude peaking (roll ratchet tendency) without restricting roll control bandwidth (with resulting sluggish or PIO prone control).

One means of reducing control sensitivity problems and roll ratchet tendency in the F-18, X-29, and other aircraft, has been to replace stick force sensing with stick displacement sensing. This results in a natural smoothing (filtering) of the command input via the manipulator

dynamic elements. This also brings into play a different set of receptors in the pilot's hand/arm neuromuscular subsystem. Results obtained from the X-29 aircraft flight test (Ref. 8) also cast doubt on the response time delay criterion of the flying qualities specification, MIL-F-8785C. This specification states that the effective time delay between application of force at the manipulator and appropriate vehicle response shall not exceed 0.1 sec for Level I and 0.2 sec for Level II flying quality ratings. Due to the use of stick displacement sensing and command prefiltering in the X-29 plus the presence of computational time delay, surface actuation and aircraft lags, etc., the total effective time delay is predicted to produce Level II pilot ratings. However the aircraft is rated a solid Level I in flight. If the feel system dynamic delay is excluded from the effective time delay calculation, Level I response is predicted.

The question raised is whether the dynamic lag of the feel mechanism is transparent to the pilot (and therefore not to be included in the calculation of forward loop effective time delay, or alternatively, the specification criteria to apply from the source of the electrical command -- force or displacement) or whether the specification criteria is too stringent and should be relaxed to allow for the dynamic lag contribution of the displacement mechanism and feel package.

The relative merits of stick displacement command versus prefiltered stick force command have not been quantified in terms of effective time delay, maximum control bandwidth, neuromuscular peaking, low and high frequency PIO tendency, etc. The goal of the experimental program reported herein is to provide such information, to compare results with the preceding force sensing investigation, and to provide design guides/tradeoffs for minimizing roll control problems in future high performance aircraft.

#### **A. SOME SIMPLE PILOT/VEHICLE CONSIDERATIONS**

A block diagram for a general compensatory control situation showing the basic human operator subsystems is presented in Fig. 2 (from Ref. 2). The major elements are the controlled element dynamics ( $Y_c$ ),

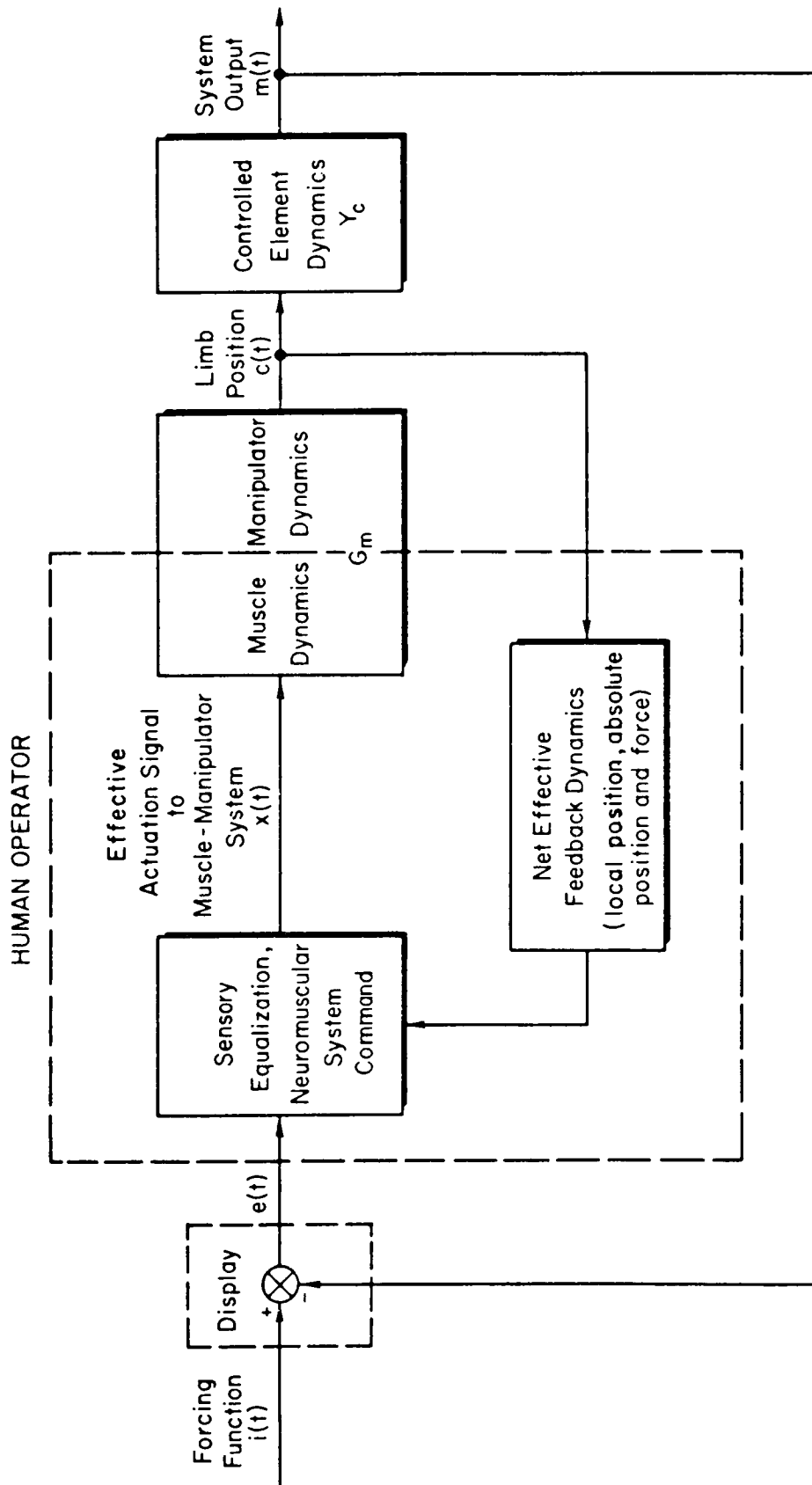


Figure 2. General Compensatory Control Situation and Basic Human Operator Subsystems

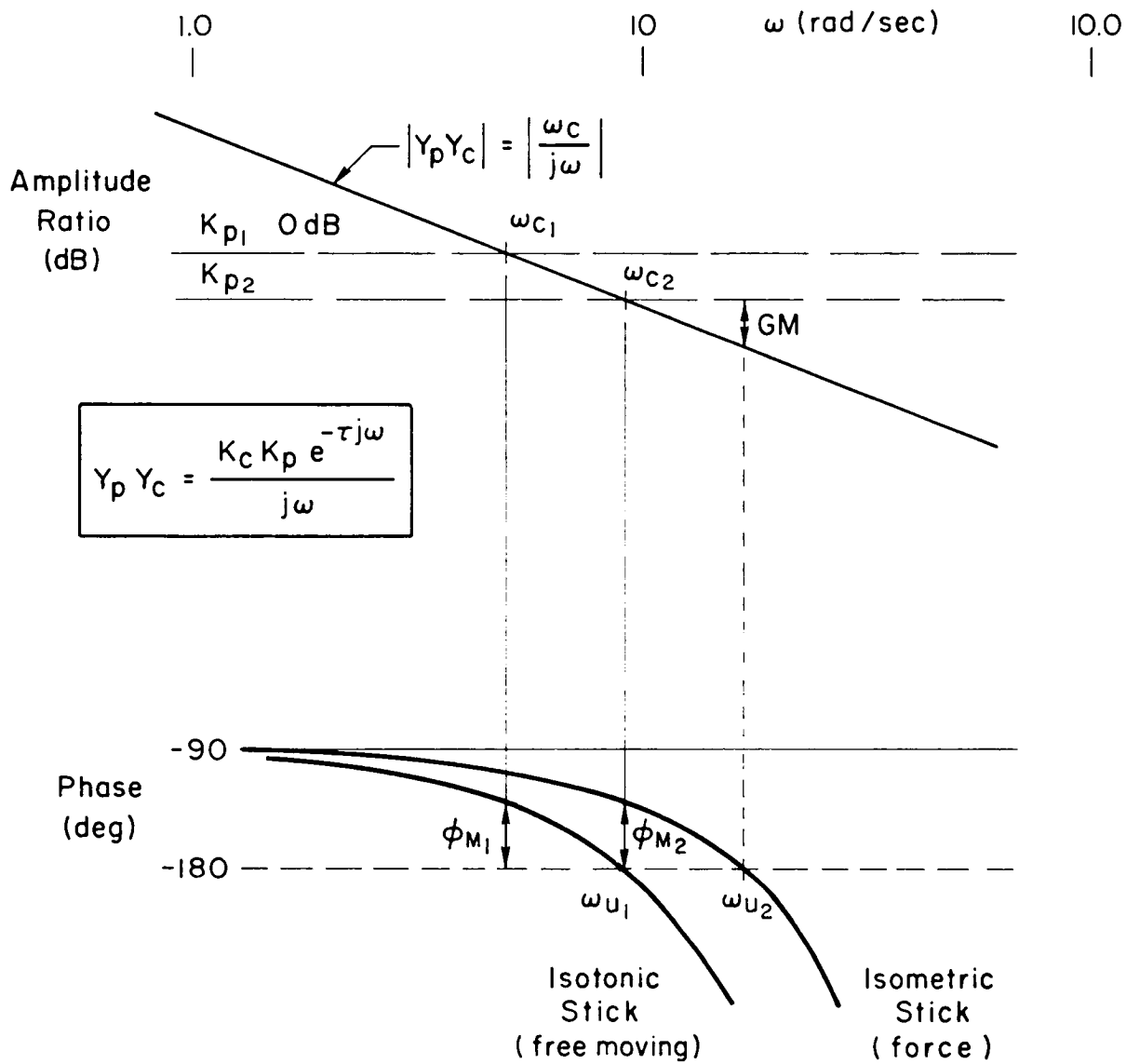
the manipulator dynamics, and the human operator which encompasses the central sensory, equalization, and neuromuscular (N.M.) command elements, the muscle actuation dynamic element, and the various N.M. force and displacement feedbacks.

Simple tracking task pilot model forms and associated pilot vehicle system properties begin with the ideal crossover model of Fig. 3 (see e.g., Ref. 4). In this model the pilot adjusts his dynamic characteristics so that the open-loop pilot-vehicle dynamics are approximately K/s over the frequency band immediately above and below the gain crossover. The prescription for K/s-like controlled element dynamics in the region of pilot vehicle system crossover as an often desirable form stems from the fundamental feature of human dynamics that no pilot lead is then required to establish good closed-loop dynamics over a wide range of pilot gains. The basic recipe is almost invariably conditioned by such statements as "in the frequency region about crossover." Such statements are made to restrict the form of the pilot model to that required only in the crossover region. In particular, the cases covered are such that an effective time delay term in the pilot model is an adequate approximation to the high frequency effects. The model also indicates that in full attention tracking operations the pilot will adjust his gain to offset any variation in controlled element gain in order to maintain a nearly fixed control system bandwidth. Thus the full attention closed-loop bandwidth  $\omega_c$  (identified as the crossover of the 0 dB gain line with the K/s amplitude plot) is independent of the controlled element gain. Furthermore, the pilot tends to keep the product of the crossover frequency and the task RMS error,  $\omega_c \sigma_e$ , constant.

In the crossover model the exponential term with time delay,  $\tau$ , approximates all the lag contributions due to pilot and vehicle high frequency dynamic modes. The effective time delay is a function of, among other things, the force/displacement characteristics of the manipulator. As shown in Fig. 3, an isometric (force) stick results in less lag than does an isotonic (free moving) stick. Past experimentation has identified the difference to be approximately 0.1 sec (e.g., Ref. 4).



$$\begin{aligned}\omega_c &\doteq \text{constant} \\ &\neq f(K_c) \\ \omega_c \sigma_e &= \text{constant}\end{aligned}$$



$$\Delta\tau = \tau_{\text{isotonic}} - \tau_{\text{isometric}} \doteq 0.1 \text{ sec}$$

Figure 3. Ideal Crossover Model

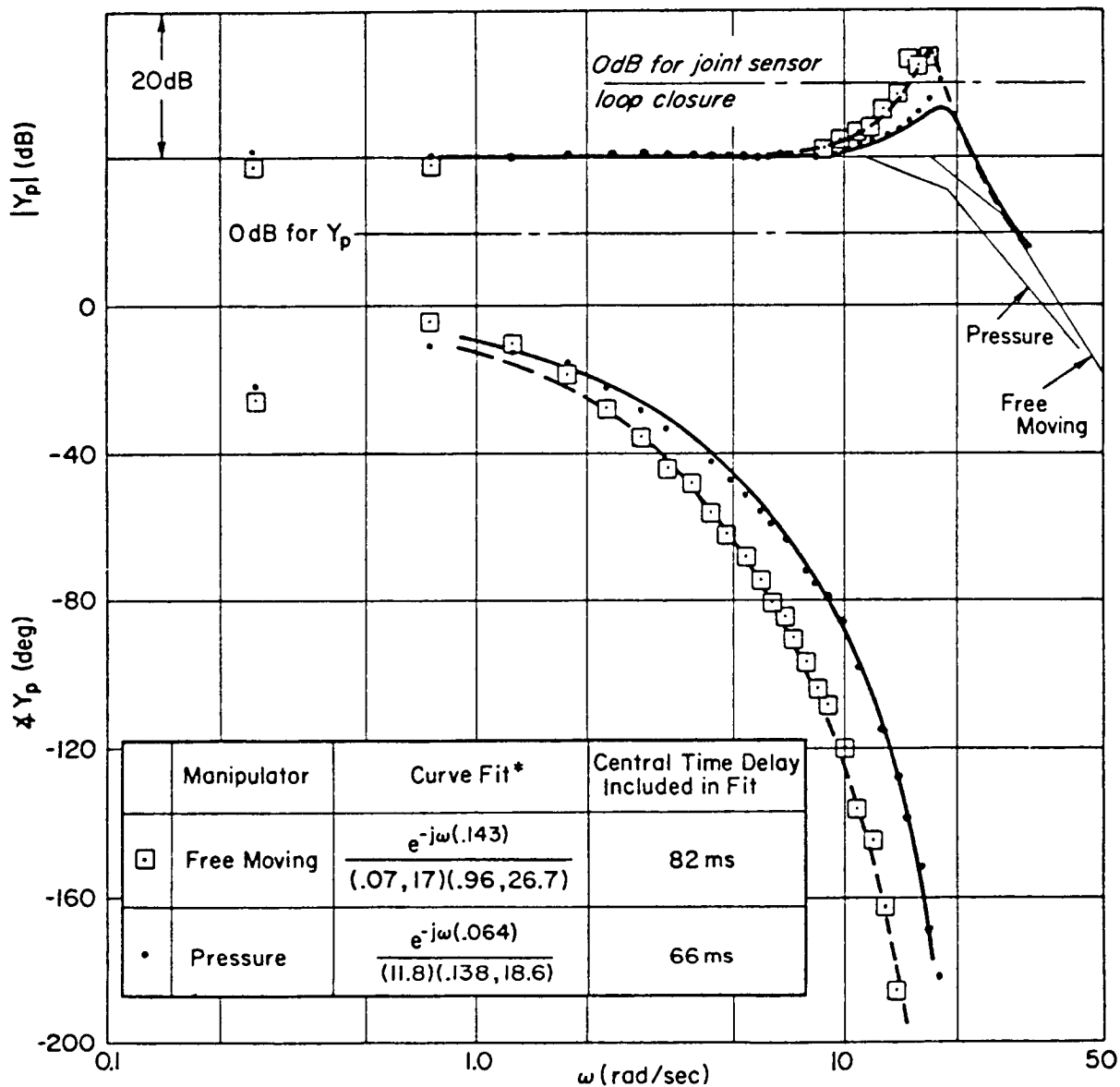
In Fig. 3 if the pilot gain were set at the value represented by  $K_{p2}$  with an isometric stick, the bandwidth would be indicated by  $\omega_{c2}$  and would result in a system stability phase margin  $\phi_{m2}$ , and gain margin, GM. If this same gain were employed with the isotonic stick, the phase margin would be 0, and a low frequency continuous oscillation (PIO) would result. This oscillation can then be alleviated by the pilot reducing his gain to the value represented by  $K_{p1}$  and accepting the reduced bandwidth. Thus Fig. 3 can be used to demonstrate the common low frequency PIO problem which generally occurs in the vicinity of 0.5 Hz and which is relieved by reducing pilot gain. Note that in the crossover model an  $\omega_u$  of 4 rad/sec corresponds to  $\tau = \pi/2\omega_u \approx 0.4$  sec for the total pilot, control system, aircraft, etc., latency.

### B. THE NEUROMUSCULAR SYSTEM MODEL

As previously noted, early studies on the neuromuscular system (e.g., Ref. 1 circa 1968) noted the presence of a neuromuscular system or limb-manipulator peak at 14-19 rad/sec, well past the usual "crossover region." The effects of various restraints on the limb/neuromuscular system are described in detail in Ref. 2. Figure 4 (from Ref. 2) shows closed-loop neuromuscular system model fits to pilot/controlled-element describing function measurements for pressure and free moving manipulators. An important part of the neuromuscular dynamics in each case is a peaking quadratic mode with damping and natural frequency of

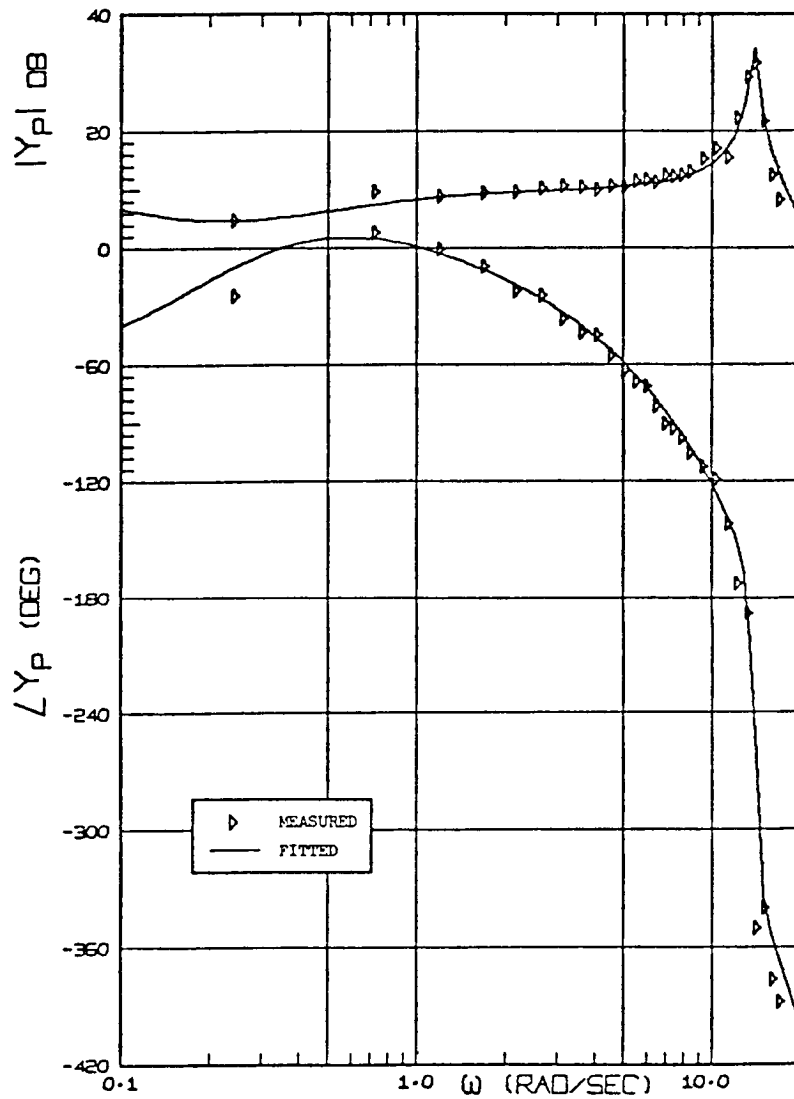
MANIPULATOR	NM/L DYNAMICS
Free Moving	[0.07, 17]
Isometric or Pressure	[0.138, 18.6]

The experiments which allowed identification of these modes used forcing functions having a low power shelf extending to higher frequencies than normally utilized in tracking tasks. The human pilot describing function data of Fig. 5 from Ref. 12, provides an example of the range of frequencies needed to completely define the resonant peak. Note in Fig. 4 that there is a second neuromuscular mode for the pressure



\*Note: To simplify the notation,  $(s^2 + 2\zeta\omega s + \omega^2)$  is written  $(\zeta, \omega)$  and  $(s + a)$  is written  $(a)$ .

Figure 4. Closed-Loop Neuromuscular System Model Fit to  $Y_p$  for Pressure and Free-Moving Manipulator ( $Y_c = 1/s$ ) from Ref. 2



RUN 4079. SUBJECT LR.  $\omega_1 = 4.0$  RAD/SEC. FREE-MOVING MANIPULATOR.

Figure 5. Example Describing Function Showing High Frequency Peak  
(Taken from Gordon-Smith, Ref. 12)

manipulator which is approximated by a first-order lag break at 11.8 rad/sec. This mode is also somewhat dependent on the nature of the manipulator restraints (Refs. 13 and 14). The free moving manipulator results in a second, highly damped second-order mode at about 27 rad/sec.

The reason that the neuromuscular actuation system dynamics differ when the manipulator restraints are changed is physiological -- the neuromuscular apparatus involved depends on the restraints and limb movements. While greatly oversimplified, the neuromuscular actuation elements of the human may be viewed in Fig. 6 as a two loop system. The inner loop feedback principally involves muscle spindle receptors (and Golgi) with short pathways directly to the spinal level and back to the musculature. Viewed from the output end this loop is primarily sensitive to forces, and because of the short neural pathways the time lags of information flow are small. The effective bandwidth of this loop can, therefore, be quite high. The second or outer loop includes joint

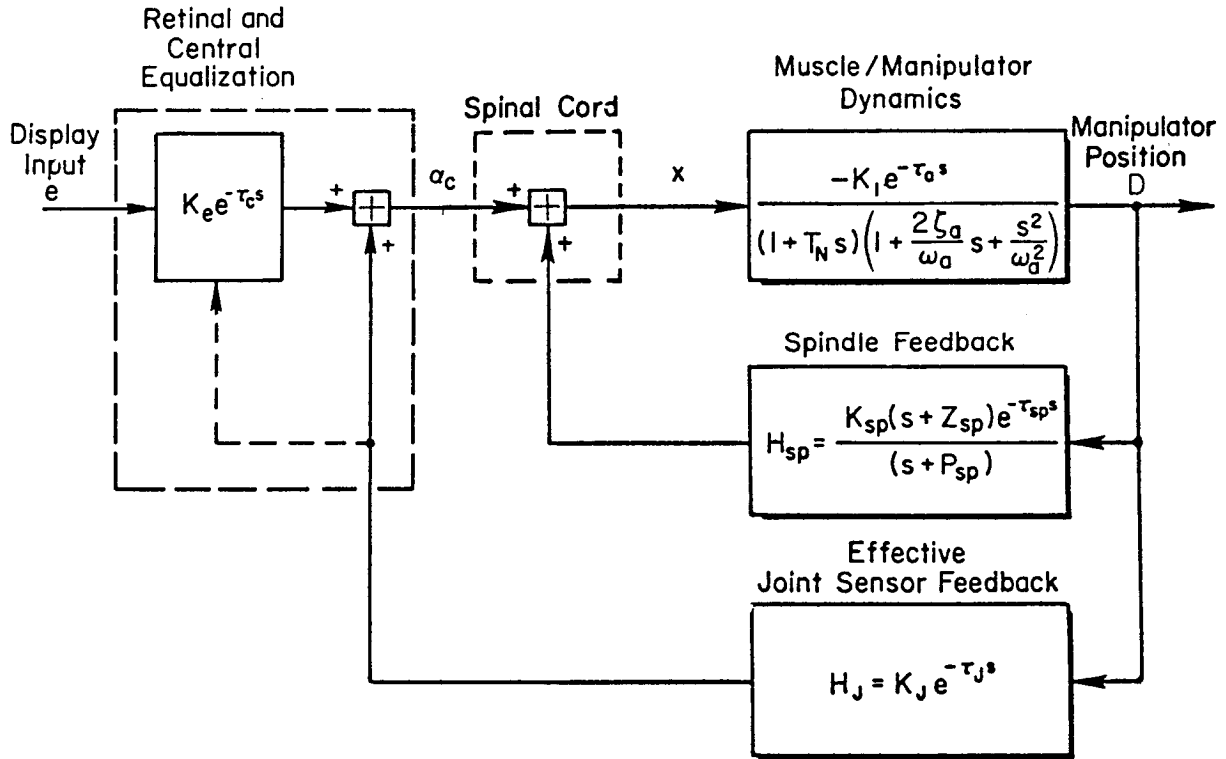


Figure 6. Neuromuscular Subsystems for Free-Moving and Pressure Manipulators and Central Equalization for Rate Dynamics

and other (e.g., peripheral vision) receptors as major feedback elements. Their neural pathways, and associated delays, are longer, leading to a lower outer loop bandwidth. Note that this simplified model does not include dynamic elements associated with the manipulator itself and the form of the retinal and central equalization term in Fig. 6 is appropriate for controlled element dynamics of the form  $Y_c = K_c/s$ . If the controlled element differs appreciably from this ideal the pilot's central equalization can include an additional lead, lag, or both.

Figure 7 (from Ref.2) presents root locus and Bode-Siggy plots showing typical closed-loop N.M. actuation subsystem root migrations for successive closures of the Fig. 6 inner (spindle, force) and outer (joint sensor, displacement) feedback loops. Increasing force or tension in the inner loop increases the frequency but decreases the damping of the complex mode and decreases the inverse time constant of the first order mode. Closure of the joint displacement loop results in a slight decrease in the complex mode frequency and further decreases mode damping. Peaking of the closed-loop N.M. mode increases with increasing joint displacement feedback gain.

In isometric (force-stick) manipulator conditions, there is little or no joint movement, so the inner loop elements should be dominant. With isotonic (free-moving stick) conditions, on the other hand, the joint receptors are major elements. As already indicated in connection with Fig. 3 the net difference, in terms of an effective latency, is approximated at low frequencies by a difference in effective time delay of about 0.1 sec.

If we now employ the Fig. 4 detailed model of the neuromuscular system (instead of only approximating its phase lag contribution as in Fig. 3) and superimpose it on the controlled element  $K/s$  as in Fig. 8, we see an open-loop resonant peak in the 2 to 3 Hz frequency range due to the neuromuscular system. The correspondence of the neuromuscular/limb quadratic mode numerical values and roll ratchet frequencies is very unlikely to be a coincidence. So, the neuromuscular/limb mode clearly should be taken into account in the analysis of roll ratchet. Since the

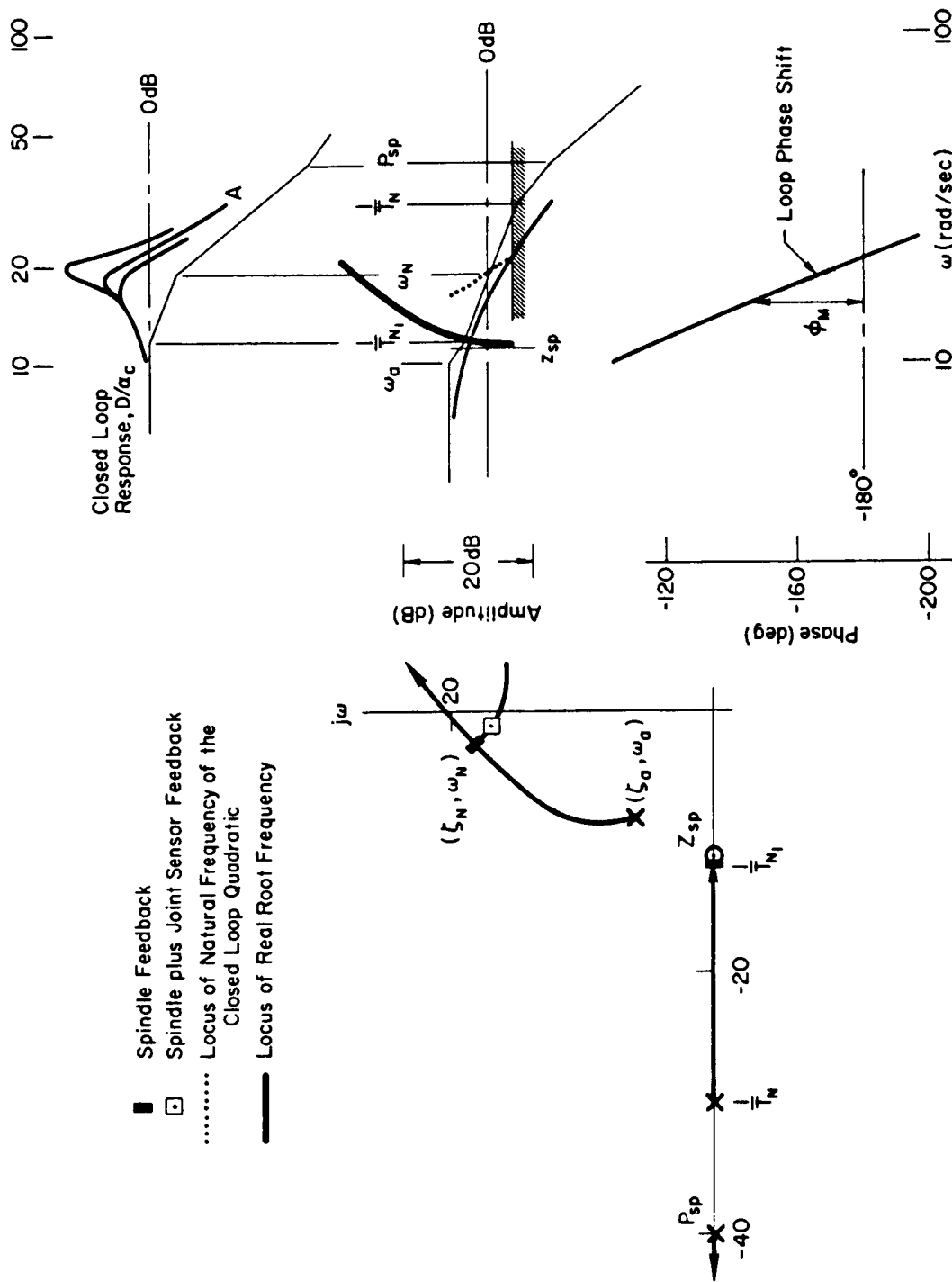


Figure 7. Bode and Root Locus for Spindle Feedback (Some Effects of Joint Sensor Feedback Shown)(Ref. 2)

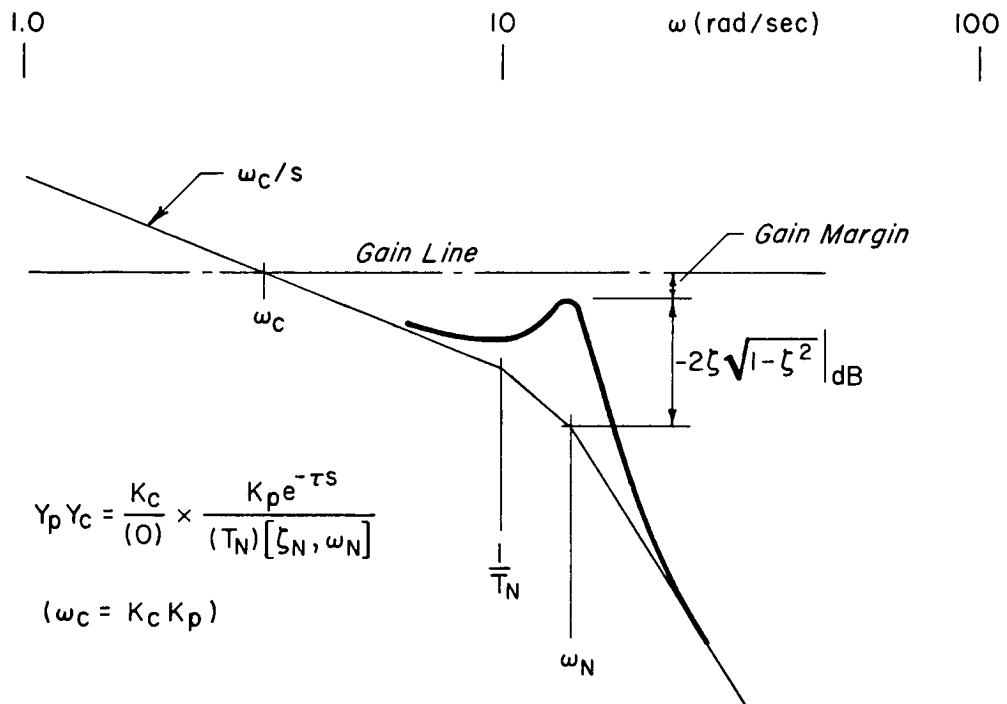


Figure 8. Bode Amplitude Ratio Plot for Neuromuscular System Contribution to Roll Ratchet Potential

primary effect is a resonant peak from which "Gain Margin" might be measured, it is quite apparent that these properties will be of central importance for high gain situations. While the "Gain Margin" shown in Fig. 8 indicates the magnitude difference between the  $\omega_N$  peak and the 0 dB line, the phase at or near this frequency may differ appreciably from that required for instability. Thus when the "Gain Margin" shown is zero only one of the two conditions for instability may be satisfied. Consequently this is not necessarily a true gain margin in the conventional sense. It does, however, indicate a resonant tendency contributed by the pilot.

### C. LIMB ACTUATION/FEEL SYSTEM INTERFACE

In the world of real aircraft, control manipulators (sticks) are not pure isotonic or isometric devices. Even the F-16 force stick has limited movement. The reason for this is to provide the pilot with some predetermined "feel" relating to aircraft state, mission task, comfort, etc. These feel systems generally involve stick displacement response



to force application through a spring-damper (dash-pot) type arrangement. They also incorporate nonlinear elements such as detents, breakouts, stops, etc. Detents and breakout are incorporated around stick neutral to provide positive centering and minimize inadvertent stick inputs due to vehicle motion, turbulence, cross axis coupling, etc. These nonlinearities are kept as small as possible and once overcome, the stick/feel system can be modelled by 2nd order dynamics.

The limb-actuation, feel system model including the linear elements is shown in the block diagram of Fig. 9 allowing for the two types of manipulator sensing (force or displacement).

### 1. Force Sensing

Closing the muscle actuation/spindle feedback loop produces the effective inner loop transfer function

$$\frac{F}{\alpha_c} = \frac{K_{NM} \left(1 + \frac{s}{P_{sp}}\right) e^{-\tau_{NM}s}}{(1 + T_{N1}'s) \left[1 + \frac{2\zeta_N' s}{\omega_N'} + \left(\frac{s}{\omega_N'}\right)^2\right]}$$

If the manipulator is fixed (no displacement) this simple transfer function then reflects the pilot's N.M. subsystem. However if stick displacement is incorporated through a feel system, the feel dynamics are encompassed in the joint receptor feedback path and contribute to the effective N.M. system as shown in Fig.10. The pilot/manipulator closed loop transfer function then is of the form

$$\frac{F}{e} = \frac{K_p \left(1 + \frac{s}{P_{sp}}\right) \left[1 + \frac{2\zeta_{FS}s}{\omega_{FS}} + \left(\frac{s}{\omega_{FS}}\right)^2\right] e^{-\tau_p s}}{(1 + T_{N1}'s) \left[1 + \frac{2\zeta_N' s}{\omega_N'} + \left(\frac{s}{\omega_N'}\right)^2\right] \left[1 + \frac{2\zeta_{FS}' s}{\omega_{FS}'} + \left(\frac{s}{\omega_{FS}'}\right)^2\right]}$$

The feel system contribution is seen to produce a complex pole/zero dipole. The residue of this dipole depends upon the separation and hence effective loop gain. Any lag or delay contribution to the effective pilot dynamics (and hence transparency to the pilot) will depend upon the location of the feel system dynamics with respect to the N.M.

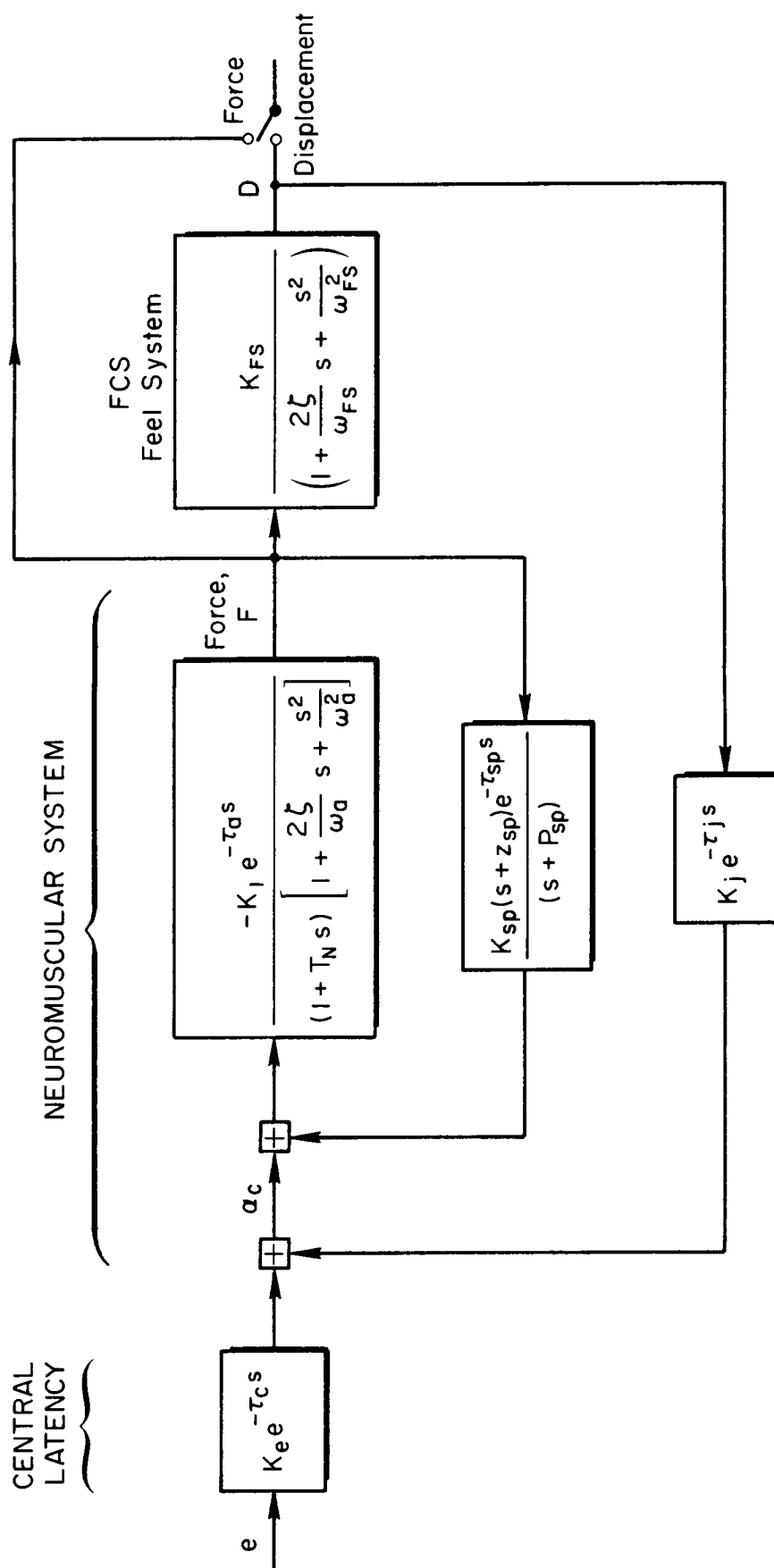


Figure 9. Pilot Closed-Loop Limb-Actuation With Feel System Dynamics

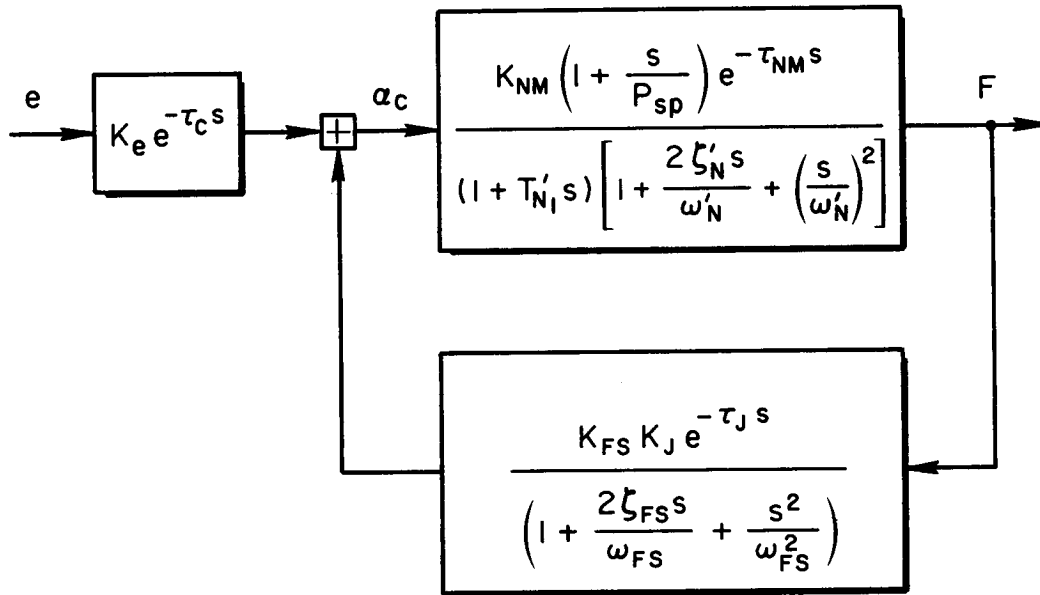


Figure 10. Closed-Loop Manipulator System With Force Sensing

system (ie., lower or higher frequency) and dipole residue. If the feel dynamics are well above the N.M. mode and the stick displacement small, then the effective closed-loop dynamics reduce to the third order noted earlier.

## 2. Displacement Sensing

When displacement sensing is employed the feel system dynamics become a part of the forward loop in Fig. 9 and the pilot/manipulator closed loop transfer function is of the form

$$\frac{D}{e} = \frac{K_p \left(1 + \frac{s}{P_{sp}}\right) e^{-\tau_p s}}{(1 + T'_{N1} s) \left[1 + \frac{2 \zeta'_N s}{\omega'_N} + \left(\frac{s}{\omega'_N}\right)^2\right] \left[1 + \frac{2 \zeta_{FS} s}{\omega_{FS}} + \left(\frac{s}{\omega_{FS}}\right)^2\right]}$$

The feel system then becomes a direct contributor to the forward loop lags. A question remains however as to whether this lag is partially or totally compensated for by a change in the pilot's central equalization (lead generation or decrease in latency) and therefore is transparent to the pilot. If this should be the case then there is room for argument

that the flying qualities time delay criterion should not be referenced to force application but rather to manipulator displacement. On the other hand, past experimentation (e.g., Fig. 4) has indicated an increase in pilot central latency with pure displacement (inertia) manipulators. This would portend a compounding effect for pilot/feel-system lags with displacement sensing. Thus the need for experimentation to resolve as many of these issues as possible.

### SECTION III

#### EXPERIMENT GOALS AND SETUP

##### A. EXPERIMENT SETUP

The experimental setup is shown in block diagram form in Fig. 11. For the greater part it is identical to that employed in the Ref. 11 experiments. A roll tracking task is used in which the pilot matches the bank angle of his controlled element with that of a "target" having pseudo-random rolling motions. The random motions are obtained via a computer generated sum of sine waves. The error is presented as an Attitude Director Indicator (ADI) type display with a rolling reference line (target) implemented on a circular CRT (Fig. 12). A grid was available in the background for estimating angular deviation of the reference line and a prominent aircraft symbol was available in the foreground. The pilot attempts to null the error by applying force to the manipulator, the output of which becomes the command to the controlled element,  $Y_c$ .

The controlled element consisted of a classical airframe roll transfer function ( $Y_\phi$ ) with time delay and an optional command filter ( $Y_{CF}$ ) of the form shown in Fig. 11.  $Y_\phi$  approximates a high gain roll rate command system. The lag parameter ( $T$ ) may be considered to be the effective roll subsidence time constant or a first order flight control system prefilter (between the pilot's stick command and the flight control system), whichever is larger. For very small values of  $\tau$  the pure time delay may be a realistic approximation to digital flight control system sample and hold dynamics. More generally it is a low frequency approximation for all the high frequency lags in the system which are not covered by the first order lag  $T$ . The parameter values for  $T$  and  $\tau$  used in the experiment are generally consistent with values that would be present in systems designed to be Level I on the basis of flying qualities specifications. Thus, the parameter values used for  $Y_\phi$ , in the main, should produce excellent effective controlled elements providing the gain is appropriately adjusted.

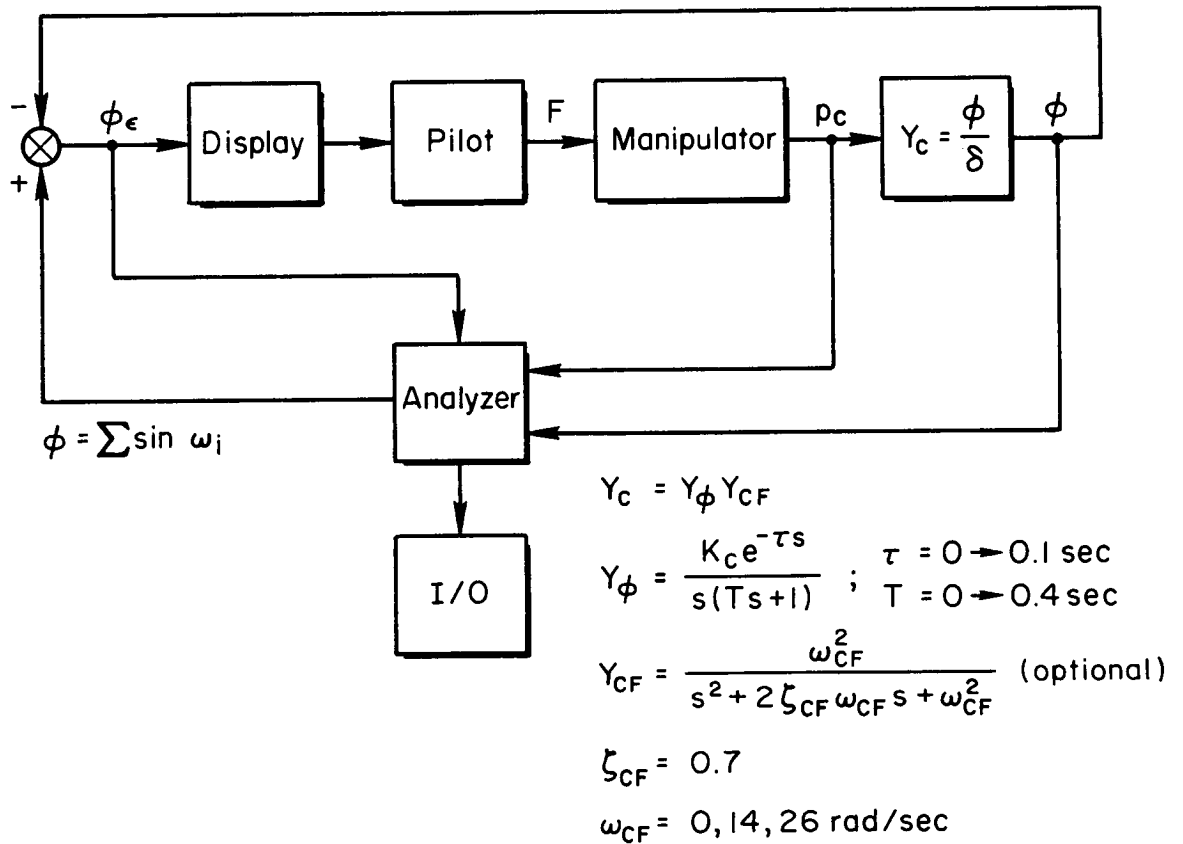


Figure 11. Experimental Setup

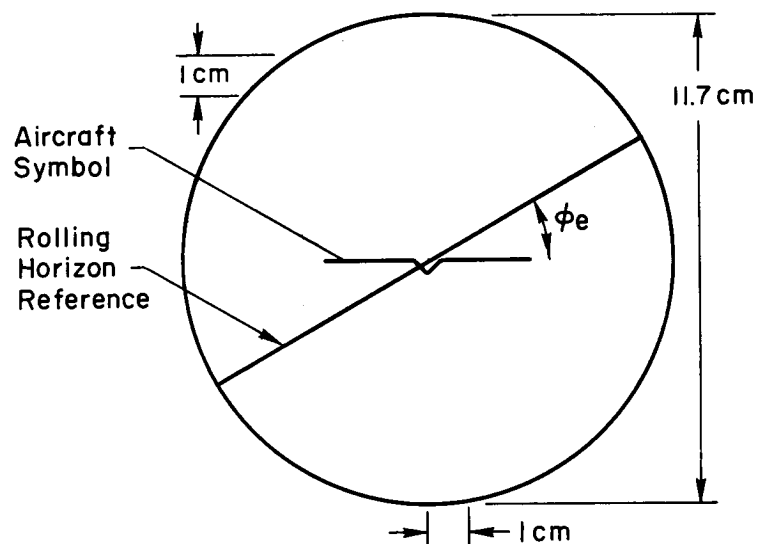


Figure 12. Display Format

An optional response command 2nd order prefilter was incorporated for some of the experiments so that the manipulator feel system and command prefilter dynamic lag contributions could be interchanged. In this manner it was possible to investigate pilot sensitivity to location of lags within the forward loop path.

The manipulators were McFadden force loader systems used in many aircraft research and development simulations. Two stick types were employed (Table 1). One was a right hand mounted side stick. Three different force gradients which fairly well encompassed those used in other experiments (Refs. 15, 16) were evaluated with this manipulator at one set of feel dynamics. The second stick was a conventional fighter type center stick. Two different sets of feel system dynamic characteristics were evaluated with this stick at one representative force gradient. Both displacement and force sensing were available as output from the stick electronics. Plots and time traces of the feel characteristics together with details of their mounting are given in Appendix A.

TABLE 1. STICK/FEEL SYSTEM CONFIGURATIONS:

SIDESTICK	$Y_{FS1}$	$Y_{FS2}$	$Y_{FS3}$
$K_{FS}$ (#/in)	14	7.5	3.75
(#/deg)	1.22	0.65	0.33
(deg/#)	0.82	1.53	3.1
$\omega_{FS}$ (rad/sec)	31.4	22.4	18.0
$\zeta_{FS}$	0.7	0.6	0.6
Breakout (#)	0.75	----->	
CENTERSTICK	$Y_{FS4}$	$Y_{FS5}$	
$K_{FS}$ (#/in)	4	4	
$\omega_{FS}$	26	14	
$\zeta_{FS}$	0.7	0.7	
Breakout (#)	1.0	1.0	

Analog signals from the manipulator sensors were passed through to the controlled element, resident in an analog computer. The controlled element roll response was in turn passed through an A to D converter to a digital computer where  $Y_p Y_c$  describing functions and various performance measures were computed using STI's Describing Function Analyser (DFA) program. The computations were essentially on-line and printed out at the conclusion of each run. Some 380 data runs were accomplished which provided a suitable data base from which to determine or identify the various interactions of interest.

## B. DISTURBANCE (TARGET) INPUT FUNCTION

Key aspects of the experimental program were that the describing function measurements must cover the limb-neuromuscular peaking frequency region, and the forcing functions should emphasize good data in the neuromuscular subsystem region. The experimental runs were accomplished using the summation of sine waves presented in Table 2. This input function was scaled to give an rms disturbance of 18.60 deg roll over a run length of approximately 27 sec. There was an approximately 11 sec "warm-up" and 1.5 sec "cool-down" period at the beginning and end, respectively, of each run where no data is taken by the DFA. This is necessary to allow for desirable initial conditions to be met before starting the describing function analysis and to assure the run length covered a full cycle of the lowest frequency sine wave.

TABLE 2. ROLL TRACKING FORCING FUNCTION

Sine Wave (i)	1	2	3	4	5	6	7	8	9
Frequency ( $\omega_i$ )	0.467	0.701	1.17	1.87	3.51	7.01	11/2	14.0	18.7
Amplitude ( $A_i$ )	15.2	15.2	15.2	7.6	3.04	0.76	0.38	0.228	0.152
Relative Amplitude	1	1	1	0.5	0.2	0.05	0.025	0.015	0.01

$$\phi_I = \sum A_i \cos \omega_i t \text{ (deg)}$$



### C. PROTOCOL

The primary subject (Subject A) completed the whole test matrix. A second subject (Subject B) was employed on approximately half of the configurations to provide a set of check results. Subject A is a flying qualities engineer with previous experience as a military pilot. Subject B is a flying qualities engineer and licensed pilot with experience as a test pilot in both simulator and actual flight situations (light and heavy fixed wing plus rotary wing aircraft).

The subjects were required to perform a minimum of three runs at each configuration before allocating a pilot rating. The Cooper-Harper Pilot Rating (CHPR) scale shown in Fig. 13 was used. Desired performance level required extended time periods of less than 1 to 2 deg roll error and peak errors during reversals of less than 11 deg. Adequate performance required short periods of 1 to 2 deg tracking error and peak errors on reversals of less than 22 deg. The background grid on the display (Fig. 12) was used to judge these angles.

The subjects were instructed to maintain tracking error as small as possible throughout the entire run.

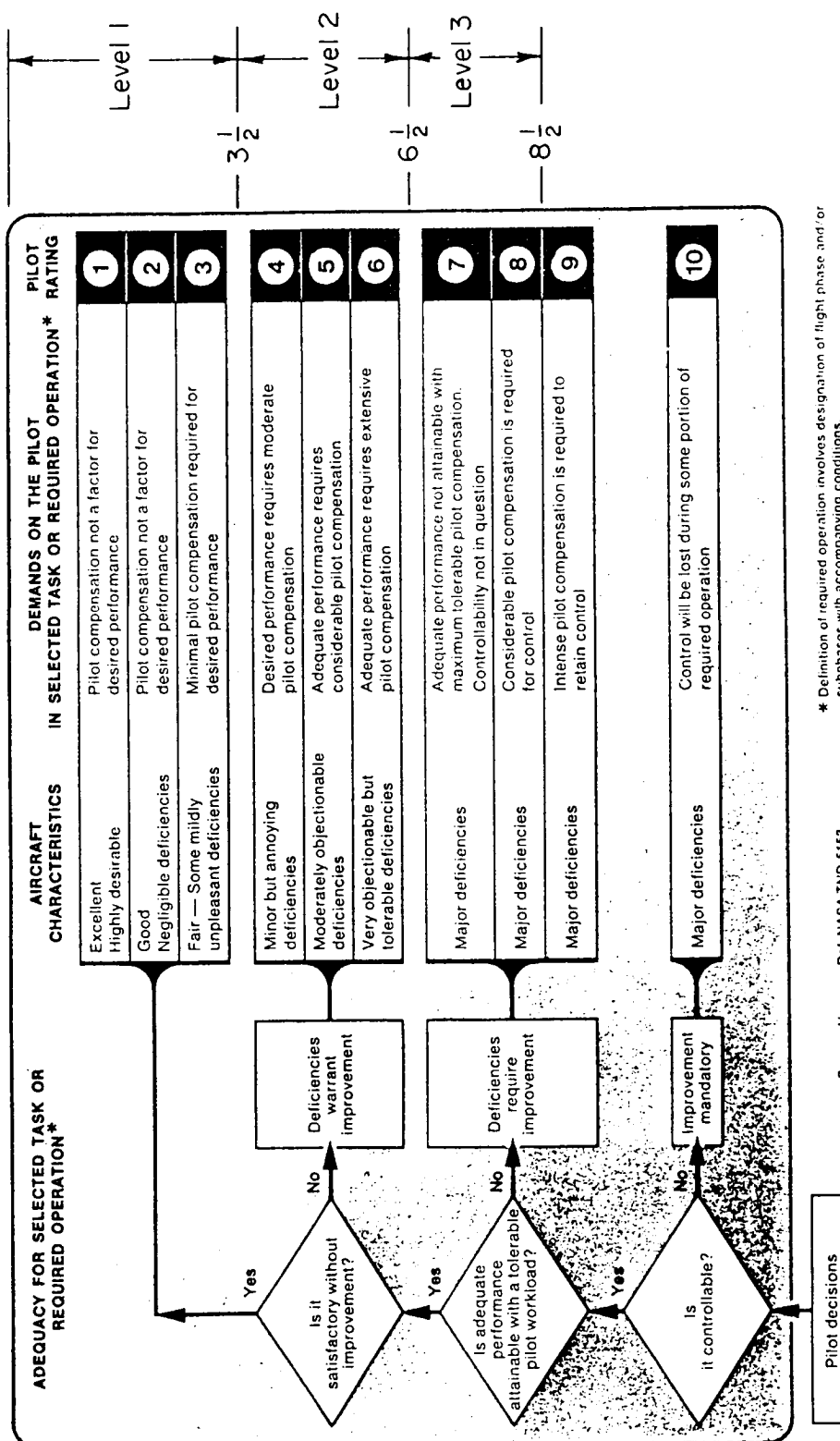


Figure 13. Definition of Flying Qualities Levels

## SECTION IV

### DISPLACEMENT SIDESTICK AND FEEL SYSTEM

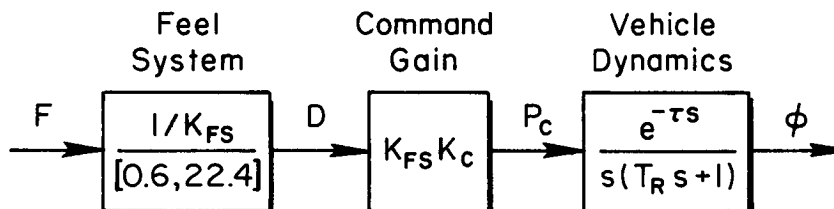
One of the key findings of the previous investigation (Ref. 11) was that the combination of a stiff sidestick manipulator and force sensing could contribute to roll ratchet tendency. A principal goal of this continuing investigation is to determine if the use of displacement sensing alters the tendency to roll ratchet, and if so, to what extent. Another goal is to identify handling performance metrics for the roll control task and to determine the influence of sidestick manipulator, feel system, and response command characteristics on task performance.

Roll ratchet tendency was related in Ref. 11 to the open-loop  $Y_p Y_c$  frequency response amplitude ratio and phase lag at the pilot's neuromuscular (referred to hereafter as N.M.) subsystem dynamic mode frequency. Therefore, we will first look at the influence of position sensing on N.M., peaking tendency, and the system phase lag at that frequency. Results will be compared with those obtained with force sensing in Ref. 11.

Attention will then be focused on roll tracking with various feel system force/displacement gradient and response command gains in order to identify the influence of these design parameters on tracking performance and pilot acceptance.

#### A. INFLUENCE ON PILOT'S NEUROMUSCULAR SYSTEM MODE

A simple block diagram representation of the effective controlled element is shown below.



For this series the experimental matrix encompassed:

- Feel gradient,  $K_{FS} = 0.33, 0.65$  and  $1.22$  lb/deg
- Command gain,  $K_C = 5$  to  $20$  deg/sec/lb
- Time delay,  $\tau = 0, 0.067$ , and  $0.1$  sec
- Roll subsidence,  $T_R = 0, 0.2$ , and  $0.4$  sec

A total of 179 data runs were required to complete this series.

### 1. Amplitude Ratio Peaking

Amplitude ratio peaking of the N.M. mode was determined by drawing straight line asymptotes of the effective controlled element ( $Y_C$ ) and moving the asymptote up or down to fit the  $Y_p Y_C$  describing function data points and satisfy the crossover model in the region of gain crossover as shown in Fig. 14. The amplitude deviation from the asymptote in the region of 11 to 19 rad/sec is then taken as the pilot's N.M. mode contribution.

Average amplitude ratio deviations obtained with an ideal K/s roll task across all command gains and two different feel system gradients (0.65 and 1.22 lb/deg) are shown in Fig. 15. The range of peak readings obtained are indicated by the bars and the number of runs by the number above the bar. The neuromuscular subsystem natural frequency is seen to be in the vicinity of 14 rad/sec for the two test subjects. The peak magnitude and form seems to be independent of the feel system gradient. The lone point which disagrees with this observation (1.22 lb/deg gradient at 19 rad/sec) was not thought to be significant due to the relatively small number of runs made with this configuration.

The latter finding is reinforced by the data of Fig. 16 which show the effects of varying feel system gradient and controlled element time delay. In essentially, all cases, the neuromuscular mode peak frequency remains at approximately 14 rad/sec. However, there are some changes in peak amplitude. Increasing stick stiffness and/or controlled element time delay may be seen to produce a weak increase in the peaking tendency.

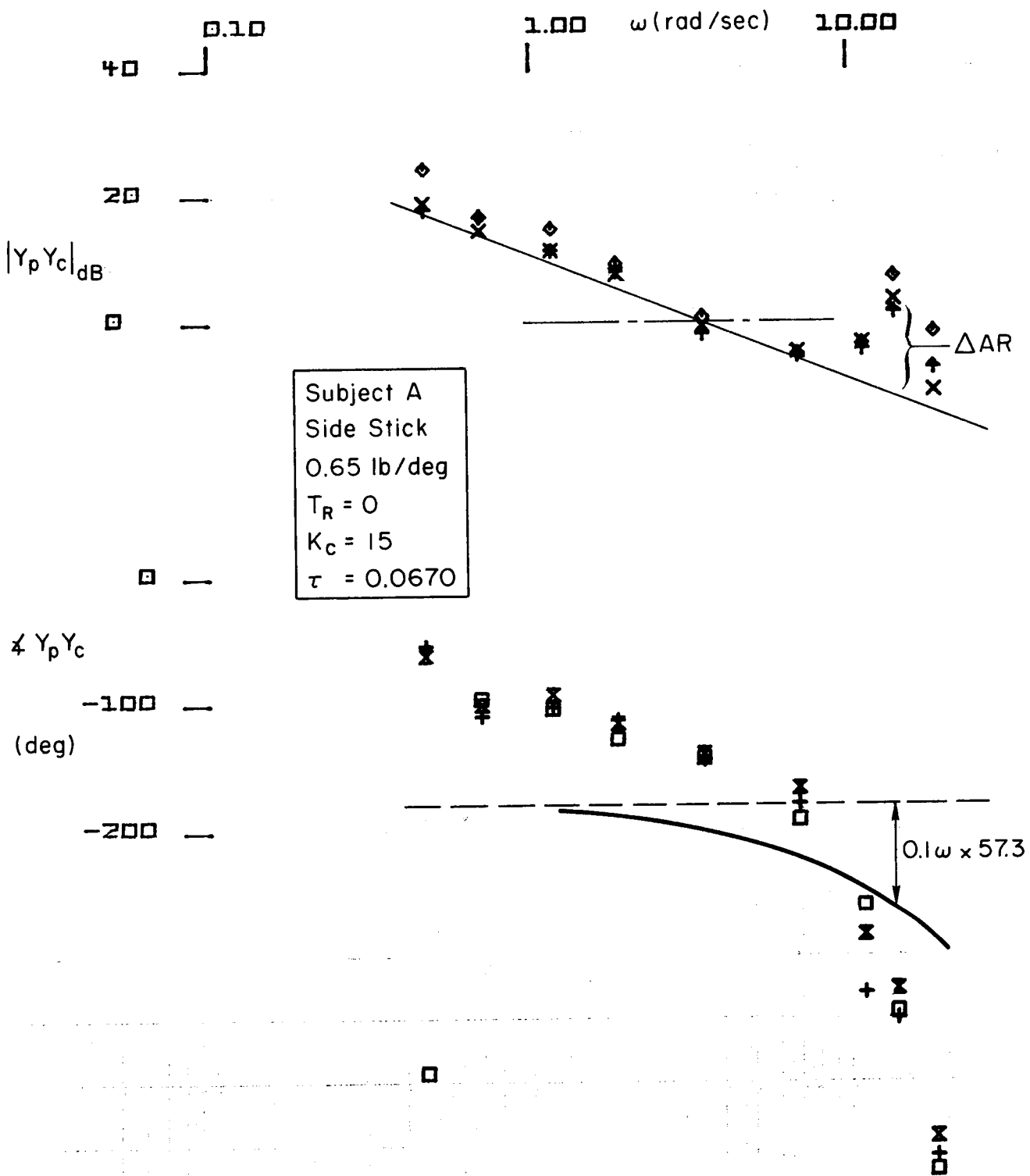


Figure 14. Example Bode Plot With K/S Fit to Obtain  $\Delta AR$

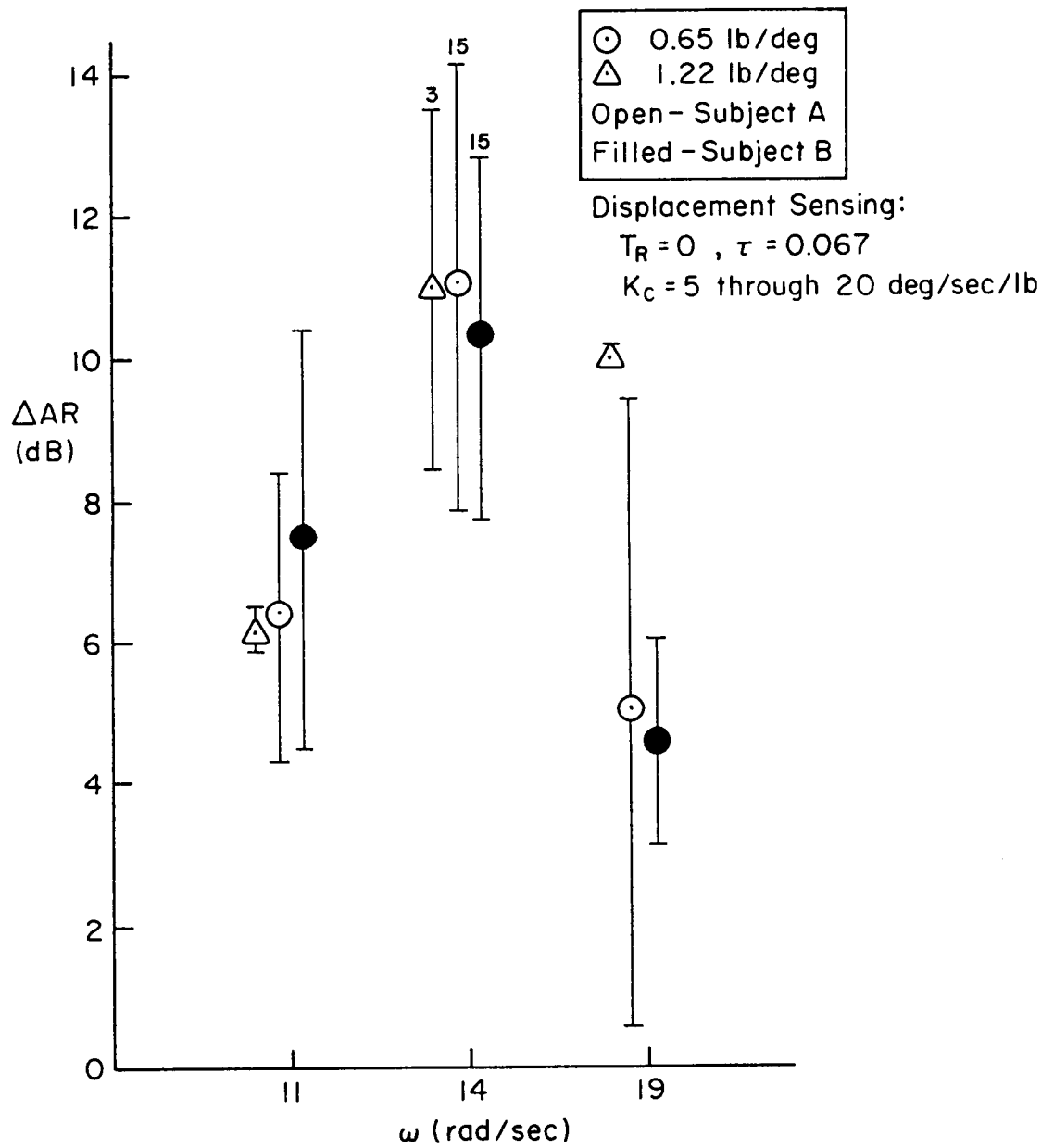


Figure 15. Amplitude Deviation From  $Y_c$  Asymptote Due to Neuromuscular Mode

Open - displacement; Filled - force  
 $K_C = 10 \text{ deg/sec/lb}$ ;  $T_R = 0$   
 Subject A

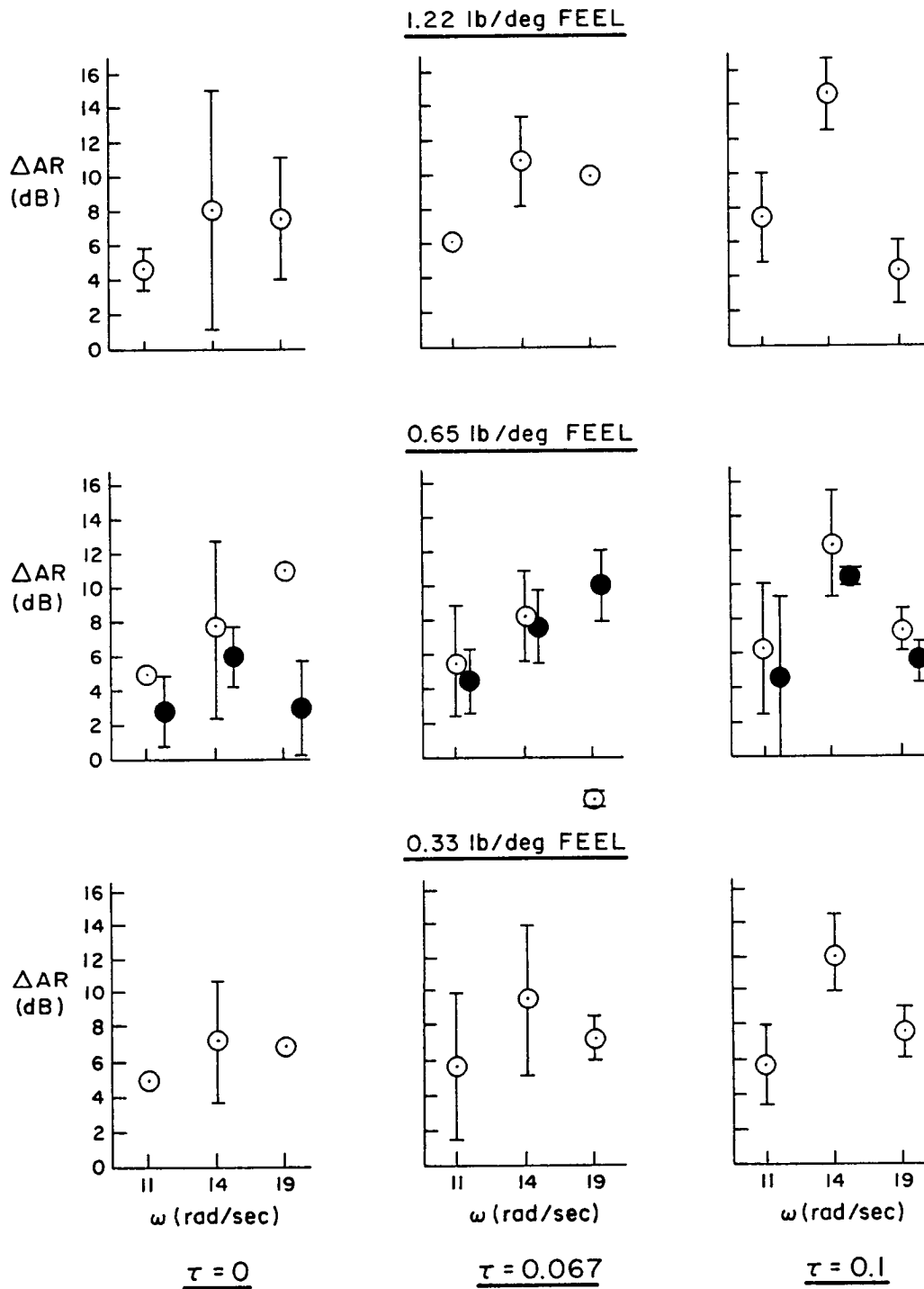


Figure 16. Influence of Feel Gradient and Effective Time Delay on Neuromuscular Mode Peaking With Stick Displacement Sensing

The influence of force vs displacement sensing on peaking was checked with the 0.65 lb/deg feel gradient over the range of time delays. These results are also shown in Fig. 16. As expected from theory, an increase in peaking with displacement sensing can be seen, however the difference is not nearly so pronounced as in the Fig. 4 cases of pure force vs. free moving manipulators.

## 2. Roll Ratchet Tendency

The Ref. 11 experiment indicated that neuromuscular peaking could lead to a roll resonance (ratchet) at the N.M. frequency if the 0 db gain line of the  $Y_p Y_c$  Bode plot cuts through the N.M. mode amplitude peak while the phase angle is very close to 180 deg. To satisfy the phase criteria, a first order correction to the measured describing function phase was required in Ref. 11 to account for the difference between no motion and the rapid rolling motion in flight where the phenomenon actually occurs. The correction is derived from Ref. 4 where it is shown the pilot's angular motion sensing neurological apparatus acts very much like a rate gyro inner loop in the frequency range near and slightly above crossover. This inner loop, present when super threshold rolling velocities are imposed on the pilot, has the effect of reducing the effective time lags in the pilot's visual input/manipulator output response. The reduction can be as much as 0.1 sec from the fixed-base data. When a phase lead of 0.1σ is made in Fig. 14 (which in effect "bends" the 180 deg phase line with respect to the  $Y_p Y_c$  describing function data points as shown by the solid line) it is apparent that the phase angle at the N.M. mode is still considerably greater than 180 deg. The rapid phase roll-off in  $Y_p Y_c$  is due to the feel system 2nd order mode lag contribution (in this case at 22.4 rad/sec) and to the low damped N.M. mode itself. Thus, in spite of the increased N.M. peaking tendency, shown in Figs. 15, 16, we would expect no roll ratchet tendency with this stick displacement sensing response-command system. This was indeed the case with all such configurations investigated.



### 3. Comparison Between Displacement And Force Sensing

It was noted above that there is slightly greater peaking of the N.M. mode with displacement vs force stick sensing. Further comparison between the two is made in Figs. 17, 18, 19. Figure 17a presents the 1.22 and 0.65 lb/deg feel gradient displacement sensing cases of Fig. 16 compared to the almost identical configurations from the Ref. 11 experiment with stick force sensing (17b). While the N.M. mode peaking generally may be greater with displacement sensing the difference is negligible.

Figure 18 allows direct comparison of typical describing function data for the same controlled element dynamics with displacement vs force sensing being the only variables. The most notable difference is the more rapid  $Y_p Y_c$  phase roll-off above roughly 5 rad/sec with displacement sensing (as predicted by Eq. 3) which reduces the roll ratchet tendency as noted above. But, it is also worth noting, that this additional phase lag results in the open-loop  $Y_p Y_c$  phase data points crossing the 180 deg line at a lower frequency. This could result in the pilot being forced to reduce his gain in order to maintain adequate gain and phase margins, thereby resulting in a slightly lower control bandwidth. This decrease in bandwidth would in turn result in degraded tracking performance. It could also result in the pilot generating slightly more lead to offset this added lag in the region of intended crossover, thereby maintaining control bandwidth and hence performance at the expense of extra pilot compensation.

Figure 19 presents survey plots of predicted roll ratchet tendency across different  $K_c$  and  $T_R$  combinations for the sidestick manipulator/feel configurations investigated in this and the Ref. 11 force sensing experiments. The open symbols represent no roll ratchet tendency, the filled symbols reflect roll ratchet. The dashed line boundary separating ratchet and no ratchet is derived from the Ref. 16 NT-33 flight test data also shown in Fig. 19. It appears from this data that the boundary could either be moved to the right by a considerable amount or eliminated entirely by use of displacement sensing.

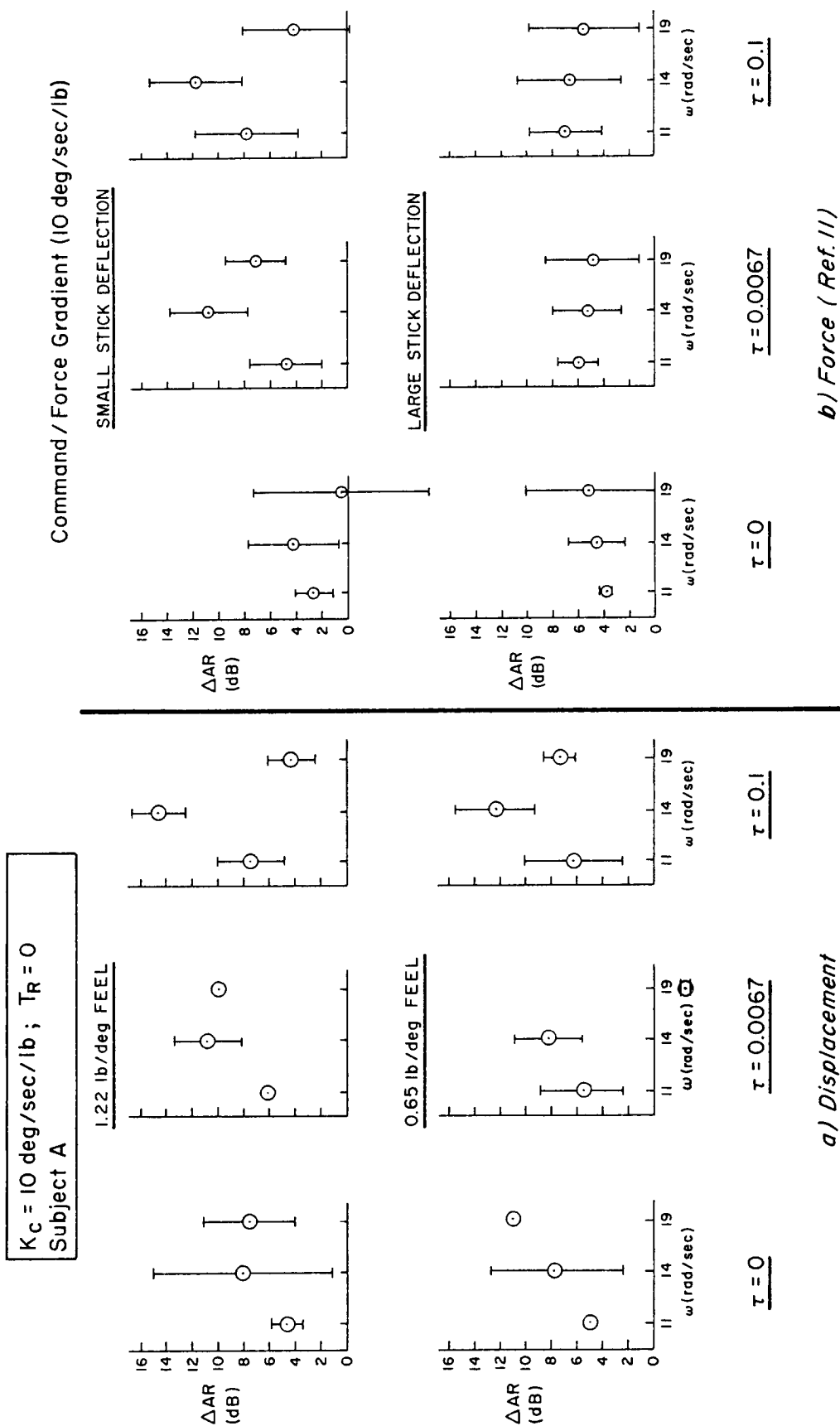


Figure 17. Comparison of Neuromuscular Peaking With Displacement vs Force Sensing

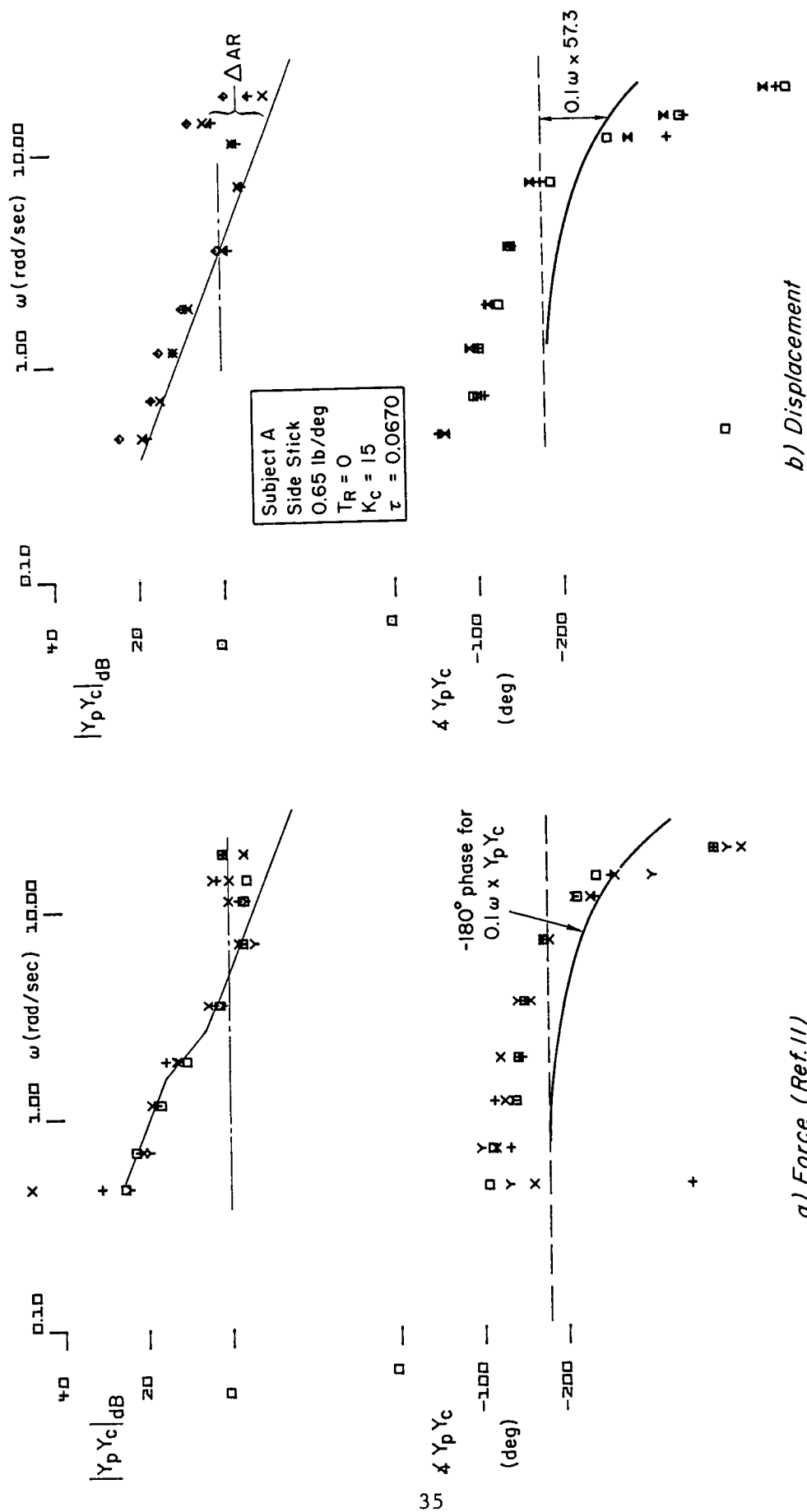
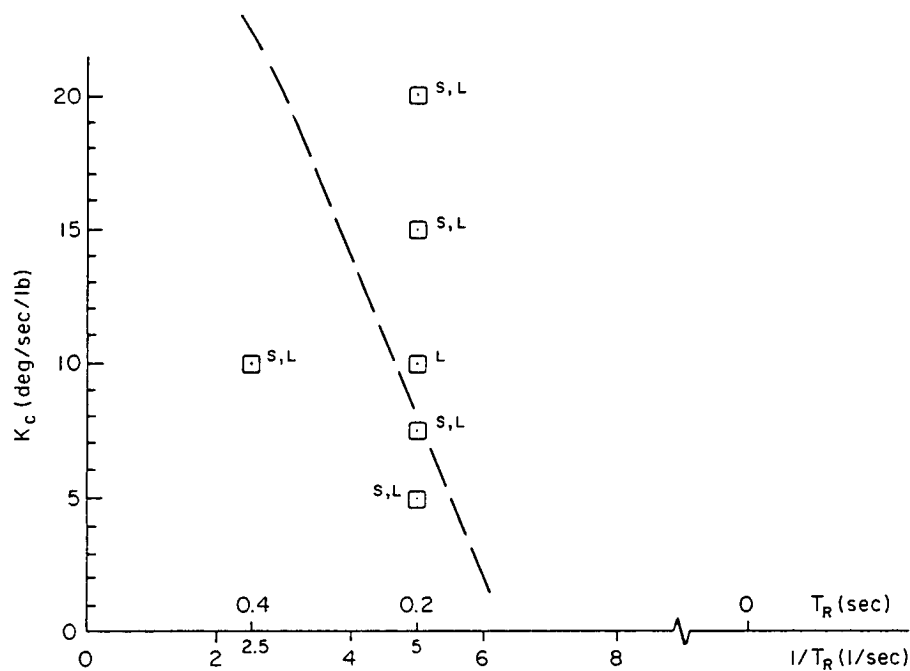
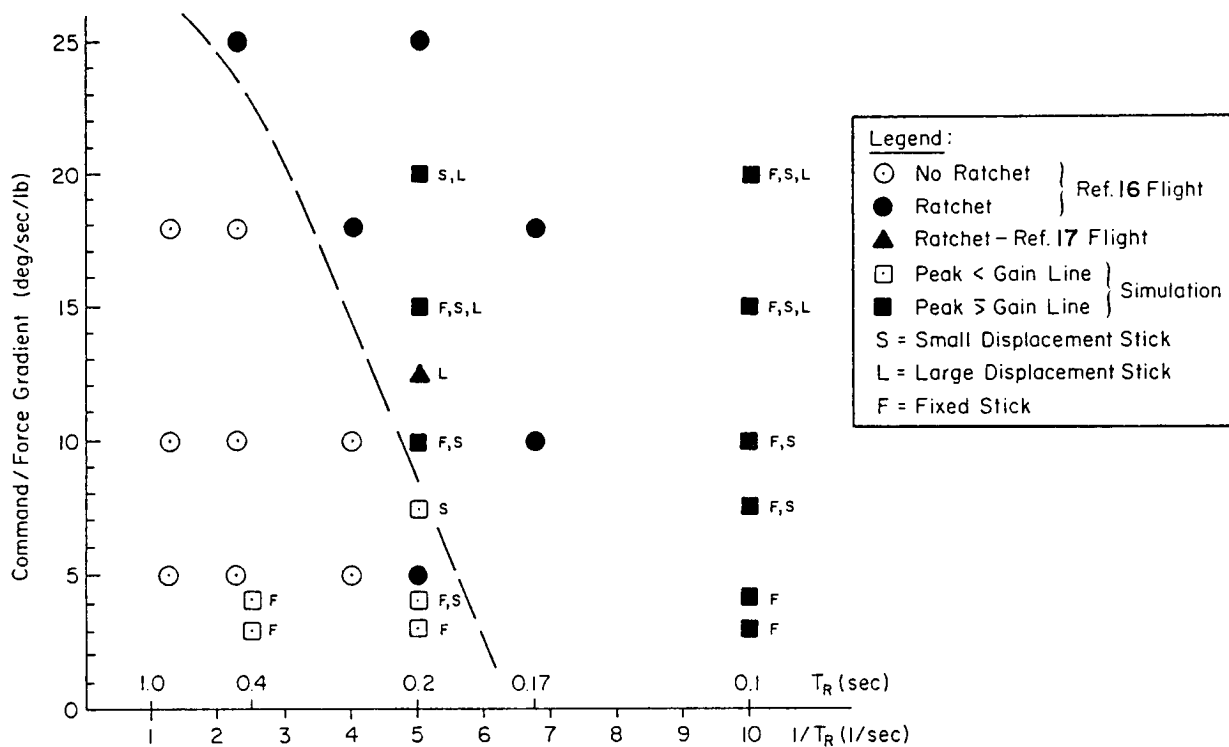


Figure 18. Typical Describing Function Plots for Displacement vs Force Sensing



a) Displacement



b) Force (Ref. 11)

Figure 19. Roll Ratchet Tendency With Variation of Roll Lag and Command Gain; Displacement vs Force Sensing

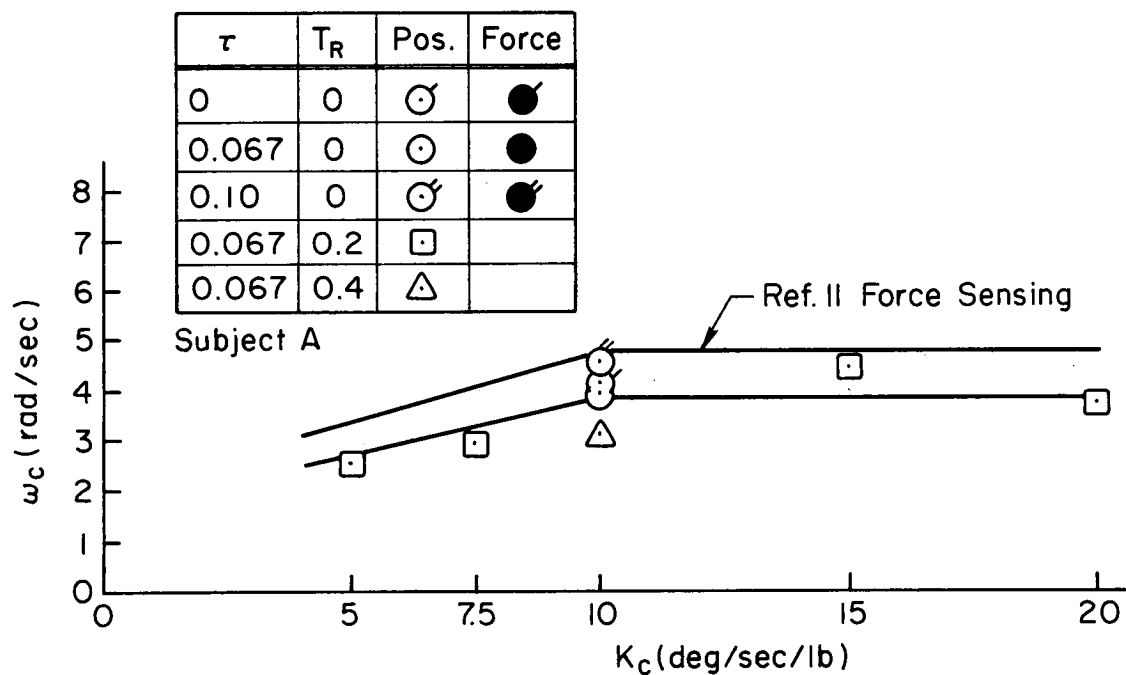
## B. INFLUENCE ON CLOSED-LOOP TRACKING PERFORMANCE

Tracking performance metrics obtained directly from the describing function measures are rms roll error ( $\sigma_e$ ) and crossover frequency ( $\omega_c$ ). These are inversely related, in that, generally for systems which obey the crossover law, higher crossovers result in lower rms error. Another measure obtained by the analysis software is rms manipulator amplitude (stick displacement or force). This measure is inversely related to command gain ( $K_c$ ). Combined, the rms error and manipulator effort constitute a measure of tracking workload. A final measure is pilot rating (CHPR), which is the pilot's opinion of the overall system (pilot and controlled element) closed-loop performance and task workload.

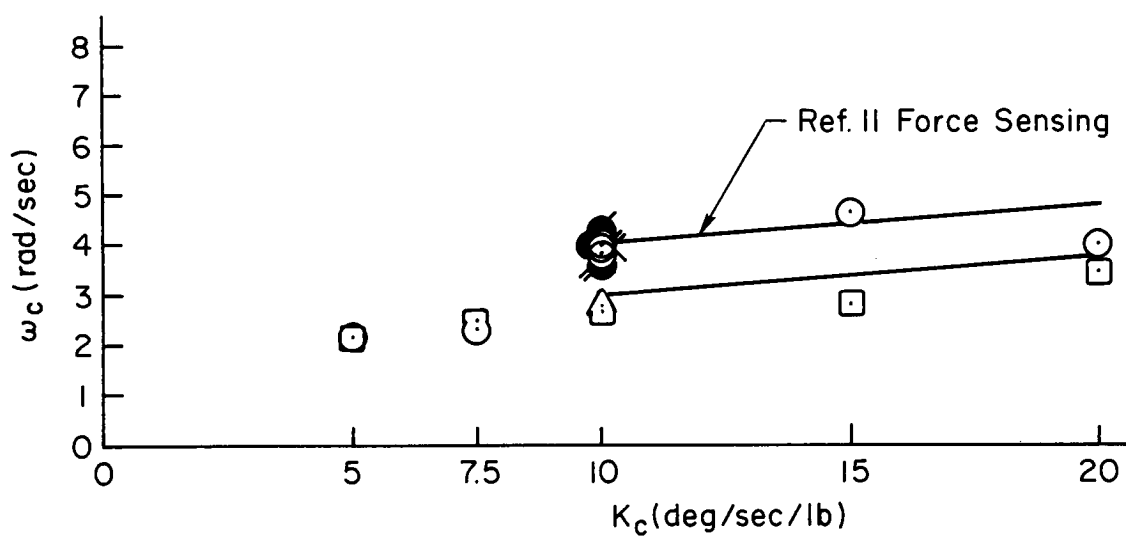
As noted previously, there were 3 runs per configuration, with the configurations being presented to the subjects in a random order. The subjects were highly trained in the tracking task, having accomplished several hundred runs each. However, the first run for each configuration often resulted in the subject adapting to the new effective controlled element dynamics by varying his control technique (gain, lead, lag) during the course of the run. This is evidenced by scatter in the first run data points. The second and third run data would then be quite consistent. Thus, only data from the last two runs for each configuration are included in the results reported herein.

### 1. Bandwidth

The performance measure for bandwidth is crossover frequency ( $\omega_c$ ). It was found in the Ref. 11 stick force sensing simulation that tracking bandwidth remained relatively constant for command gains above 10 deg/sec/lb., but decreased linearly for gains below 10 deg/sec/lb. A similar trend was observed with stick displacement sensing. Fig. 20 presents a plot of crossover frequency versus command gain obtained for the 1.22 and 0.65 lb/deg feel gradient sticks over all values of  $\tau$  and  $T_R$ . Boundaries for data from the Ref. 11 experiments are also shown. The data from Ref. 11 (force sensing) and the new displacement sensing results show so little difference that all the data points at each



a) 1.22 lb/deg Stick



b) 0.65 lb/deg Stick

Figure 20. Roll Tracking Crossover vs Command Gain  
With Displacement Sensing

command gain have been averaged in Fig. 21. This represents a summation of all values of  $\tau$  and roll subsidence, the 1.22 and 0.65 lb/deg feel gradients, and force and displacement command sensing. The data means are represented by the open symbol and the  $1\sigma$  range by the lines. The data show quite remarkable consistency. It may be noted at the lowest values of  $K_c$  that the mean crossover frequency is slightly higher for force sensing than for displacement sensing. This does not hold true for higher command gains. However, it was found that the values for the 1.22 lb/deg feel gradient generally lie within the  $+1\sigma$  bound from the overall mean and the values for the 0.65 lb/deg feel gradient (displacement and force) lie within the  $-1\sigma$  region. Thus, the stiffer feel gradient results in a slight increase in closed-loop bandwidth, but there is no significant difference between displacement and force command sensing.

#### GENERALLY:

Mean value for  $K_{FS} = 1.22$  lies within  $+1\sigma$  value

Mean value for  $K_{FS} = 0.65$  lies within  $-1\sigma$  value

#### SUMMATION OF:

$K_{FS} = 1.22$  and  $0.65$  lb/deg

All values of  $\tau$  and  $T$

Force and Displacement sensing

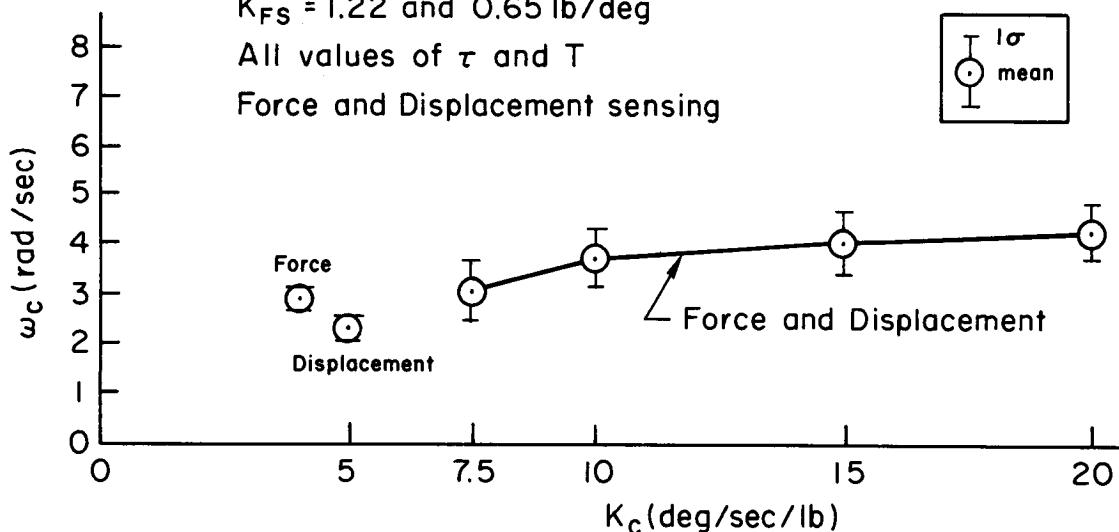


Figure 21. Roll Tracking Crossover vs Command Gain  
With Force and Displacement Sensing

It has been established in this and the previous experiment that the crossover "droop" at low command gain is due principally to a physical inability on the part of the pilot to overcome the high stick forces and move the manipulator far enough to generate the required correction signal in a timely manner. There is also evidence from pilot commentary that at the high end of the gain scale the problem of PIO begins to arise and any further increase in command gain may result in a decrease in crossover. On this basis, it would appear that command gains between 10 and 20 deg/sec/lb may be optimum (subject, of course, to flight verification).

## **2. Tracking Error And Pilot Effort**

A measure of pilot effort in achieving either desired or best obtainable performance was selected to be the product of rms tracking error ( $\sigma_e$ ) and rms manipulator displacement ( $\sigma_c$ ) or force when using force sensing. This product of performance and effort might be considered a measure of workload. It will be shown later that this parameter correlates well with Cooper-Harper pilot ratings (CHPR) obtained. Figure 22 presents a plot of the workload parameter ( $\sigma_e \times \sigma_c$ ) versus the reciprocal of the product of crossover ( $\omega_c$ ) and command gain ( $K_c$ ). As should be expected from the crossover model (Ref. 4), this indicates good correlation between the parameters. Decreasing crossover and/or command gain results in increasing workload -- or vice-versa. However, the data also tend to indicate a relative insensitivity of workload, over the range of  $1/(\text{gain} \times \text{crossover})$  between about 0.75 and 2 lb/(rad/sec)<sup>2</sup>. The data points within this region generally reflect a command gain of 20 deg/sec/lb and this may suggest that this gain is sufficiently high that tracking effort becomes minimal and other factors such as higher frequency time delays begin to dominate.



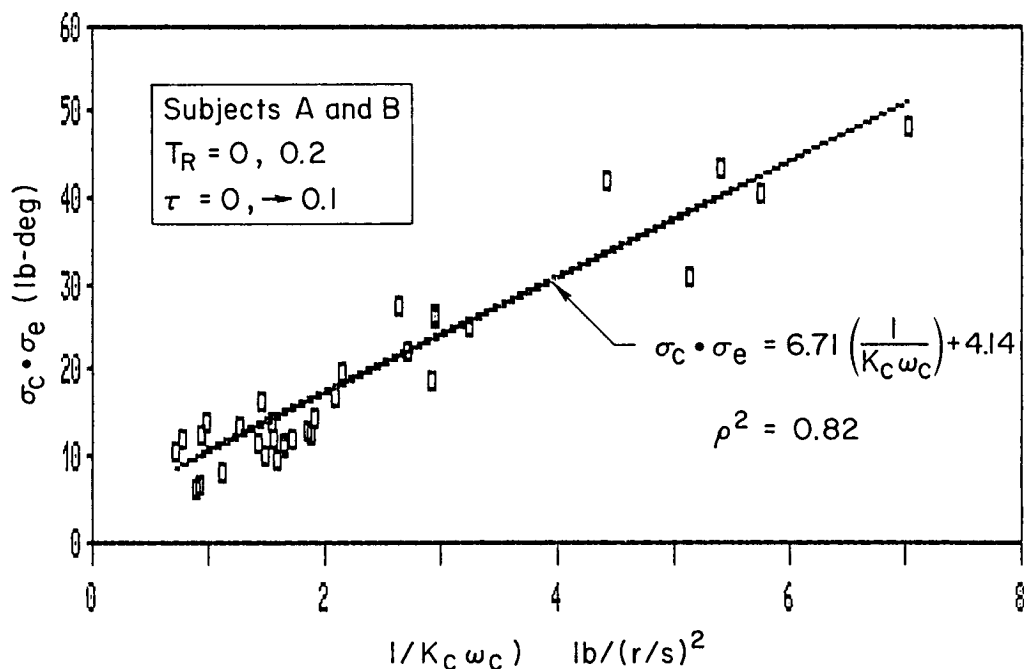


Figure 22. Relationship Between Tracking Performance and Loop Closure Parameters

## C. INFLUENCE ON PILOT RATING

### 1. Command Gain And Feel Gradient Variation

Previous plots indicated the influence of command gain ( $K_c$ ) on tracking bandwidth and workload. It is of interest to determine if and how this may correlate with the Cooper-Harper pilot ratings obtained. Figure 23 presents a crossplot of CHPR and command gain for the two best roll subsidence and the three feel system configurations. These data represent only one pilot subject because only the one was given the entire matrix of configurations. However, it will be shown subsequently that ratings were quite consistent between the two subjects.

The trend with CHPR reflects that of crossover (Fig. 20) in that there is a general degradation with decreasing command gain. Command gains less than 10 deg/sec/lb were unacceptable for anything other than a K/s equivalent aircraft.  $K_c = 10$  deg/sec/lb was marginal depending upon feel system gradient and roll subsidence time constant. There was

$$Y_c = \frac{K_c e^{-0.067s}}{s(T_R s + 1)}$$

Sidestick - Displacement Sensing  
Subject-A

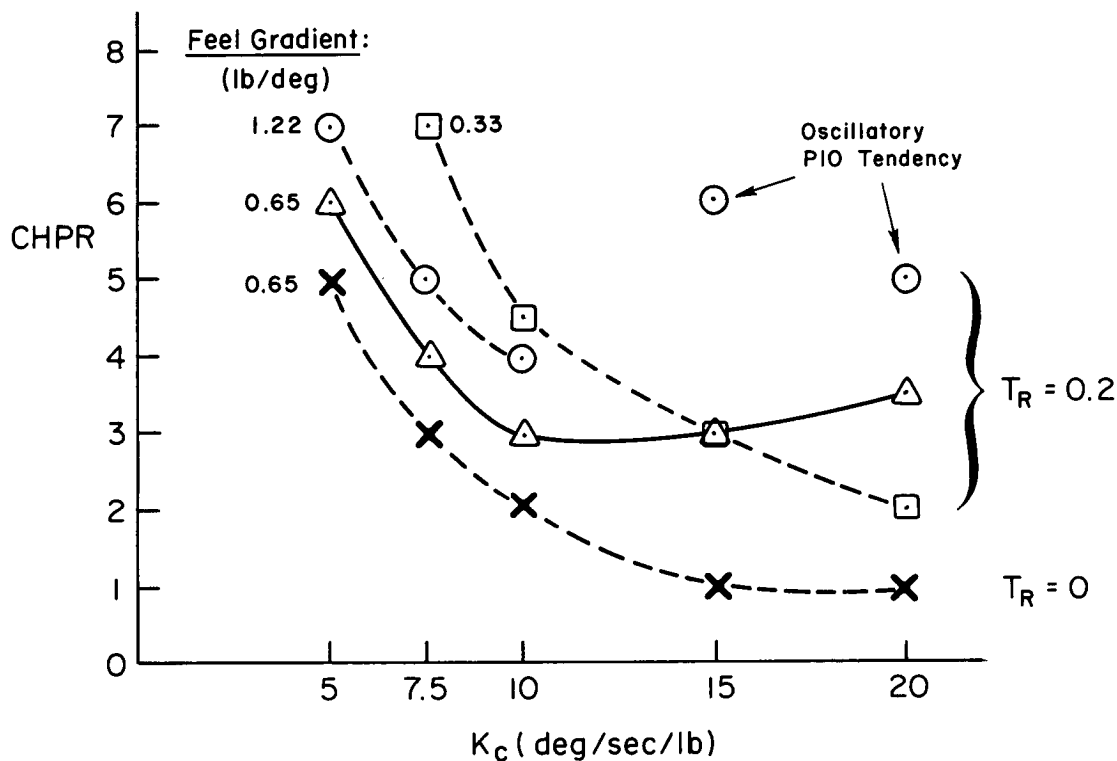


Figure 23. Variation of CHPR With Position Sensing Command Gain and Feel Gradient

a general complaint about the stiffest feel gradient (1.22 lb/deg) that forces were too high and tiring, especially at gains below 10 deg/sec/lb and at the higher gains there was some tendency to low frequency PIO which degraded ratings significantly. The lowest feel gradient (0.33 lb/deg) seemed to induce larger stick deflections and required a high command gain to avoid hitting the stick travel limits in the larger maneuvers. It therefore, gave the impression of inadequate control authority, and was downgraded accordingly. Also, this configuration would not be expected to be acceptable in flight, because it would be too difficult to avoid inadvertent stick inputs in turbulence. The best compromise feel gradient was found to be 0.65 lb/deg.

There was a significant improvement in CHPR in going from a  $T_R$  of 0.2 to zero (K/s) with the 0.65 lb/deg stick gradient and higher command gains. This may reflect a requirement for pilot generated lead and/or a tendency to oscillation at the higher  $T_R$ .

## 2. Comparison With NT-33 Flight Data

It should be recalled at this point that the response command gradient gain ( $K_C$ ) generally is not a fixed parameter in a flight control system, but is changed as a function of stick force or displacement input. A low response gain is provided around stick neutral to avoid inadvertent command inputs and/or over control in situations requiring small precise command inputs. For larger stick inputs as required for gross maneuvering, the response command gradient is increased to obtain faster motion response with lower stick force or displacement. In most instances two or more discrete gradient are employed to cover the range of flight tasks from air refueling or air-to-air tracking to gross maneuvers as in air combat. The Ref. 16 flight test in the NT-33 investigated several response command gradients (Fig. 24) in air-to-air tracking and gross maneuvering tasks.

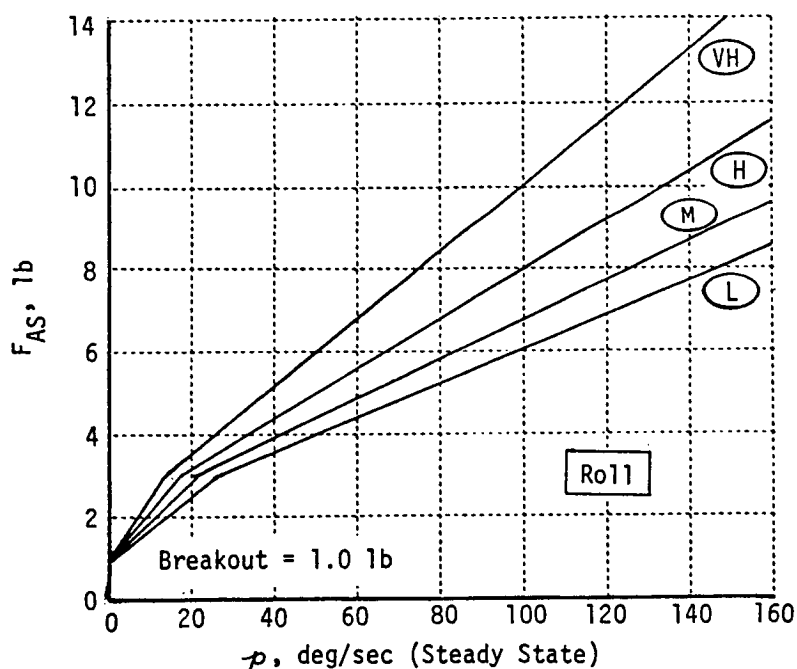


Figure 24. Control Force-Response Gains, Up-and-Away Flight (Ref. 16)

In general the first gradient was dominant in the tracking task and the second gradient was dominant in the gross maneuvers. One objective of the test was to select the best gradients. The flight test also investigated three different feel system configurations: fixed stick, "small" deflection (1.3 lb/deg measured at the center of the stick grip), and "large" deflection (0.7 lb/deg).

Figure 25 presents a plot of CHPR vs.  $K_c$  made up from data for the 1.3 lb/deg stick in Ref. 16. Across the bottom of the figure is a superimposed guide to the NT-33 first and second command gradients and associated evaluation tasks. The average pilot rating is identified (X) along with the range obtained. Also shown in the figure are the ratings obtained with the 1.22 lb/deg feel configuration (O) in this simulation. For the region corresponding to the NT-33 1st gradient (tracking) there is excellent agreement between the two. For command gains appropriate for the 2nd gradient, the CHPR for our tracking task was downgraded because of a tendency to PIO. The existence of this PIO tendency in the tracking task is probably related to the relatively high bandwidth, closed-loop nature of the task when compared with a relatively open-loop gross maneuvering task. The "target" which was being tracked did produce some gross maneuvers (60 deg right to 60 deg left and vice versa) but the subjects were not required to rate these separately.

Figure 26 presents similar data for the NT-33 0.7 lb/deg ( $\square$ ) and our 0.65 lb/deg feel configurations ( $\triangle$ ). Here the correlation in the 1st gradient range (only two data points) is not good because in-flight tracking produced PIO tendencies (Level II) whereas in the simulation at similar command gains the task was rated Level I. For the gross maneuvering range the correlation is much better (Level I for both). This implies that our subject pilot was able to track the gross and small maneuvers well with no tendency to PIO.

The data points for the NT-33 1.3 lb/deg ( $\times$ ) are also shown in Fig. 26 and interestingly match our simulation results for the 0.65 lb/deg feel system quite well over the command gain range from 10 to 20 deg/sec/lb. However, the match below 10 deg/sec/lb is not as good as in Fig. 25.

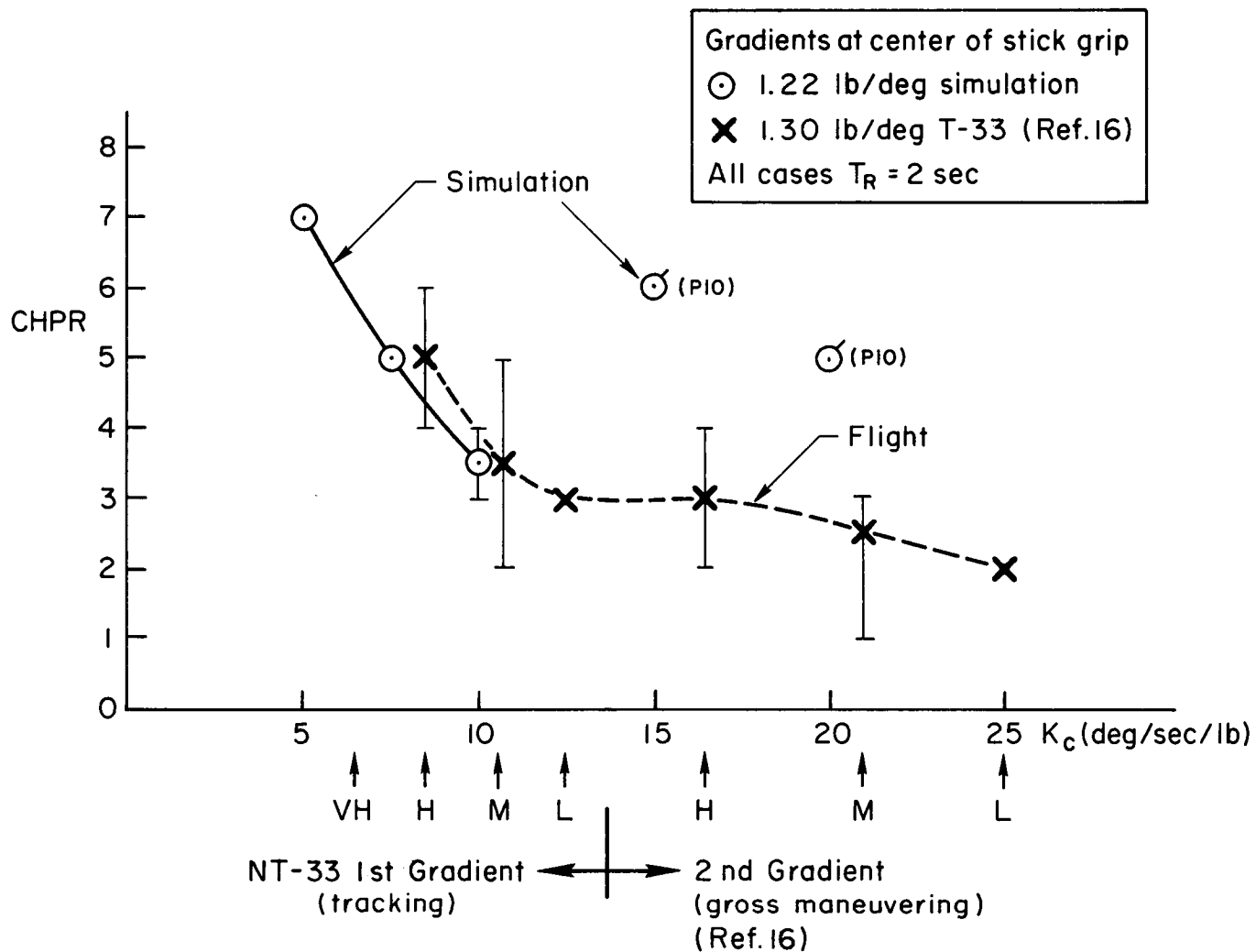


Figure 25. Comparison of CHPR vs Command Gain for Flight and Lab With Feel Gradient 1.2 - 1.3 lb/deg

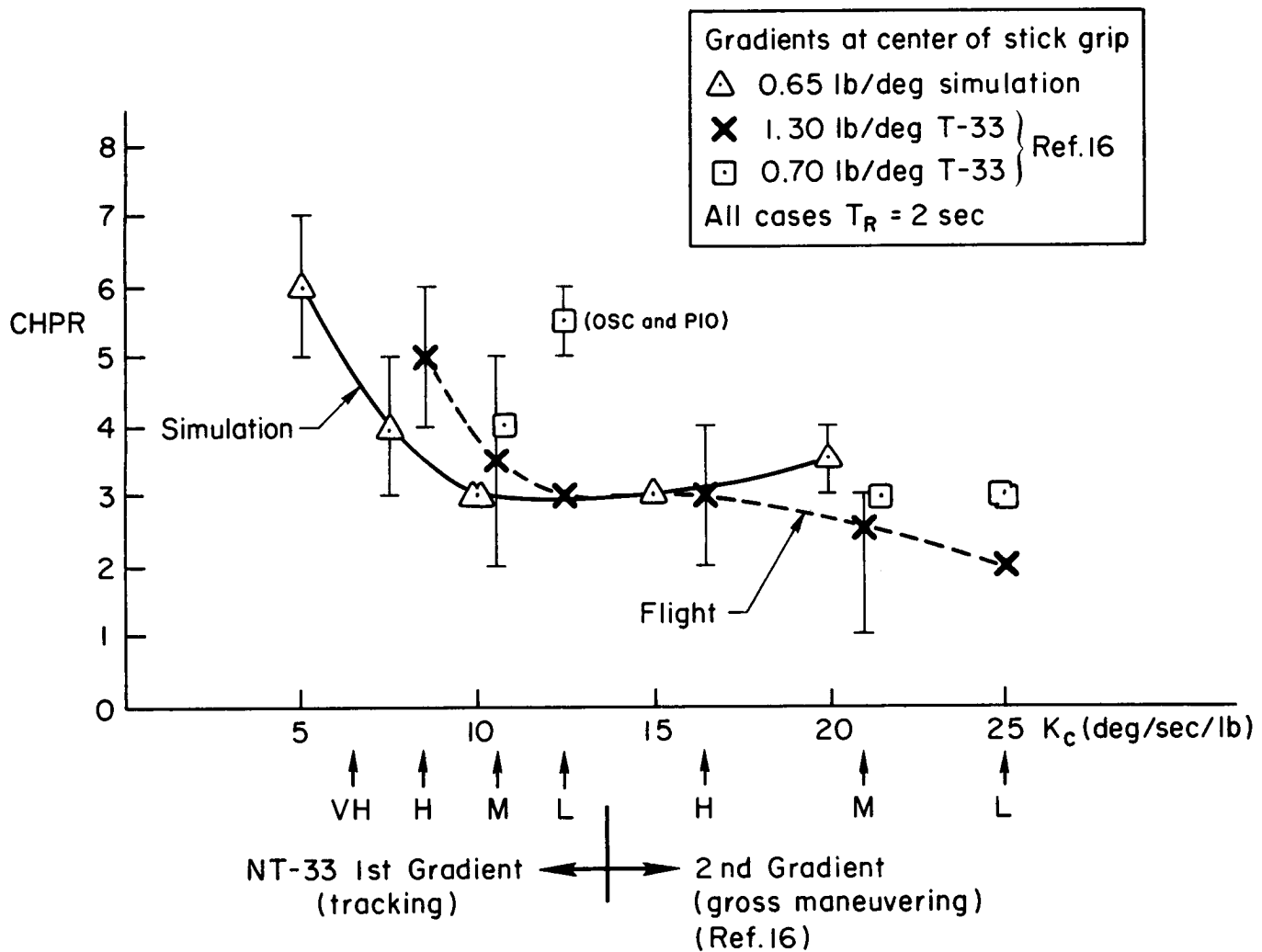


Figure 26. Comparison of CHPR vs Command Gain for Flight and Lab with Feel Gradient 0.65 - 0.7 lb/deg

There are several potential design lessons in these results:

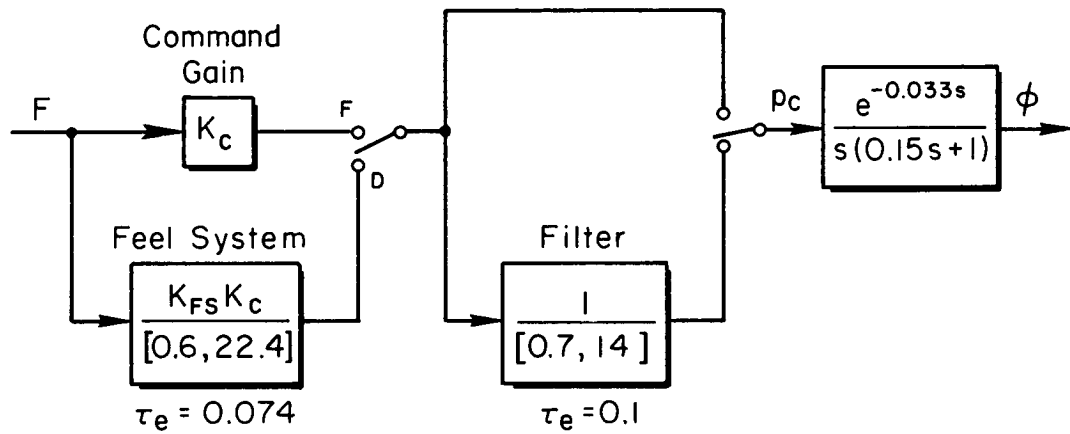
- The fixed base simulation indicated the 0.65 lb/deg feel to be the best overall force/displacement gradient but flight results show the stiffer 1.3 lb/deg feel to be the better. The difference may well be due to motion effects and minimization of inadvertent inputs in turbulence, etc., but may also have been related to the particular stick design or installation. On the other hand, a feel gradient somewhere between the two may offer a better compromise. Such factors should be checked in flight.
- Flying quality rating degrades very rapidly as response command initial gradient is decreased below 10 deg/sec/lb. For Level 1 rating the initial gradient should be above 10 deg/sec/lb.
- Flying quality rating does not change appreciably for 2nd gradient command gains appropriate for gross maneuvering although there is flight evidence from Figs. 25, 26 that  $K_c = 20$  deg/sec/lb or higher is to be preferred when the stick force gradient is high.

#### **D. ADDITION OF 2ND ORDER COMMAND FILTER LAG**

Using the "best" feel gradient (0.65 lb/deg) and command gains (10 and 20 deg/sec/lb), a set of 57 additional runs was made with a second order filter inserted in the command path. The basic purpose was to determine the effect on tracking performance and pilot rating of such a command filter tuned to the pilot's N.M. subsystem. For this set of runs the effective controlled element was as shown by the block diagram of Fig. 27. Both displacement and force stick sensing were employed. Thus, four configurations were involved; the force to roll response equivalent time delay of the four varies from 0.033 sec to 0.207 sec.

##### **1. Influence of Effective Time Delay On Pilot Rating**

Figure 28 presents a summary of pilot ratings versus effective time delay across the four configurations and two command gains (10 and 20 deg/sec/lb). Ratings by the two subject pilots are within one rating point of each other for each gain and all but one configuration ( $D_1$ ).



Configuration	Sensing	Filter	$\sum \tau$ (sec)	$\tau_e$ (sec)
A <sub>1</sub>	Force	OUT	0.033	0.033
B <sub>1</sub>	Disp.	OUT	0.074 + 0.033	0.107
C <sub>1</sub>	Force	IN	0.1 + 0.033	0.133
D <sub>1</sub>	Disp.	IN	0.074 + 0.1 + 0.033	0.207

Figure 27. Effective Controlled Element Dynamics for 2nd Order Command Filter Experiment With Sidestick



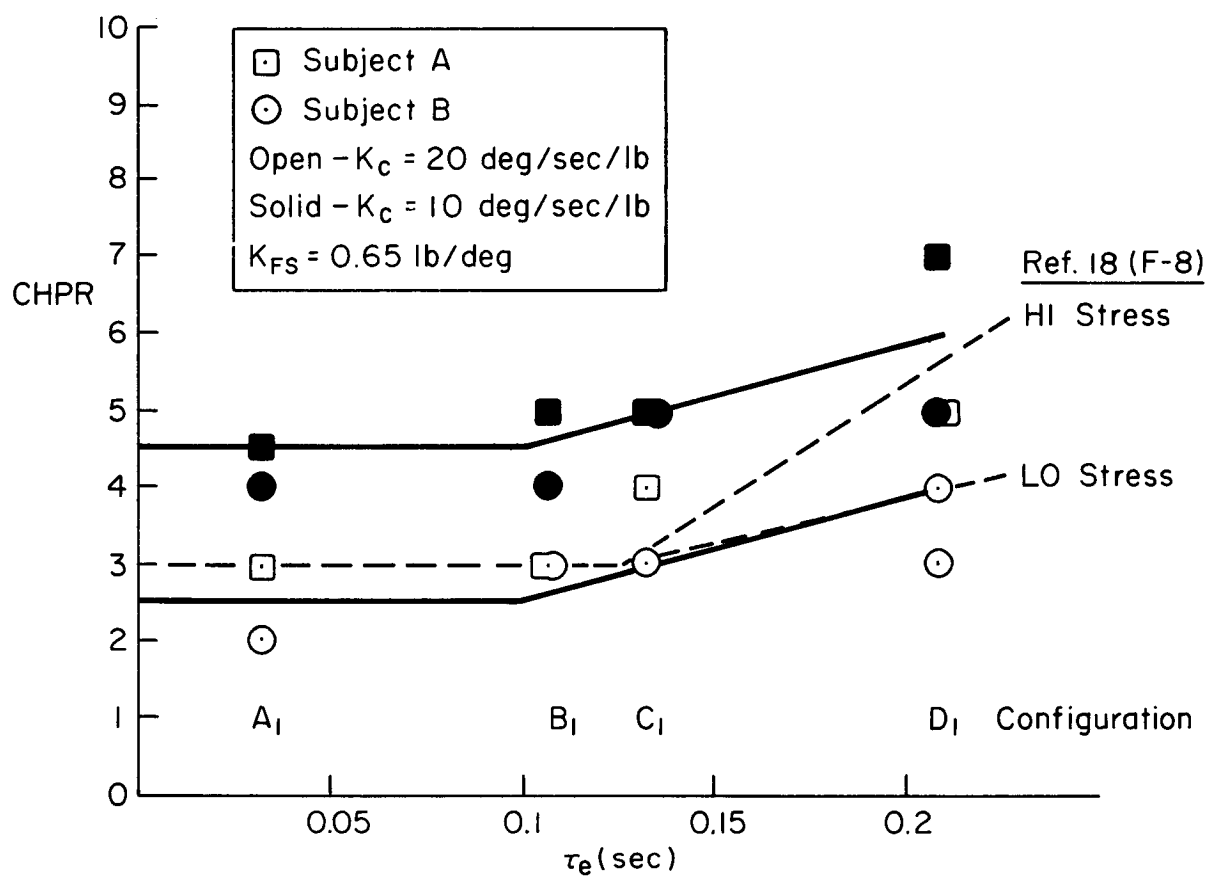


Figure 28. Influence of Effective Time Delay and Command Gain on CHPR (0.65 lb/deg Sidestick)

The ratings show a general degradation with increasing effective time delay similar to that reported in Ref. 18 for a low stress task. However, it will be noted that the 20 deg/sec/lb gain fared better than the 10 deg/sec/lb gain by about 1.5 to 2 rating points across all configurations. This trend is opposite that shown in Fig. 23 but is supported by the flight data of Fig. 26. Thus, it is suspected that the  $K_c = 20$  (0.65 lb/deg and  $T_R = 0.2$ ) data run in Fig. 23 may have been adversely influenced by some unknown factor.

As a further check on the CHPR differential for the two command gains, a plot of effective workload ( $\sigma_e \times \sigma_c$ ) versus effective  $\tau$  is shown in Fig. 29 for the four configurations. This also shows a distinct separation for the two gains. This might be expected since a doubling in gain should reduce the rms stick input by roughly a factor of two and this is the case here. If the workload parameter is normalized with command gain as shown in Fig. 30 the resulting error measure is shown to be independent of command gain. Thus, the CHPR rating differential between the command gains can be related to amplitude of stick activity (effort) required. (It also becomes apparent that the pilots were employing different error criteria in performing their tracking task. Subject A consistently tracked tighter than Subject B).

The influence of the effective time delay now becomes more clear in Fig. 30. Displacement sensing added a small increment in tracking error to that obtained with force sensing, and the 2nd order filter added a significant increase. If we now eliminate the effect of command gain on CHPR in Fig. 28 and concentrate on change in CHPR with increasing  $\tau$  (referenced to the initial ratings for each subject in each case) we obtain the plot of Fig. 31. The end result is that addition of the second order filter at the pilot's N.M. mode frequency to the force sensing stick produced essentially the same decrement in rating as did changing to displacement sensing but without the filter (increase in  $\tau_e$  is almost the same in both cases). Adding the filter to the displacement sensed input degraded the rating by about 1 to 1.5 rating points. Obviously, since the use of displacement sensing alone essentially eliminates any tendency to roll ratchet (Fig. 19), there is little need for this added lag.

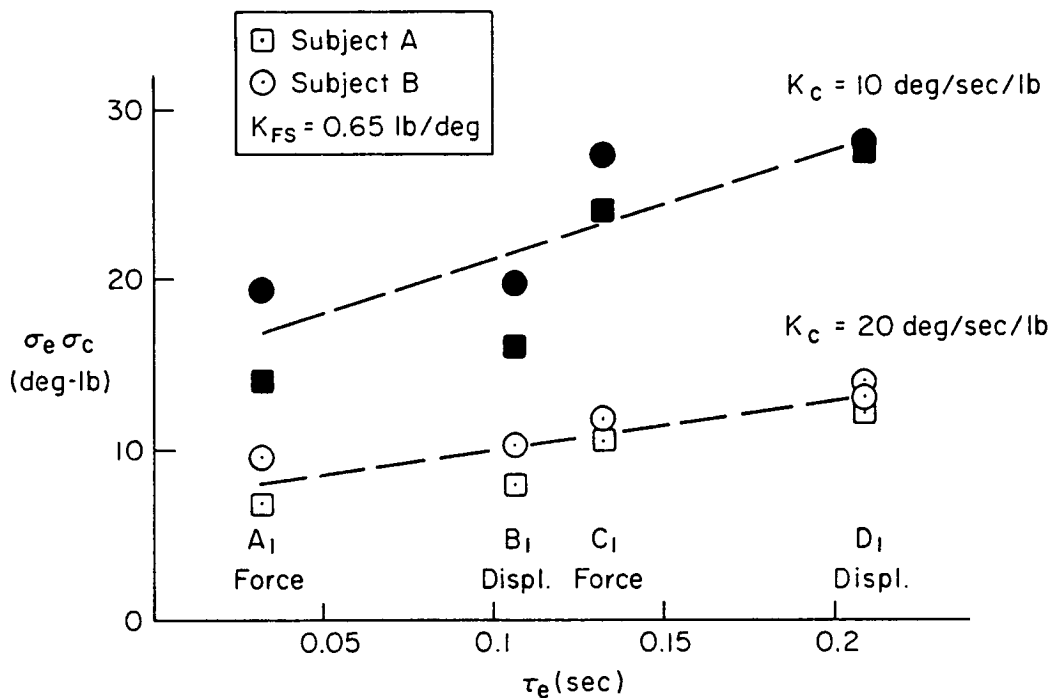


Figure 29. Influence of Effective Time Delay and Command Gain on Roll Tracking Performance (0.65 lb/deg Sidestick)

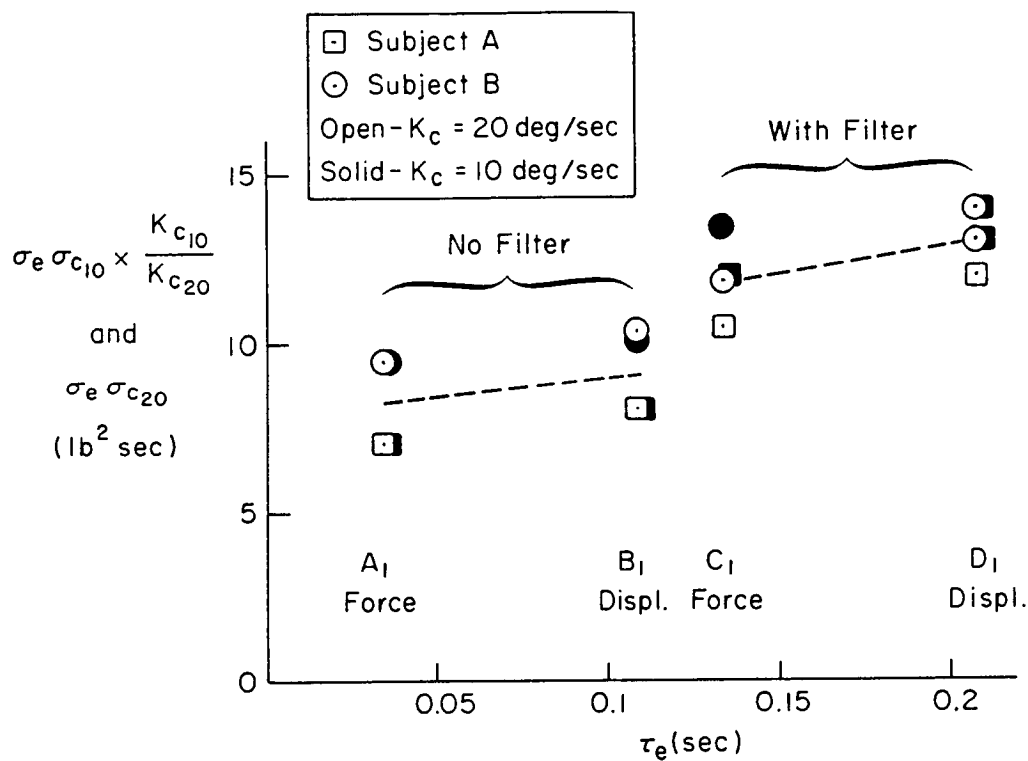


Figure 30. Command Gain Normalized Tracking Performance Measures Variation With Effective Time Delay (0.65 lb/deg Sidestick)

## 2. Comparison With MIL-Spec Time Delay Criteria

There is some controversy over whether the allowable time delay criterion of MIL-F-8785C should be referenced from the force input to the manipulator or the resulting manipulator deflection (Ref. 9). Figure 32 presents the average values of rating degradation from Fig. 31 for each configuration but with an initial CHPR rating selected to be the average of the two ratings given for  $\tau = 0.033$  and  $K_c = 20$  in Fig. 28. This configuration was chosen as it is the baseline airframe which received Level I ratings i.e.,  $K_c$  was optimal and not a factor in the ratings. The data presented in Fig. 32a, where the feel system lag is included in the calculation of the effective time delay, seems to support an increase in the allowable Levels I and II time delays from the present MIL-F-8785C limits. In Fig. 32b the feel system lag has been excluded from the effective controlled element time delay. In this case the data points lie within the appropriate boundaries.

This limited set of data supports the contention that the allowable time delay criterion should not require inclusion of the feel system dynamics. If the feel system dynamics are included, it supports an increase in the allowable Levels I and II time delays from their present (MIL-F-8785C) limits. It is also worth noting that this data was obtained with, and is therefore valid for, a sidestick manipulator.

## E. SUMMARY

The goals of this experiment were to determine whether stick displacement sensing decreases the tendency to neuromuscular (NM) system related roll ratchet and to assess the influence of displacement sensing and related feel system and command filter dynamics on tracking performance and pilot acceptance. It has been shown that stick displacement sensing decreases the tendency to NM mode induced roll ratchet due to the additional forward loop phase lag introduced by the feel system dynamics. This additional lag, in effect, serves the same smoothing purpose as the command prefilter lag required with stick force sensing configurations.

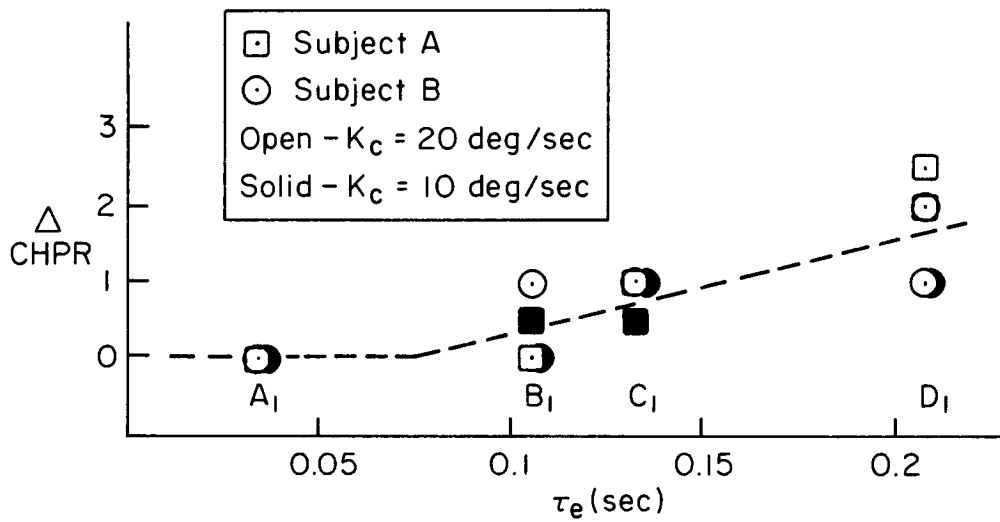


Figure 31. Command Gain Normalized CHPR Variation With Effective Time Delay (0.65 lb/deg Sidestick)

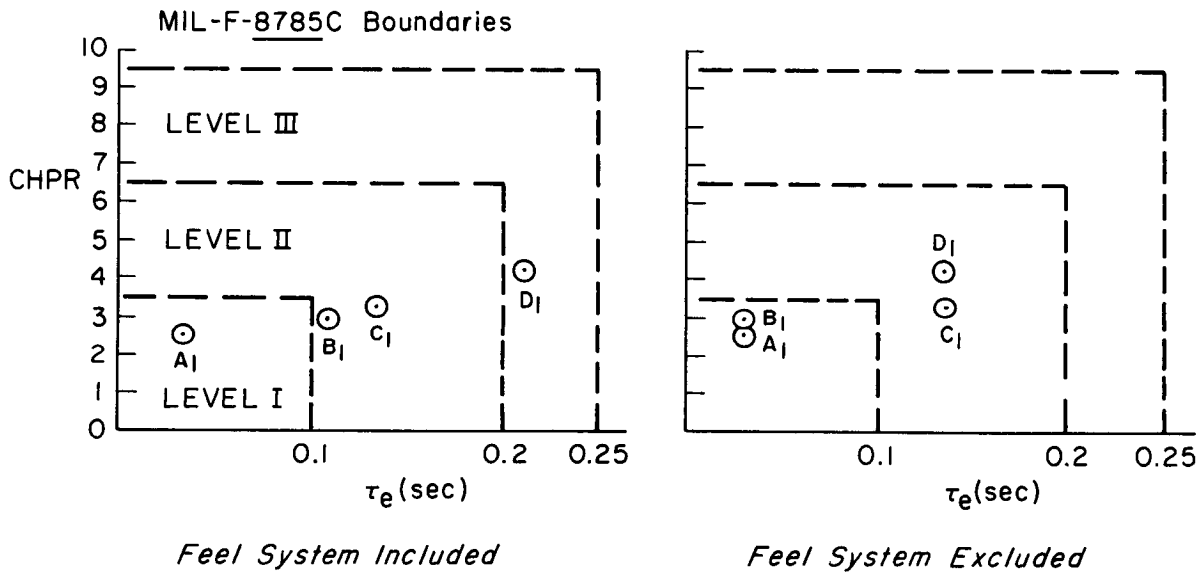


Figure 32. Comparison of CHPR With MIL-F-8785C Effective Time Delay Criteria (0.65 lb/deg Sidestick)

It was found that displacement sensing does not result in appreciable change in the NM mode frequency (about 14 rad/sec) and amplitude peaking from that noted previously with force sensing. As with force sensing, the peak amplitudes tended to increase with stiffer feel gradients (0.65 to 1.22 lb/deg) and increasing effective time delay (up to 0.1 sec). However, this is not as significant with displacement sensing compared to force sensing because of the concomitant phase lag contribution of the feel system in the frequency region near the NM mode.

As with force sensing, tracking bandwidth increased as controlled element command gain ( $K_c$ ) increased. The sensitivity to command gain is quite high for  $K_c$  less than 10 deg/sec/lb, with bandwidth, tracking performance, and pilot acceptance all degrading rapidly as command gain is decreased. Performance and pilot acceptance improved slightly with increasing command gain in the range  $K_c = 10$  to 20 deg/sec/lb.

Tracking bandwidth, performance, and pilot acceptance were influenced somewhat by feel system force/displacement gradient. A gradient of 0.65 lb/deg appeared best for this fixed base tracking task. The 0.33 lb/deg gradient was too weak and allowed excessive stick deflection when trying to follow large changes in target motion. The 1.22 lb/deg gradient was considered too stiff and tiring. However, under flight motion conditions, a gradient between 0.65 and 1.22 lb/deg might be more appropriate.

It was found that use of displacement sensing without command prefiltering was rated about the same as force sensing with a second order command prefilter tuned to attenuate the NM mode. Addition of the second order prefilter to displacement sensing produced excessive high frequency lag and degraded handling quality ratings by 1 to 1.5 rating points. Again, there is little or no need for such filtering with stick displacement sensing.

Concerning the -8785C flying qualities specification for allowable effective time delay, data from this limited experiment with a side-stick manipulator supports the Ref. 9 contention that the feel system dynamics should not be included in calculation of the effective forward loop time delay or, if the feel system is included, the -8785C criteria boundaries should be relaxed.

## **SECTION V**

### **CENTER STICK WITH DISPLACEMENT VS FORCE SENSING**

A NASA DFRF flight test program is planned to be accomplished in the USAF NT-33 aircraft to help resolve several issues concerning the influence of force vs. displacement stick sensing, feel system dynamic lags, and command prefiltering on the roll control characteristics of highly augmented aircraft. Among the issues is whether the calculated time delay for the effective aircraft dynamics as viewed by the pilot should be referenced to force applied to the manipulator (and hence the feel lag included) as called for in MIL-F-8785C, or whether the feel system dynamics are transparent to the pilot (and hence not to be included in the calculated time delay). Other issues pertain to the influence of roll mode time constant and stick command gain (or sensitivity) on roll ratchet. Since this simulation preceeds the flight test, one set of objectives was to:

- duplicate a few typical configurations to be tested in flight
- preview possible flight results
- obtain describing function and other closed-loop task performance measures which might provide insight to results
- suggest possible improvements to the flight experiments.

This section will be devoted to a description of the configurations investigated, the influence of force versus displacement sensing on closed-loop tracking performance and pilot rating, the influence of interchanging the feel and command filter lag contributions, and finally an assessment of results based on overall effective time delay.

#### **A. CONFIGURATIONS INVESTIGATED**

A block diagram showing the simulation of the feel system, the force vs. displacement option, the command gain and filter option, the NT-33

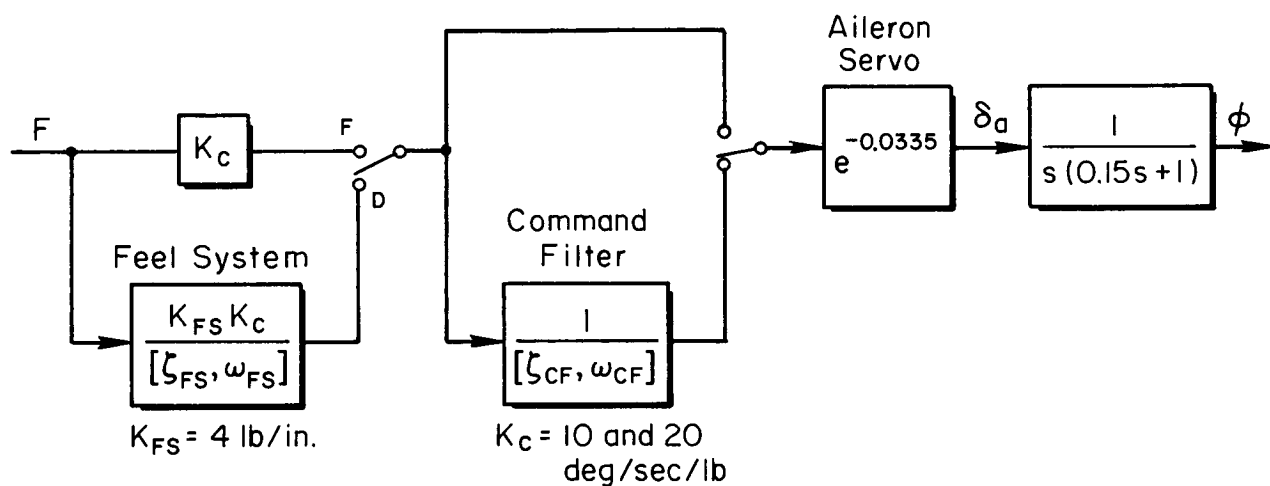
aileron servo effective time delay and simplified augmented roll dynamics (roll subsidence of 0.15 sec.) is presented in Fig. 33. The matrix of configurations investigated is shown in the accompanying table. The configurations are coded in the left column with the subscript 2 to indicate use of the fighter type center-stick. The type of stick sensing is indicated in the second column. Two sets of feel characteristics were employed: one with the regular NT-33 system second order dynamics (26 rad/sec frequency and 0.7 damping ratio) and the second with 14 rad/sec frequency and 0.7 damping (to approximate the X-29 aircraft lateral feel). The latter actually is 13 rad/sec but this could not be duplicated in the lab. In both of our cases the force/displacement gradient was 4 lb/in measured at the top of the stick.

The command filter second order lag and feel dynamics were interchanged in four cases ( $E_2 - H_2$ ) but with the total lag between force application to the stick and roll response held constant. However the effective time delay between force input and roll response varied with the sensed stick input as reflected by the effective time delay shown in the right hand column.

Roll acceleration time responses to step stick force inputs are presented in Fig. 34 for the 26 and 14 rad/sec feel system with no command filter lag (representing configurations  $C_2$  and  $F_2$  respectively) and for the combined feel and filter lags (representing configurations  $G_2$  and  $H_2$ ). These traces demonstrate the large differences in response characteristics produced by the various lags and the quite sluggish response which results when both the feel system and command filter lags are in the command path.

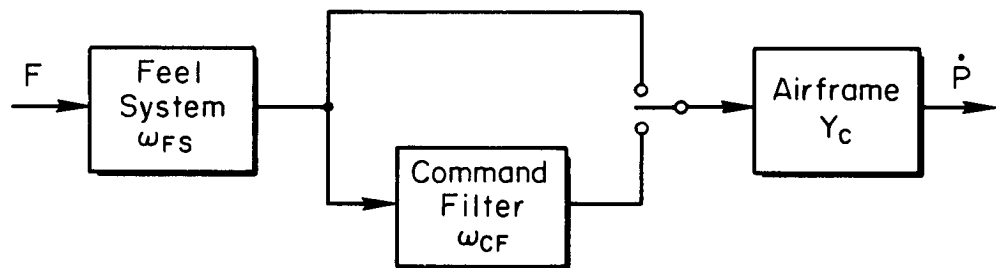
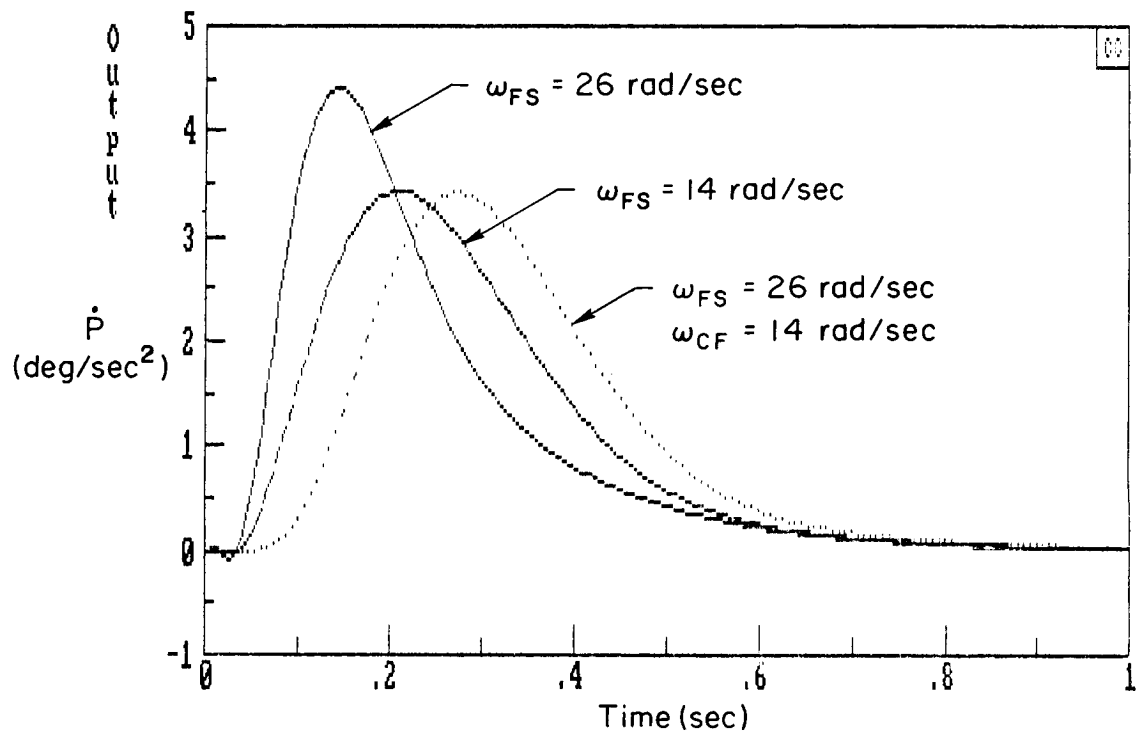
To provide additional comparison between force and displacement sensing and the influence of low and high frequency feel dynamics, the second order filter was switched out in four cases ( $A_2 - D_2$ ). Finally, two command gains were employed ( $K_c$  of 10 and 20 deg/sec/lb) for each of the 8 configurations. Accomplishment of this overall test matrix with the two test subjects required a total of 141 runs.





Configuration	Sensor	$\omega_{FS}$ (rad/sec)	$\omega_{CF}$ (rad/sec)	$\tau(F \rightarrow \delta_a)$ (sec)	$\tau_e$ (sec)
A <sub>2</sub>	F	26	—	0.033	0.033
B <sub>2</sub>	F	14	—	0.033	0.033
C <sub>2</sub>	D	26	—	0.033 + 0.055	0.088
D <sub>2</sub>	F	14	26	0.033 + 0.055	0.088
E <sub>2</sub>	F	26	14	0.033 + 0.102	0.135
F <sub>2</sub>	D	14	—	0.033 + 0.102	0.135
G <sub>2</sub>	D	26	14	0.033 + 0.055 + 0.102	0.190
H <sub>2</sub>	D	14	26	0.033 + 0.102 + 0.055	0.190

Figure 33. Effective Controlled Element Configurations  
Employed -- Roll Tracking With Center Stick



$$Y_c = \frac{K_c(0)^2 e^{-0.033s}}{(0)(6.67)}$$

Figure 34. Roll Acceleration Time Response to Step Stick Force

## B. FORCE VERSUS DISPLACEMENT SENSING

For this comparison, attention is focused on closed-loop crossover frequency ( $\omega_c$ ), tracking error ( $\sigma_e$ ), and pilot ratings as metrics to identify the possible differences in performance resulting from force and displacement stick usage in closed-loop roll tracking tasks.

### 1. Tracking Performance

Figure 35 presents a plot of average tracking bandwidth (crossover frequency,  $\omega_c$ ) achieved by each subject pilot for the eight configurations and two command gains. Each data point reflects an average taken over three runs. The configurations are paired to emphasize any difference due to the different stick input sensing methods. It is apparent from this plot that there is no consistent difference due to the type of sensing. The only clear trend shown is that Subject A consistently produced a higher crossover which in turn indicates tighter tracking.

This trend is further demonstrated by Fig. 36 which presents averages across all data points for each subject at each command gain. The symbols reflect the average and the bars reflect the maximum and minimum values, respectively. This plot also reveals that both subjects tended to achieve higher crossover with the higher command gain, however the difference is more pronounced for Subject A.

The influence of the two different types of stick input sensing on rms tracking error is shown in Fig. 37 where each data point represents an average of the rms error measures from three tracking runs. The difference obtained is quite striking. Tracking error is consistently greater with the displacement stick. The degradation varies from approximately 5 to 25 percent. The influence of command gain on tracking error is small but it is again apparent that subject A is consistently using a tighter tracking technique.

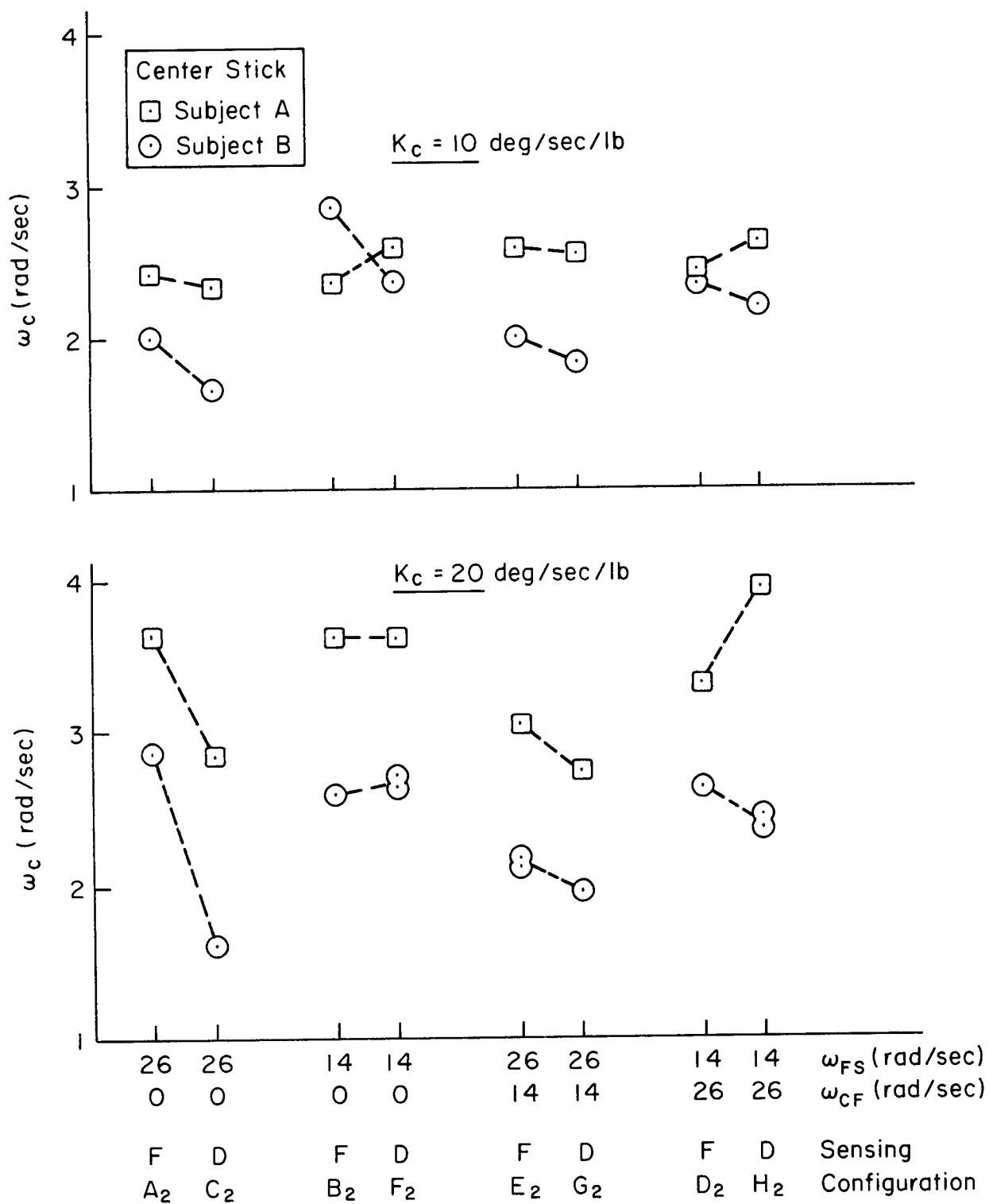


Figure 35. Influence of Feel and Filter Dynamics on Tracking Bandwidth With Center Stick Displacement and Force Sensing

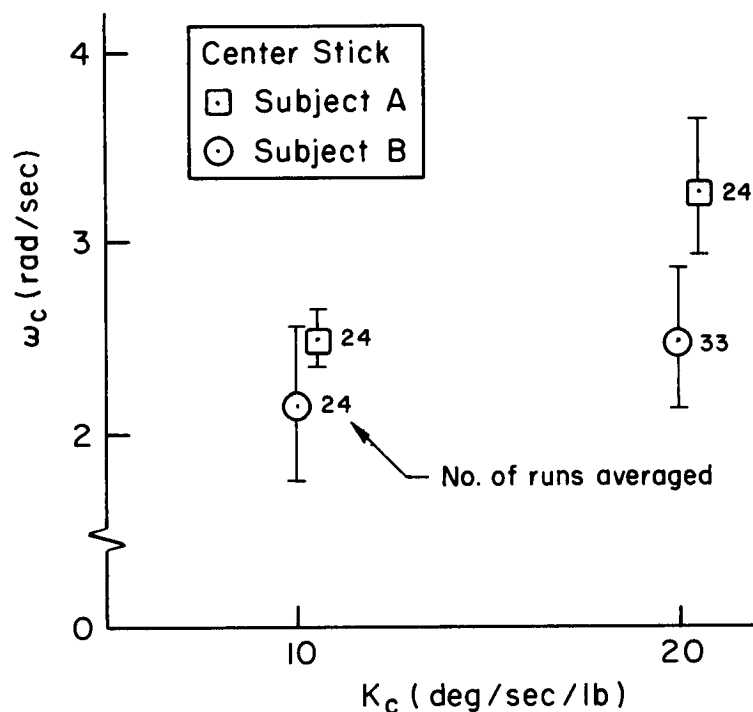


Figure 36. Influence of Command Gain on Tracking Bandwidth (Center Stick)

## 2. Pilot Rating

Pilot ratings elicited by the different configurations are summarized in Fig. 38. There are three specific points to be noted from this plot. First, the ratings given by the two subjects are very consistent, the average difference being two-thirds of a rating point. Second, the CHPR ratings tend to reflect tracking error performance and show a preference for force sensing. Third, with the 10 deg/sec/lb command gain almost all configurations lie in the Level II handling rating range. When the gain is increased to 20 deg/sec/lb all configurations with force sensing move into the Level I range.

In summary, the data show a decided preference on the part of both subjects for force sensing and the 20 deg/sec/lb command gain with this center stick. This preference would appear to be due to better tracking performance.

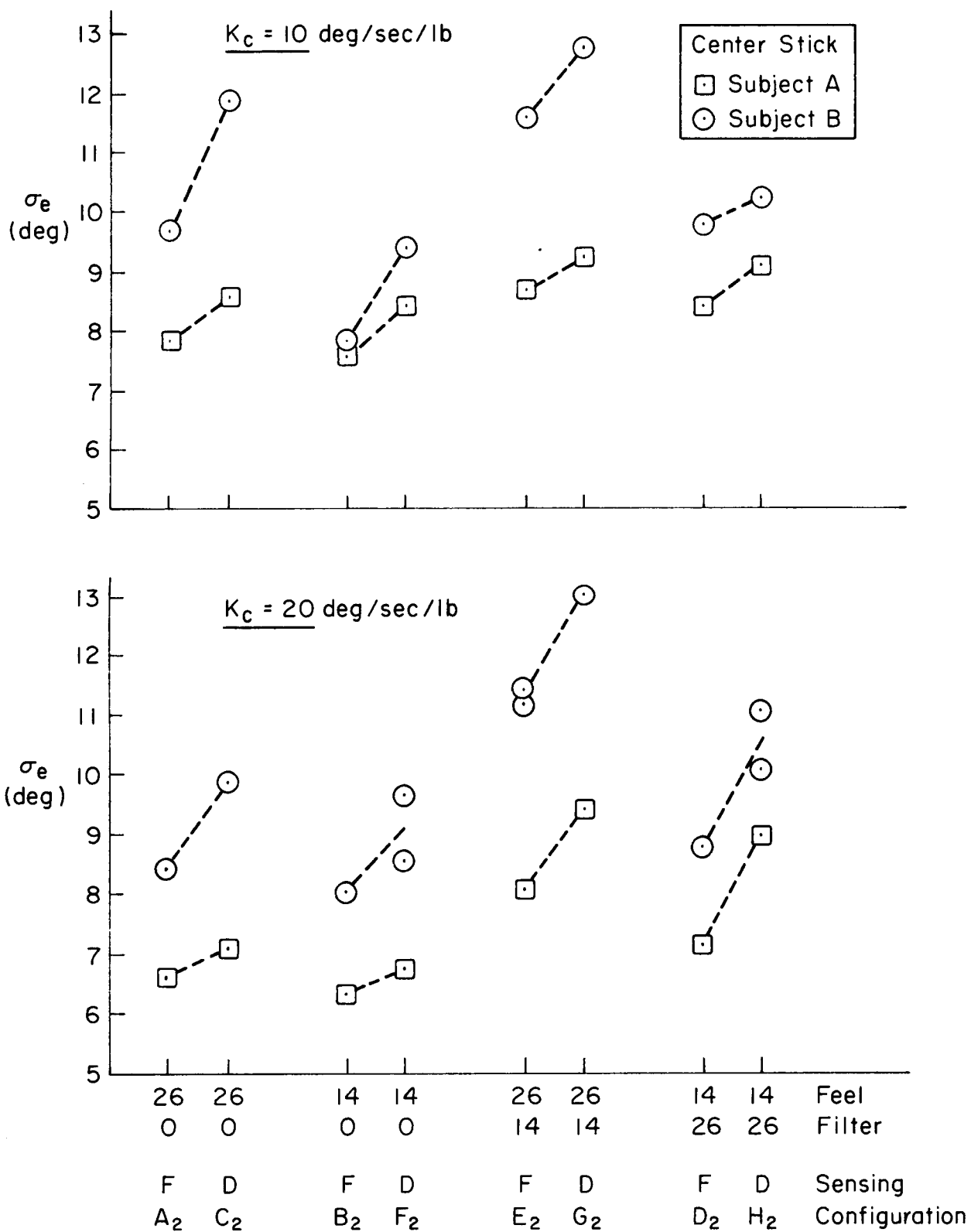


Figure 37. Influence of Feel and Filter Dynamics on Tracking Performance With Center Stick Displacement and Force Sensing

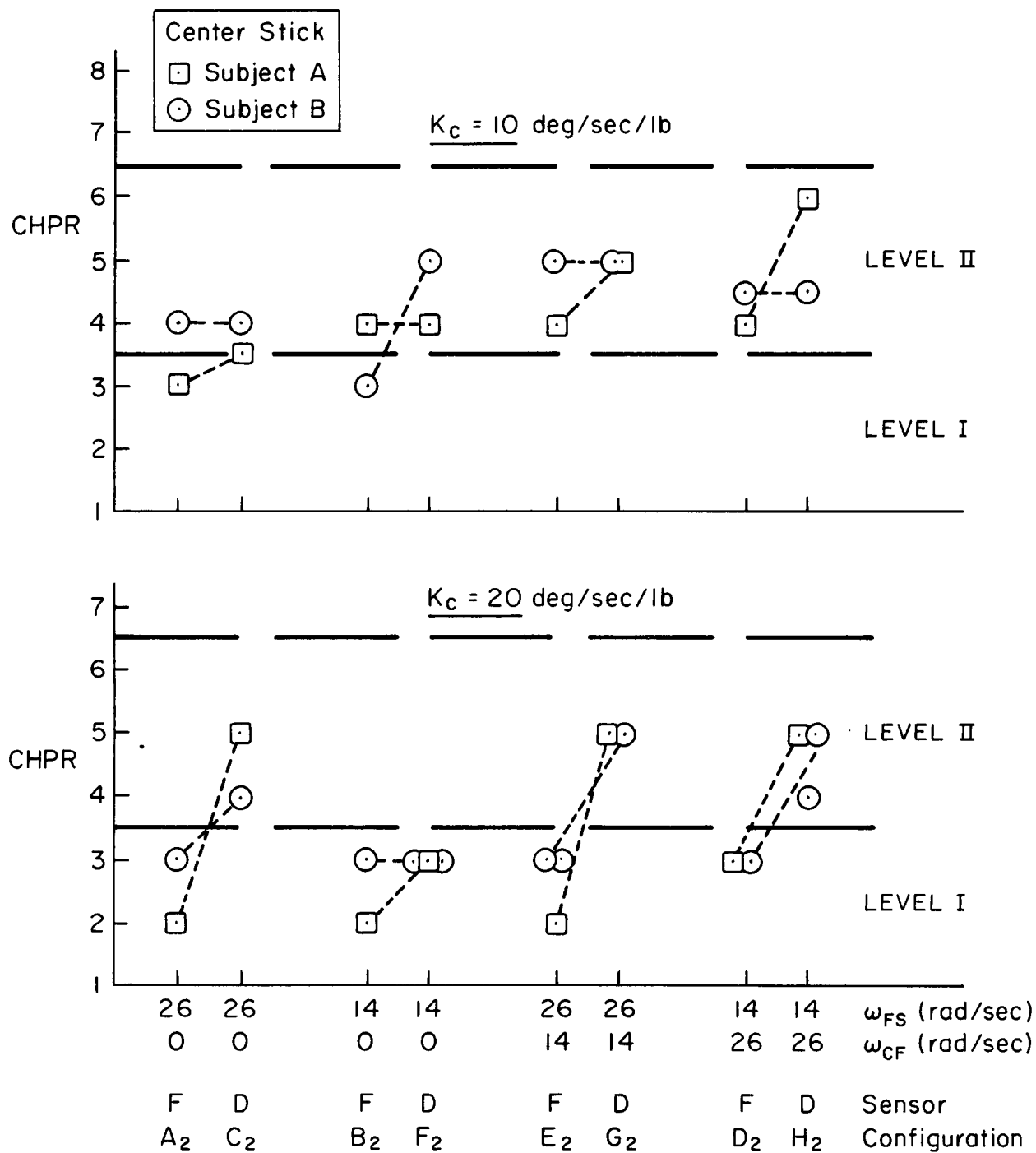


Figure 38. Influence of Feel and Filter Dynamics on CHPR  
With Center Stick Displacement and Force Sensing

### C. INFLUENCE OF DYNAMIC LAG LOCATION

The influence of dynamic lag location on tracking performance and pilot rating may be observed by comparing configurations  $D_2$  and  $E_2$  (force sensing) and configurations  $G_2$  and  $H_2$  (displacement sensing) in which the low and high frequency dynamic lags are interchanged between the feel and command filter locations while keeping the overall forward loop path lag constant.

#### 1. Tracking Performance

Figures 39 and 40 show the influence on tracking bandwidth and rms error, respectively. Separate comparisons are made for force and displacement sensing at each command gain. Results in both figures

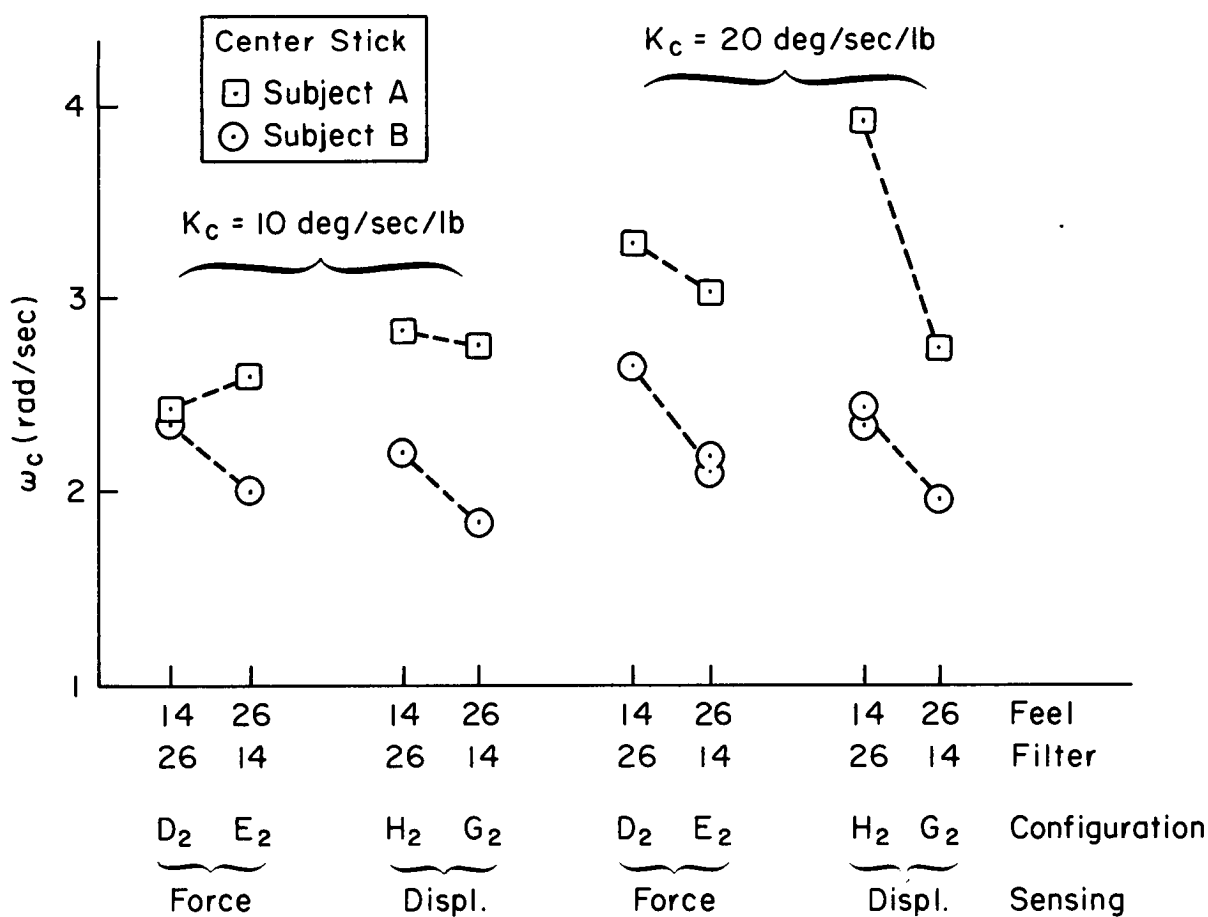


Figure 39. Influence of Dynamic Lag Location on Tracking Bandwidth (Center Stick)



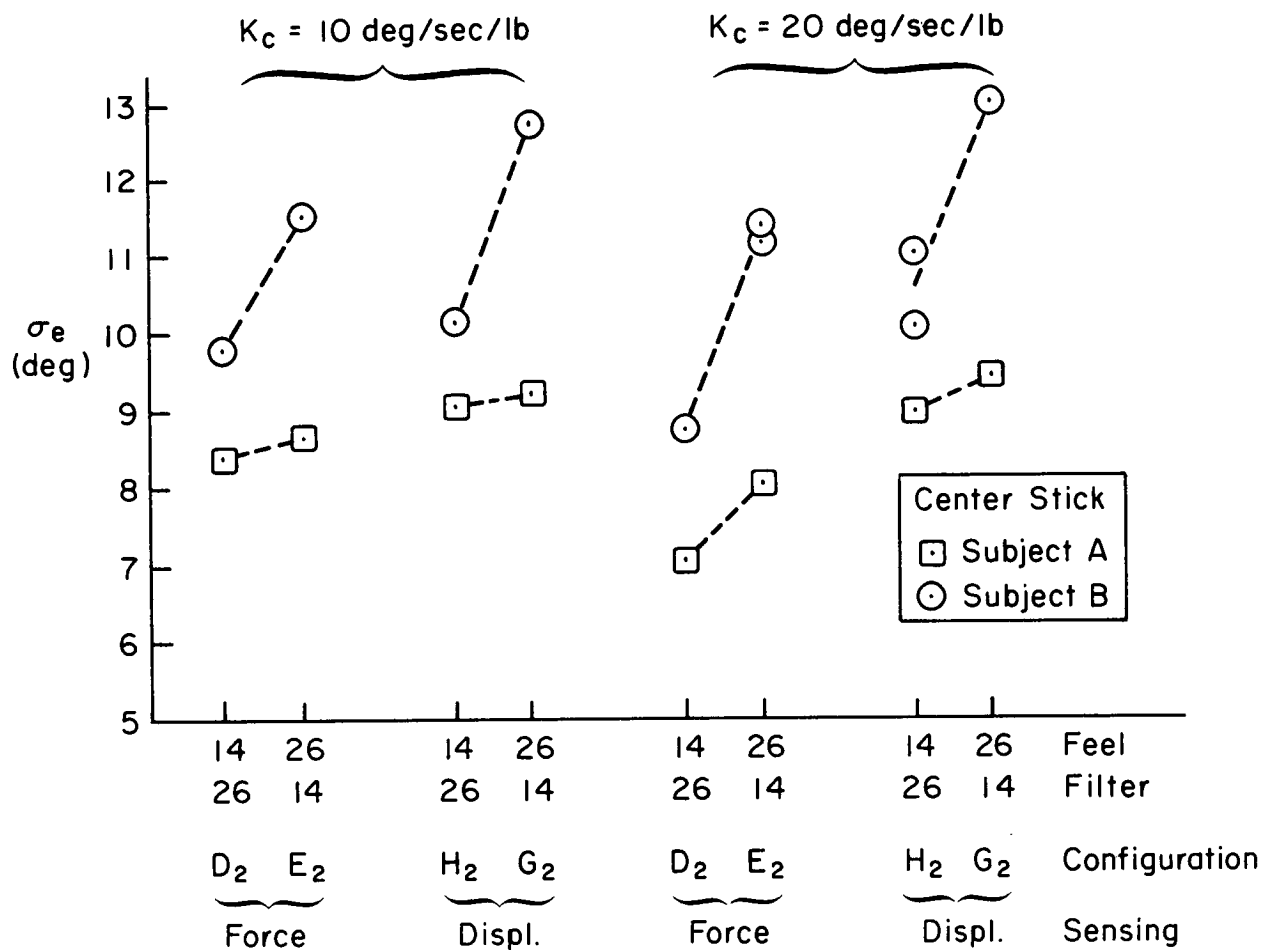


Figure 40. Influence of Dynamic Lag Location on Tracking Error (Center Stick)

indicate placing the 14 rad/sec lag in the command filter location has a decidedly adverse effect on these tracking performance measures. The difference is more pronounced for Subject B than for Subject A. Referring back to Figs. 35 and 37, it may be observed on the other hand that there is no adverse effect when the 14 rad/sec feel dynamics are substituted for the 26 rad/sec feel system with the command filter lag eliminated. These results support the findings of Refs. 8 and 9.

## 2. Pilot Rating

Figure 41 shows that pilot ratings are not changed significantly by interchanging the 14 rad/sec lag between the feel system and the command filter locations. This is probably due to the accumulative system lag being so great as to result in Level II flying qualities in three sets of comparisons and borderline Level I-II in the fourth. But, referring back to Fig. 38 it may be observed again that there is no adverse effect on pilot rating when the 14 rad/sec feel dynamics are substituted for the 26 rad/sec feel system. This too supports the flight results of Refs. 8 and 9 concerning the lack of adverse effect on flying qualities when a feel system having relatively low frequency dynamics is employed in the roll axis.

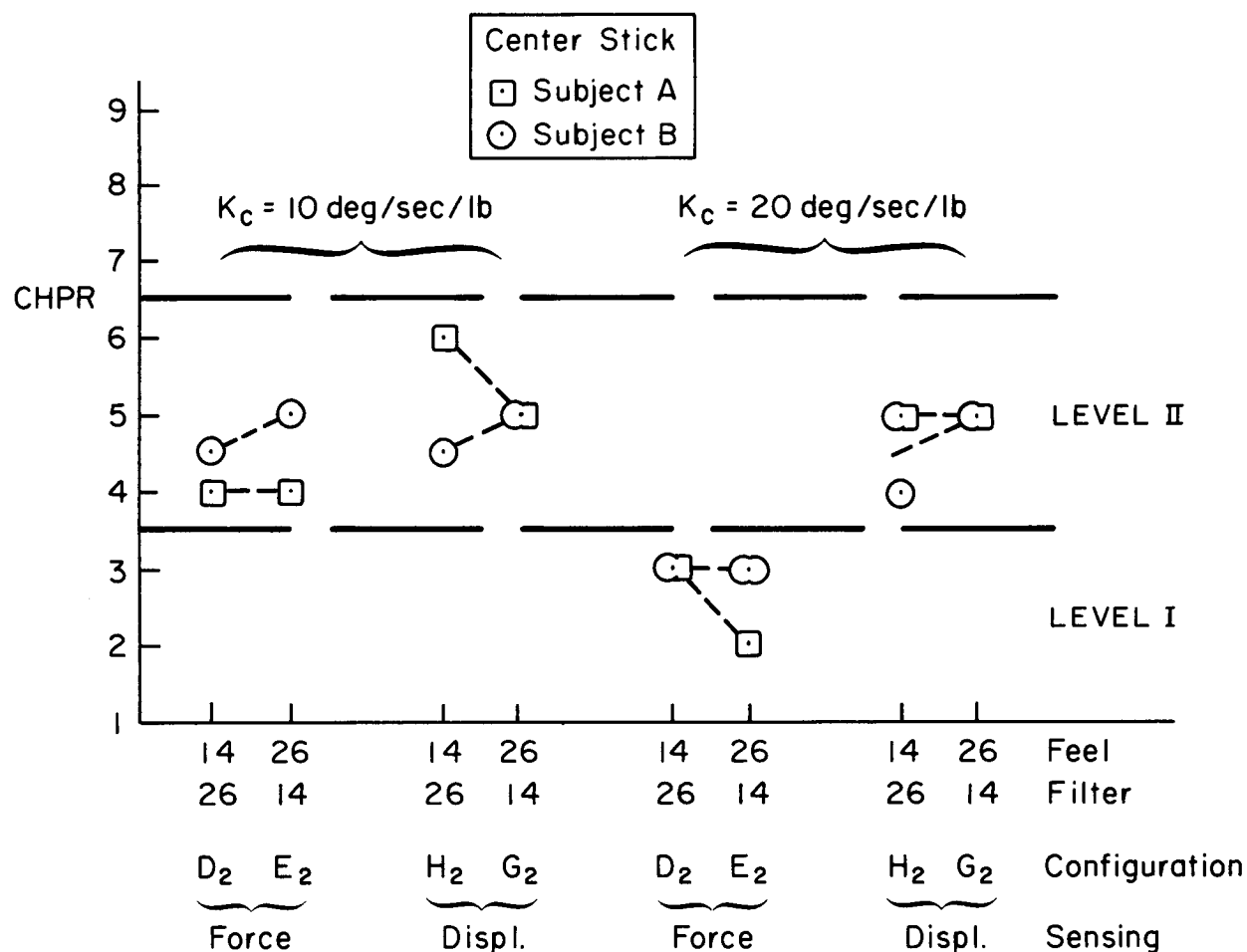


Figure 41. Influence of Dynamic Lag Location on CHPR (Center Stick)

## D. INFLUENCE OF CUMULATIVE EFFECTIVE TIME DELAY

Having looked at the various direct comparisons between mechanizational elements, it is of interest to view the results in terms of the computed cumulative buildup in effective time delay with the different configurations. The table in Fig. 33 shows this effective delay, from force application to roll response, extends from 0.033 sec to 0.19 sec in four nearly equal time increments.

### 1. Tracking Performance

Figures 42 and 43 present rms tracking error ( $\sigma_e$ ) plotted against cumulative effective  $\tau_e$  for subjects A and B, respectively. The data of Fig. 42 show for Subject A a linear increase in error with increasing time delay. There is a distinct difference in performance between the low and high command gains which begins at the lowest effective time delay configurations and diminishes as  $\tau_e$  increases. The lower rms error for  $K_c = 20$  was noted in the previous plots but here it becomes most noticeable that the gain influence decreases at the higher effective time delay values.

Figure 43 for Subject B also indicates a linear increase in tracking error as controlled element effective time delay increases. However this plot tends to bring out the wider spread in error due to a less consistent tracking gain loop closure of Subject B as compared to Subject A.

In summary, the rms tracking error measures show a linear degradation in performance proportional to an increase in overall controlled element effective time delay.

### 2. Pilot Ratings

A summary plot of CHPR versus controlled element effective time delay is presented in Fig. 44. This shows the mean and 1  $\sigma$  values obtained by combining data from both subjects at each command gain. The numbers beside the symbols indicate the number of runs involved. Not only is the data very consistent (one half rating point 1  $\sigma$  ranges), but

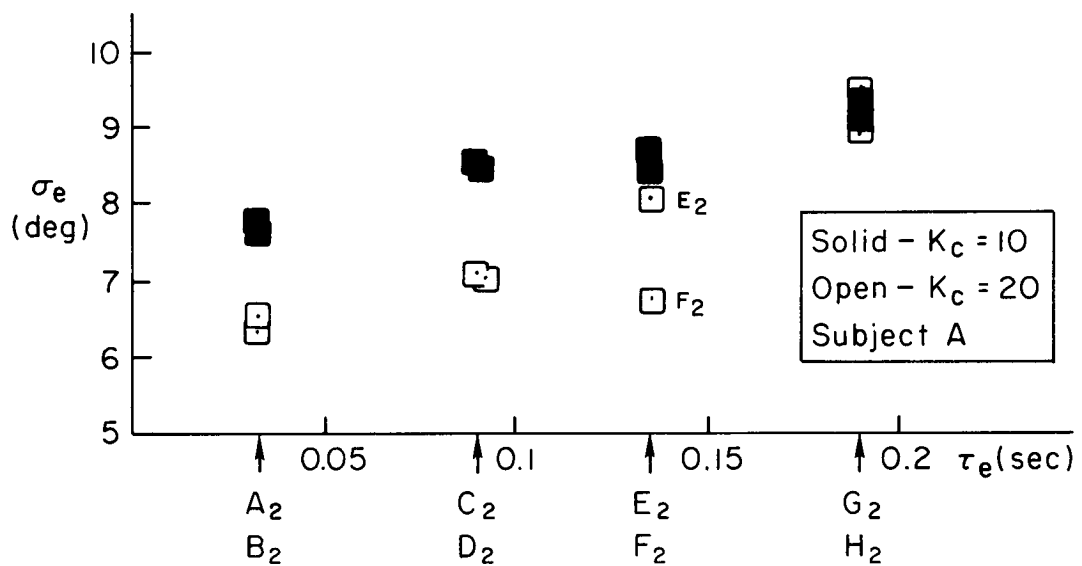


Figure 42. RMS Tracking Error vs Effective Time Delay, Subject A (Center Stick)

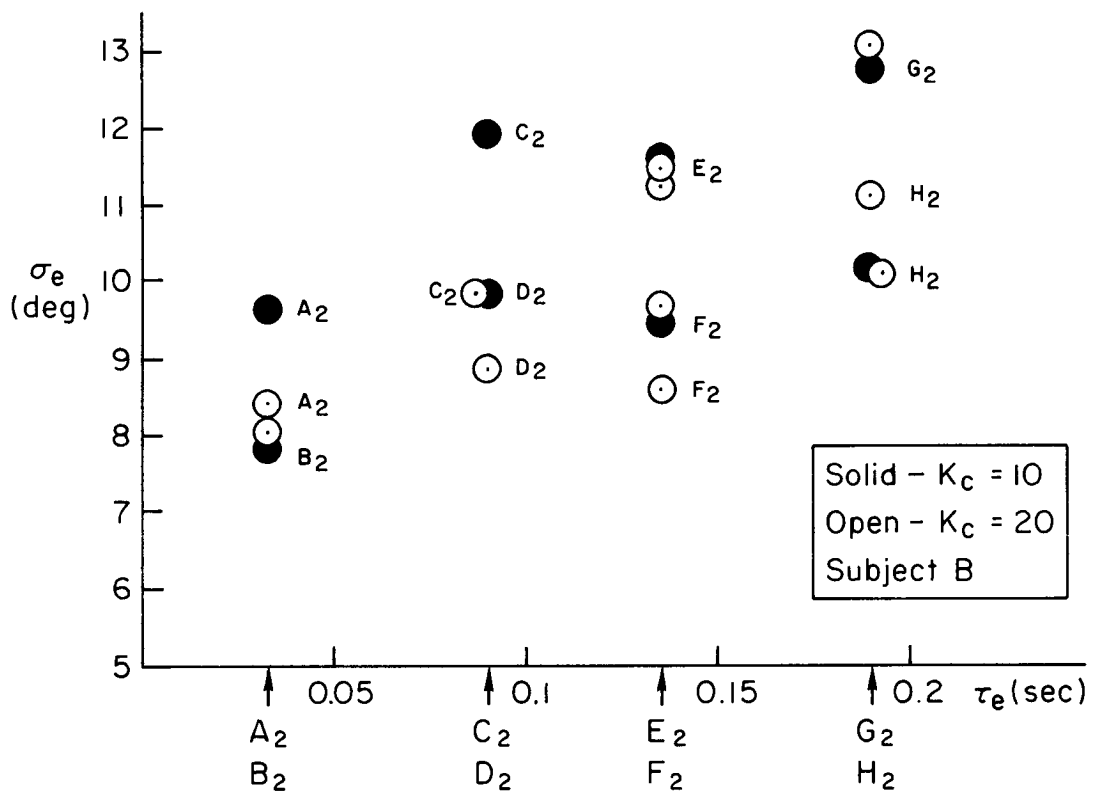


Figure 43. RMS Tracking Error vs Effective Time Delay, Subject B (Center Stick)

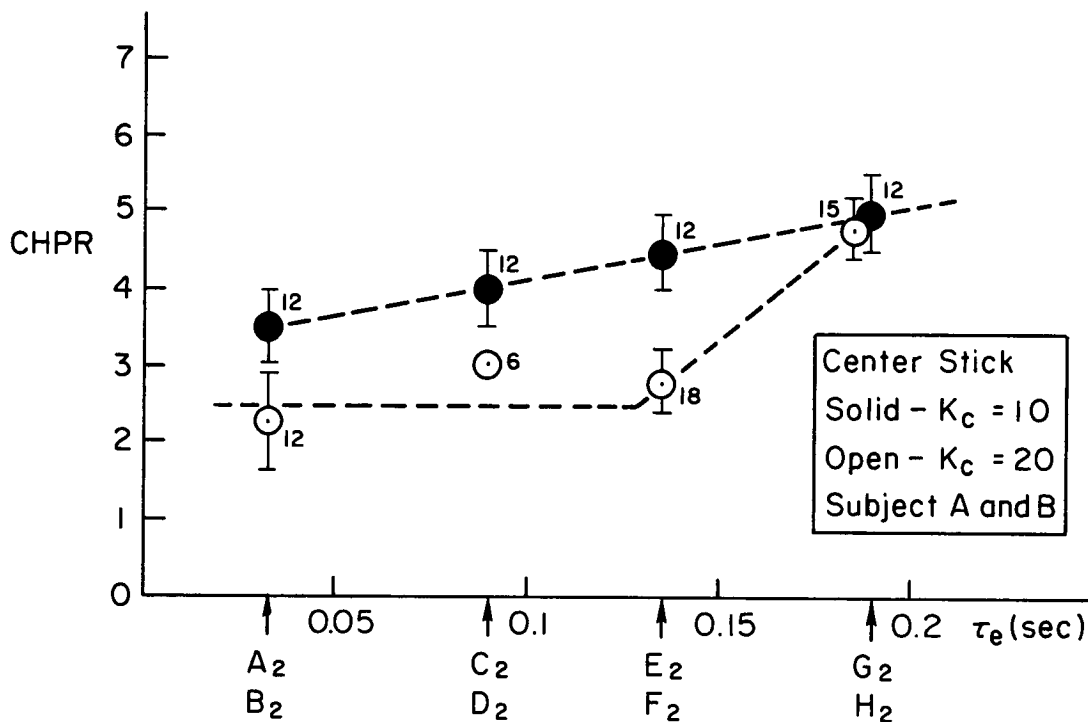


Figure 44. CHPR Variation With Effective Time Delay and Command Gain (Center Stick)

this plot again shows the definite preference for the  $K_c = 20$  command gain at  $\tau$  less than 0.19 sec.

### 3. Comparison With MIL-Spec Time Delay Criteria

It was noted in Section II-D-2 that the question has been raised as to whether the time delay criterion of MIL-F-8785C should be referenced to manipulator force or displacement (i.e., whether the feel system lag should be included when the command input is manipulator displacement). Figure 45 presents summary plots of average CHPR vs  $\tau_e$  data including the feel system lag (per 8785C) and excluding the feel lag (per Ref. 9). Since results of this simulation show a sensitivity to command gain, data are plotted for each gain separately and for the average of the two. The upper plots reflect  $K_c = 10$ , the middle plots reflect  $K_c = 20$ , and the lower plots the average for both gains. All plots reflect the averaged CHPRs from Fig. 44.

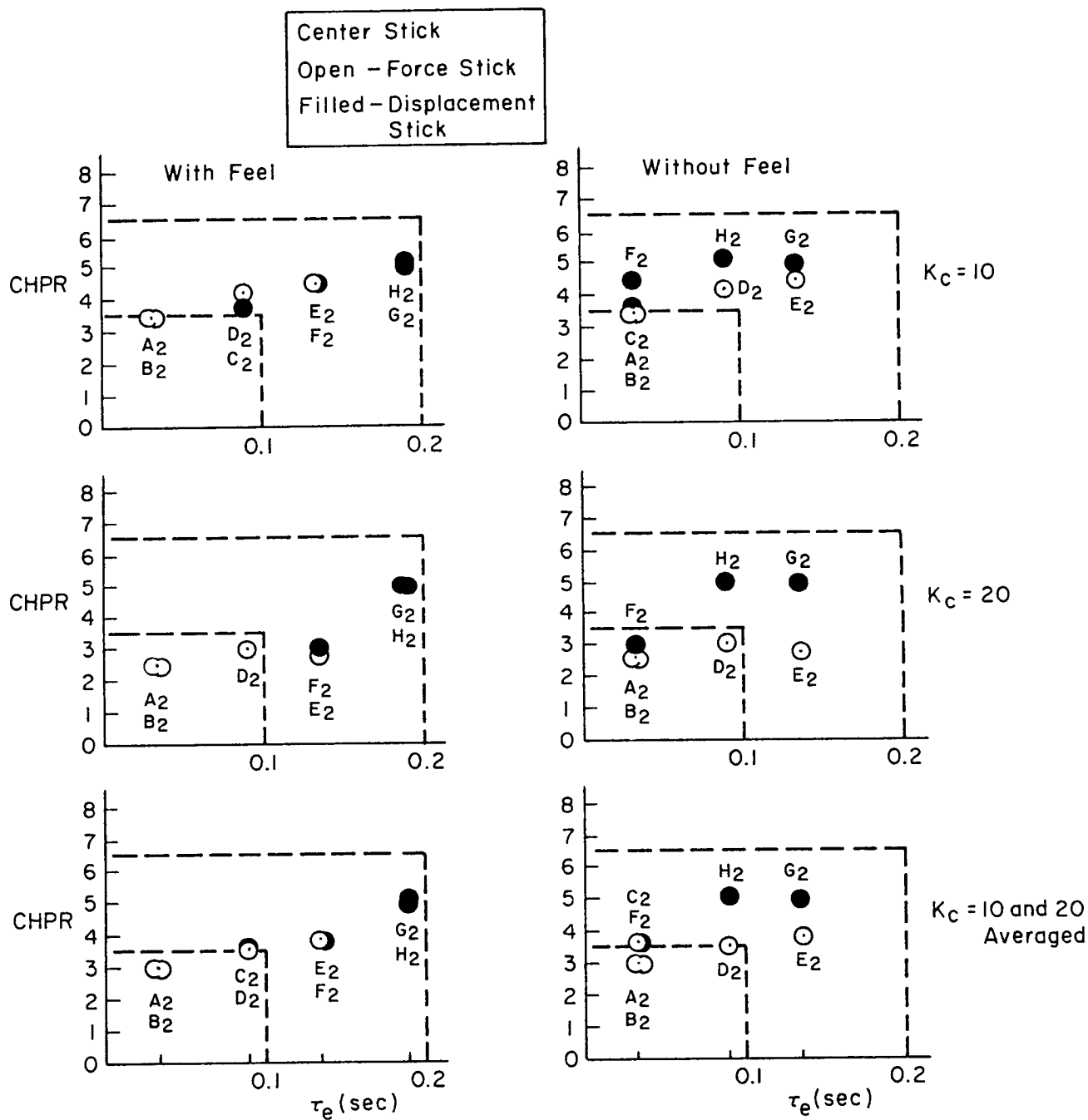


Figure 45. Comparison of CHPR With MIL-F-8785C Effective Time Delay Criteria (4 lb/in Center Stick)

When the effective time delay is computed from force application (therefore feel dynamics included), there is a steady progression of increasing CHPR with increasing  $\tau$  which supports the -8785C Level I boundary but may indicate the boundary between Level II and III is too conservative. On the other hand, when the feel dynamics are excluded in the calculation of the effective time delay, two different CHPRs result for each value of  $\tau$  and the ratings for the displacement sensing center stick (shaded symbols) definitely do not fit the criteria boundaries. The data are not consistent with the contention that the feel system dynamic lag should be excluded when calculating the overall vehicle effective time delay. It should also be noted that these results for the center stick are not consistent with those of Fig. 32 for the side stick. There was not so much difference in pilot rating between force and displacement stick sensing for the side stick.

It seems obvious from these comparisons that the more appropriate criterion is that of MIL-F-8785C which includes the feel lag contribution in the overall vehicle computed effective time delay when stick displacement sensing is employed.

#### **E. SUMMARY**

This set of experiments was performed to obtain lab data for later comparison with flight. Results of this limited simulation forecast that for a center stick configuration in a roll tracking task:

- Force sensing results in lower tracking error and is rated better than displacement sensing.
- In the absence of appreciable command filter lag, there is no difference in tracking performance or pilot preference between feel system dynamics of 26 and 14 rad/sec.
- A 14 rad/sec command filter in series with a 26 rad/sec feel system has a decidedly adverse effect on tracking error in comparison with a 26 rad/sec command filter and a 14 rad/sec feel system, however it appears to make no difference in pilot rating. (The latter probably is due to the excessive total effective time delay for both configurations).

- Pilot ratings obtained for effective time delays up to 0.19 sec support the MIL-F-8785C criterion which requires the time delay be referenced to force applied to the manipulator regardless of whether force or displacement sensing is used. Results also fell within the 8785C Level I and II boundaries.



## SECTION VI

### PILOT DYNAMIC MODEL WITH FORCE VS DISPLACEMENT CENTER STICK

It was shown in the previous section that stick displacement sensing (feel dynamics in the forward path of Fig. 9) degraded CHPR an average of 1 rating point compared to force sensing (feel dynamics in the feedback path). However, based on Refs. 8, 9 and other findings of the previous section, there also is evidence that use of a comparatively sluggish feel system does not degrade flying qualities ratings appreciably, providing there is little or no command filter lag in the outer (tracking) loop path.

An explanation for the latter in the case of displacement sensing is advanced in Ref. 9 by noting that closure of the limb/manipulator loop via the pilot's arm joint receptors moves the open-loop feel dynamic mode to higher frequency and therefore reduces the closed-loop effective lag contribution of this dynamic element. Figure 46 presents an example root locus plot for closure of the positional limb/manipulator loop of Fig. 9 using typical 3rd order NM system parameter values and the 14 rad/sec, 0.07 damped, feel system dynamics. (The second order mode above 40 rad/sec is the Pade' approximation for the time delays in the forward and feedback paths of Fig. 9.) This locus shows the feel system mode moves to higher frequency and lower damping as loop gain is increased. Conversely, the NM 2nd order mode moves to a lower frequency but at lower damping. For the maximum stable gain shown, the closed-loop feel mode moves to about 17 rad/sec.

Another possible explanation is that the feel system lag contribution is partially or totally compensated for by a change in the pilot's central compensation (decrease in latency and/or generation of lead). But, if the feel lag is offset by pilot appreciable lead generation, then one might expect an accompanying degradation in flying quality rating. This has not necessarily been noted.

In this subsection an attempt is made to shed light on the subject by applying two different model fitting approaches to the data obtained.

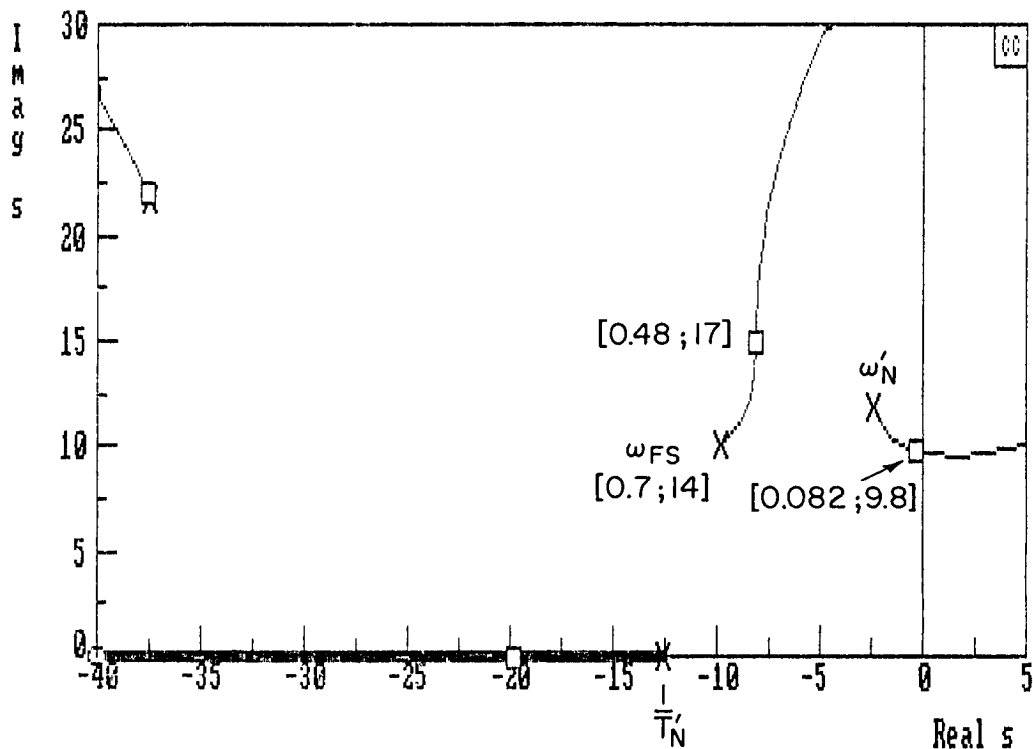


Figure 46. Example Root Locus of the Limb/Manipulator Positional Loop Closure

In the first,  $Y_p Y_c$  describing function data from several typical center-stick tracking runs were fitted with transfer function models appropriate for the various elements in the loop. Parameter values for the "known" control system and aircraft were considered fixed while values for the "unknown" pilot were adjusted until an adequate fit was obtained. This approach appears to provide some of the needed insight to the above uncertainties concerning high frequency mode contributions. Additional insight is obtained by taking a much simplified crossover model fit to identify dominant factors in the region of tracking loop closure frequency.

#### A. HIGH ORDER DYNAMIC MODEL

The STI Describing Function Analyzer (DFA) program computationally extracts opened-loop describing function amplitude and phase data from

the closed-loop tracking task. Therefore it is appropriate to start with known open-loop dynamic models and parameter values for the feel, command filter, and aircraft elements and assume models and parameter values for the pilot. The latter are then iterated until acceptable fits are obtained to the amplitude and phase data points. Adjustments to the feel dynamics are considered if adequate matches cannot be obtained through this method. The example configurations which were fitted are listed in Table 3. All included the 2nd order command filter.

The matches to the describing function data points are presented in Figs. 47 through 52. The transfer functions employed in the various fits are included in each figure. It should be noted that the pilot NM mode in each instance is modeled by second order rather than third order dynamics. The first order lag is either beyond the frequencies employed or is effectively canceled by the NM mode zero (see Eqs. 1, 2, 3). In some cases it is also necessary to include lead/lag terms in the pilot model to achieve an adequate fit. In all cases excellent amplitude and phase fits are achieved out through 14 rad/sec. At the highest frequency (19 rad/sec) the amplitude data points generally are somewhat higher than the models predict and the phase matches vary. This is not

TABLE 3. CONFIGURATIONS FITTED WITH HIGH ORDER MODELS

FIGURE	CONFIG.	COMMAND SENSING	FEEL SYSTEM	COMMAND FILTER	SUBJECT
47	E <sub>2</sub>	Force	26	14	A
48	D <sub>2</sub>	Force	14	26	A
49	H <sub>2</sub>	Displacement	14	26	A
50	G <sub>2</sub>	Displacement	26	14	A
51	H <sub>2</sub>	Displacement	14	26	A
52	H <sub>2</sub>	Displacement	14	26	B

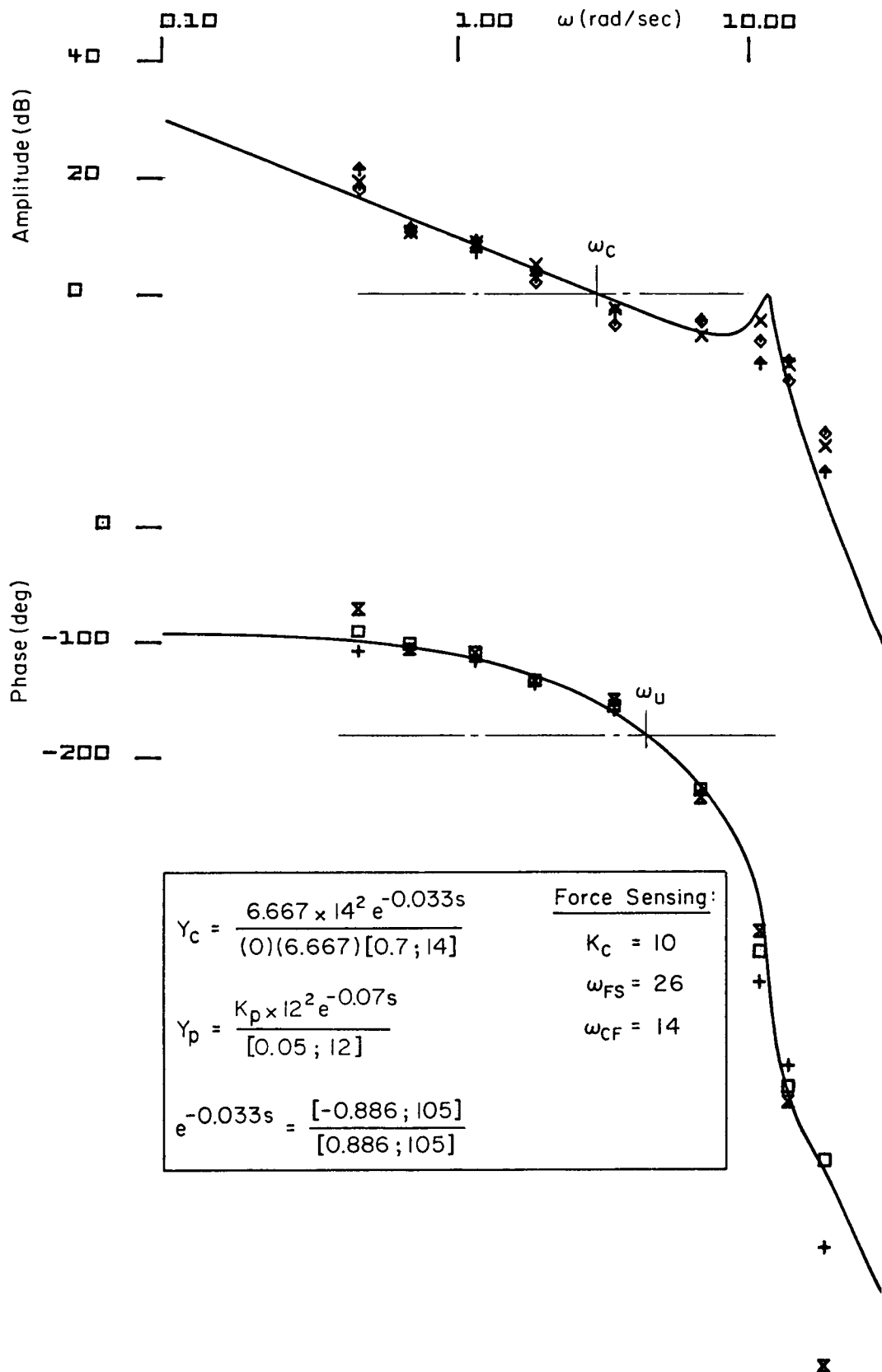


Figure 47. Dynamic Model Match to Describing Function Data, Force Sensing Center Stick, Subject A,  $\omega_{FS} = 26$ ,  $\omega_{CF} = 14$

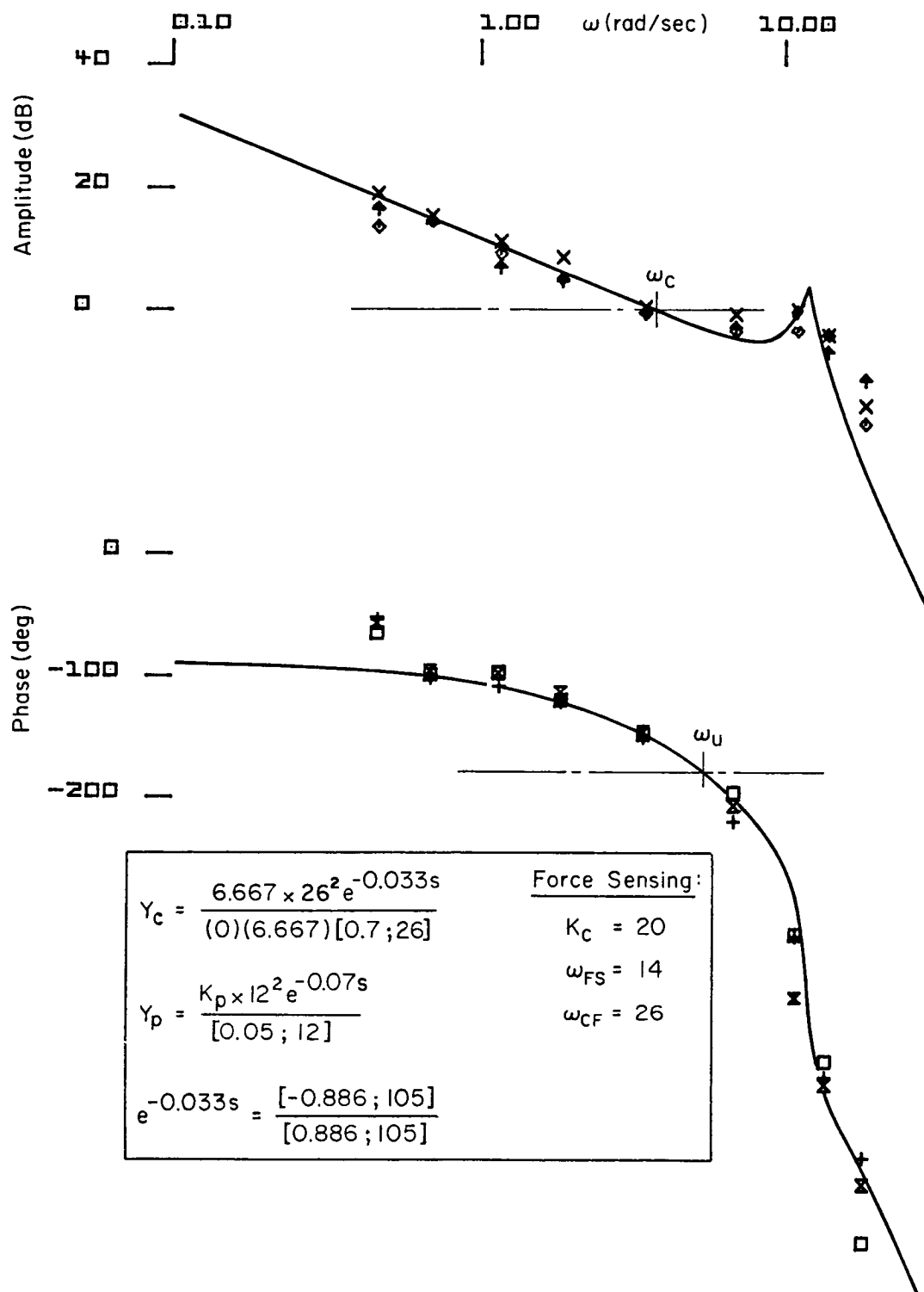


Figure 48. Dynamic Model Match to Describing Function Data, Force Sensing Center Stick, Subject A,  $\omega_{FS} = 14$ ,  $\omega_{CF} = 26$

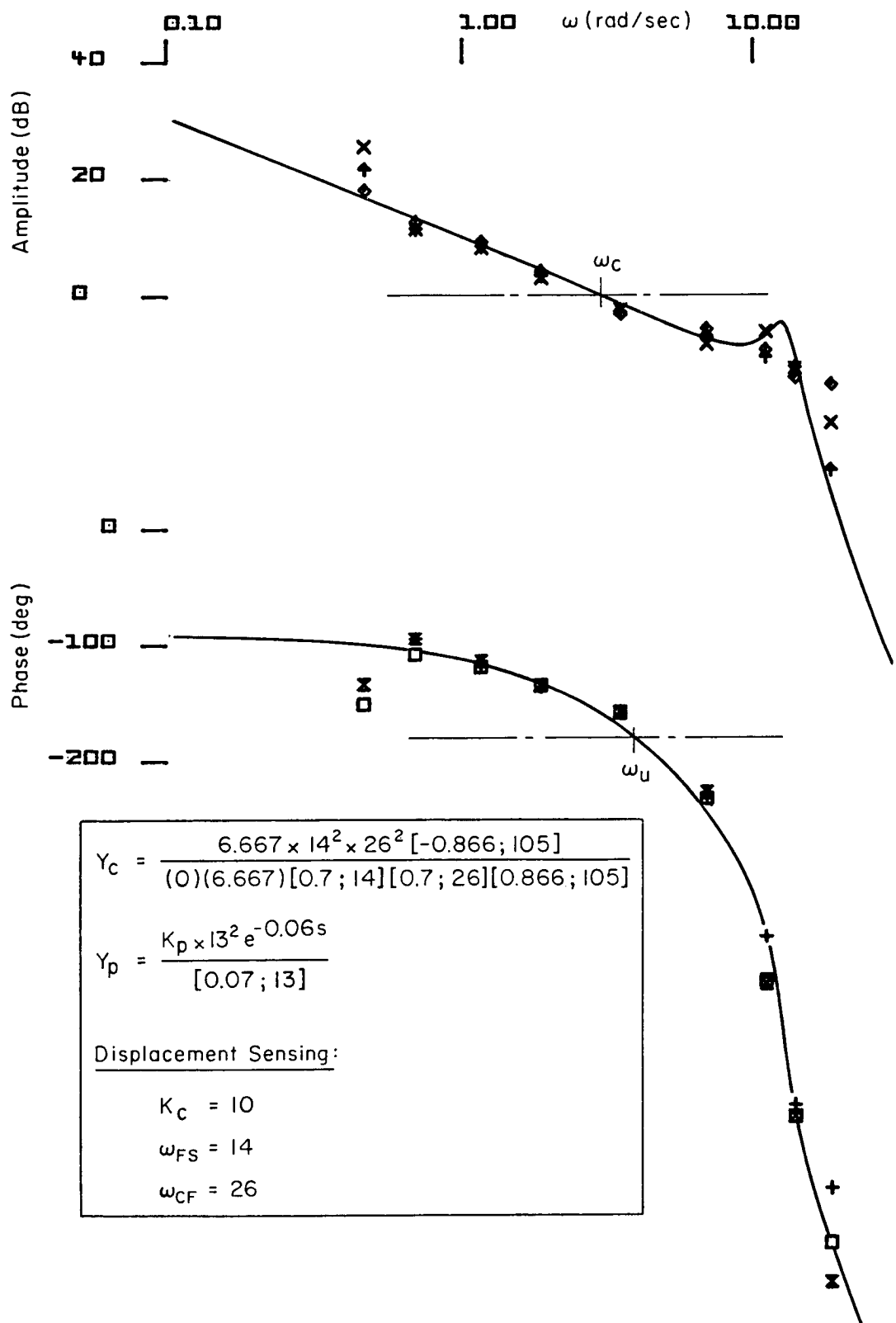


Figure 49. Dynamic Model Match to Describing Function Data  
 Displacement Sensing Center Stick, Subject A  
 $\omega_{FS} = 14$ ,  $\omega_{CF} = 26$

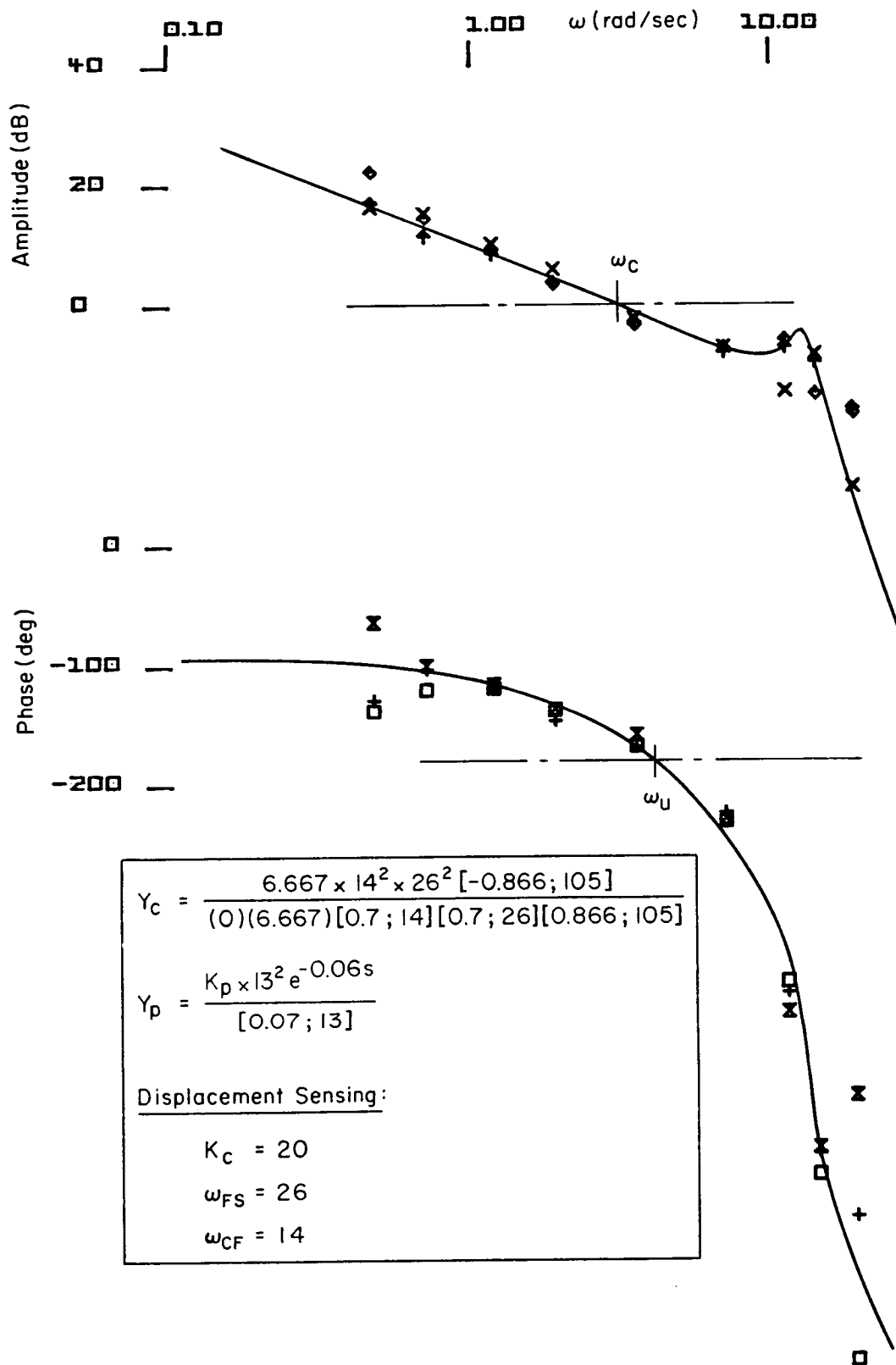


Figure 50. Dynamic Model Match to Describing Function Data,  
Displacement Sensing Center Stick, Subject A,  
 $\omega_{FS} = 26$ ,  $\omega_{CF} = 14$

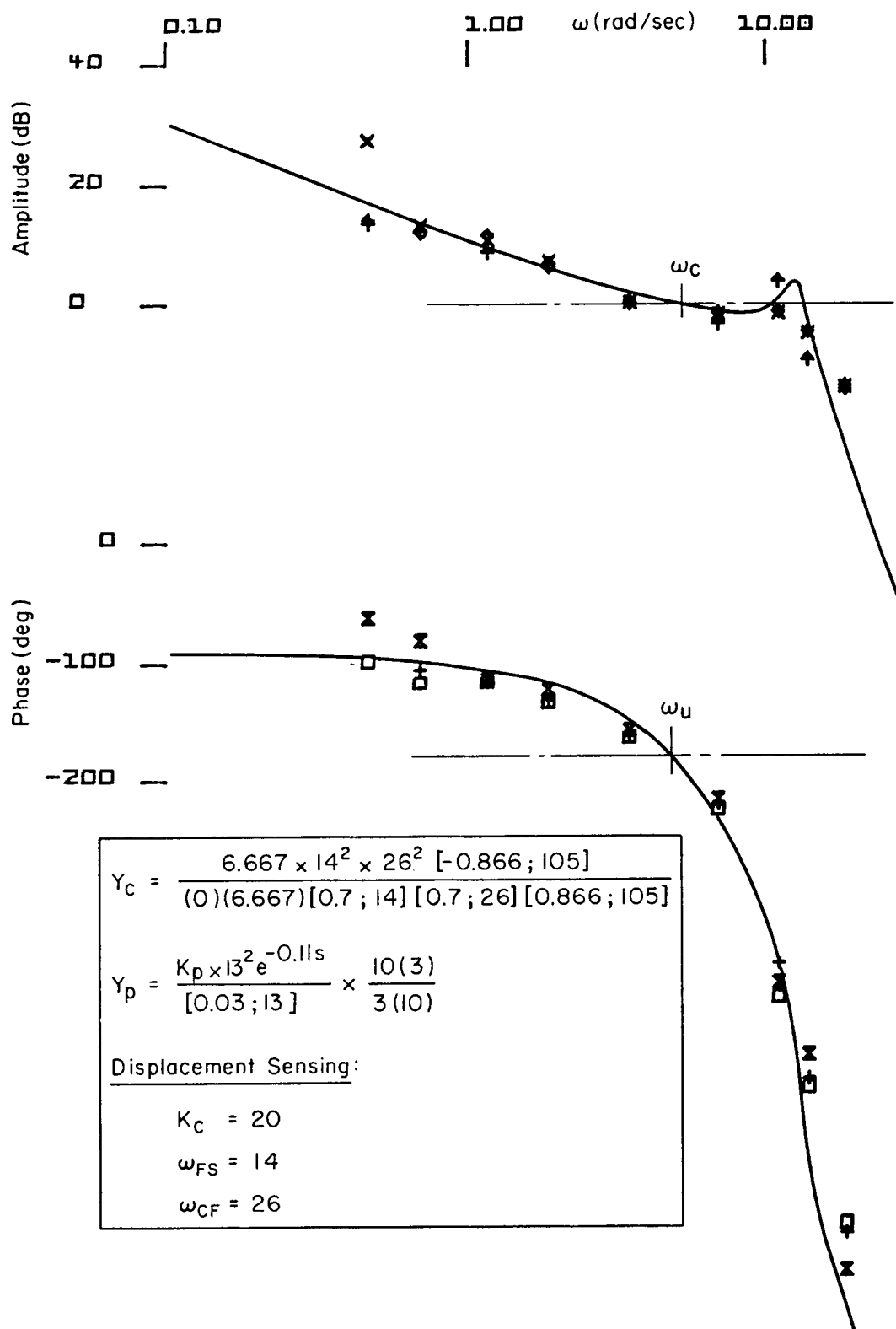


Figure 51. Pilot Generation of Lead With Displacement Sensing Center Stick, Subject A,  $\omega_{FS} = 14$ ,  $\omega_{CF} = 26$



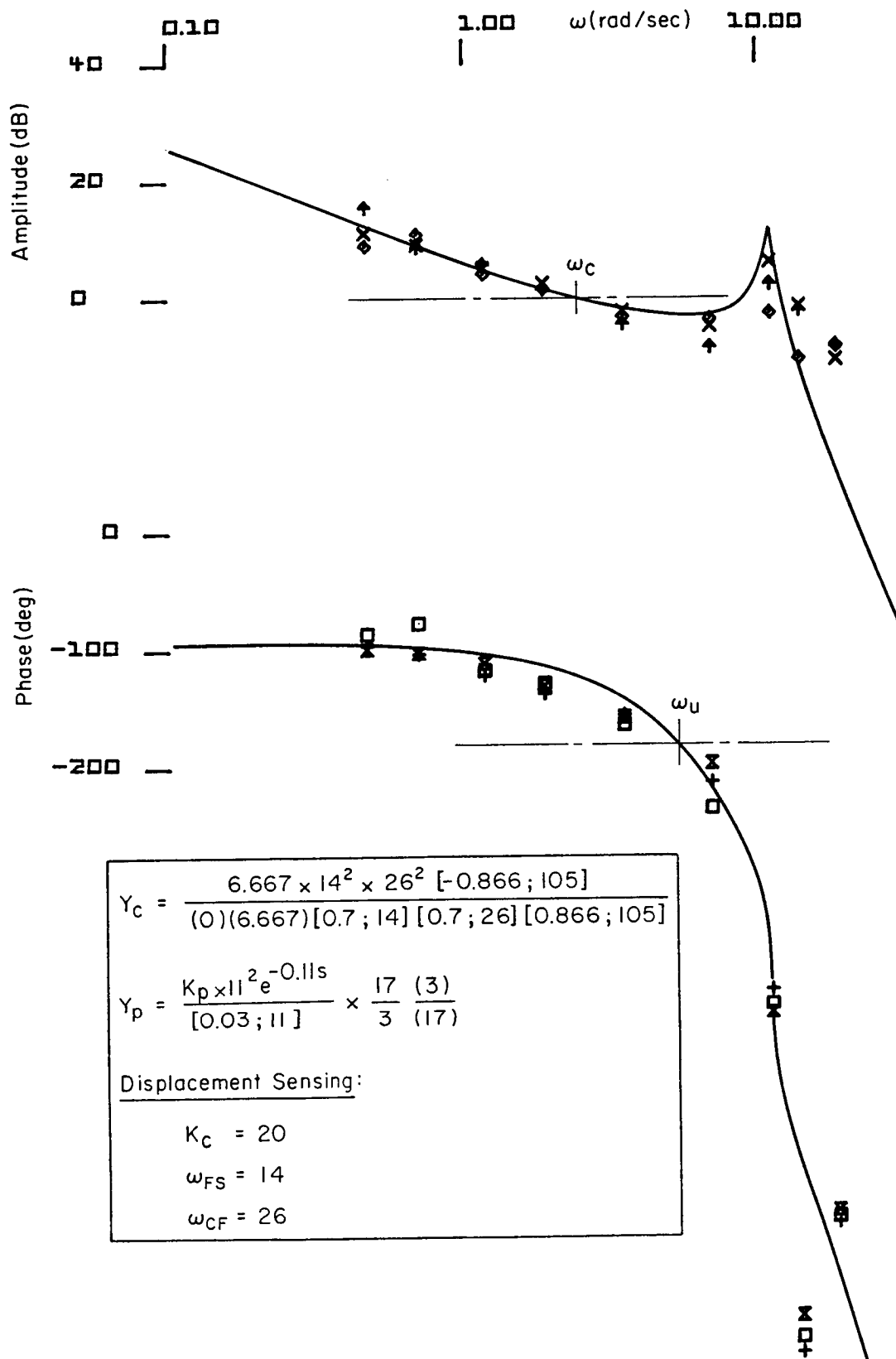


Figure 52. Pilot Generation of Lead With Displacement Sensing Center Stick, Subject B,  $\omega_{FS} = 14$ ,  $\omega_{CF} = 26$

too disconcerting as the forcing function amplitude is quite small at this frequency and the closed-loop response power is also very low allowing system noise and other sources of remnant to dominate. Therefore there is considerably more scatter in the data at this frequency.

Comparison between the figures reveals the following:

#### **1. Force Vs Displacement Sensing (Figs. 47, 48 vs 49, 50)**

The fits to the force sensing configurations are shown in Figs. 47, 48. These configurations reflect command filters of 14 and 26 rad/sec and gains of 10 and 20 deg/sec/lb, respectively. Both are characterized by the absence of the feel dynamics lag. The pilot model consists of a time delay of 0.07 sec and the 2nd order NM mode at 12 rad/sec and 0.05 damping. In both cases excellent matches are obtained. The gain line crossover with the amplitude fit ( $\omega_c$ ) is above 3 rad/sec, the phase crossover ( $\omega_u$ ) is close to 5 rad/sec, and the phase margin at  $\omega_c$  is 30 deg in both cases. These were given CHPR ratings of 3 and 4.

Two matches to displacement sensing configurations in which the subject pilots did not employ lead/lag compensation are shown in Figs. 49, 50. These are characterized by the presence of the feel system lag modeled with the open-loop parameter values. Figure 49 is for the 14 rad/sec feel, 26 rad/sec filter, and 10 deg/sec/lb gain. Figure 50 is for the 26 rad/sec feel, 14 rad/sec filter, and 20 deg/sec/lb gain. In both of these cases an excellent match is obtained with a pilot time delay of 0.06 second 2nd order NM mode of 13 rad/sec and 0.07 damping. Thus there is very little difference in the pilot model parameters between this displacement and the previous force sensing fits. But it will be noted that the amplitude crossover is barely 3 rad/sec in both of the displacement stick cases, the phase crossover is less than 4 rad/sec, and the phase margin is 20 deg or less. These elicited CHPR ratings of 5 and 6.

It should be pointed out that the two force and the two displacement sensing cases shown represent an interchange of feel and command filter dynamic lag values. In these examples there obviously is no influence on the pilot model or parameter values.

## 2. Pilot Generation Of Lead

Although the interchange of the 14 and 26 rad/sec dynamic elements had little influence, there was considerable evidence in the describing function amplitude and phase data that the additional phase lag of the two elements caused the subjects to adopt lead/lag compensation in many runs with the displacement sensing stick. Two of the more extreme examples of this behavior are presented in Figs. 51, 52. Figure 51 shows Subject A adopted a lead at 3 rad/sec and lag at 10 rad/sec. His central latency increased to 0.11 sec but there was no change in his NM mode. This particular set of runs indicates gain crossover very near to the phase crossover frequency (zero phase margin), a PIO condition. It resulted in a CHPR of 5.

Another set of example runs for the same controlled element but with Subject B is presented in Fig. 52. This was again fit with a lead at 3 rad/sec but a lag at 17 rad/sec. Note that this resulted in a little too much phase lead in the region around crossover. Thus a slightly higher lead break would probably produce a better match. This Subject also increased his central latency to 0.11 sec and reduced his NM mode to 11 rad/sec, 0.03 damping. The equalization increased the phase crossover ( $\omega_{\phi}$ ) to almost 5.5 rad/sec but the accompanying increase in amplitude ratio at frequencies above 3 rad/sec caused a gain regression which resulted in an amplitude crossover of only 2.5 rad/sec. Also the amplitude peaking of the NM mode is greater than in any of the previous plots. Despite these adverse influences, the Subject gave the configuration a CHPR rating of 4. Quite possibly this is due to the phase margin at gain crossover being increased to about 60 deg.

In both Figs. 51, 52 it is apparent the adoption of lead causes a flattening of the amplitude ratio plot in the region of desired crossover (e.g., 2.5 to 4 rad/sec) and therefore non-K/s like characteristic. This results in increased sensitivity of crossover frequency and/ or phase margin to pilot gain and may help to explain the Level II ratings given to these configurations in Fig. 41.

### 3. Summary

Results of these higher order mode data fits have shown no appreciable difference in pilot model form or parameter values for configurations in which the dynamic lag contributions of the feel and command filter elements were interchanged. Presence of the 14 rad/sec 2nd order lag (either feel or filter) with a displacement sensing stick either reduces closed-loop bandwidth and phase margin (if  $Y_p$  is unchanged from the force sensing cases) or induces the pilot to adopt lead/lag compensation in an attempt to improve bandwidth and phase margin. The latter results in an offsetting increase in pilot central latency and increased sensitivity of closed-loop performance to pilot gain.

Excellent high order fits have been obtained over the entire frequency range through the use of feel system parameter values representative of open-loop limb/manipulator characteristics. This tends to indicate that the limb/manipulator position loop is not closed sufficiently tight to appreciably modify either set of dynamic characteristics.

#### B. CROSSOVER MODEL APPROACH

The foregoing high order models provide excellent fits to six example cases but one might question whether these results are representative of all 105 describing function data runs. Detailed fits to accommodate the nuances of all runs could not be accomplished within time and budget constraints. Therefore the much simpler crossover model approach was employed. This approach focuses on the region around crossover ( $\omega_c$ ) since this is the region which dominates the pilot's perception of system performance (e.g., bandwidth, phase margin, gain margin, need for lead compensation).

In this simplified model the lag contribution of all higher frequency dynamic modes are approximated by the summation of their equivalent time delays (see Fig. 53). The describing function data points reflect the total open-loop pilot/feel/filter/aircraft system,

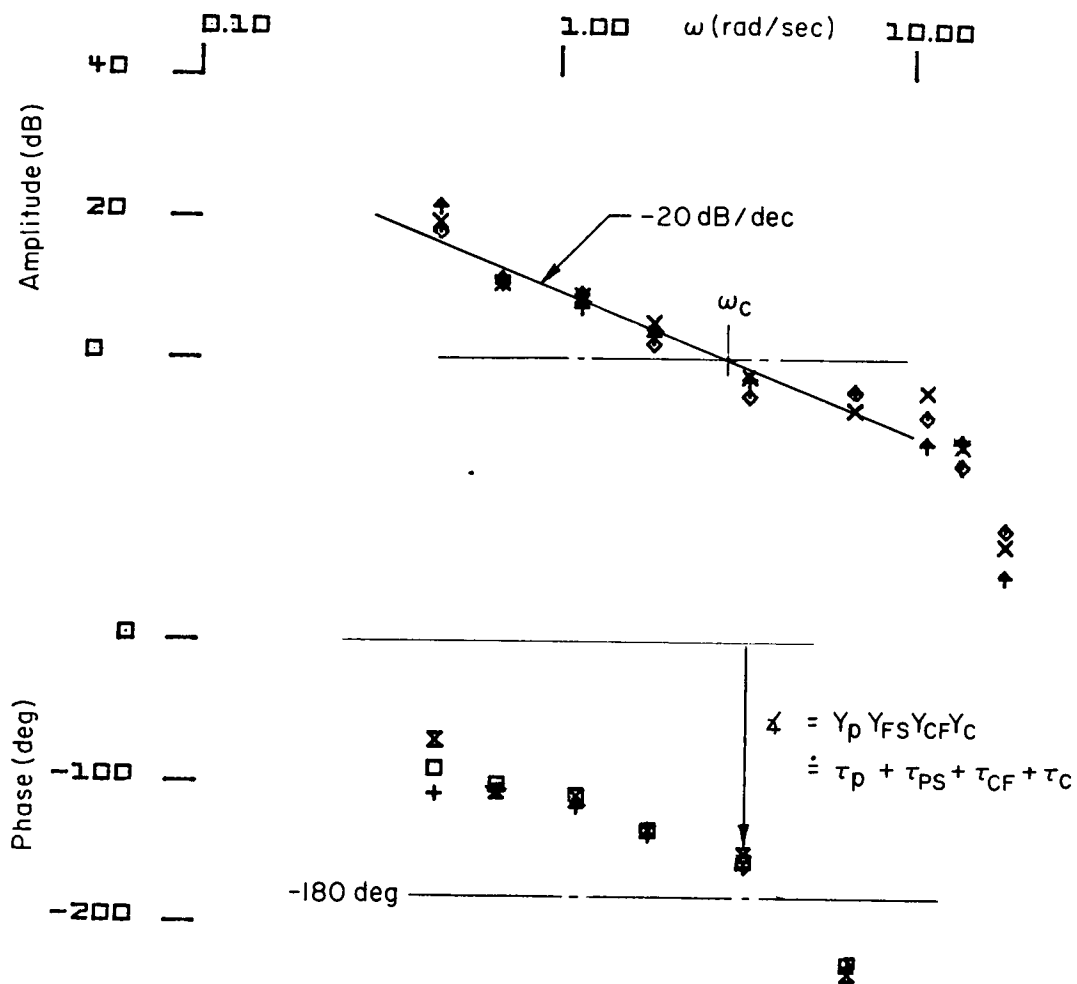
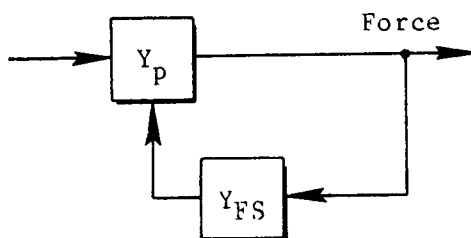


Figure 53. Effective Controlled Element Time Delay Summation for Crossover Model

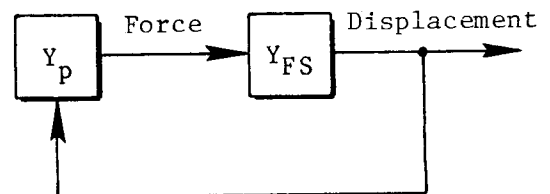
$Y_p Y_{FS} Y_{CF} Y_c$ . Since the dynamic parameters of  $Y_{CF} Y_c$  are known, the equivalent time delay contribution of these elements can be subtracted and the residual for the unknown  $Y_p Y_{FS}$  is left. The average values for the "residuals" from the 105 data runs are indicated below for the force and displacement sensing sticks.

$\tau_p$ (sec)	$\omega_{FS}$ (rad/sec)
0.076	14
0.08	26

$(\tau_p + \tau_{FS})$	$\omega_{FS}$
0.125	14
0.105	26



Force sensing sticks



Displacement sensing sticks

For the force stick the residual consists of the pilot effective time delay  $\tau_p$ . The values obtained with the 14 and 26 rad/sec feel dynamics are essentially the same. If we calculate the total effective pilot time delay based on the high order model of Figs. 47, 48 we obtain:

$$\begin{aligned}
 \tau_e &= \tau_p + \frac{2\zeta_{NM}}{\omega_{NM}} \\
 &= 0.07 + \frac{2(0.07)}{12} \\
 &= 0.082 \text{ sec}
 \end{aligned}$$

This is within about 5 percent of the average of the two values noted above. Thus the higher order model fit derived for the force sensing stick is consistent with all force sensor runs.

For the displacement sensing stick the residual reflects the pilot and feel dynamics ( $\tau_p + \tau_{FS}$ ). If we calculate the total effective time delay using the dynamic models of Figs. 49, 50 with the 14 rad/sec feel system we obtain:

$$\begin{aligned}\tau_e &= \tau_p + \frac{2\zeta_{NM}}{\omega_{NM}} + \frac{2\zeta_{FS}}{\omega_{FS}} \\ &= 0.06 + \frac{2(0.07)}{13} + \frac{2(0.7)}{14} \\ &= 0.06 + 0.0108 + 0.1 \\ &= 0.1708 \text{ sec}\end{aligned}$$

This is about 37 percent higher than the 0.125 sec extracted from the data runs. If the difference (0.0458 sec) were to be attributed to a shift in the feel system frequency and damping due to closure of the pilot limb/manipulator loop, it would require nearly doubling the feel system frequency. This is not likely based on the root locus of Fig. 46. On the other hand, the differential could be accounted for by a relatively modest first order pilot lead/lag. This also is consistent with the phase plots of Figs. 49, 50 where it can be noted that the describing function data points are about 10 deg above (lead) the fitted curve over a small range at, and slightly above, the crossover frequency.

A similar calculation of the effective time delay with the 26 rad/sec feel system shows:

$$\begin{aligned}\tau_e &= 0.06 + \frac{2(0.07)}{13} + \frac{2(0.7)}{26} \\ &= 0.06 + 0.0108 + 0.055 \\ &= 0.1258 \text{ sec}\end{aligned}$$

This is about 20 percent higher than the 0.105 sec from the data runs. Again this can be accounted for by a small pilot lead.

Thus it appears the subject pilots were consistently adopting lead to partially offset the lag introduced by the displacement sensing stick

configuration. But the lead time constant is so small that it may not adversely effect the handling quality rating.

### **C. ROLL RATCHET POTENTIAL**

Consistent with the side-stick portion of the experiment, it is of interest to look at the roll ratchet potential for the center-stick configurations. A comparison of the typical phase lag data points in the vicinity of the NM frequency in Figs. 47 through 52 with the similar phase data points of Fig. 18 (sidestick) shows the controller/aircraft configurations used with the center-stick have much greater phase lag and therefore definitely are not candidates for roll ratchet. This excess lag is due to the cumulative effect of the command filter, the aircraft roll subsidence ( $T_R = 0.15$  sec), and the feel system lag (with displacement sensing).



## SECTION VII

### CONCLUSIONS AND RECOMMENDATIONS

Results of the experiments discussed herein together with those of Ref. 11 provide insight to key interactions between the pilot's neuromuscular system and the manipulator, feel system, control response command gain, and command prefilter elements in roll tracking type control tasks. The relative merits of stick displacement command versus stick force command have been quantified in terms of effective time delay, maximum control bandwidth, tracking performance, low and high frequency PIO tendency, pilot's neuromuscular mode peaking, etc. Potential trade-offs between response command gradient (gain), feel system force/displacement gradient, and effective time delay have been noted. The overall results provide insight and design guides for minimizing roll control problems in future high performance aircraft. Specific conclusions are:

- Manipulator Force Vs Displacement Sensing
  - Force Sensing
    - Minimizes forward loop dynamic lag because the manipulator/feel system lag is relegated to the feedback path of the pilot's neuromuscular limb position system
    - Results in lower tracking error in the simulation task
    - Minimum phase lag plus the associated decrease in signal attenuation at frequencies near the neuromuscular mode amplitude peak increases susceptibility to roll ratchet
    - Command prefiltering is generally required to prevent roll ratchet and other high frequency extraneous inputs
    - Caution must be exercised in selecting the prefilter time constant because excessive lag leads to low frequency PIO

- As a rule of thumb, the prefilter inverse time constant should be double the closed-loop control bandwidth required.

#### • Displacement Sensing

- Moves the manipulator/feel system dynamic characteristics to the forward loop command path
- Increases (slightly) the neuromuscular mode peaking over that obtained with force sensing
- Increases high frequency phase lag and command attenuation
- Reduces or eliminates any tendency to neuromuscular system induced roll ratchet if the manipulator/feel system dynamics lie in the region of the neuromuscular system 2nd order mode
- Reduces or eliminates the need for command prefiltering
- As a rule of thumb, the manipulator/feel system principal dynamic mode should be greater than the pilot's neuromuscular mode (approximately 12-13 rad/sec) to avoid adverse effect on tracking performance and flying qualities rating

#### • Side- vs Center -Stick

- The above apply equally to both types

#### • Response Command Gradient (Gain)

- All results (side- and center-stick) showed a preference for command gain of about 20 deg/sec/lb in both tracking and gross maneuvering in the simulation
- Based upon comparison with previous NT-33 flight experiments, it appears 10 deg/sec/lb is more appropriate for actual flight with small precise control input tasks (formation, tracking) but the 20 deg/sec/lb remains appropriate for gross maneuvering

- Command gains of less than 10 deg/sec/lb result in rapid degradation in control performance (bandwidth, tracking error) and flying qualities rating due to the high forces involved
- Degradation of CHPR with increasing effective time delay was less with command gain of 20 deg/sec/lb than with 10 deg/sec/lb
- Feel System Force/Displacement Gradient (for side-stick)
  - 0.65 lb/deg was rated best for precise tracking and following gross attitude changes
  - 1.22 lb/deg was found to be stiff and tiring
  - 0.33 lb/deg was too soft, producing a tendency to excessive stick deflection
  - Based upon flight test in the NT-33, it appears that gradients as high as 1.33 lb/deg may be acceptable in the presence of motion and atmospheric disturbances
- Manipulator/Feel System Dynamics
  - In the absence of appreciable command filter lag, there appears to be no difference in tracking performance or pilot preference (CHPR) between feel system dynamics as low as 14 rad/sec and 26 rad/sec.
- Feel/Command Filter Effective Time Delay
  - Flying quality rating degradation with increasing  $\tau_e$  was found to be consistent with the criterion of MIL-F-8785C with both the side- and center-stick configurations although there is some indication the Level I and II boundaries could be relaxed somewhat (especially for the side-stick)
  - Sensitivity to  $\tau_e$  decreased as command gain ( $K_c$ ) increased

- The distribution of principal lag between feel and command prefilter has essentially no influence on flying quality rating but tracking performance measures show preference for the lessor lag being located in the command filter
- Manipulator Configuration (side- vs center-stick)
  - Use of the side-stick resulted in significantly higher closed-loop control bandwidth and lower tracking error in the roll tracking task simulated, however, there was no significant difference in pilot rating

## REFERENCES

1. Magdaleno, Raymond E., Duane T. McRuer, and George P. Moore, Small Perturbation Dynamics of the Neuromuscular System in Tracking Tasks, NASA CR-1212, Dec. 1968.
2. Magdaleno, R. E., and D. T. McRuer, Experimental Validation and Analytical Elaboration for Models of the Pilot's Neuromuscular Subsystem in Tracking Tasks, NASA CR-1757, Apr. 1971.
3. McRuer, D. T., L. G. Hofmann, H. R. Jex, et al., New Approaches to Human-Pilot/Vehicle Dynamic Analysis, AFFDL-TR-67-150, Feb. 1968.
4. McRuer, D. T., and E. S. Krendel, Mathematical Models of Human Pilot Behavior, AGARDograph No. 188, Jan. 1974.
5. Powers, B. G., "An Adaptive Stick-Gain to Reduce Pilot-Induced Oscillation Tendencies," AIAA Journal of Guidance, Control, and Dynamics, Vol. 5, No. 2, Mar., Apr. 1982.
6. Garland, Michael P., Michael K. Nelson, and Richard C. Patterson, F-16 Flying Qualities with External Stores, AFFTC-TR-80-29, Feb. 1981.
7. Burton, R. A. and B. T. Kneeland Jr., "F/A-18 High Authority/High Gain Digital Flight Control System Development and Flight Testing," AIAA 81-2465, AIAA/SETP/SFTE/SAE/ITEA/IEEE First Flight Testing Conference, Las Vegas, NV, Nov. 11-13, 1981.
8. Sarrafian, S. K., "Flying Qualities Result," in X-29A Symposium, Initial Flight Results, Sept. 17-19, 1985.
9. Smith, R. E., and S. K. Sarrafian, "Effect of Time Delay on Flying Qualities: An Update," AIAA 86-2202, Aug. 1986.
10. Hoh, R. H., D. G. Mitchell, I. L. Ashkenas, et al., Proposed MIL Standard and Handbook - Flying Qualities of Air Vehicles, AFWAL-TR-82-3081, Vol. II, Nov. 1982.
11. Johnston, D. E., and D. T. McRuer, Investigation of Interactions Between Limb-Manipulator Dynamics and Effective Vehicle Roll Control Characteristics, NASA-CR-3983, May 1986.
12. Gordon-Smith, M., An Investigation into Certain Aspects of the Describing Function of a Human Operator Controlling a System of One Degree of Freedom, Univ. of Toronto, UTIAS Rept. No. 149, Feb. 1970.

13. Magdaleno, R. E., and D. T. McRuer, Effects of Manipulator Restraints on Human Operator Performance, AFFDL-TR-66-72, Dec. 1966.
14. McRuer, D. T., and R. E. Magdaleno, Human Pilot Dynamics with Various Manipulators, AFFDL-TR-66-138, Dec. 1966.
15. Mooij, H. A., W. P. de Boer, and M. F. C. van Gool Determination of Low-Speed Longitudinal Maneuvering Criteria for Transport Aircraft with Advanced Flight Control Systems, NLR TR-79127 U, Dec. 1979.
16. Hall, G. Warren, and Rogers E. Smith, Flight Investigation of Fighter Side-Stick Force-Deflection Characteristics, AFFDL-TR-75-39, May 1975.
17. Monagan, Stephen J., Rogers E. Smith, and Randall E. Bailey, Lateral Flying Qualities of Highly Augmented Fighter Aircraft, AFWAL-TR-81-3171, Mar. 1982.
18. Berry, D., "In-Flight Evaluation of Pure Time Delays in Pitch and Roll," AIAA 85-1852, Aug. 1985.

## APPENDIX A

### TRACKING STATION AND FEEL SYSTEM SET-UP

A sketch of the tracking station set-up with the right hand side-stick is presented in Fig. A-1. Key dimensions, angles, pivots, etc., are identified. It should be noted especially that the stick grip orientation was set to maximize comfort and minimize cross-axis coupling (although the experiment task was single axis). The center-stick set-up was essentially the same except for location of the stick and its pivot near the floor.

Manipulator/feel system force-displacement calibration plots are contained in Figs. A-2 through A-5. Also shown in each figure is a time trace of stick displacement to a step force release, i.e., the stick was held to one side and then the force released.

The force-displacement gradients shown here reflect measurements made at the top of the stick (for convenience). In the main text the side-stick gradients are referenced to the center of the grip for comparison with similar data from referenced experiments. The conversion is:

top of stick (lb/in)	center of grip (lb/deg)
6.39	1.22
3.44	0.65
1.71	0.33

When using the force sensing stick configurations it is necessary to incorporate a force signal deadboard (breakout) which matches the force-displacement breakout of the feel system. A calibration plot for this feature is presented in Fig. A-6.

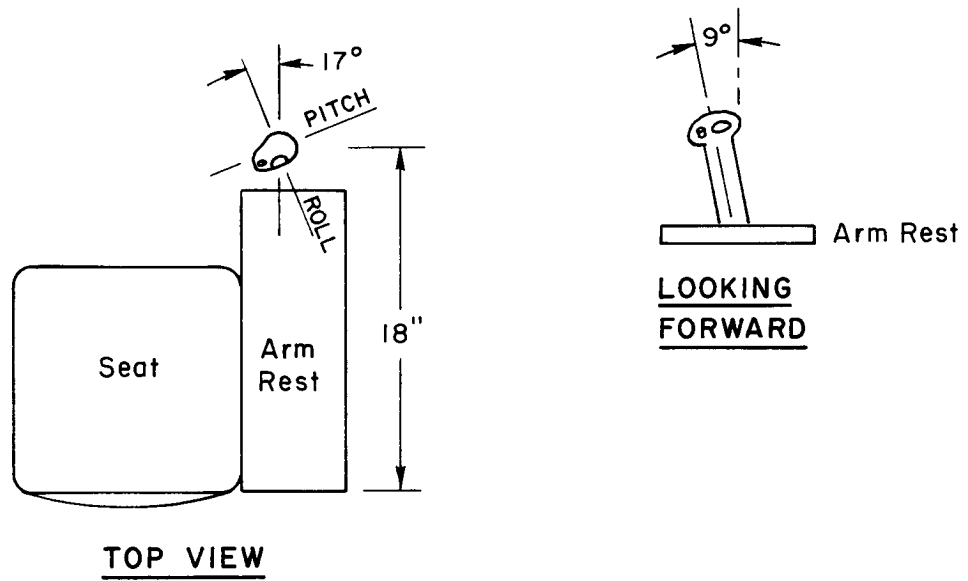
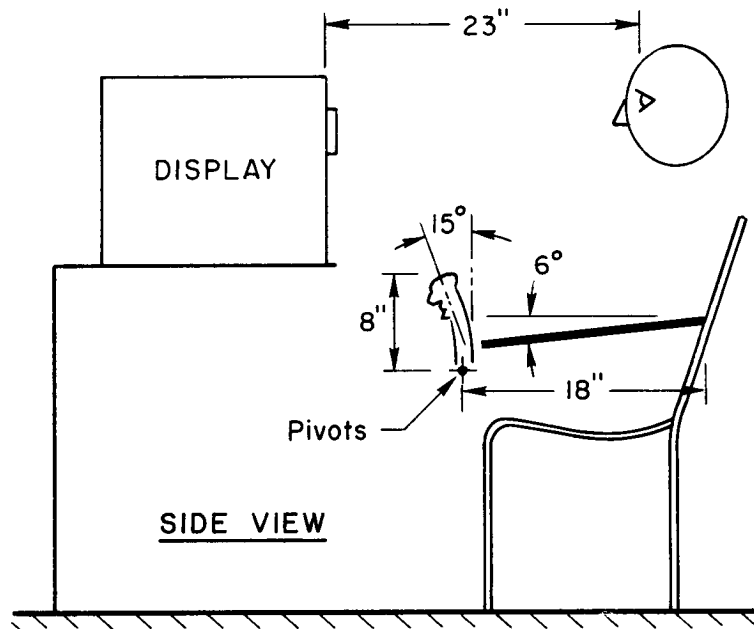
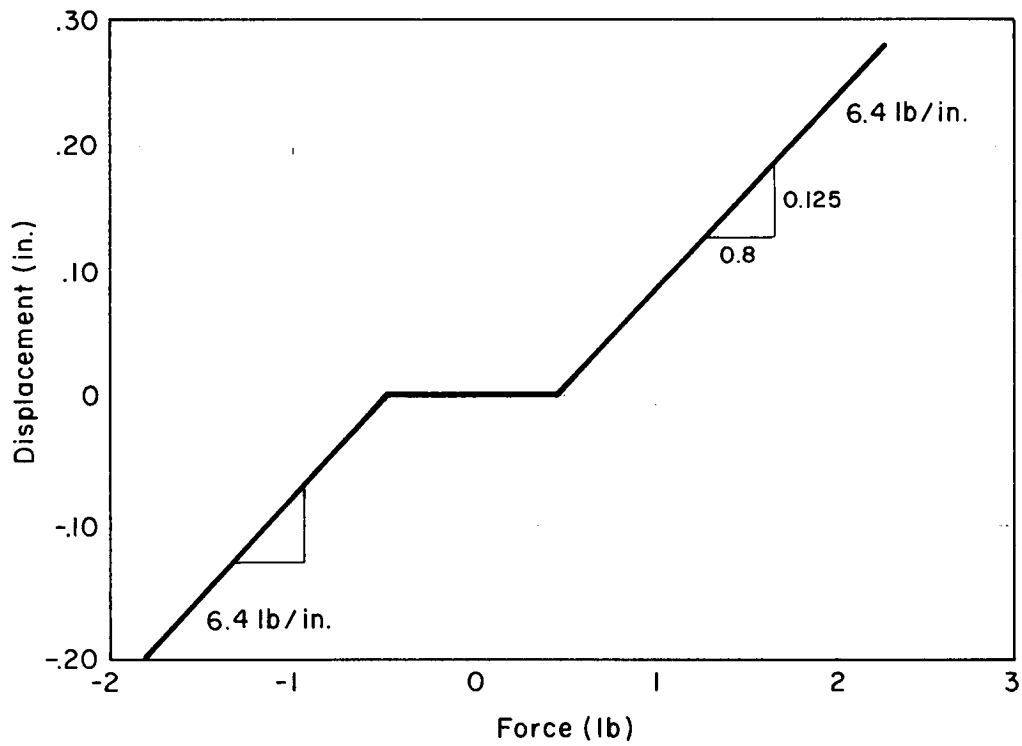
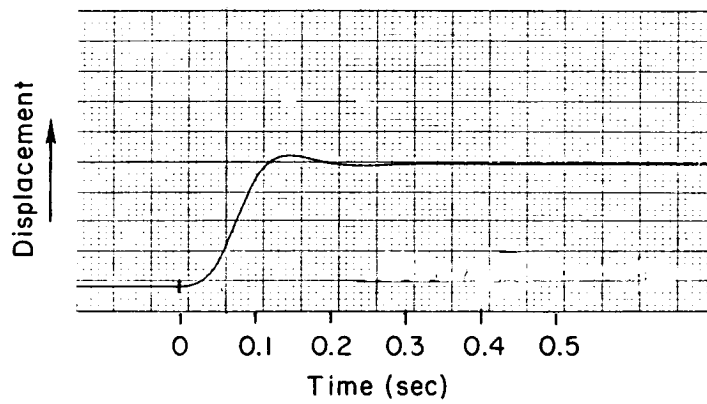


Figure A-1. Sidestick Tracking Station Set-Up



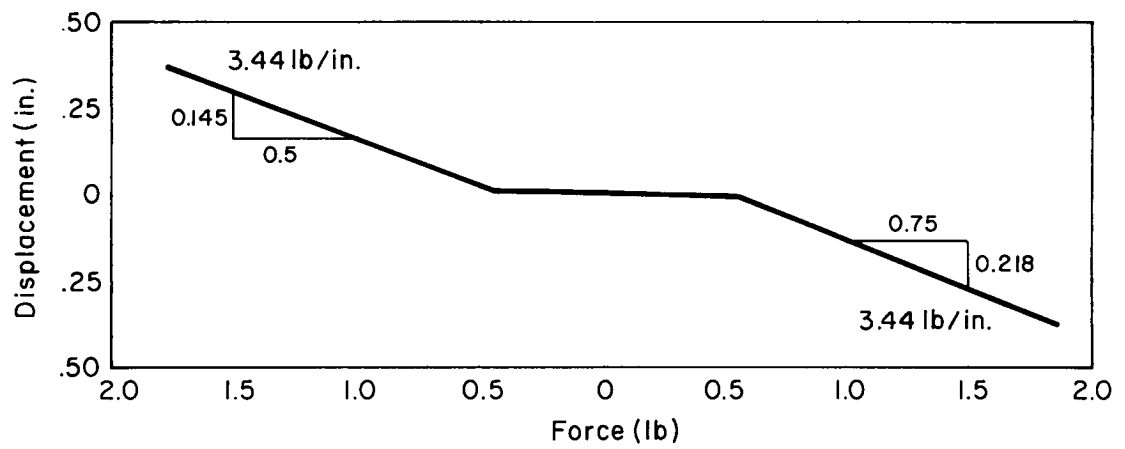


Force Gradient (top of stick)

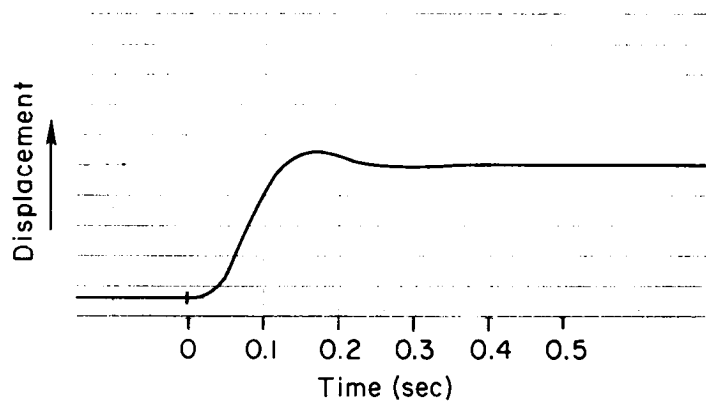


Step Response  $[\zeta; \omega] \doteq [0.7; 31.4]$

Figure A-2. Small Displacement (Stiff) Sidestick Calibration

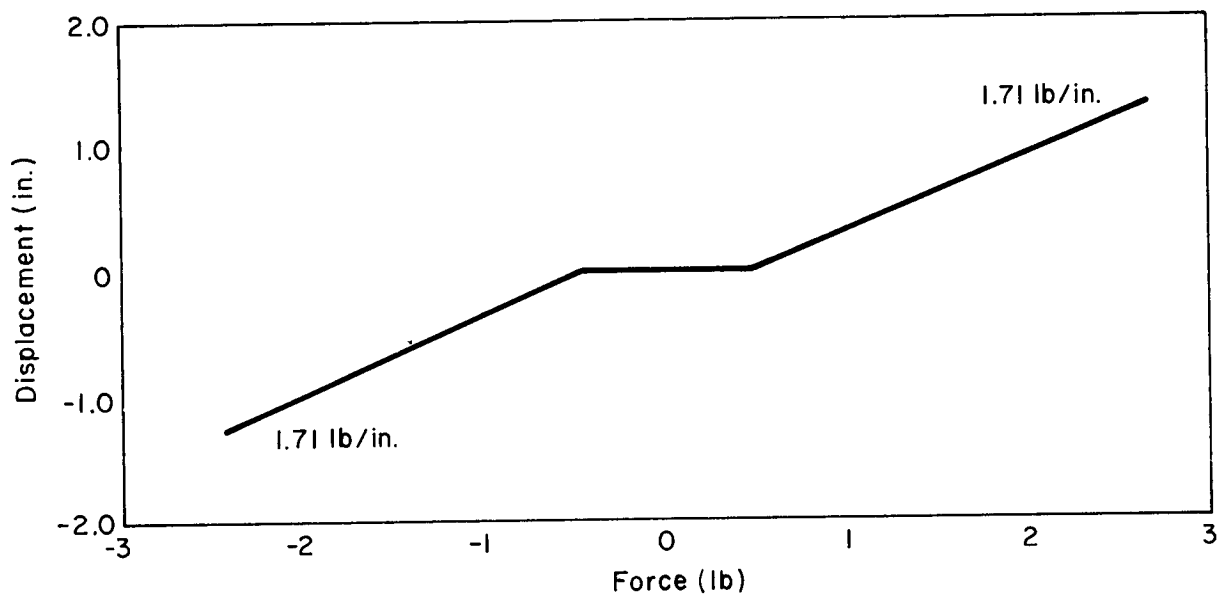


Force Gradient (top of stick)

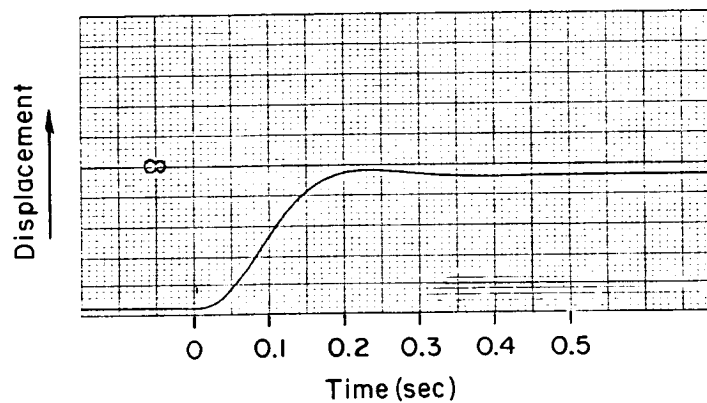


Step Response  $[\zeta; \omega] \doteq [0.6; 22.4]$

Figure A-3. Large Displacement (Medium) Sidestick Calibration

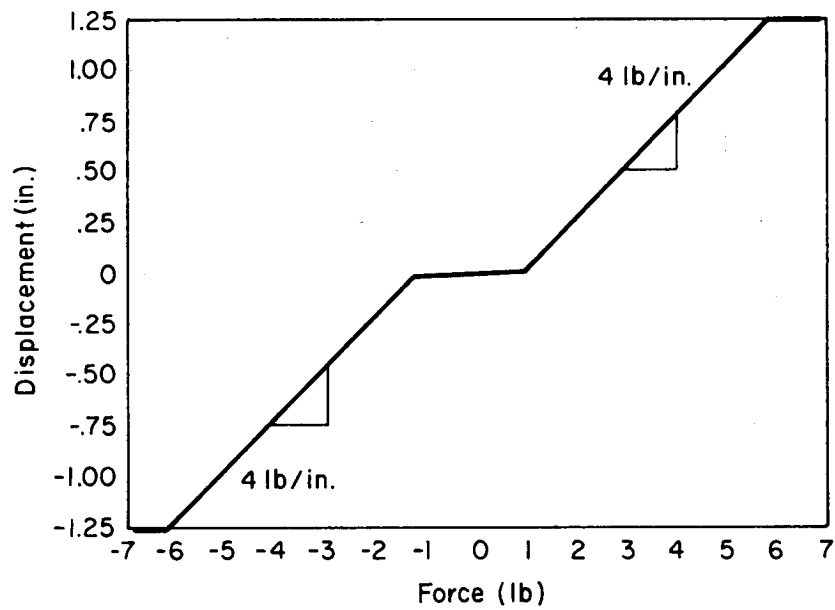


Force Gradient (top of stick)

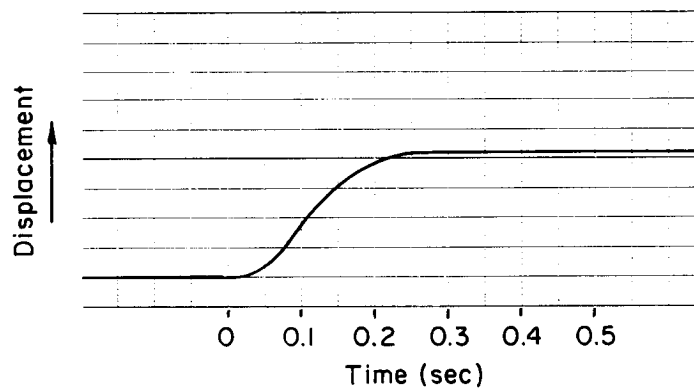


Step Response  $[\zeta; \omega] \doteq [0.71; 18.0]$

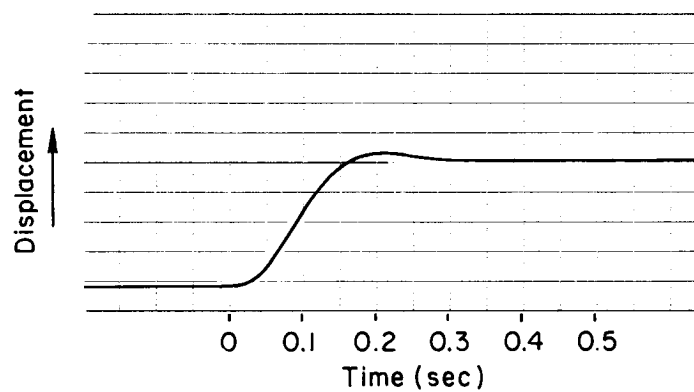
Figure A-4. Very Large Displacement (Soft) Sidestick Calibration



Force Gradient (top of stick)



Step Response  $[\zeta; \omega] \doteq [0.7; 14.0]$



Step Response  $[\zeta; \omega] \doteq [0.7; 26.0]$

Figure A-5. Center-Stick Calibration

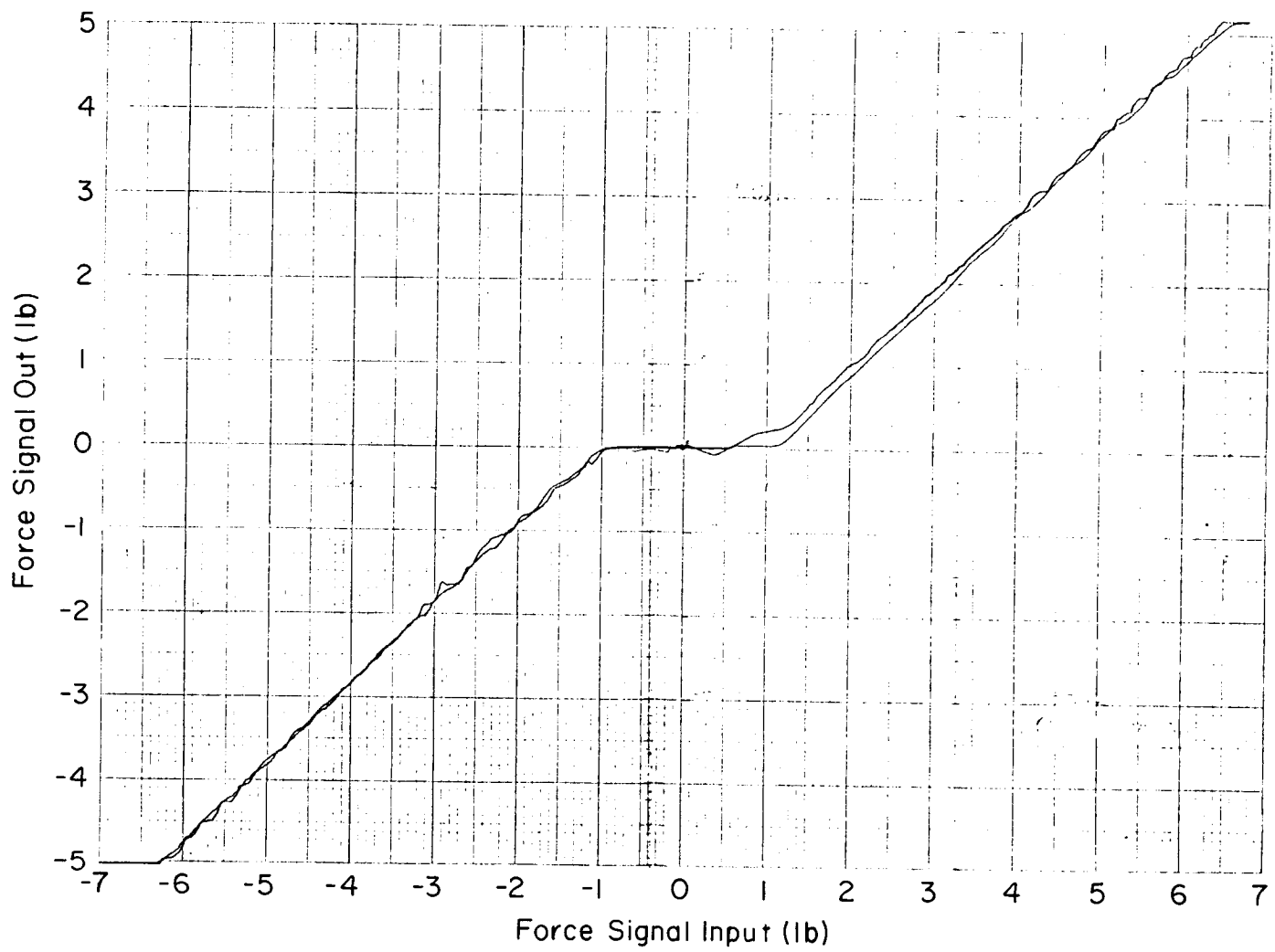
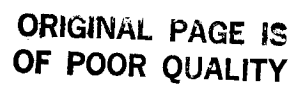


Figure A-6. Force Sensing Electrical Signal Breakout Calibration

## **APPENDIX B**

### **ANALOG COMPUTER CODING**

The roll tracking controlled element dynamics were implemented on an EAI-231-R analog computer. The computer coding diagram from the McFadden force loader analog signal inputs through to the display and strip chart recorder outputs is presented here. Also shown are the forcing function inputs from the digitally generated sum of sine waves and the various signals fed to the analog to digital (A/D) conversion for calculation of performance metrics and describing functions.



103

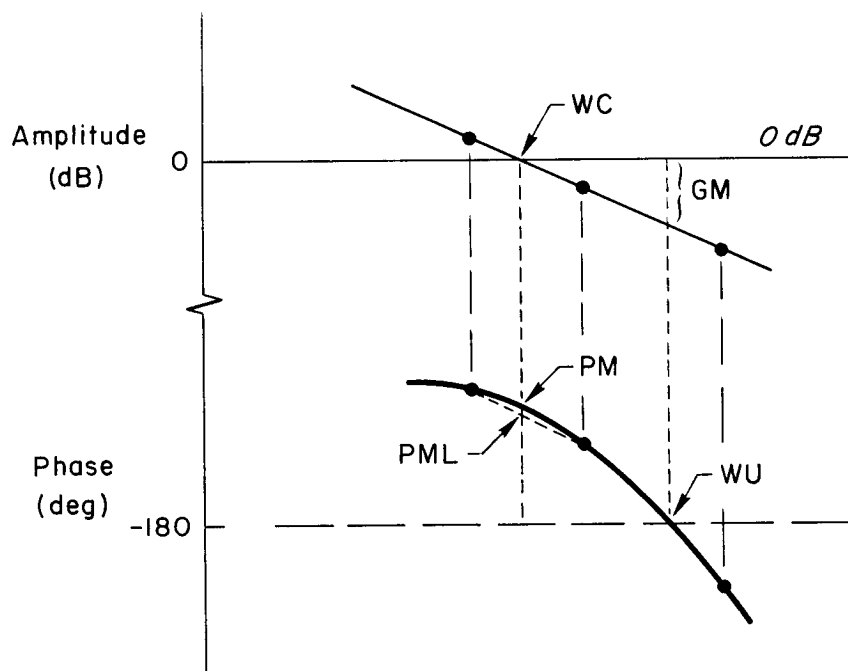
## APPENDIX C

### EXPERIMENT DATA

#### 1. Closed-Loop Performance Measures

Open and closed-loop describing function measures and parameters are calculated at the conclusion of each experiment run. Summary tables of closed-loop performance measures, interpolated open-loop describing function parameters, and experiment configuration parameter values across all experiment runs are contained in Table C-1 (center-stick experiment) and Table C-2 (side-stick experiment). The open and closed-loop parameters extracted are based on the extended crossover model (Ref. C-1) where the plant is assumed to be of the form

$$Y = \frac{K e^{-j(\tau_e \omega - \alpha/\omega)}}{s}$$





in the region of the crossover. A best "fit" to the describing function amplitude and phase data points for each run is made and the resulting plant and loop closure parameter extracted. These are identified in the table (and sketch) as follows:

ALPHA	-- plant open-loop low frequency phase droop parameter from the exponential $\alpha/\omega$
CBAR	-- average manipulator deflection during the data run (identifies any trim bias)
CHPR	-- Cooper-Harper Pilot Rating given for run
CSIG	-- one sigma rms value for manipulator deflection during the run
EBAR	-- average roll error in tracking run
ESIG	-- one sigma rms roll tracking error
F	-- force sensing stick (experiment configuration)
GM	-- Bode open-loop gain margin at frequency of $180^\circ$ phase crossover, $\omega_u$ ; computed from straight line interpolation between describing function amplitude data points immediately above and below computed $\omega_u$
$K_c$	-- Response command gain (experiment configuration)
P	-- position (displacement) sensing sticks (experiment configuration)
P	-- Bode open-loop phase margin at frequency of closed-loop gain crossover, $\omega_c$ ; computed from the complete extended crossover model
PML	-- Bode open-loop phase margin at frequency of closed-loop gain crossover, $\omega_c$ ; computed from a straight line interpolation between the two describing function data points immediately above and below $\omega_c$
SLOPE	-- slope of Bode open-loop amplitude asymptote between two data points immediately above and below gain crossover frequency
Tau	-- equivalent time delay set into effective controlled element
TE	-- plant open-loop high frequency time delay parameter from the exponential $\tau\omega$

$T_r$	-- first order lag time constant set into effective controlled element (represents aircraft roll subsidence mode or first order command prefilter)
WC	-- crossover frequency - frequency of crossover between open-loop 0 db line and Bode amplitude asymptote calculated from straight line fit between two describing function data points immediately above and below crossover
WF	-- command filter frequency (second order) (experiment configuration)
WS	-- feel system (stick) frequency (second order) (experiment configuration)
WU	-- unstable frequency - frequency at which system open-loop phase plot crosses the 180 deg line (calculated from complete extended crossover model)

## 2. $Y_p Y_c$ Describing Function Plots

The remainder of Appendix C contains the computer generated opened-loop  $Y_p Y_c$  plots for all experimental runs. Runs 01A1 through 8A141 were with the center-stick. Runs 15A142 through 22A379 reflect the side-stick manipulator with the various feel system gradient, filter, and time delay configurations.

## 3. Reference

- C-1 Jex, Henry R., R. Wade Allen, and Raymond E. Magdaleno, Display Format Effects on Precision Tracking Performance, Describing Functions, and Remnant, AMRL-TR-71-6, Aug. 1971.

TABLE C-1. CLOSED-LOOP TRACKING MEASURES, CENTER-STICK

RUN	TYPE	WS	WF	CHPR	EBAR	ESIG	ROLL	TRACKING 1 AUG 86				PML	SLOPE	TE	ALPHA	MU	GM
							CENTER	STICK	CSIG	WC	PH						
01A1	F	14	26		0.67	10.55	-0.10	5.26	5.03	7.06	2.00	-17.5	0.22	1.71	5.27	0.4	
01A2	F	14	26		0.83	9.19	-0.13	3.45	3.22	34.14	32.98	-14.6	0.29	0.16	4.27	1.5	
01A3	F	14	26		0.73	8.75	-0.14	3.76	4.16	26.11	22.77	-6.2	0.31	-0.01	5.22	0.6	
01A4	F	14	26	3	1.30	9.60	-0.12	3.26	3.63	20.97	20.10	-16.3	0.30	-0.09	5.00	2.3	
01A5	F	14	26	3	1.27	9.07	-0.13	3.26	2.79	43.59	41.51	-23.5	0.25	0.35	5.09	3.2	
01A6	F	14	26	3	1.52	8.73	-0.19	3.20	3.33	31.98	31.22	-17.6	0.29	0.11	5.00	1.6	
01A7	F	14	0	2	0.35	8.34	-0.12	2.06	3.13	34.49	32.98	-19.7	0.20	0.32	5.69	4.2	
01A8	F	14	0	2	0.44	7.69	-0.17	2.93	3.16	37.64	36.33	-21.6	0.26	0.32	5.43	2.3	
01A9	F	14	0	2	-0.54	8.55	-0.17	2.98	2.75	42.07	40.74	-20.3	0.30	-0.01	4.06	3.5	
01A10	P	14	0	3	-0.61	9.03	-0.15	2.69	2.59	36.03	34.18	-24.0	0.30	0.40	4.60	5.5	
01A11	P	14	0	3	-0.54	10.00	-0.18	2.73	2.50	42.01	39.61	-15.3	0.26	0.46	5.00	3.2	
01A12	P	14	0	3	-0.00	9.11	-0.20	3.04	3.01	37.91	36.14	-16.4	0.27	0.32	4.53	1.9	
01A13	P	14	26	4	-1.22	11.65	-0.14	3.04	2.62	35.00	33.12	-17.0	0.20	0.56	4.74	3.4	
01A14	P	14	26	4	0.13	11.44	-0.14	2.82	2.30	43.00	40.76	-17.5	0.37	-0.07	4.14	3.3	
01A15	P	14	26	4	-1.00	10.35	-0.10	2.42	2.20	45.10	43.23	-21.6	0.32	0.19	5.29	6.7	

TABLE C-1. (CONTINUED)

RUN	FILE	TYPE	Kc	HS	HF	CHPR	EBAR	ROLL TRACKING RUNS OF 4-AUG-86				ALPHA	MU	GM				
								STICK	CSIG	WC	FORCE							
16	4R16	F	10.00	14.00	0.00		-0.13	7.60	-0.14	2.30	2.04	43.22	41.29	-24.70	0.30	-0.08	6.21	10.40
17	4R17	F	10.00	14.00	0.00	3.00	0.12	6.57	-0.15	2.41	3.11	39.04	30.42	-26.50	0.26	0.25	5.19	7.30
18	4R18	F	10.00	14.00	0.00	3.00	0.00	6.01	-0.15	2.35	2.09	46.75	45.00	-30.30	0.23	0.29	5.84	5.90
19	4R19	F	10.00	14.00	0.00	3.00	-1.33	7.29	-0.15	2.50	3.09	45.00	44.59	-17.60	0.22	0.29	5.69	4.50
20	4R20	P	10.00	14.00	0.00	4.00	0.15	8.31	-0.13	2.61	2.84	33.69	31.34	-25.70	0.34	0.06	5.24	5.20
21	4R21	P	10.00	14.00	0.00	4.00	-0.54	8.72	-0.17	2.41	2.30	43.67	41.42	-27.00	0.26	0.46	4.72	6.00
22	4R22	P	10.00	14.00	0.00	4.00	1.32	8.12	-0.15	2.30	2.55	30.72	36.15	-25.20	0.30	0.31	4.56	5.00
23	4R23	P	10.00	14.00	0.00	6.00	0.99	9.71	-0.16	2.07	2.68	32.76	30.01	-19.50	0.31	0.44	4.20	4.00
24	4R24	P	10.00	14.00	0.00	6.00	-1.41	8.49	-0.14	2.62	2.65	35.27	32.61	-27.00	0.30	0.39	4.32	4.10
25	4R25	P	10.00	14.00	0.00	6.00	0.75	9.10	-0.15	2.70	2.63	34.36	31.64	-23.00	0.31	0.38	4.34	4.10
26	4R26	F	10.00	14.00	0.00	3.00	0.00	7.82	-0.17	2.43	2.93	42.04	40.22	-22.70	0.26	0.19	4.79	4.90
27	4R27	F	10.00	14.00	0.00	3.00	0.34	7.19	-0.16	2.43	3.07	41.49	40.02	-26.70	0.25	0.23	4.96	3.60
28	4R28	F	10.00	14.00	0.00	3.00	-0.26	7.46	-0.13	2.45	2.81	41.71	39.62	-25.60	0.28	0.13	5.10	4.20
29	4R29	F	10.00	14.00	0.00	2.00	0.40	6.04	-0.15	2.41	3.10	46.48	45.21	-29.00	0.21	0.37	5.45	4.90
30	4R30	F	10.00	14.00	0.00	2.00	-0.52	6.31	-0.17	2.25	2.72	54.26	52.59	-34.90	0.20	0.23	5.46	5.70
31	4R31	P	20.00	14.00	0.00		-0.32	7.13	-0.11	2.95	3.71	20.31	24.52	-13.10	0.31	-0.05	4.09	1.00
32	4R32	P	20.00	14.00	0.00	3.00	-0.01	6.17	-0.16	2.62	3.94	20.36	25.69	-11.90	0.39	-1.77	4.77	1.00
33	4R33	P	20.00	14.00	0.00	3.00	-0.07	6.05	-0.13	2.71	3.40	32.03	32.36	-22.10	0.26	0.44	4.64	1.60
34	4R34	P	20.00	14.00	0.00	3.00	-0.19	7.08	-0.17	3.10	4.22	23.26	20.63	-13.30	0.28	0.32	5.10	1.60
35	4R35	F	20.00	14.00	0.00	2.00	-0.03	5.56	-0.13	3.14	5.13	11.49	6.00	-19.20	0.26	0.31	5.66	0.00
36	4R36	F	20.00	14.00	0.00	2.00	-1.10	6.34	-0.13	3.10	5.27	10.55	6.06	-20.50	0.25	0.30	5.74	0.00
37	4R37	F	20.00	14.00	0.00	5.00	-0.34	9.00	-0.14	3.77	4.02	10.31	6.00	-6.30	0.31	0.61	4.30	0.20
38	4R38	P	20.00	14.00	0.00	5.00	-2.96	9.40	-0.14	3.02	4.25	4.96	0.45	-6.50	0.32	0.48	4.20	0.00
39	4R39	P	20.00	14.00	0.00	5.00	0.32	8.49	-0.13	3.20	3.65	20.67	19.62	-11.50	0.30	0.37	4.61	1.20
40	4R40	P	20.00	14.00	0.00	2.00	-0.48	7.42	-0.13	3.19	3.71	26.69	25.33	-9.40	0.28	0.24	5.13	1.30
41	4R41	F	20.00	14.00	0.00	2.00	0.35	7.02	-0.14	3.12	4.44	13.40	0.93	-13.30	0.30	0.07	4.93	0.60
42	4R42	F	20.00	14.00	0.00	2.00	-0.35	6.94	-0.15	3.32	4.74	0.01	3.02	-13.30	0.28	0.56	4.93	0.20
43	4R43	F	20.00	14.00	0.00	2.00	-0.39	6.94	-0.15	3.32	4.74	0.01	3.02	-13.30	0.28	0.56	4.93	0.20
44	4R44	F	20.00	26.00	14.00	7.00	0.00	12.60	-0.13	5.31	3.09	30.39	20.72	-23.90	0.35	-0.17	6.50	5.20
45	4R45	F	20.00	26.00	14.00	7.00	-0.13	10.53	-0.23	4.49	0.20	-53.54	-57.00	-95.00	-0.01	21.24	4.04	-2.40
46	4R46	F	20.00	26.00	14.00	7.00	-1.09	9.19	-0.23	4.24	4.46	11.74	7.19	-0.10	0.29	4.09	4.09	0.30
47	4R47	F	20.00	26.00	14.00	7.00	-1.51	8.14	-0.09	3.04	4.07	11.65	7.93	-16.90	0.36	-0.43	4.30	0.50
48	4R48	P	20.00	26.00	0.00	5.00	-0.06	7.13	-0.16	2.51	2.72	30.33	35.91	-33.10	0.29	0.31	4.93	4.30
49	4R49	P	20.00	26.00	0.00	5.00	-1.41	7.01	-0.16	2.45	2.91	45.30	43.51	-25.60	0.20	0.54	5.40	3.20
50	4R50	P	20.00	26.00	0.00	5.00	-2.55	7.08	-0.14	2.73	2.99	30.33	36.72	-30.10	0.26	0.59	6.05	3.70
51	4R51	F	20.00	26.00	0.00	3.00	-1.16	7.24	-0.16	3.01	3.73	29.67	20.33	-14.00	0.24	0.58	5.04	2.70
52	4R52	F	20.00	26.00	0.00	3.00	-0.79	6.65	-0.13	3.70	4.00	16.34	11.05	-14.00	0.24	0.57	5.78	1.20
53	4R53	F	20.00	26.00	0.00	3.00	-1.69	6.02	-0.11	3.37	4.64	26.30	22.52	-16.10	0.23	0.11	0.54	-23.20
54	4R54	P	20.00	26.00	14.00	5.00	-0.40	10.04	-0.14	3.43	2.94	19.97	17.20	-29.70	0.34	0.70	8.04	3.30
55	4R55	P	20.00	26.00	14.00	5.00	-0.34	9.34	-0.12	2.93	2.56	30.23	27.25	-24.00	0.37	0.20	4.00	4.10
56	4R56	P	20.00	26.00	14.00	5.00	-1.42	9.05	-0.17	2.70	2.65	33.94	31.21	-24.40	0.30	0.45	4.32	4.00
57	4R57	F	20.00	26.00	14.00	4.00	-0.20	9.01	-0.10	4.10	5.11	3.72	-1.32	-3.70	0.34	-1.00	5.05	0.00
58	4R58	F	20.00	26.00	14.00	4.00	-3.00	9.07	-0.14	3.79	3.52	22.56	22.47	-9.90	0.36	-0.37	4.32	0.90

TABLE C-1. (CONTINUED)

FILE	TYPE	Kc	Ws	WF	CHPR	EBAR	RUNS OF 5-RUG-86			DSIG	WC	PH	PML	SLOPE	TE	ALPHA	HU	GM
							STICK	ROLL	TRACKING									
CENTER																		
IN POS & FORCE)																		
ESTG																		
CBAR																		
DSIG																		
WC																		
PH																		
PML																		
SLOPE																		
TE																		
ALPHA																		
HU																		
GM																		
59	F	20.00	26.00	0.00	3.00	-0.37	8.07	-0.12	2.51	2.55	30.31	35.72	-25.20	0.29	0.42	5.65	5.30	
5959	F	20.00	26.00	0.00	3.00	-0.71	8.73	-0.18	3.01	2.91	36.45	34.36	-20.30	0.28	0.32	5.16	4.08	
5960	F	20.00	26.00	0.00	3.00	0.24	7.76	-0.16	2.87	3.19	37.24	36.02	-20.10	0.25	0.35	4.81	2.30	
5961	F	20.00	26.00	0.00	3.00	-0.62	11.20	-0.19	2.80	2.10	41.12	39.89	-17.60	0.36	0.16	4.02	2.30	
5962	F	20.00	26.00	14.00	3.00	-0.24	11.12	-0.11	2.72	2.30	39.77	36.22	-20.00	0.39	-0.06	3.01	3.40	
5963	F	20.00	26.00	14.00	3.00	-1.26	12.01	-0.13	2.61	1.92	40.20	36.22	-20.00	0.42	-0.16	3.68	6.40	
5964	F	20.00	26.00	14.00	3.00	-1.28	14.20	-0.19	2.73	1.52	52.61	51.60	-22.20	0.35	0.18	3.47	11.40	
5965	P	20.00	26.00	14.00	5.00	-1.28	14.20	-0.19	2.73	1.52	52.61	51.60	-22.20	0.35	0.18	3.47	11.40	
5966	P	20.00	26.00	14.00	5.00	-0.03	11.75	-0.18	3.01	2.09	39.32	36.64	-20.50	0.39	0.17	3.69	4.30	
5967	P	20.00	26.00	14.00	5.00	-1.41	13.31	-0.09	2.97	2.15	34.77	32.69	-15.60	0.39	0.25	3.90	4.00	
5968	P	20.00	26.00	0.00	4.00	-1.44	9.78	-0.19	2.91	2.11	52.21	50.91	-22.40	0.20	0.16	4.71	5.10	
5969	P	20.00	26.00	0.00	4.00	-2.16	10.49	-0.16	2.34	2.03	53.31	52.33	-21.50	0.30	0.08	5.55	6.10	
5970	P	20.00	26.00	0.00	4.00	-2.03	9.29	-0.13	2.70	2.71	47.74	45.01	-16.60	0.34	-0.53	7.10	6.30	
5971	F	20.00	26.00	14.00	3.00	-2.36	11.00	-0.16	2.84	2.24	46.36	44.46	-16.50	0.29	0.27	4.60	3.70	
5972	F	20.00	26.00	14.00	3.00	-0.99	9.73	-0.12	2.94	2.45	44.76	42.46	-21.10	0.35	-0.20	4.10	3.50	
5973	F	20.00	26.00	14.00	3.00	-1.01	13.00	-0.06	2.53	1.72	49.05	48.46	-15.00	0.50	-0.24	4.46	5.60	
5974	F	10.00	26.00	14.00	5.00	-7.96	20.48	-0.08	3.41	1.74	50.77	50.47	-56.90	0.60	-0.49	0.49	-5.00	
5975	F	10.00	26.00	14.00	5.00	-2.09	11.32	-0.07	2.90	2.21	45.65	43.76	-19.10	0.35	0.00	4.55	5.00	
5976	F	10.00	26.00	14.00	5.00	-0.79	9.69	-0.06	2.34	1.94	47.48	46.92	-22.30	0.36	0.07	4.35	5.70	
5977	F	10.00	26.00	0.00	4.00	-1.20	10.06	-0.10	1.97	1.88	55.16	55.19	-24.40	0.19	0.09	6.70	9.00	
5978	F	10.00	26.00	0.00	4.00	-0.72	10.06	-0.10	1.97	1.94	59.56	59.19	-18.50	0.25	0.09	4.84	7.40	
5979	F	10.00	26.00	0.00	4.00	-0.40	9.31	-0.11	2.11	2.19	57.52	56.16	-23.40	0.27	-0.07	4.92	5.40	
5980	P	10.00	26.00	14.00	5.00	-2.16	13.44	-0.06	2.10	1.74	49.55	49.06	-18.70	0.52	-0.34	4.02	8.10	
5981	P	10.00	26.00	14.00	5.00	-2.36	12.46	-0.11	2.20	1.70	59.02	59.55	-11.50	0.28	0.04	3.09	5.50	
5982	P	10.00	26.00	14.00	5.00	-1.79	12.40	-0.11	2.34	1.96	56.53	55.90	-19.50	0.39	-0.37	4.11	7.00	
5983	P	10.00	26.00	0.00	4.00	0.01	12.53	-0.11	1.96	1.26	67.56	67.23	-14.00	0.17	0.22	4.00	11.00	
5984	P	10.00	26.00	0.00	4.00	-2.14	13.41	-0.11	1.75	1.33	70.23	69.73	-10.90	0.37	-0.20	4.53	0.30	
5985	P	10.00	26.00	0.00	4.00	-1.54	9.77	-0.11	2.17	2.36	60.31	59.09	-25.20	0.16	0.35	5.11	4.70	

FILE	TYPE	Kc	Ms	Wf	CHPR	EDBR	ESIG	CBRR	CSIG	WC	PH	PHL	SLOPE	YE	ALPHA	WU	G1
7866	F	10.00	26.00	0.00	Practice	0.68	7.27	-0.14	2.57	2.94	42.13	40.37	-26.78	0.28	0.83	5.18	4.48
7867	F	20.00	26.00	0.00	1.00	-0.06	6.55	-0.14	2.95	3.79	29.53	27.91	-12.00	0.23	0.73	6.17	2.70
7868	F	20.00	26.00	0.00	1.00	0.09	6.33	-0.14	2.76	3.57	31.41	31.08	-13.70	0.25	0.51	5.74	2.88
7869	F	20.00	26.00	0.00	1.00	0.18	6.95	-0.12	2.82	3.55	28.19	27.94	-14.40	0.19	1.40	7.04	4.20
7890	F	20.00	26.00	14.00	2.00	0.24	6.00	-0.09	2.69	3.00	32.62	30.72	-23.00	0.35	-0.14	4.65	2.80
7891	F	20.00	26.00	14.00	2.00	0.07	8.26	-0.09	2.72	3.41	32.63	33.41	-23.10	0.36	-0.56	4.61	2.40
7892	F	20.00	26.00	14.00	2.00	-1.19	7.96	-0.13	2.73	3.03	36.08	34.36	-21.50	0.32	-0.11	4.77	3.20
7893	F	10.00	26.00	0.00	3.00	0.06	7.02	-0.14	2.32	2.50	50.78	40.83	-20.90	0.19	0.55	5.84	5.10
7894	F	10.00	26.00	0.00	3.00	0.21	7.73	-0.14	2.28	2.41	40.29	46.24	-31.60	0.22	0.48	5.69	6.08
7895	F	10.00	26.00	0.00	3.00	0.08	7.89	-0.11	2.10	2.30	52.00	50.98	-27.30	0.22	0.28	6.45	5.68
7896	P	10.00	26.00	0.00	3.50	0.67	8.94	-0.15	2.29	2.22	44.56	42.67	-25.60	0.27	0.43	4.43	6.48
7897	P	10.00	26.00	0.00	3.50	-0.05	8.56	-0.13	2.22	2.34	51.71	49.81	-25.00	0.33	-0.23	5.14	5.30
7898	P	10.00	26.00	0.00	3.50	0.95	8.10	-0.15	2.38	2.44	45.72	43.53	-22.60	0.23	0.50	5.80	6.10
7899	F	10.00	26.00	14.00	4.00	0.08	8.97	-0.13	2.05	2.88	30.34	27.91	-27.00	0.31	0.45	4.32	3.00
78100	F	10.00	26.00	14.00	4.00	-0.66	8.54	-0.14	2.29	2.27	42.42	40.30	-27.30	0.29	0.39	4.47	5.00
78101	F	10.00	26.00	14.00	4.00	-0.36	8.59	-0.15	2.49	2.64	40.23	37.79	-22.30	0.26	0.52	4.50	3.48
78102	P	10.00	26.00	14.00	5.00	-0.70	9.03	-0.12	2.61	2.42	35.53	32.09	-21.90	0.40	-0.01	4.38	6.10
78103	P	10.00	26.00	14.00	5.00	-0.34	8.96	-0.09	2.62	2.67	30.78	27.05	-21.80	0.35	0.26	4.20	3.00
78104	P	10.00	26.00	14.00	5.00	-1.02	8.96	-0.16	2.75	2.63	29.50	26.62	-25.90	0.33	0.48	4.06	3.90

TABLE C-1. (CONCLUDED)

RUN	FILE	TYPE	Kc	M5	WF	CHPR	EBAR	ROLL TRACKING RUNS OF 8-AUG-86										G1
								STICK (1 lb. BO IN POS & FORCE)										
								RHH										
CENTER								ESTG	CBAR	CSIG	MC	PH	PML	SLOPE	TE	RLPHA	WU	
105	8A105	F	18.00	14.00	0.00	3.00	-0.82	7.74	-0.13	2.44	2.97	43.79	42.17	-21.98	0.28	-0.08	5.69	5.10
106	8A106	F	18.00	14.00	0.00	3.00	-0.13	8.21	-0.11	2.42	2.81	49.64	47.91	-19.88	0.26	-0.84	5.57	5.59
107	8A107	F	18.00	14.00	0.00	3.00	-0.12	7.42	-0.12	2.28	2.87	51.83	49.44	-29.30	0.23	0.09	5.76	5.20
108	8A108	P	18.00	14.00	0.00	5.00	-0.32	9.39	-0.14	2.50	2.51	43.11	48.75	-23.70	0.31	0.08	4.72	4.90
109	8A109	P	18.00	0.00	0.00	5.00	-1.72	9.20	-0.12	2.24	2.27	48.25	46.32	-21.58	0.31	0.05	4.84	5.70
110	8A110	P	18.00	14.00	0.00	5.00	-0.78	9.51	-0.15	2.33	2.36	46.37	44.23	-21.08	0.31	0.08	4.25	6.70
111	8A111	F	18.00	26.00	4.50	4.50	-0.83	9.45	-0.14	2.64	2.71	45.69	47.40	-17.40	0.30	-0.21	4.77	2.60
112	8A112	F	18.00	14.00	26.00	4.50	-1.27	10.14	-0.15	2.30	2.39	50.35	48.37	-20.70	0.29	-0.82	6.87	8.30
113	8A113	F	18.00	14.00	26.00	4.50	-1.71	9.82	-0.13	2.11	1.93	58.69	58.38	-20.50	0.30	-0.05	4.53	7.20
114	8A114	P	18.00	14.00	26.00	4.50	-0.75	10.22	-0.13	2.22	2.02	52.08	51.09	-21.08	0.35	-0.13	4.89	7.70
115	8A115	P	18.00	14.00	26.00	4.50	-1.67	9.56	-0.13	2.47	2.48	48.59	38.09	-22.90	0.33	0.08	4.21	4.20
116	8A116	P	18.00	14.00	26.00	4.50	-1.04	10.84	-0.17	2.31	2.09	47.85	45.67	-22.60	0.29	0.30	4.49	14.60
117	8A117	P	20.00	14.00	26.00	5.00	-0.91	10.34	-0.15	2.73	2.40	42.31	39.93	-29.30	0.34	0.05	4.10	6.80
118	8A118	P	20.00	14.00	26.00	5.00	-1.98	9.90	-0.12	3.23	2.42	42.89	40.54	-12.90	0.30	0.23	4.36	2.50
119	8A119	P	20.00	14.00	26.00	5.00	-1.71	10.13	-0.14	3.35	2.51	42.68	48.31	-15.90	0.24	-0.59	4.92	-0.70
120	8A120	F	20.00	14.00	26.00	3.00	-1.90	8.76	-0.15	2.61	2.03	52.84	51.32	-31.00	0.28	-0.39	5.35	4.00
121	8A121	F	20.00	14.00	26.00	3.00	-2.66	8.91	-0.17	2.54	2.44	52.84	50.97	-15.10	0.26	0.04	4.84	3.70
122	8A122	F	20.00	14.00	26.00	3.00	-0.79	8.70	-0.12	2.29	2.64	49.51	47.55	-19.90	0.32	-0.34	4.85	5.20
123	8A123	F	20.00	0.00	0.00	3.00	-2.74	9.09	-0.13	2.02	2.07	60.08	59.94	-20.30	0.26	-0.08	7.34	7.40
124	8A124	F	20.00	14.00	0.00	3.00	-1.19	8.18	-0.15	2.45	2.79	50.94	49.21	-25.10	0.21	0.24	5.74	4.30
125	8A125	F	20.00	0.00	0.00	3.00	-0.68	6.87	-0.13	2.35	2.91	53.61	52.27	-27.40	0.28	-0.49	6.11	5.40
126	8A126	P	20.00	14.00	0.00	3.00	-0.21	8.68	-0.14	2.16	2.42	53.42	51.58	-24.48	0.27	-0.84	5.26	6.60
128	8A128	P	20.00	14.00	0.00	3.00	-2.16	8.42	-0.17	2.73	2.52	58.25	48.25	-25.70	0.29	-0.09	5.61	4.50
129	8A129	P	20.00	14.00	0.00	3.00	-0.78	8.71	-0.17	2.08	2.93	39.55	37.67	-18.10	0.30	0.01	4.73	3.70

	F	20.00	14.00	0.00	2.00	0.26	6.71	-0.13	2.67	3.57	36.58	36.22	-13.40	0.24	0.22	6.06	3.10
130	001130																
131	001131	F	20.00	14.00	0.00	0.49	6.09	-0.13	2.54	3.69	36.97	35.90	-13.90	0.25	0.82	6.00	3.00
132	001132	F	20.00	14.00	0.00	-0.91	6.10	-0.13	2.62	3.64	36.10	35.31	-15.40	0.23	0.35	6.30	3.00
135	001135	F	20.00	14.00	26.00	0.48	6.55	-0.14	2.96	4.94	7.99	3.84	-4.90	0.33	-0.30	4.69	0.10
134	001134	F	20.00	14.00	26.00	0.43	7.23	-0.11	2.72	3.31	35.69	34.94	-20.40	0.29	-0.04	5.56	2.50
135	001135	F	20.00	14.00	26.00	-0.26	7.68	-0.13	2.57	3.27	38.27	37.43	-19.60	0.30	-0.25	5.15	1.90
136	001136	F	10.00	14.00	26.00	1.62	9.15	-0.16	2.42	2.40	41.17	30.00	-27.60	0.25	0.63	4.82	6.30
137	001137	F	10.00	14.00	26.00	1.62	8.02	-0.15	2.53	2.55	43.39	41.06	-27.60	0.25	0.45	4.60	4.60
138	001138	F	10.00	14.00	26.00	0.29	8.11	-0.16	2.15	2.29	51.67	49.06	-24.00	0.31	-0.09	4.99	5.00
139	001139	F	10.00	14.00	0.00	0.11	8.10	-0.14	2.06	2.17	56.20	54.06	-22.50	0.24	0.15	5.60	7.10
140	001140	F	10.00	14.00	0.00	1.48	7.00	-0.15	2.26	2.51	49.23	47.34	-24.00	0.24	0.30	5.40	7.50
141	001141	F	10.00	14.00	0.00	0.32	6.92	-0.14	2.00	2.55	51.01	49.06	-20.00	0.24	0.14	5.90	6.70

TABLE C-2. CLOSED-LOOP TRACKING MEASURES, SIDE-STICK

RHH RUNS OF 15-RUG-86

SIDE STICK (3.44 lb/in.; 5 lb. 80. IN POS &amp; FORCE)

RUN	FILE	TYPE	Kc	MS	WF	CHPR	EBRR	ESIG	CBRR	CSIG	WC	PM	PHL	SLOPE	TE	ALPHA	WU	GH
142	15A142	F	10.00	22.00	out	practice	-2.39	14.61	-0.16	2.02	1.34	66.67	66.67	-17.60	8.47	-0.31	7.22	14.60
143	15A143	F	10.00	22.00	out	4.00	0.01	0.00	-0.13	2.03	2.28	57.46	55.91	-21.78	8.28	-0.17	5.61	9.00
144	15A144	F	10.00	22.00	out	4.00	-0.92	7.92	-0.11	2.54	2.69	43.08	40.85	-26.10	0.26	0.31	5.01	5.00
145	15A145	F	10.00	22.00	out	4.00	-0.28	9.24	-0.14	2.03	2.10	72.29	71.56	-18.50	0.27	-0.52	6.20	7.20
146	15A146	F	10.00	22.00	14.00	5.00	-1.44	11.63	-0.14	2.31	1.98	52.99	52.25	-18.40	0.33	-0.83	4.59	6.50
147	15A147	F	10.00	22.00	14.00	5.00	0.37	11.74	-0.12	2.50	2.12	56.37	55.18	-14.30	0.31	-0.17	4.35	3.00
148	15A148	F	10.00	22.00	14.00	5.00	-0.67	10.62	-0.14	2.34	2.07	50.82	48.82	-15.20	0.30	0.15	4.53	4.70
149	15A149	P	10.00	22.00	14.00	5.00	-0.40	10.85	-0.16	2.41	2.17	45.26	43.46	-19.90	0.34	0.07	4.07	4.50
150	15A150	P	10.00	22.00	14.00	5.00	-1.65	11.93	-0.15	2.59	2.06	79.08	78.44	-24.78	0.43	-1.45	4.20	3.90
151	15A151	P	10.00	22.00	14.00	5.00	-0.90	10.30	-0.15	2.43	2.26	45.97	43.97	-19.40	0.32	0.09	4.06	4.00
152	15A152	P	10.00	22.00	out	4.00	-1.44	9.27	-0.11	2.28	2.26	57.00	56.42	-17.00	0.25	0.00	5.79	3.90
153	15A153	P	10.00	22.00	out	4.00	-0.41	9.60	-0.13	1.96	2.03	60.45	59.67	-23.20	0.28	-0.18	7.83	6.60
154	15A154	P	10.00	22.00	out	4.00	0.32	8.60	-0.14	2.35	2.64	49.39	47.41	-25.10	0.23	0.24	5.37	5.40
155	15A155	P	20.00	22.00	out	3.00	-0.46	8.47	-0.15	2.35	2.62	48.61	46.60	-23.50	0.32	-0.27	4.74	4.20
156	15A156	P	20.00	22.00	out	3.00	-1.50	9.56	-0.12	2.22	2.21	55.93	54.47	-25.70	0.26	0.07	4.05	4.70
157	15A157	P	20.00	22.00	out	3.00	0.20	6.00	-0.12	2.04	3.60	31.83	31.20	-9.70	0.31	-0.35	5.02	1.40
158	15A158	F	20.00	22.00	14.00	3.00	-0.25	9.59	-0.14	2.33	2.50	46.30	44.09	-22.70	0.32	-0.11	4.41	6.00
159	15A159	F	20.00	22.00	14.00	3.00	-0.00	9.29	-0.17	2.63	2.54	46.50	44.48	-19.40	0.28	0.13	4.31	2.50
160	15A160	F	20.00	22.00	14.00	3.00	-2.13	8.63	-0.17	2.50	2.77	44.31	42.29	-21.00	0.30	-0.06	4.30	2.00
161	15A161	P	20.00	22.00	14.00	4.00	-1.30	9.95	-0.12	2.02	2.63	38.84	36.35	-19.10	0.36	-0.14	4.13	3.50
162	15A162	P	20.00	22.00	14.00	4.00	-1.36	9.05	-0.17	2.49	2.33	54.65	52.84	-19.10	0.30	-0.64	4.32	4.10
163	15A163	P	20.00	22.00	14.00	4.00	-1.57	10.15	-0.16	3.03	2.68	45.37	43.26	-19.90	0.31	-0.12	4.26	4.10
164	15A164	F	20.00	22.00	out	2.00	-0.70	9.92	-0.15	1.96	2.09	60.45	59.45	-20.20	0.25	-0.02	7.11	6.70
165	15A165	F	20.00	22.00	out	2.00	-0.73	8.30	-0.17	2.43	2.35	55.19	53.48	-26.30	0.27	-0.07	5.70	4.10
166	15A166	F	20.00	22.00	out	2.00	-1.39	7.95	-0.18	2.30	2.52	51.00	49.97	-25.90	0.24	0.14	7.05	7.60
167	15A167	P	20.00	22.00	14.00	3.00	-0.04	10.20	-0.12	2.83	2.26	51.01	50.01	-17.20	0.35	-0.29	4.27	4.30
168	15A168	P	20.00	22.00	14.00	3.00	-1.52	10.72	-0.19	2.00	2.18	50.06	49.25	-19.50	0.32	-0.05	4.11	2.50
169	15A169	P	20.00	22.00	14.00	n/a	0.90	11.73	-0.19	2.47	1.90	56.69	56.01	-23.30	0.34	-0.19	3.03	4.60
170	15A170	P	20.00	22.00	14.00	3.00	-2.06	9.55	-0.11	2.33	2.13	51.92	50.47	-20.00	0.33	-0.10	4.30	4.10

TABLE C-2. (CONTINUED)

DEJ RUNS OF 15-AUG-86  
SIDE STICK (3.44 lb/in.; 5 lb. 80. IN POS & FORCE)

RUN	FILE	TYPE	Kc	W5	WF	CHPR	EBAR	ESIG	CBAR	CSIG	WC	PH	PHL	SLOPE	TE	ALPHA	HU	GM
171	15A171	F	20.00	22.00	out	practice	0.70	5.02	-0.16	2.75	3.99	28.76	26.21	-28.20	0.26	0.14	5.69	3.10
172	15A172	F	20.00	22.00	out	practice	0.61	5.17	-0.13	2.54	3.95	30.87	27.78	-19.80	0.25	0.21	5.87	3.48
173	15A173	F	20.00	22.00	out	3.00	1.09	5.50	-0.13	2.71	3.98	39.10	30.98	-30.20	0.22	0.41	6.24	4.20
174	15A174	F	20.00	22.00	out	3.00	1.76	5.15	-0.14	2.61	4.07	35.44	32.91	-17.30	0.24	0.41	6.53	3.68
175	15A175	F	20.00	22.00	out	3.00	0.94	5.44	-0.14	2.64	3.52	43.00	43.00	-14.50	0.23	-0.05	6.60	4.00
176	15A176	P	20.00	22.00	out	3.00	0.56	5.62	-0.13	2.64	4.11	29.71	26.73	-17.10	0.28	-0.42	5.61	2.30
177	15A177	P	20.00	22.00	out	3.00	1.20	6.23	-0.13	2.50	3.43	35.10	34.08	-26.40	0.27	0.08	5.50	4.10
178	15A178	P	20.00	22.00	out	3.00	0.69	5.90	-0.15	2.67	3.58	37.91	37.47	-12.80	0.25	0.03	5.81	2.90
179	15A179	P	20.00	22.00	14.00	5.00	-0.44	9.76	-0.07	3.95	4.25	8.97	4.71	-7.00	0.30	0.55	4.50	0.20
180	15A180	P	20.00	22.00	14.00	5.00	0.68	7.91	-0.13	2.98	3.56	24.70	24.31	-15.30	0.37	-0.56	4.41	1.40
181	15A181	P	20.00	22.00	14.00	5.00	0.38	8.60	-0.13	2.87	2.92	33.52	31.35	-21.70	0.32	0.18	4.24	3.50
182	15A182	P	20.00	22.00	14.00	5.00	0.48	8.33	-0.16	2.62	2.99	37.02	35.15	-20.50	0.26	0.44	4.39	2.20
183	15A183	F	20.00	22.00	14.00	n/a	0.48	7.10	-0.17	2.50	3.41	40.05	39.66	-21.70	0.23	0.34	4.66	1.40
184	15A184	F	20.00	22.00	14.00	4.00	0.78	8.68	-0.17	2.56	3.09	39.44	38.02	-24.60	0.31	-0.21	4.61	1.90
185	15A185	F	20.00	22.00	14.00	4.00	2.64	8.60	-0.13	2.39	2.57	43.70	41.39	-23.30	0.29	0.18	4.94	4.20
186	15A186	F	20.00	22.00	14.00	4.00	1.11	8.41	-0.13	2.18	2.05	47.63	46.47	-19.50	0.27	0.38	4.42	6.40
187	15A187	F	20.00	22.00	14.00	5.00	0.26	9.05	-0.12	2.38	2.17	41.05	39.15	-22.20	0.32	0.35	4.47	5.60
188	15A188	F	20.00	22.00	14.00	5.00	2.53	10.34	-0.15	2.37	2.05	40.99	39.66	-22.00	0.32	0.41	4.19	5.60
189	15A189	F	20.00	22.00	14.00	4.50	2.03	7.47	-0.15	2.00	2.36	59.43	57.96	-25.40	0.17	0.31	5.47	6.20
190	15A190	F	20.00	22.00	out	4.50	2.49	8.06	-0.17	1.85	1.84	67.51	67.43	-27.40	0.24	-0.08	5.23	5.70
191	15A191	F	20.00	22.00	out	4.50	2.07	6.90	-0.15	2.07	1.84	55.30	53.66	-26.90	0.18	0.33	5.92	6.10
192	15A192	F	20.00	22.00	out	4.50	2.89	6.32	-0.15	2.16	3.00	50.83	49.70	-25.90	0.22	0.05	5.76	7.20
193	15A193	P	20.00	22.00	out	5.00	1.69	6.75	-0.13	2.40	3.15	40.00	30.81	-22.00	0.26	0.16	5.10	3.80
194	15A194	P	20.00	22.00	out	5.00	1.91	6.50	-0.15	2.36	2.93	44.31	42.56	-32.60	0.23	0.34	5.47	4.40
195	15A195	P	20.00	22.00	out	5.00	1.70	6.03	-0.15	2.44	3.39	43.97	43.92	-20.90	0.19	0.56	5.21	3.00
196	15A196	P	20.00	22.00	14.00	7.00	-0.41	8.91	-0.13	3.56	3.67	10.94	17.60	-10.90	0.30	-0.62	4.26	0.70
197	15A197	P	20.00	22.00	14.00	7.00	1.54	9.23	-0.11	3.46	3.32	22.98	22.03	-21.60	0.32	0.33	4.43	2.90
198	15A198	P	20.00	22.00	14.00	7.00	1.29	6.27	-0.17	2.82	3.03	32.32	30.41	-30.60	0.29	0.35	4.14	3.20

DEJ RUNS OF 10-AUG-86

SIDE STICK (3.44 lb/in.; 8.5 lb. 80. IN POS. & FORCE)

RUN	FILE	TYPE	Kc	Tr	Tau	CHPR	EBAR	ESIG	CBAR	CSIG	WC	PH	PHL	SLOPE	TE	ALPHA	HU	GM
200	18A200	F	10.00	0.00	0.000	practice	2.55	8.03	-0.19	1.73	2.27	57.01	66.02	-27.10	0.14	0.17	7.42	7.90
201	18A201	F	10.00	0.00	0.000	practice	0.07	5.20	-0.20	2.14	3.53	54.40	54.40	-19.70	0.10	0.00	8.72	5.60
202	18A202	F	10.00	0.00	0.000	2.00	0.10	4.75	-0.19	2.05	3.00	50.29	40.87	-19.70	0.19	-0.16	7.90	6.00
203	18A203	F	10.00	0.00	0.000	2.00	-0.00	4.62	-0.10	2.11	3.02	49.02	47.75	-19.00	0.10	0.15	8.49	4.00
204	18A204	F	10.00	0.00	0.000	2.00	0.00	4.76	-0.18	1.94	3.46	59.16	59.03	-30.30	0.15	0.05	9.56	6.40
205	18A205	P	10.00	0.00	0.000	2.00	-0.67	5.24	-0.19	2.19	3.54	49.50	49.50	-18.40	0.20	-0.06	7.40	5.40
206	18A206	P	10.00	0.00	0.000	2.00	-0.54	4.93	-0.19	2.15	3.63	46.23	45.64	-20.40	0.18	0.43	7.74	5.60
207	18A207	P	10.00	0.00	0.000	2.00	0.55	5.40	-0.19	2.11	3.36	54.75	54.34	-30.40	0.14	0.52	7.22	5.40
208	18A208	P	10.00	0.00	0.000	2.00	-0.71	5.74	-0.16	2.24	3.48	43.05	44.93	-26.40	0.16	0.35	6.24	3.90
209	18A209	P	10.00	0.00	0.000	2.00	-1.73	7.60	-0.21	2.17	2.05	50.60	40.90	-21.40	0.26	-0.13	4.92	4.30
210	18A210	P	10.00	0.00	0.000	2.00	2.59	6.59	-0.23	2.27	3.00	43.03	41.37	-29.00	0.22	0.47	5.65	4.00
211	18A211	P	10.00	0.00	0.000	2.00	2.46	6.00	-0.18	2.00	2.99	52.90	51.74	-25.50	0.22	-0.08	6.40	5.40
212	18A212	F	10.00	0.00	0.000	no good	6.43	11.09	-0.27	2.37	4.17	46.29	43.92	-27.00	0.24	-1.00	6.52	-0.10
213	18A213	F	10.00	0.00	0.000	2.00	1.69	5.18	-0.22	2.13	3.37	49.57	49.13	-31.40	0.18	0.32	6.99	5.00
214	18A214	F	10.00	0.00	0.000	2.00	0.76	5.57	-0.20	2.07	3.36	50.82	50.36	-20.10	0.17	0.36	7.13	5.40
215	18A215	F	10.00	0.00	0.000	2.00	0.64	5.23	-0.21	2.16	3.66	50.14	49.44	-21.70	0.23	-0.08	7.13	6.10
216	18A216	F	10.00	0.00	0.000	2.00	2.81	6.47	-0.19	2.01	2.90	51.50	50.84	-20.00	0.19	0.30	6.76	5.20
217	18A217	F	10.00	0.00	0.000	2.00	1.45	6.50	-0.20	1.90	2.79	55.02	53.46	-26.20	0.10	0.27	7.10	6.00
218	18A218	F	10.00	0.00	0.000	2.00	0.70	5.78	-0.20	2.18	3.39	43.02	43.41	-27.20	0.22	0.15	6.63	5.40
219	18A219	P	10.00	0.00	0.000	2.00	0.42	6.13	-0.20	2.19	3.07	45.50	42.16	-35.60	0.22	0.39	6.04	4.20
220	18A220	P	10.00	0.00	0.000	2.00	0.77	6.28	-0.10	2.17	3.02	40.56	47.14	-28.00	0.19	0.47	6.14	3.80
221	18A221	P	10.00	0.00	0.000	2.00	0.06	5.71	-0.20	2.11	3.21	51.45	50.50	-32.50	0.16	0.52	6.00	3.40



TABLE C-2. (CONTINUED)

RUN	FILE	TYPE	Kc	Tr	Tau	CHPR	EBPR	SIDE STICK (3.44 lb/in ; 0.5 lb. BO. IN POS & FORCE )				PH	PML	SLOPE	TE	ALPHA	HU	GM
								DEJ	TASK 1	RUNS OF	19 & 20	AUG-86						
224	19A224	P	15.00	0.00	0.067	1.00	0.10		ESIG	CBPR	CSIG	WC	PH	PML	SLOPE	TE	ALPHA	HU
225	19A225	P	15.00	0.00	0.067	1.00	0.29		5.84	-0.17	2.29	3.35	38.97	38.42	-38.30	0.29	-0.31	7.06
226	19A226	P	15.00	0.00	0.067	1.00	0.29		4.98	-0.19	2.38	3.88	33.09	31.08	-19.68	0.25	0.13	6.05
227	19A227	P	20.00	0.00	0.067	1.00	-0.70		5.59	-0.17	2.19	3.13	46.38	45.24	-35.40	0.25	-0.84	7.41
228	19A228	P	20.00	0.00	0.067	1.00	0.33		5.74	-0.19	2.35	3.51	48.52	48.58	-16.38	0.25	-0.86	6.11
229	19A229	P	20.00	0.00	0.067	1.00	1.05		5.54	-0.16	2.28	3.36	45.84	44.52	-32.00	0.20	0.37	7.07
230	19A230	P	20.00	0.00	0.067	1.00	0.65		6.14	-0.19	2.11	3.87	58.93	49.73	-29.58	0.20	0.19	7.14
231	19A231	P	7.50	0.00	0.067	3.00	0.61		7.63	-0.20	1.94	2.56	58.78	57.27	-28.98	0.18	0.27	6.87
232	19A232	P	7.50	0.00	0.067	3.00	0.63		7.56	-0.19	1.99	2.33	55.97	54.37	-25.78	0.28	0.32	5.97
233	19A233	P	7.50	0.00	0.067	3.00	-0.33		6.35	-0.17	2.12	3.01	48.71	47.23	-23.28	0.16	0.73	5.73
234	19A234	P	5.00	0.00	0.067	5.00	-0.58		7.16	-0.18	2.02	2.58	53.85	51.21	-26.88	0.28	0.32	6.28
235	19A235	P	5.00	0.00	0.067	5.00	0.74		7.93	-0.17	1.91	2.24	58.11	56.65	-24.58	0.27	-0.12	6.43
236	19A236	P	5.00	0.00	0.067	5.00	-0.39		8.21	-0.17	1.94	2.23	54.86	52.95	-25.40	0.21	0.37	6.54
237	19A237	P	15.00	0.20	0.067	3.00	0.85		7.61	-0.15	2.58	2.87	35.82	32.77	-28.08	0.38	0.26	4.88
238	19A238	P	15.00	0.20	0.067	3.00	0.40		7.53	-0.15	2.54	2.88	35.64	33.48	-38.38	0.34	-0.05	4.78
239	19A239	P	15.00	0.20	0.067	3.00	1.26		7.48	-0.20	2.93	3.21	38.58	29.28	-28.68	0.27	0.53	4.35
240	19A240	P	15.00	0.20	0.067	5.00	2.38		11.98	-0.18	2.11	1.65	51.35	50.56	-23.58	0.38	0.87	4.15
241	19A241	P	5.00	0.20	0.067	5.00	1.69		12.01	-0.20	2.17	1.64	48.67	47.81	-28.88	0.45	-0.83	3.83
242	19A242	P	5.00	0.20	0.067	5.00	1.99		11.41	-0.16	1.96	1.62	55.51	54.74	-23.18	0.36	0.03	3.93
243	19A243	P	20.00	0.20	0.067	3.00	-2.42		7.52	-0.16	2.91	3.39	32.64	32.15	-13.58	0.28	0.19	4.43
244	19A244	P	20.00	0.20	0.067	3.00	0.69		7.86	-0.22	2.88	2.98	36.88	34.18	-27.28	0.29	0.24	4.31
245	19A245	P	20.00	0.20	0.067	3.00	0.35		8.55	-0.17	3.16	3.14	38.89	29.39	-25.58	0.33	-0.81	4.32
246	19A246	P	10.00	0.20	0.067	3.00	2.13		18.88	-0.20	2.28	1.78	49.18	48.74	-28.68	0.42	-0.87	4.55
247	19A247	P	10.00	0.20	0.067	3.00	1.12		9.65	-0.16	2.48	2.16	39.88	37.17	-24.98	0.29	0.57	4.31
248	19A248	P	10.00	0.20	0.067	3.00	0.18		8.86	-0.22	2.38	2.87	46.17	44.87	-28.58	0.29	0.34	4.27
249	19A249	P	10.00	0.20	0.067	3.00	0.88		8.58	-0.16	2.51	2.62	48.64	38.21	-21.38	0.28	0.34	4.78
250	19A250	P	10.00	0.20	0.067	3.00	-0.18		7.88	-0.15	2.55	2.88	39.68	37.45	-24.18	0.26	0.39	4.55
251	19A251	P	10.00	0.20	0.067	3.00	-0.51		8.84	-0.17	2.43	2.55	39.44	36.91	-38.18	0.28	0.44	4.34
252	19A252	P	10.00	0.20	0.067	3.00	2.20		8.22	-0.19	2.43	2.48	41.88	39.39	-25.88	0.27	0.45	4.23
253	19A253	P	7.50	0.20	0.067	5.00	1.46		7.89	-0.21	2.55	2.68	38.96	36.43	-28.98	0.26	0.55	4.27
254	19A254	P	7.50	0.20	0.067	5.00	0.84		7.84	-0.20	2.57	2.58	39.57	37.06	-27.78	0.27	0.50	4.49
255	19A255	P	7.50	0.20	0.067	5.00	0.77		7.69	-0.13	2.81	3.85	44.95	43.54	-23.88	0.25	0.86	5.82
256	19A256	P	20.00	0.20	0.067	4.00	-1.87		7.88	-0.14	2.94	3.75	28.69	27.86	-18.88	0.34	-0.82	4.88
257	19A257	P	20.00	0.20	0.067	4.00	0.31		7.18	-0.15	3.15	4.35	15.22	11.88	-8.88	0.38	0.84	4.95
258	19A258	P	20.00	0.20	0.067	4.00	1.78		18.17	-0.19	2.41	2.12	43.37	41.79	-23.88	0.38	0.39	4.27
259	19A259	P	5.00	0.20	0.067	7.00	3.25		9.41	-0.18	2.32	2.18	47.13	45.66	-24.18	0.34	0.86	4.17
260	19A260	P	5.00	0.20	0.067	7.00	1.68		9.34	-0.18	2.33	2.15	44.14	42.44	-26.78	0.28	0.44	4.53
261	19A261	P	10.00	0.40	0.067	7.00	0.84		18.83	-0.19	3.55	2.46	23.11	19.78	-29.18	0.36	0.67	3.73
262	19A262	P	10.00	0.40	0.067	7.00	0.53		9.78	-0.16	3.41	2.46	28.98	25.93	-28.28	0.34	0.55	4.12
263	19A263	P	10.00	0.48	0.067	7.00	0.98		8.76	-0.15	3.39	2.58	24.17	20.89	-33.38	0.32	0.81	3.97

TABLE C-2. (CONTINUED)

PHH TASK 1 RUNS OF 20-RUG-86  
SIDE STICK (3.44 lb/in : 8.5 lb 80, IN POS. & FORCE )

RUN	FILE	TYPE	Kc	Tr	Tau	CHPR	EBAR	ESIG	CBAR	CSIG	WC	PH	PHL	SLOPE	TE	ALPHA	MU	GH
283	20R283	P	10.00	0.00	0.067	4.00	-0.82	0.41	0.54	3.76	2.66	45.68	43.47	-22.50	0.28	0.95	7.26	5.40
284	20R284	P	10.00	0.00	0.067	4.00	-0.75	7.44	8.21	4.80	3.04	48.48	38.96	-24.90	0.31	-0.24	5.58	6.50
285	20R285	P	10.00	0.00	0.067	4.00	-0.43	8.36	8.40	3.73	2.51	48.42	46.34	-27.60	0.23	0.37	6.99	5.60
286	20R286	P	15.00	0.00	0.067	4.00	-1.87	7.28	8.53	2.93	2.92	44.82	43.06	-30.70	0.24	0.29	5.99	7.20
287	20R287	P	15.00	0.00	0.067	4.00	-0.95	7.48	-0.17	2.99	2.86	43.66	43.05	-32.10	0.27	-0.81	4.99	3.30
288	20R288	P	15.00	0.00	0.067	4.00	-0.85	6.50	-0.17	2.92	2.53	59.27	57.72	-23.30	0.25	-0.24	5.56	3.18
289	20R289	P	20.00	0.00	0.067	3.00	-1.75	7.52	8.24	2.84	2.89	48.97	30.99	-32.70	0.25	0.36	5.54	5.20
290	20R290	P	20.00	0.00	0.067	3.00	-0.78	6.65	8.09	1.98	3.68	42.14	41.69	-61.60	0.16	0.94	7.80	16.30
291	20R291	P	20.00	0.00	0.067	3.00	-0.39	7.21	-0.88	2.85	2.79	45.79	43.82	-25.00	0.24	0.31	6.28	3.40
292	20R292	P	5.00	0.00	0.067	6.00	-1.83	11.24	-0.19	6.90	1.47	70.16	69.61	-11.50	0.39	-0.34	6.82	9.10
293	20R293	P	5.00	0.00	0.067	6.00	0.21	9.95	-0.18	8.17	2.16	54.01	52.62	-23.20	0.24	0.22	6.72	7.70
294	20R294	P	5.00	0.00	0.067	6.00	-0.86	9.73	-0.19	8.26	1.86	61.23	61.21	-23.30	0.29	-0.87	5.88	5.30
300	20R300	P	20.00	0.20	0.067	6.00	-1.57	9.83	-0.14	2.98	2.52	37.93	35.31	-25.30	0.32	0.27	4.74	4.40
301	20R301	P	20.00	0.20	0.067	6.00	1.49	12.07	-0.19	2.12	1.72	53.37	52.05	-17.00	0.38	-0.83	4.25	7.10
302	20R302	P	20.00	0.20	0.067	6.00	0.99	11.83	-0.12	1.99	1.62	68.19	59.54	-16.00	0.31	0.83	4.64	9.10
303	20R303	P	10.00	0.20	0.067	6.00	0.23	11.31	0.82	4.74	2.09	51.81	59.41	-26.10	0.45	-0.58	3.78	6.70
304	20R304	P	10.00	0.20	0.067	6.00	0.66	11.25	-0.83	4.74	2.08	53.36	52.28	-20.80	0.27	0.18	4.65	8.00
305	20R305	P	10.00	0.20	0.067	6.00	0.87	10.90	-0.84	4.73	1.83	57.26	57.14	-18.70	0.30	0.05	4.75	7.80
306	20R306	P	15.00	0.20	0.067	5.00	0.68	9.43	-0.87	3.76	2.53	46.73	44.56	-15.20	0.24	0.35	4.77	3.40
307	20R307	P	15.00	0.20	0.067	5.00	-0.89	9.10	-0.86	3.85	2.64	37.87	35.33	-25.90	0.31	0.21	4.35	4.90
308	20R308	P	15.00	0.20	0.067	5.00	-0.66	9.80	0.17	3.44	2.65	38.68	36.11	-19.20	0.31	0.19	4.57	3.60
309	20R309	P	7.50	0.00	0.067	4.00	0.21	9.22	-0.84	4.01	2.14	62.85	61.74	-27.80	0.29	-0.31	6.22	6.40
310	20R310	P	7.50	0.00	0.067	4.00	-0.29	8.58	-0.18	5.22	2.26	56.77	55.28	-25.50	0.22	0.18	7.10	7.50
311	20R311	P	7.50	0.00	0.067	4.00	1.64	9.11	-0.81	6.19	2.47	63.84	61.68	-15.20	0.19	0.82	6.56	4.40

DEJ RUNS OF 21-RUG-86

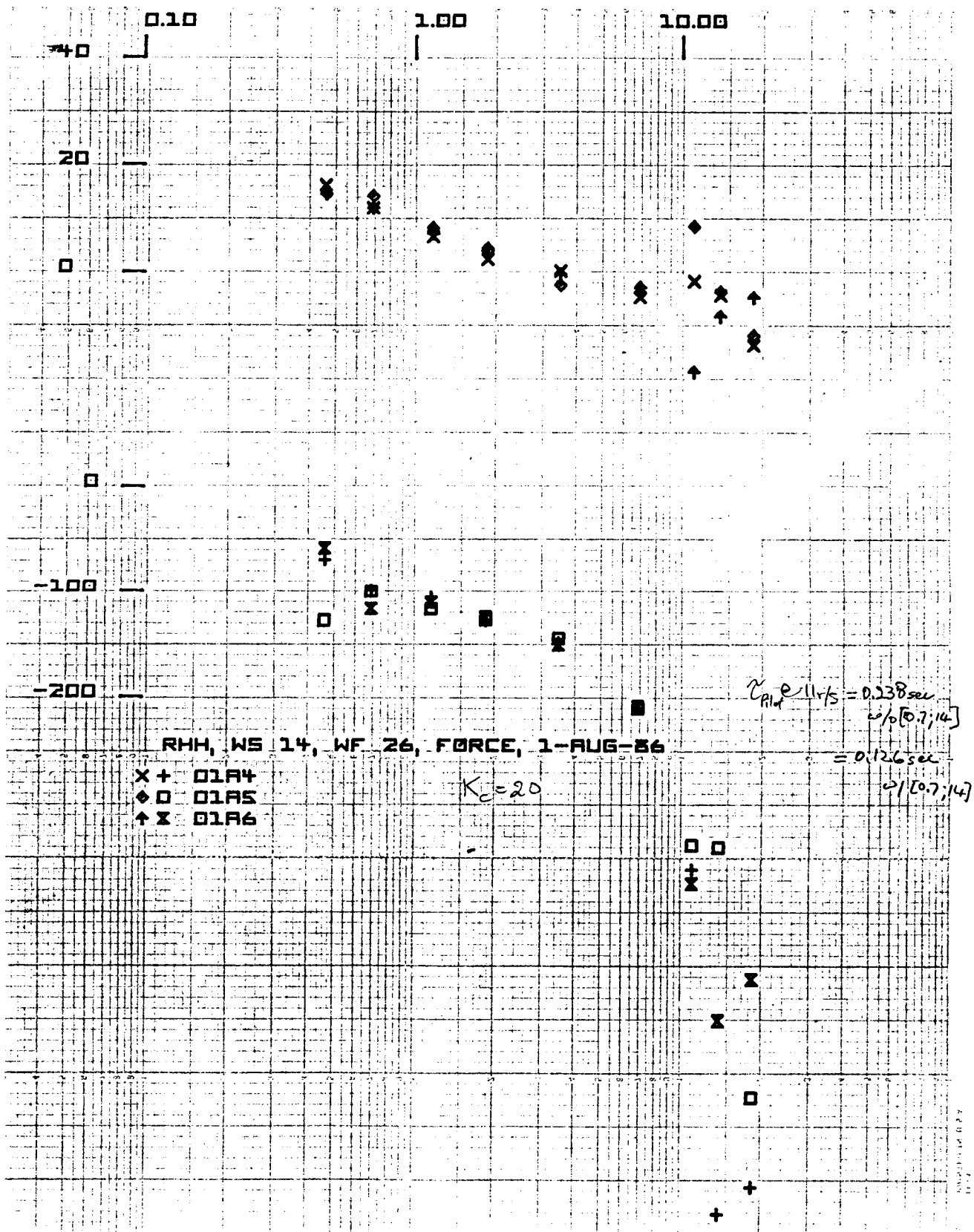
SIDE STICK (6.4 LB/IN : 8.5 LB 80, IN POS. &amp; FORCE )

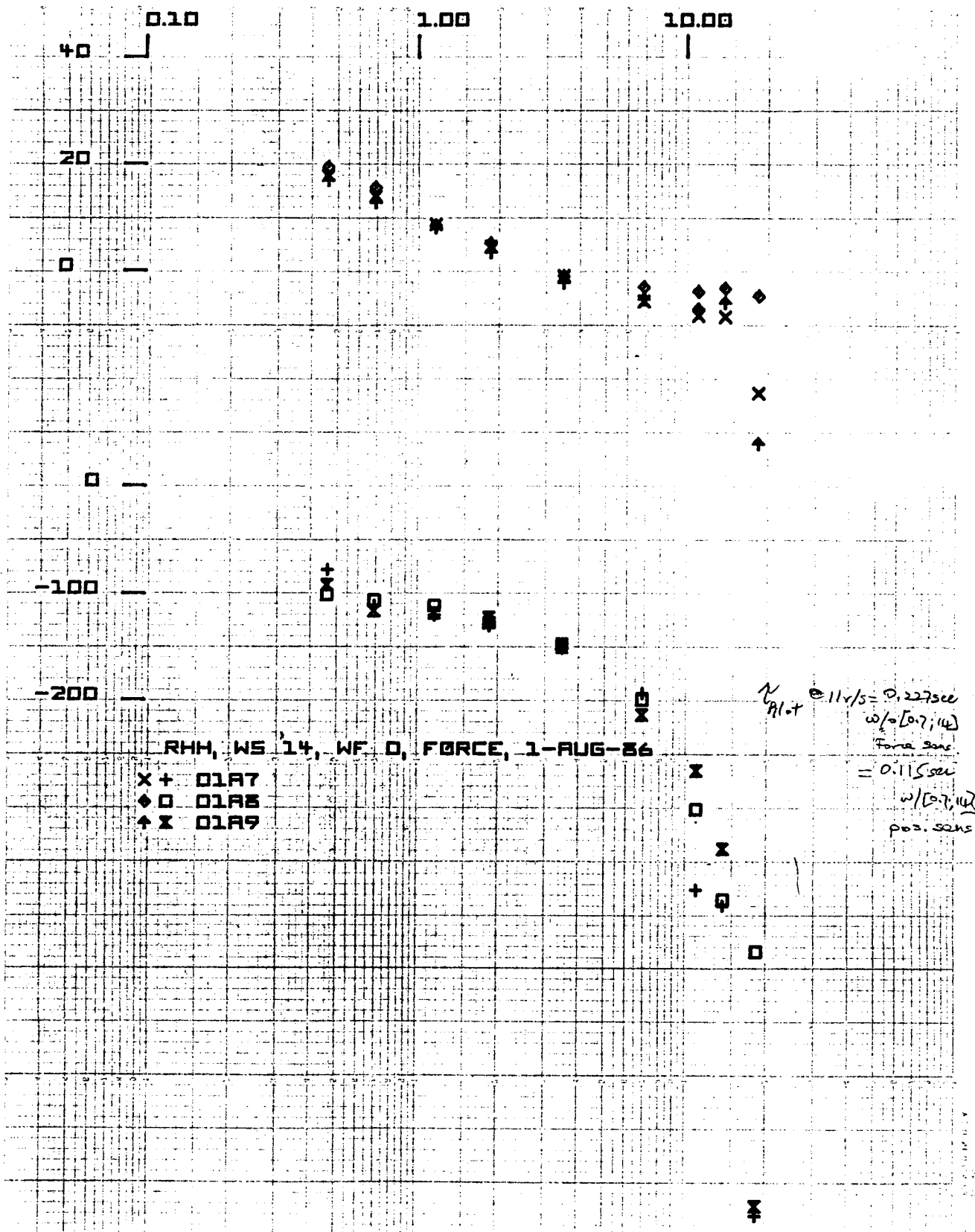
RUN	FILE	TYPE	Kc	Tr	Tau	CHPR	EBAR	ESIG	CBAR	CSIG	WC	PH	PHL	SLOPE	TE	ALPHA	MU	GH
312	21R312	P	10.00	0.00	0.000	practice	0.77	4.94	-0.18	4.84	4.77	38.46	26.85	-23.50	0.18	0.90	7.63	3.70
313	21R313	P	10.00	0.00	0.000	4.00	0.80	4.73	-0.15	4.51	4.12	41.23	39.86	-21.80	0.28	0.88	7.53	5.80
314	21R314	P	10.00	0.00	0.000	4.00	0.37	4.71	-0.80	4.37	3.88	42.90	41.40	-23.10	0.17	0.59	8.02	5.60
315	21R315	P	10.00	0.00	0.000	4.00	0.86	4.38	-0.12	4.52	3.87	43.17	41.59	-18.90	0.19	0.35	7.62	4.80
316	21R316	P	10.00	0.00	0.100	4.00	0.29	5.90	-0.15	5.29	4.27	23.51	19.91	-15.90	0.26	0.18	5.60	1.80
317	21R317	P	10.00	0.00	0.100	4.00	0.44	5.63	-0.13	4.97	3.67	35.92	34.92	-11.90	0.28	-0.36	5.50	2.10
318	21R318	P	10.00	0.00	0.100	4.00	0.80	5.74	-0.16	5.83	3.76	38.98	29.49	-16.30	0.24	0.51	6.01	3.30
319	21R319	P	10.00	0.00	0.067	3.00	1.11	5.41	-0.16	5.11	3.88	38.66	36.84	-13.40	0.24	-0.87	6.61	3.10
320	21R320	P	10.00	0.00	0.067	3.00	1.83	5.87	-0.13	4.72	3.69	43.48	42.55	-17.00	0.24	-0.24	6.66	4.40
321	21R321	P	10.00	0.00	0.067	3.00	0.94	5.86	-0.11	4.75	3.78	45.21	44.23	-14.50	0.24	-0.38	6.73	3.80
322	21R322	P	15.00	0.20	0.067	6.00	0.96	7.16	-0.88	5.38	3.67	25.76	24.65	-14.80	0.26	1.12	4.82	0.10
323	21R323	P	15.00	0.20	0.067	6.00	0.52	6.37	-0.16	4.88	4.26	15.40	11.50	-17.60	0.30	0.14	4.92	1.90
324	21R324	P	15.00	0.20	0.067	6.00	1.29	6.85	-0.11	4.51	4.26	15.40	11.50	-17.60	0.26	0.90	5.18	1.40
325	21R325	P	7.50	0.20	0.067	5.00	0.16	8.27	-0.15	7.95	2.72	38.19	27.39	-32.80	0.31	0.57	4.52	4.90
326	21R326	P	7.50	0.20	0.067	5.00	0.56	7.12	-0.15	7.29	2.89	34.45	32.21	-29.60	0.28	0.43	4.83	4.40
327	21R327	P	7.50	0.20	0.067	5.00	0.85	7.61	-0.13	7.68	2.93	32.72	30.53	-31.60	0.32	0.19	4.87	4.50
328	21R328	P	5.00	0.20	0.067	7.00	0.48	9.10	-0.84	11.82	2.35	36.66	34.14	-25.40	0.29	0.61	4.26	5.70
329	21R329	P	5.00	0.20	0.067	7.00	0.80	8.11	-0.17	10.54	2.53	36.92	34.26	-24.90	0.28	0.54	4.67	5.30
330	21R330	P	5.00	0.20	0.067	7.00	0.84	7.65	-0.16	10.80	2.66	35.51	32.86	-29.10	0.26	0.68	4.54	5.10
331	21R331	P	20.00	0.20	0.067	5.00	1.55	6.54	-0.84	3.48	7.82	-36.41	-36.40	-94.00	0.34	-1.35	4.72	-1.80
332	21R332	P	20.00	0.20	0.067	5.00	1.20	6.90	-0.12	3.06	3.15	42.55	41.38	-25.50	0.25	0.89	5.68	2.80
333	21R333	P	20.00	0.20	0.067	5.00	1.09	7.72	-0.88	3.45	3.45	11.88	7.24	-11.50	0.29	0.33	0.53	-15.80
334	21R334	P	10.00	0.40	0.067	8.00	1.85	8.67	-0.81	8.01	2.79	24.79	21.88	-34.50	0.35	0.42	3.96	4.20
335	21R335	P	10.00	0.40	0.067	8.00	-0.81	7.49	-0.18	6.82	2.76	25.79	22.82	-37.40	0.28	0.94	4.71	5.50
336	21R336	P	10.00	0.40	0.067	8.00	-0.66	8.98	-0.85	8.95	3.06	25.71	23.67	-26.90	0.31	0.52	4.44	4.80

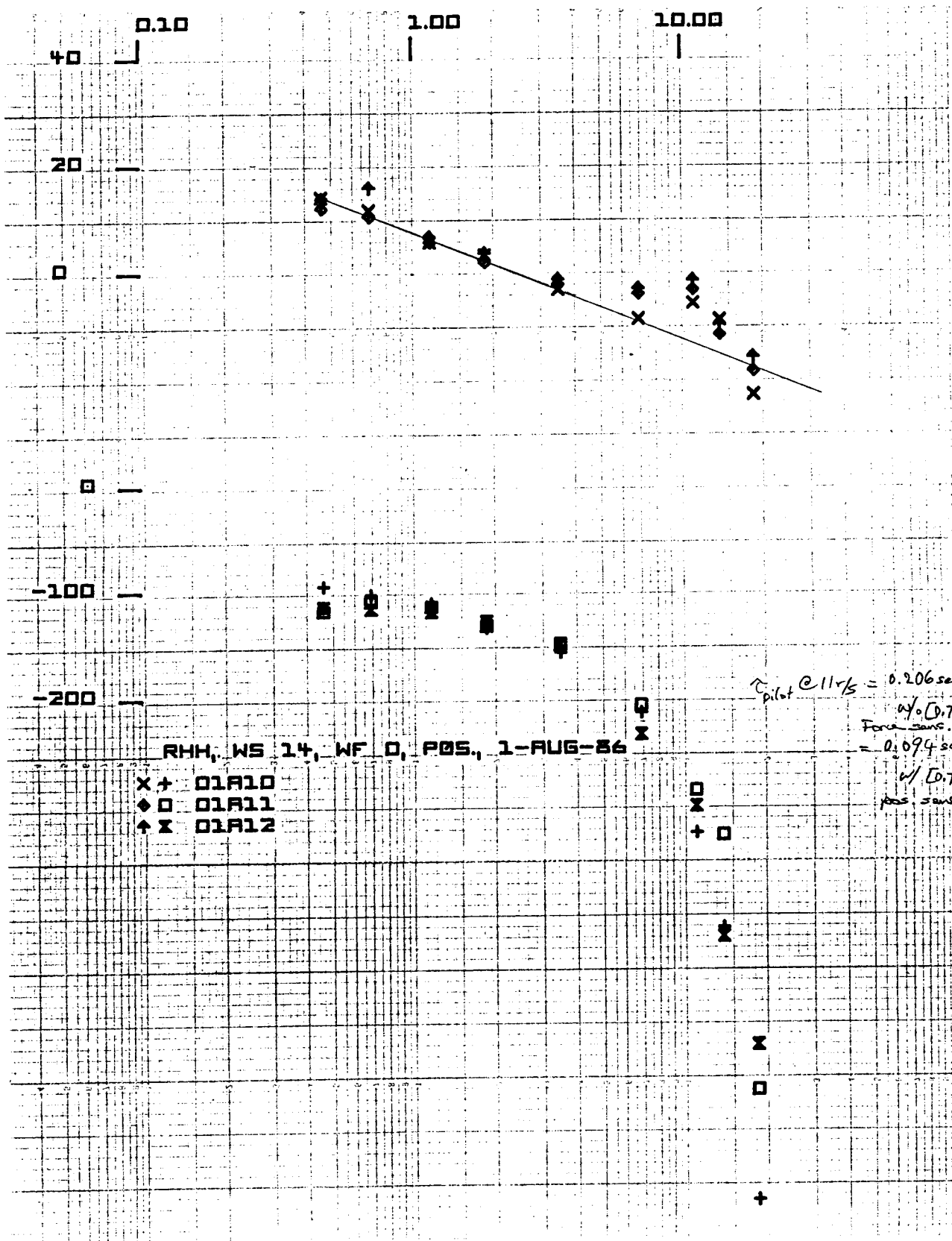
TABLE C-2. (CONCLUDED)

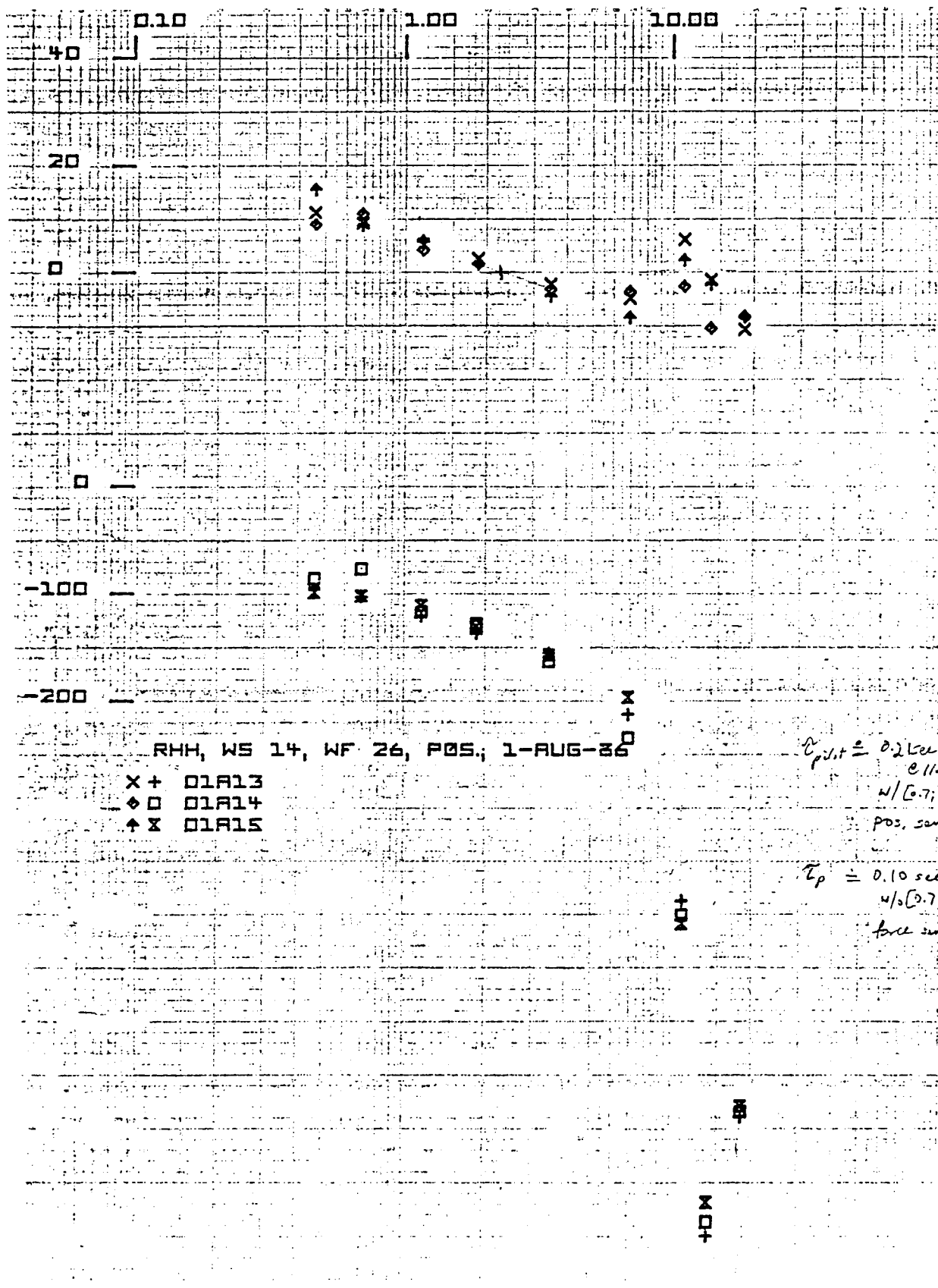
[illegible]

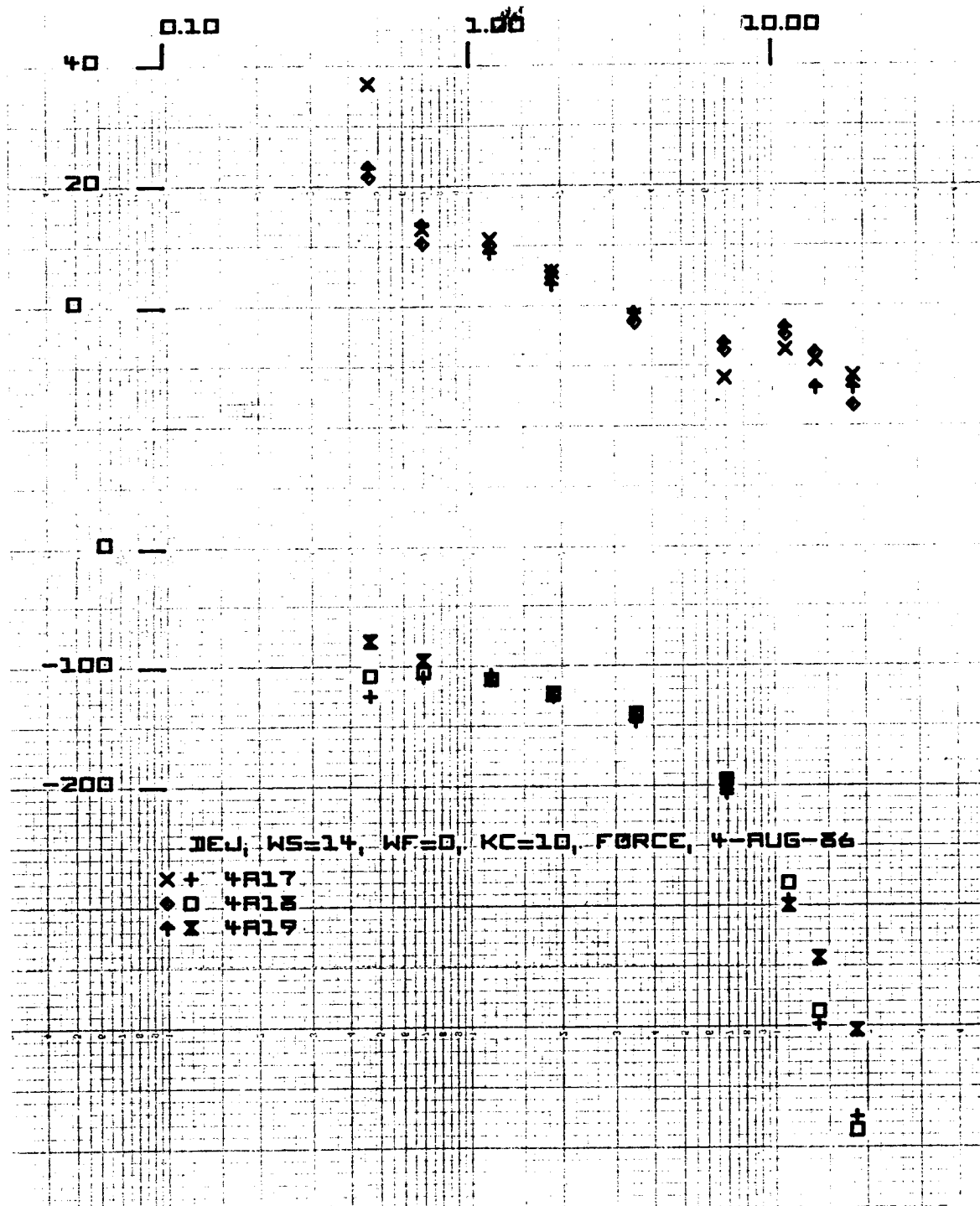
RUN	FILE	TYPE	Kc	Tr	Tau	CHPR	SIDE	STICK	RHH	RUNS OF 22-AUG-86										
										( 1.7 LB/IN ; 0.5 LB BD. IN POS. & FORCE )										
										ESIG	CBAR	CSIG	MC	PH	PML	SLOPE	TE	ALPHA	WU	GM
362	22R362	P	10.00	0.00	0.000	practice		-0.30		10.73	-0.12	3.43	1.75	73.29	73.07	-11.50	0.13	0.10	7.21	7.90
363	22R363	P	10.00	0.00	0.000	4.00		-1.45		9.48	0.02	3.50	2.14	73.55	72.09	-20.50	0.10	-0.19	8.12	7.60
364	22R364	P	10.00	0.00	0.000	4.00		-0.00		7.97	-0.13	3.01	2.44	68.67	59.19	-20.50	0.21	0.01	7.31	6.80
365	22R365	P	10.00	0.00	0.000	4.00		-0.42		7.70	-0.13	3.99	2.50	58.73	57.10	-29.40	0.25	-0.24	7.20	9.10
366	22R366	P	10.00	0.00	0.100	5.00		-2.70		9.21	-0.11	4.10	2.31	51.65	49.01	-26.90	0.29	0.00	4.96	6.00
367	22R367	P	10.00	0.00	0.100	5.00		0.71		9.63	-0.12	3.04	2.06	63.11	62.23	-29.00	0.30	-0.32	6.99	7.20
368	22R368	P	10.00	0.00	0.100	5.00		-1.70		8.60	-0.13	4.13	2.20	54.09	53.27	-23.30	0.24	0.13	5.40	6.40
369	22R369	P	10.00	0.00	0.067	3.00		-1.49		9.72	-0.12	4.15	2.35	53.47	51.67	-20.60	0.29	-0.10	5.15	6.00
370	22R370	P	10.00	0.00	0.067	3.00		0.40		8.19	-0.14	4.02	2.70	40.48	46.52	-22.70	0.26	0.00	7.22	9.90
271	22R371	P	10.00	0.00	0.067	3.00		-0.63		7.71	-0.17	3.82	2.42	56.03	54.32	-27.30	0.26	-0.09	6.65	6.90
372	22R372	P	10.00	0.00	0.067	3.00		-0.07		8.47	-0.15	3.71	2.22	60.20	58.00	-25.30	0.24	-0.05	5.68	6.90
373	22R373	P	15.00	0.20	0.067	5.00		0.51		10.73	-0.13	3.64	2.35	42.93	40.63	-26.00	0.35	0.00	4.19	5.10
374	22R374	P	15.00	0.20	0.067	5.00		0.09		10.54	-0.09	3.10	1.90	54.96	54.20	-20.10	0.30	-0.29	4.00	5.30
375	22R375	P	15.00	0.20	0.067	5.00		-1.03		10.20	-0.09	2.81	2.20	50.23	40.45	-24.00	0.42	-0.40	4.09	6.50
376	22R376	P	10.00	0.20	0.067	6.00		0.12		12.30	-0.14	3.99	1.60	60.79	60.12	-14.90	0.37	-0.14	4.71	8.10
377	22R377	P	10.00	0.20	0.067	6.00		-0.03		12.16	-0.13	4.00	1.50	57.33	56.55	-10.20	0.46	-0.25	4.92	10.20
378	22R378	P	20.00	0.20	0.067	5.00		-0.64		10.21	-0.15	2.34	2.17	47.03	46.16	-26.20	0.30	0.20	4.41	6.60
379	22R379	P	20.00	0.20	0.067	5.00		-0.60		10.15	-0.15	2.62	2.20	46.57	44.77	-10.50	0.29	0.24	4.05	3.70







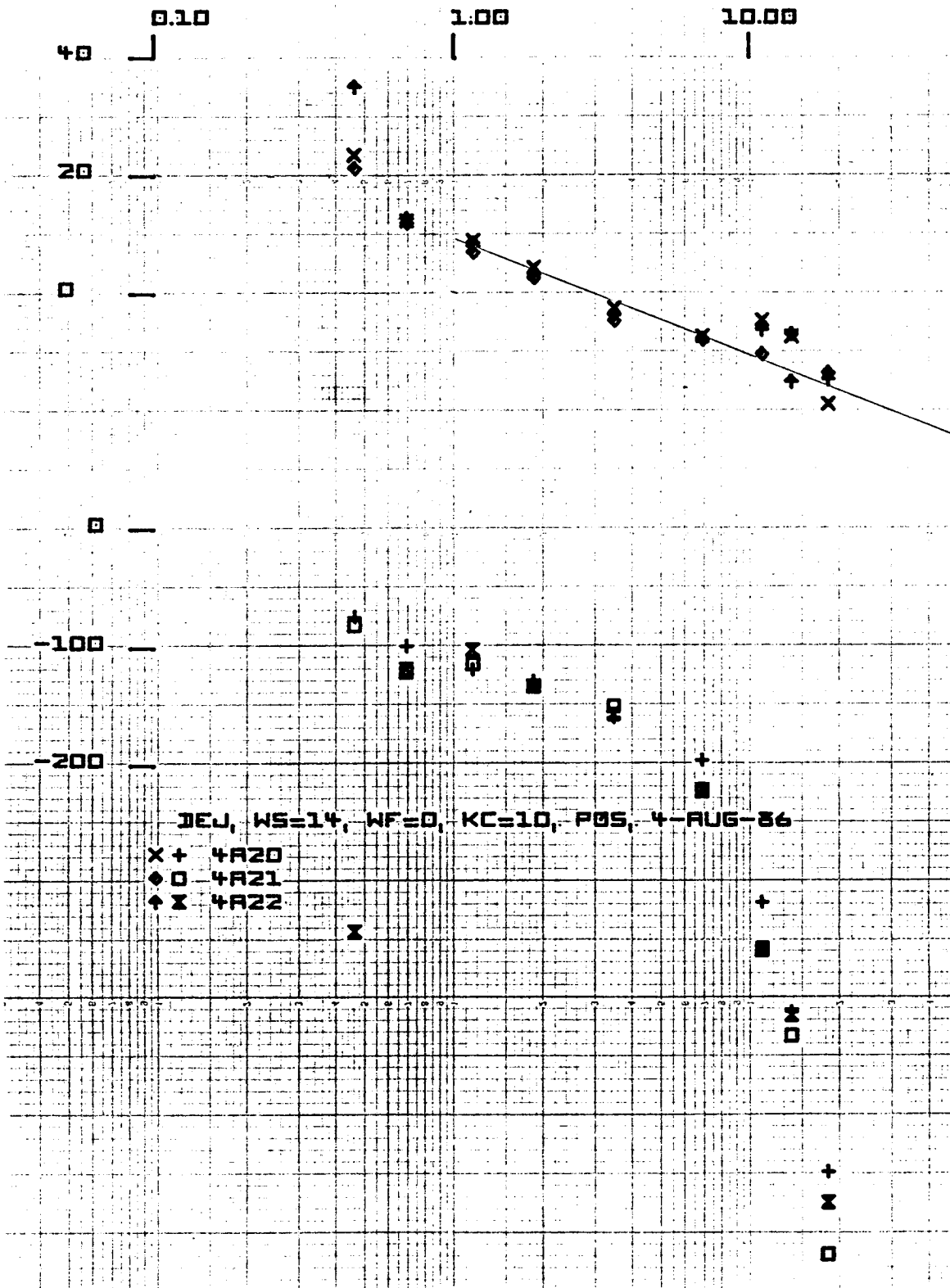


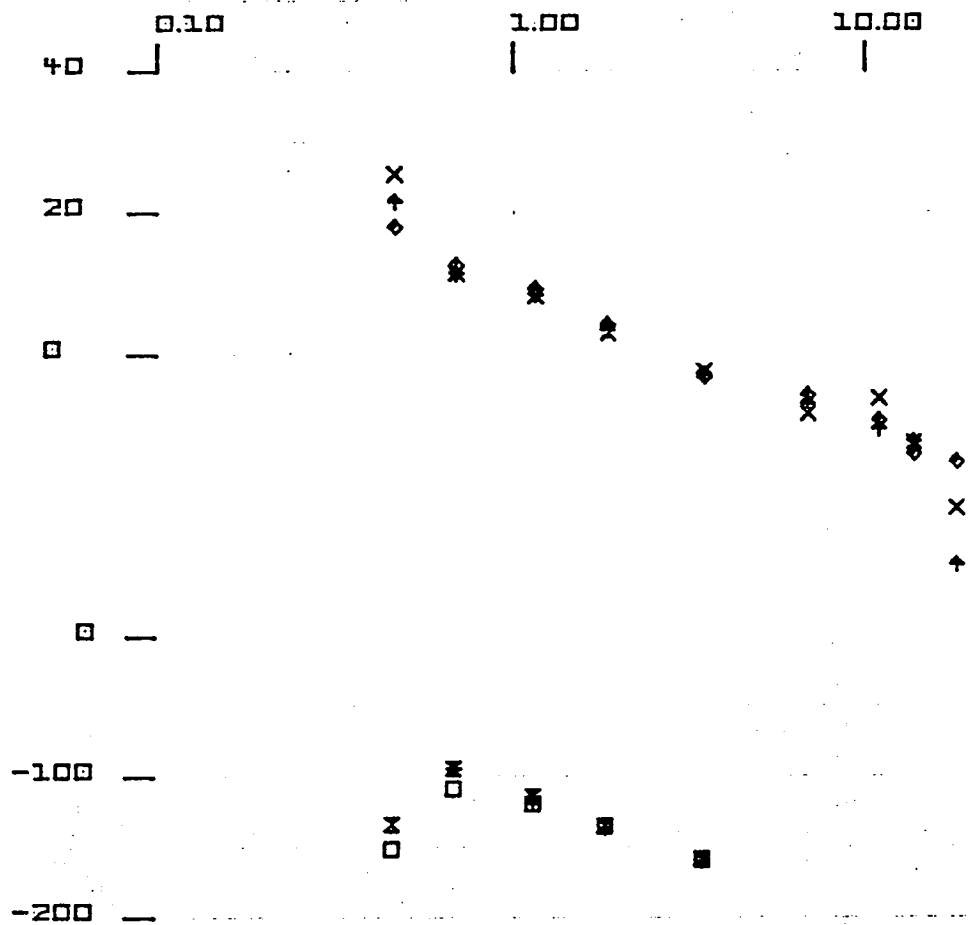


ORIGINAL PAGE IS  
OF POOR QUALITY



ORIGINAL PAGE IS  
OF POOR QUALITY

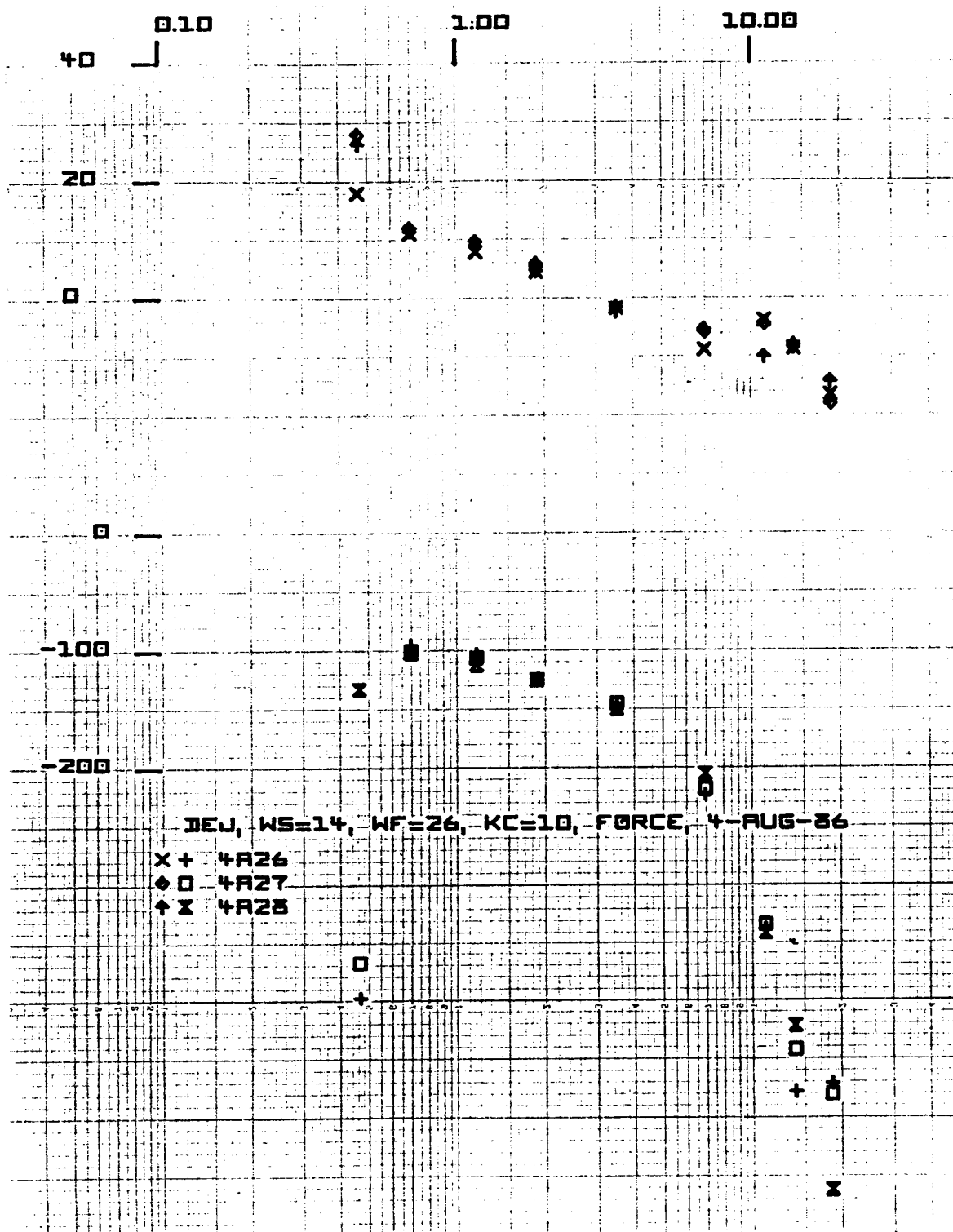


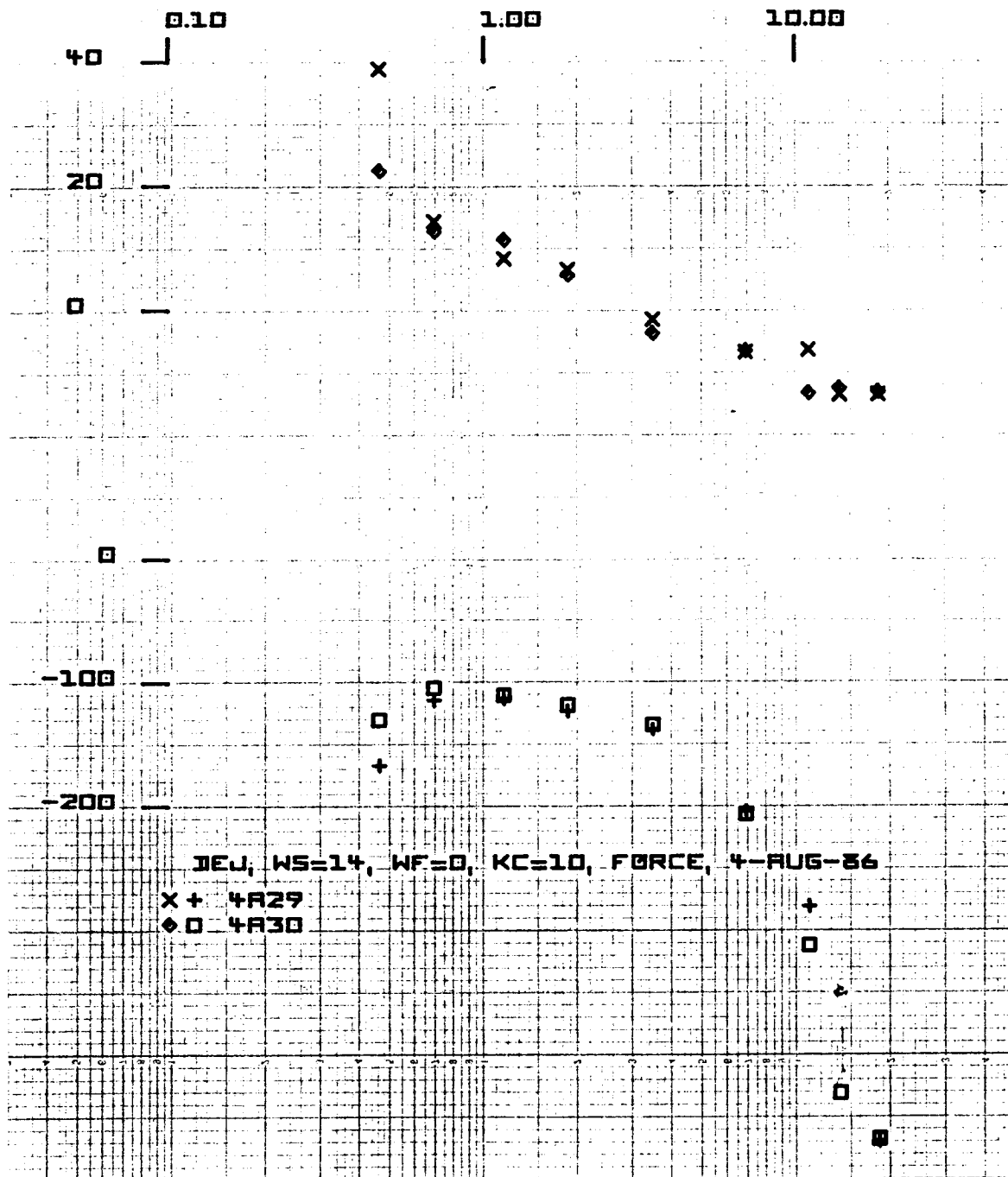


DEU, WS=14, WF=26, KC=10, POS, 4-AUG-86

X+ 4A23  
 diamond 4A24  
 X 4A25

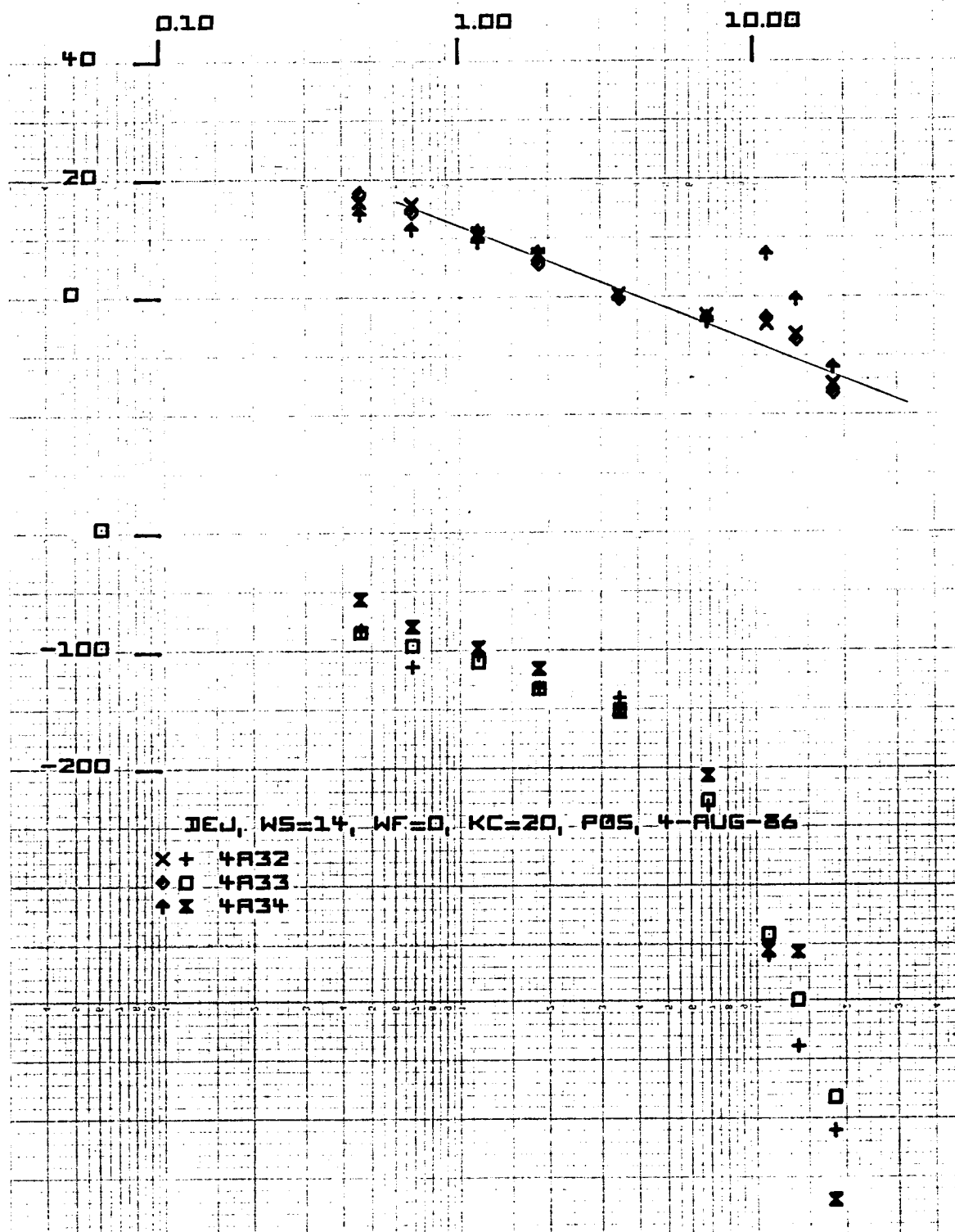
ORIGINAL PAGE IS  
OF POOR QUALITY

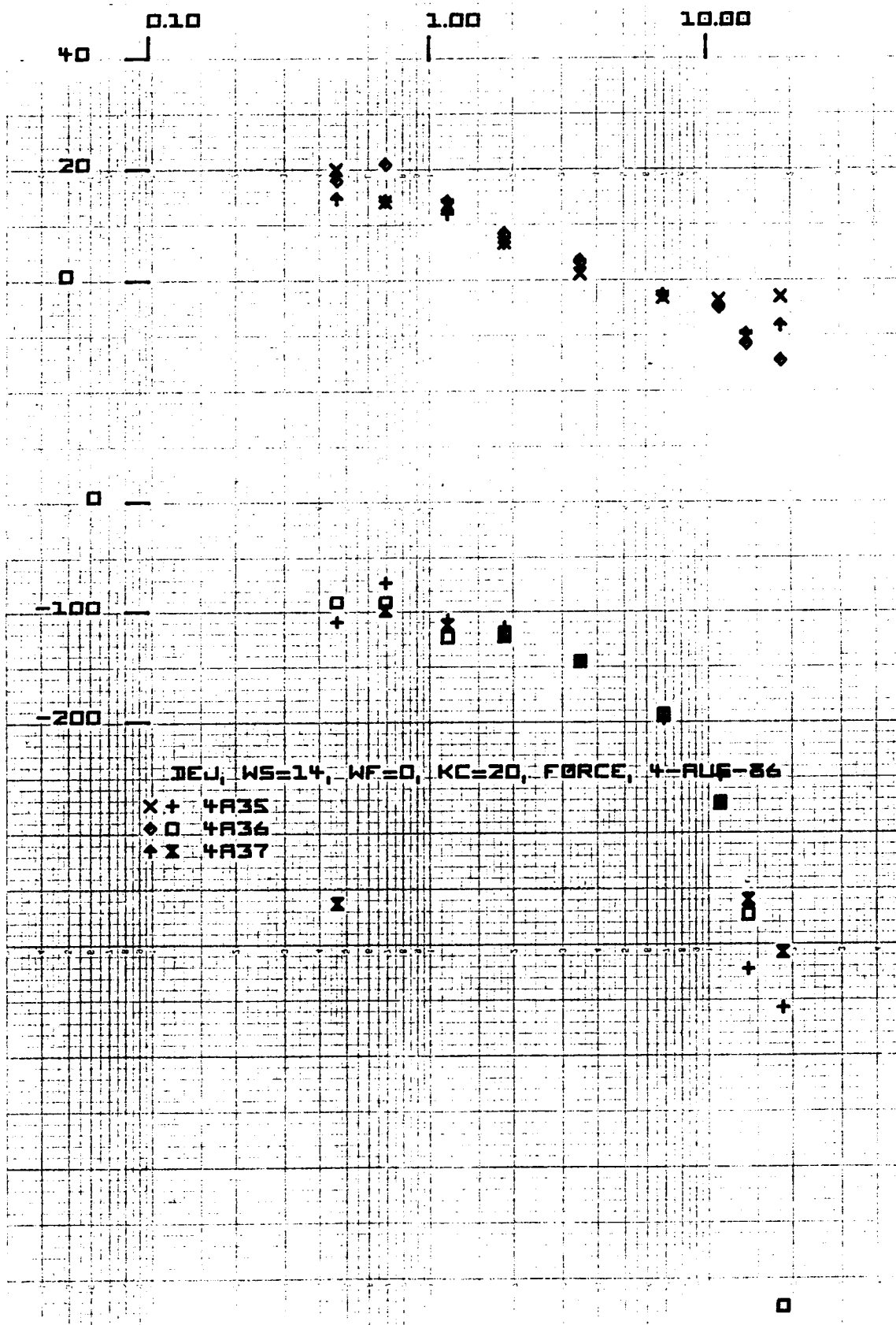




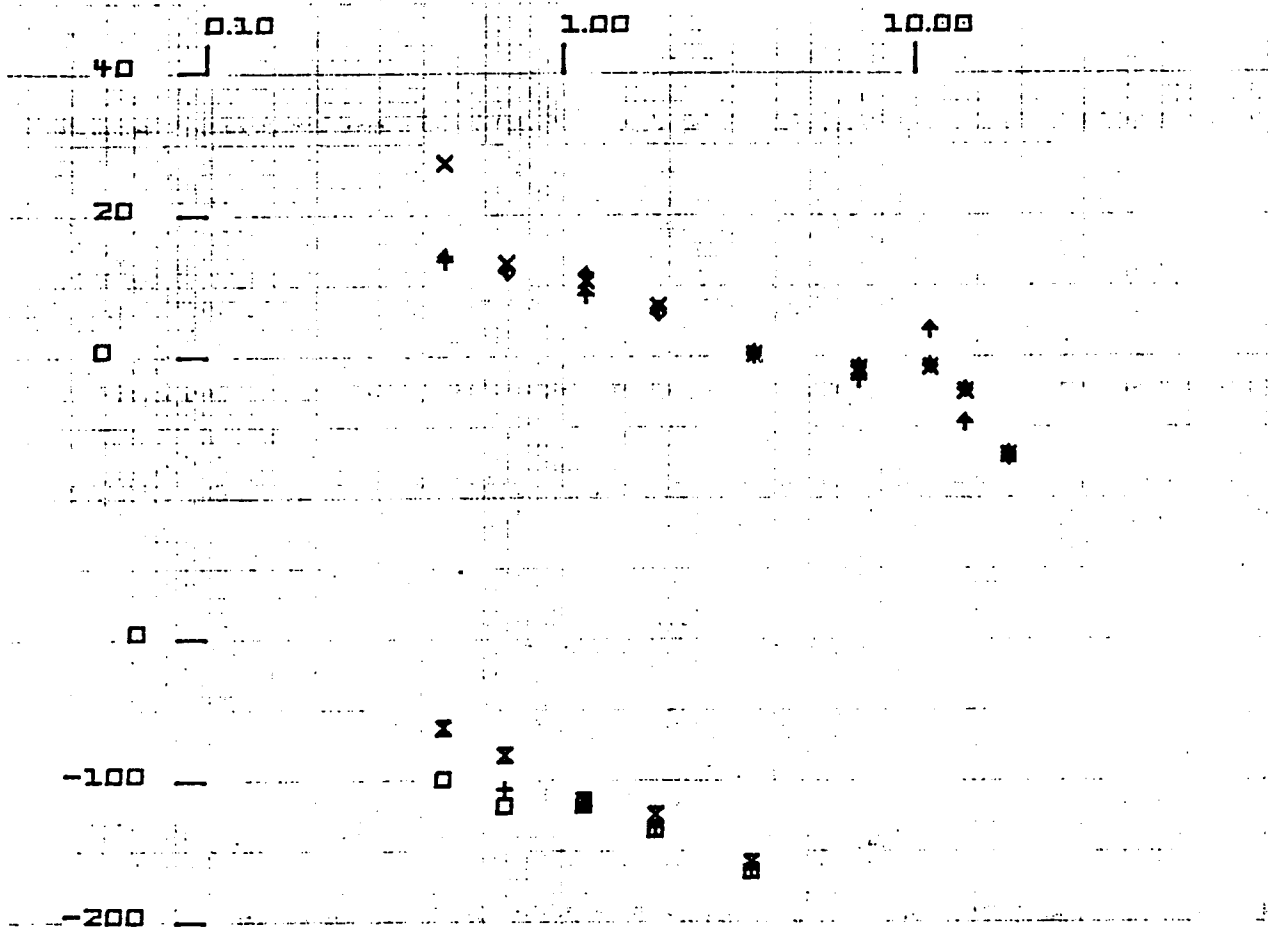
ORIGINAL PAGE IS  
OF POOR QUALITY

ORIGINAL PAGE IS  
OF POOR QUALITY



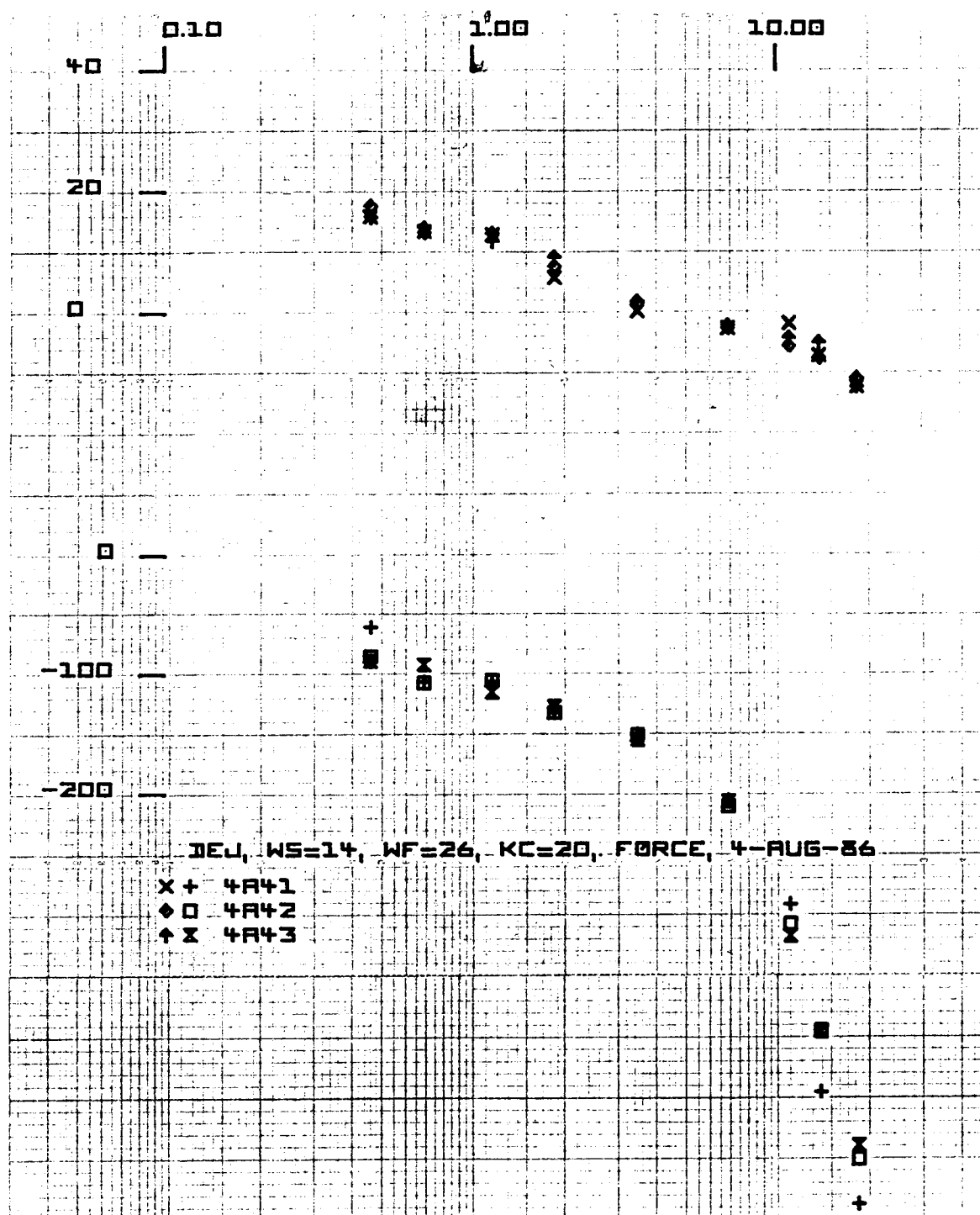


ORIGINAL PAGE IS  
OF POOR QUALITY



DEJ, WS=14, WF=26, KC=20, POS, 4-AUG-86

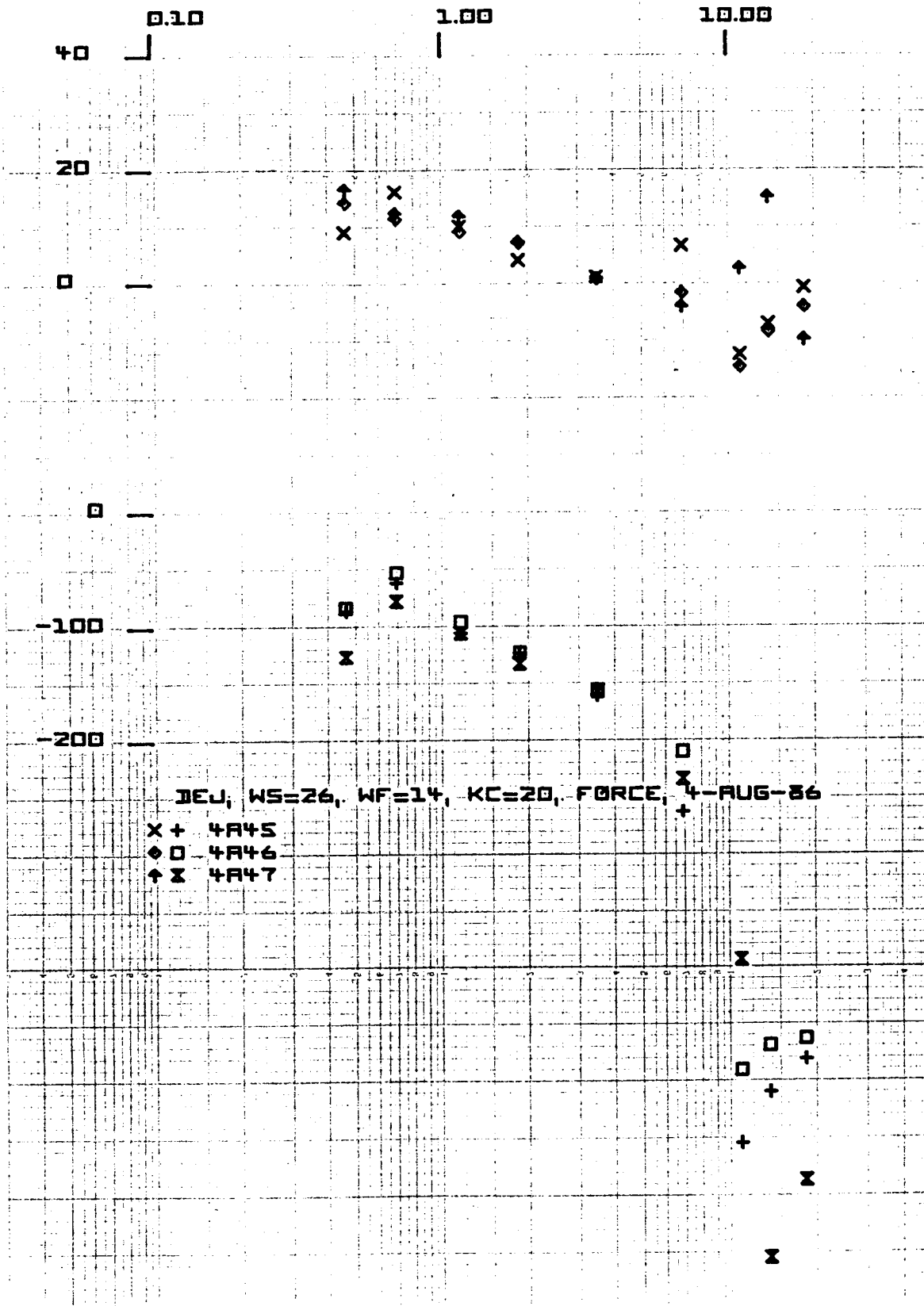
X+ 4A38  
 o 4A39  
 +X 4A40

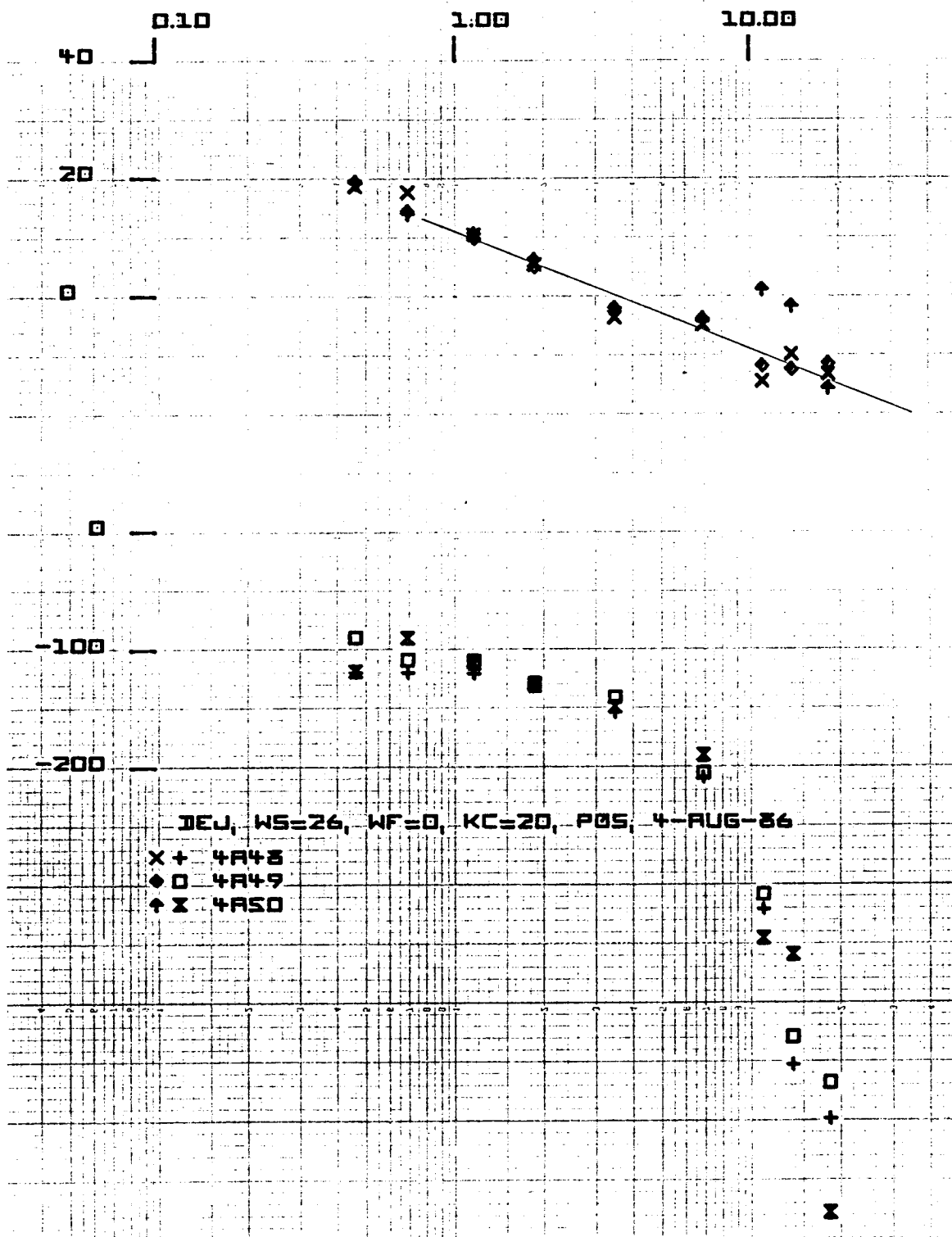


ORIGINAL PAGE IS  
OF POOR QUALITY

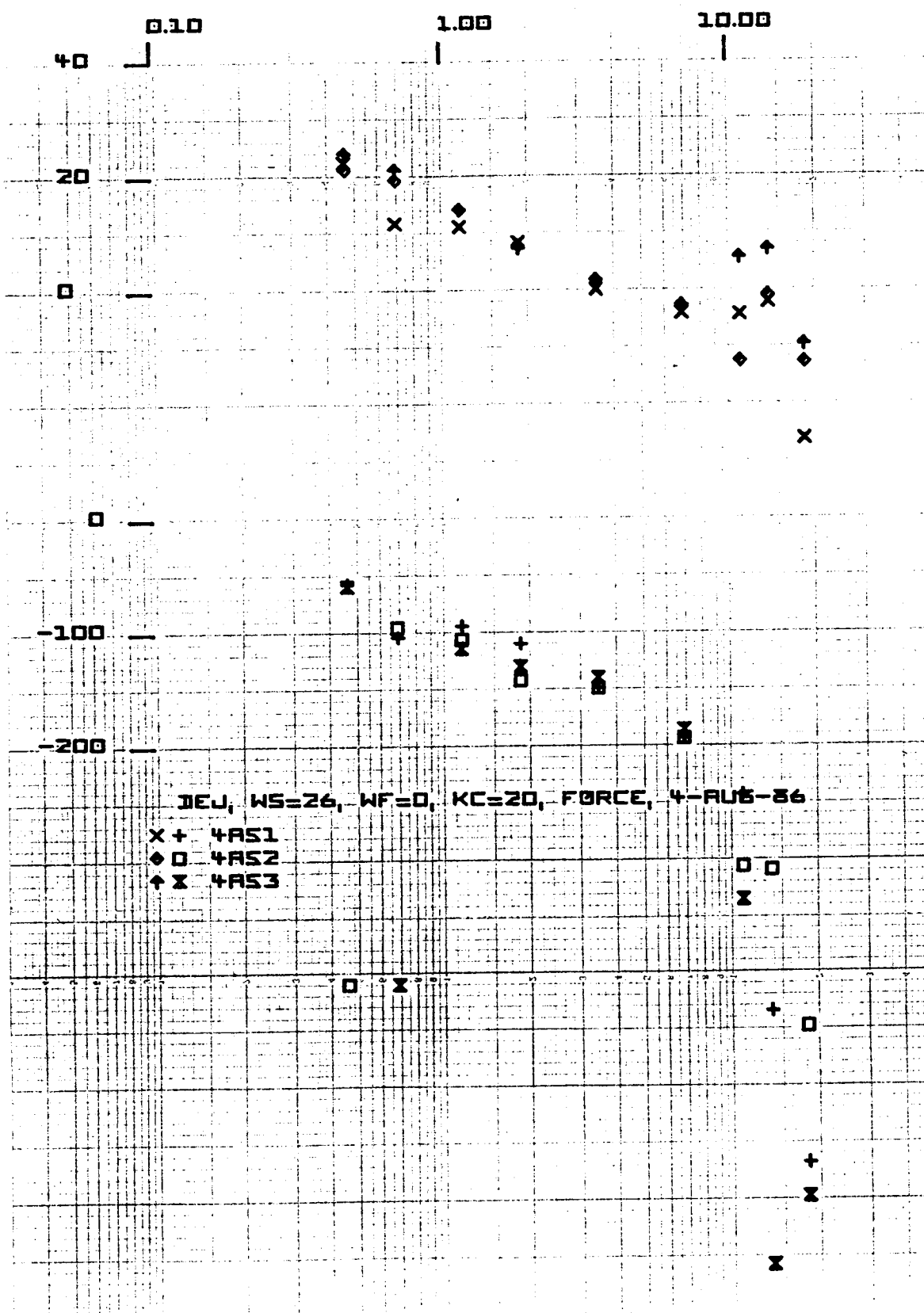


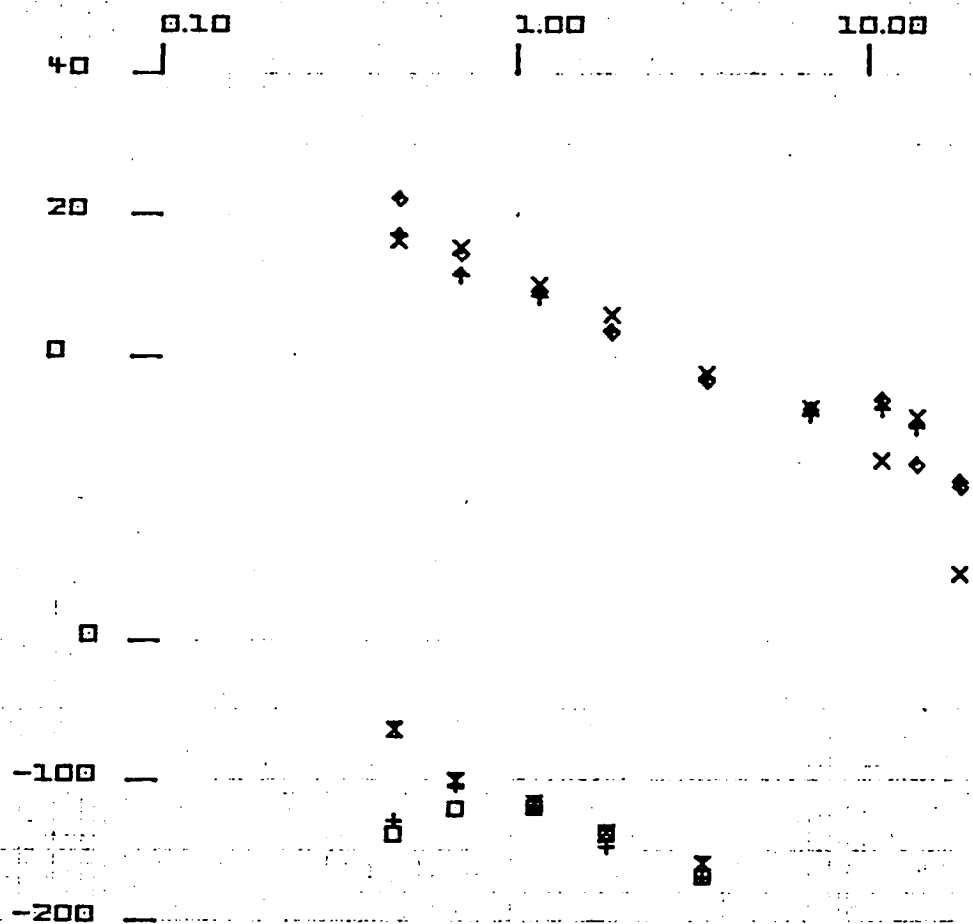
ORIGINAL PAGE IS  
OF POOR QUALITY

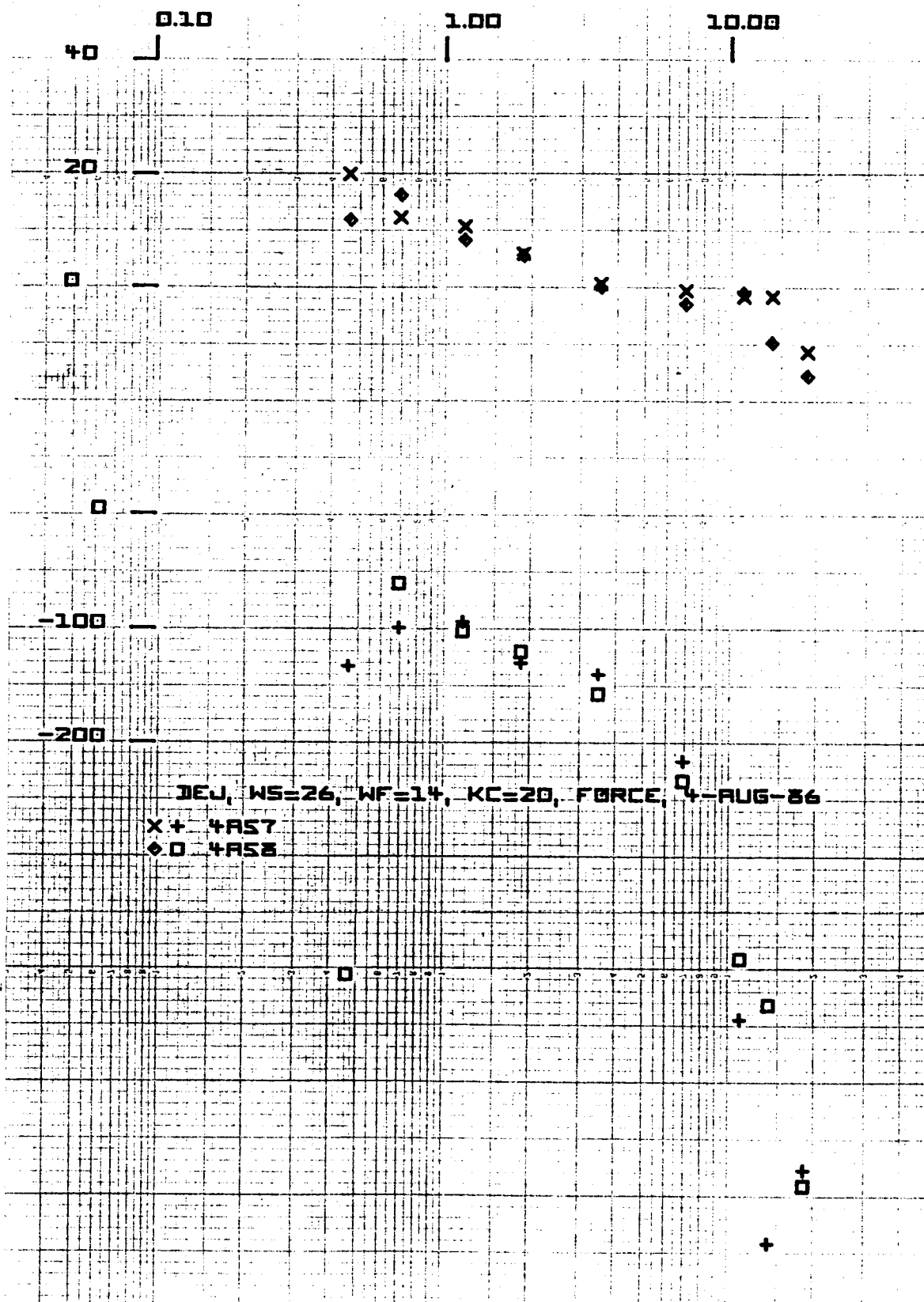


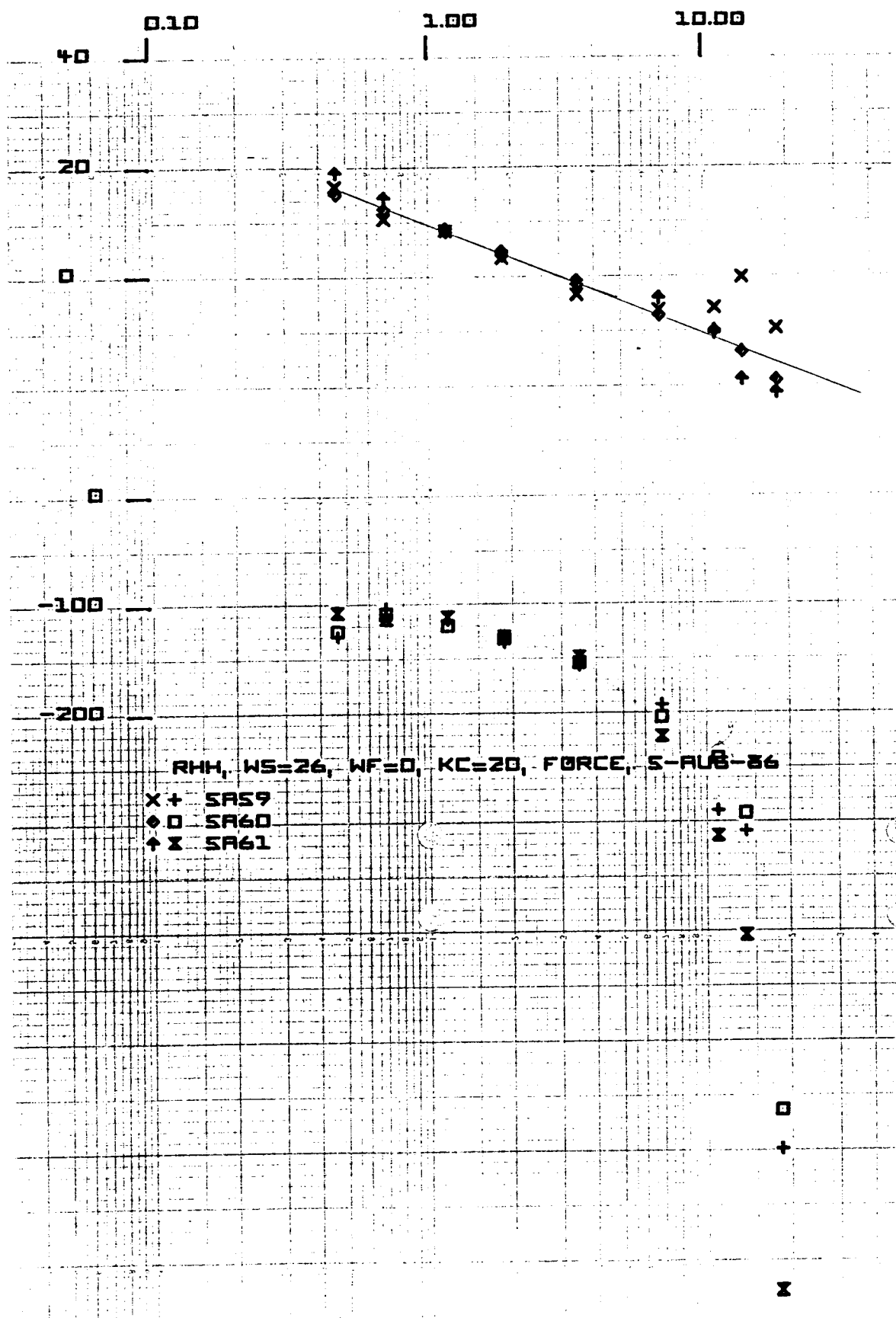


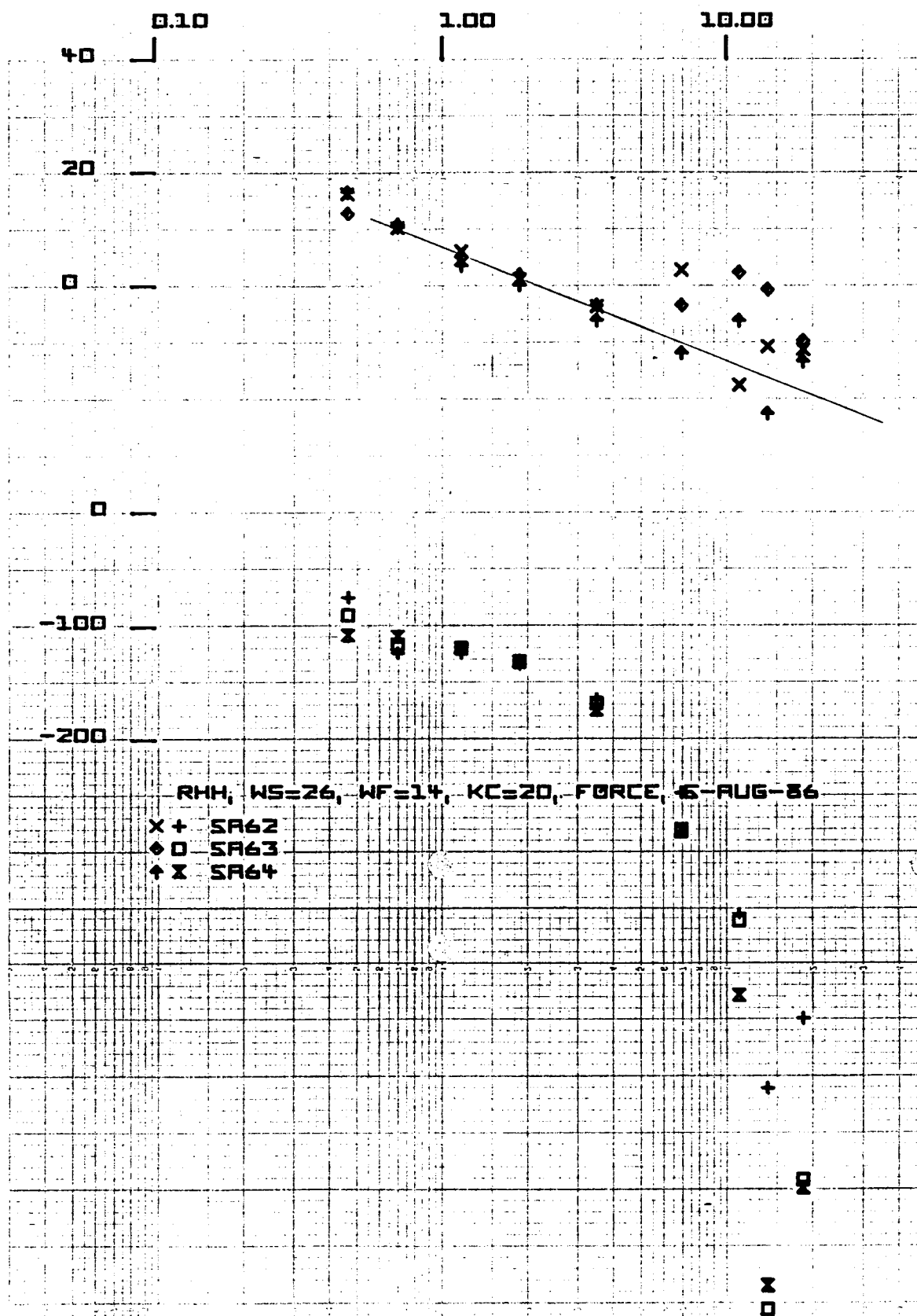
ORIGINAL PAGE IS  
OF POOR QUALITY

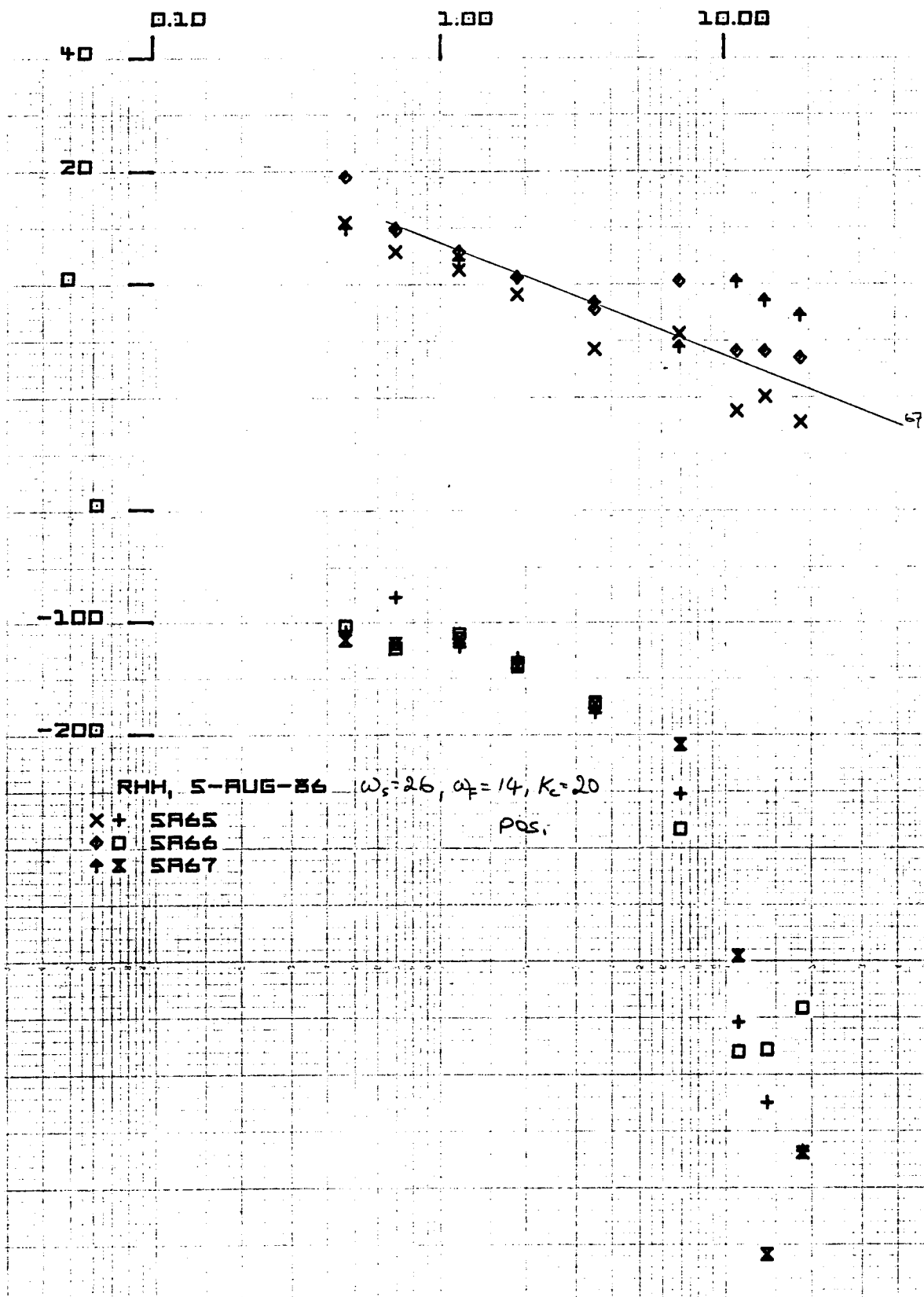




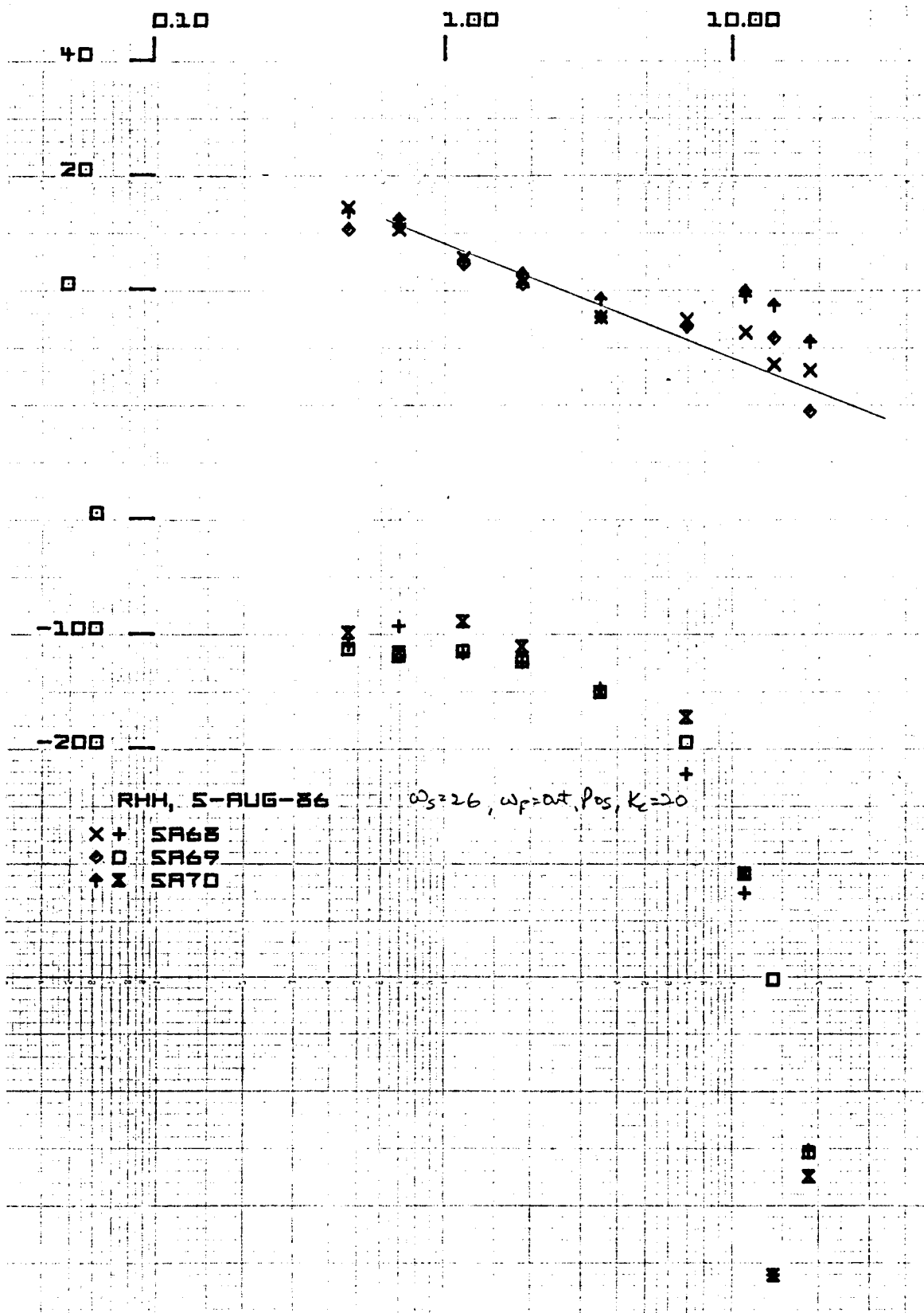


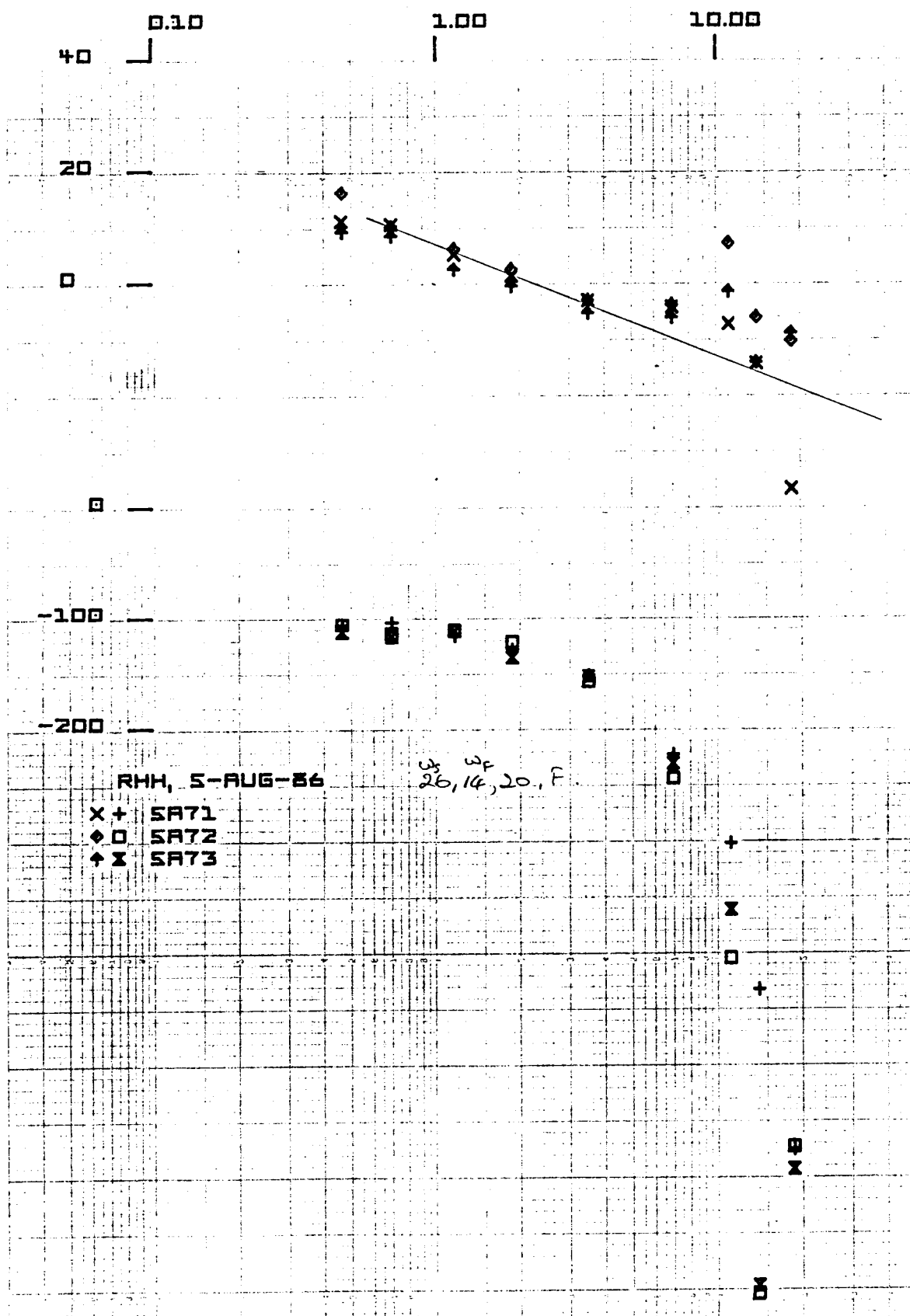


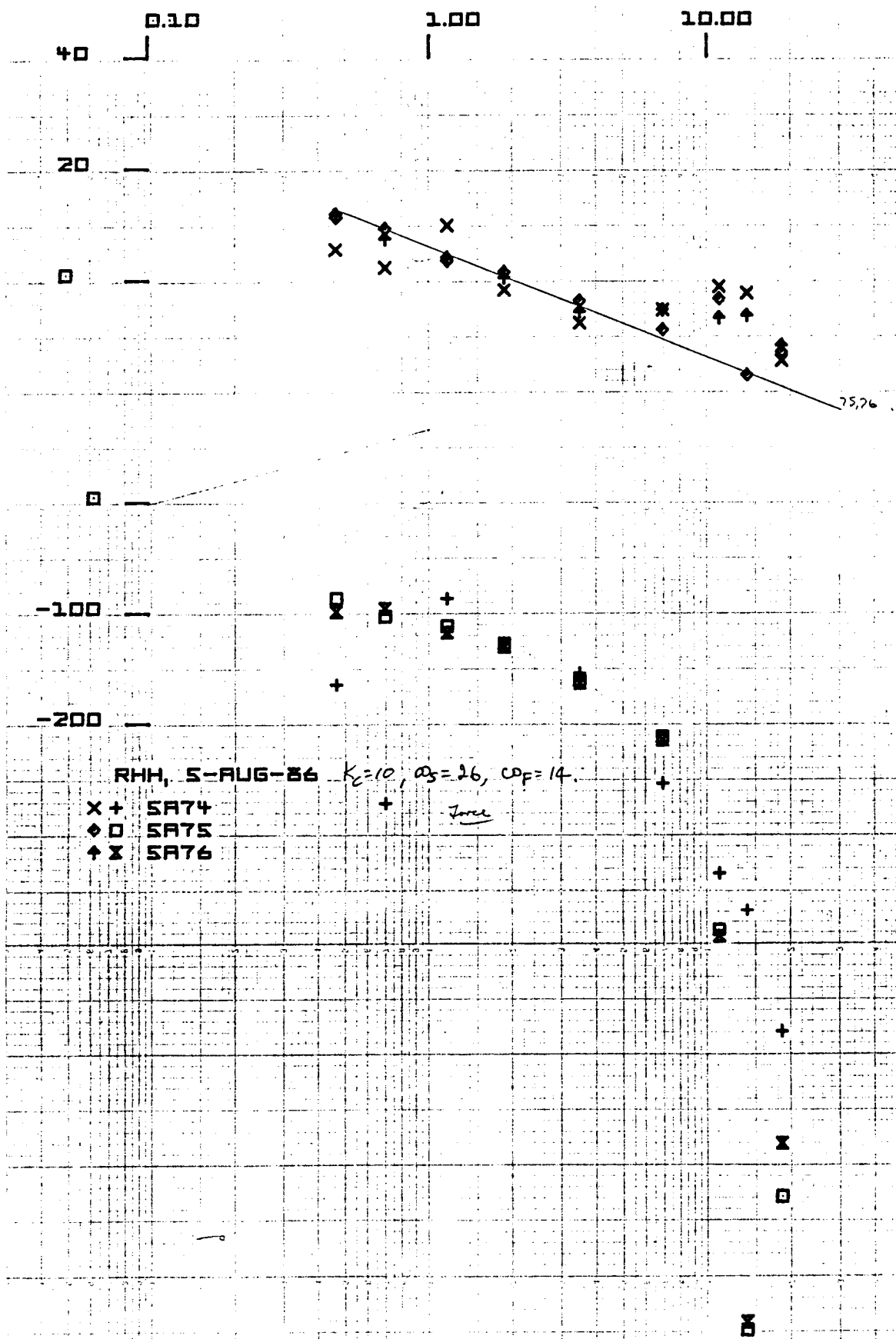


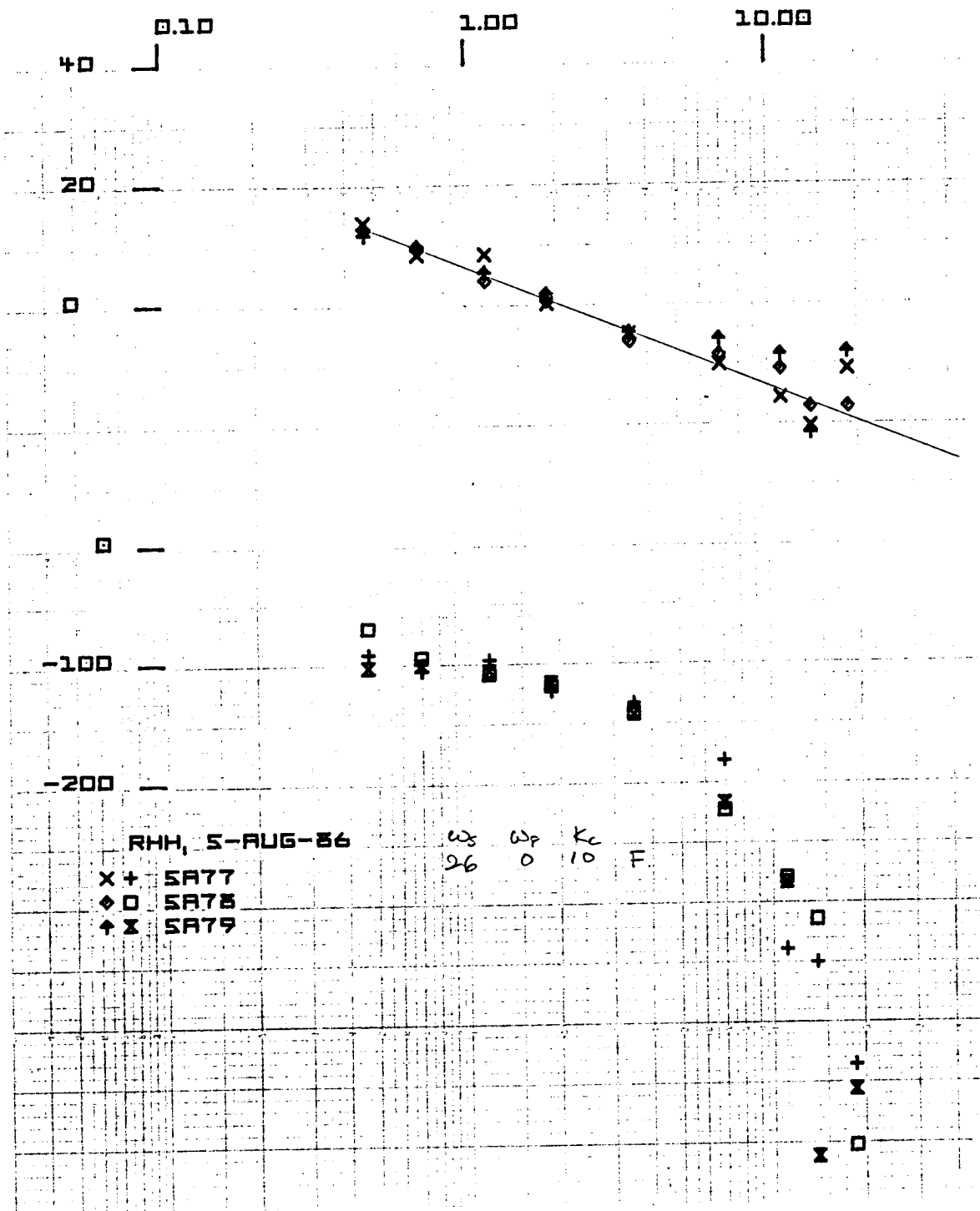


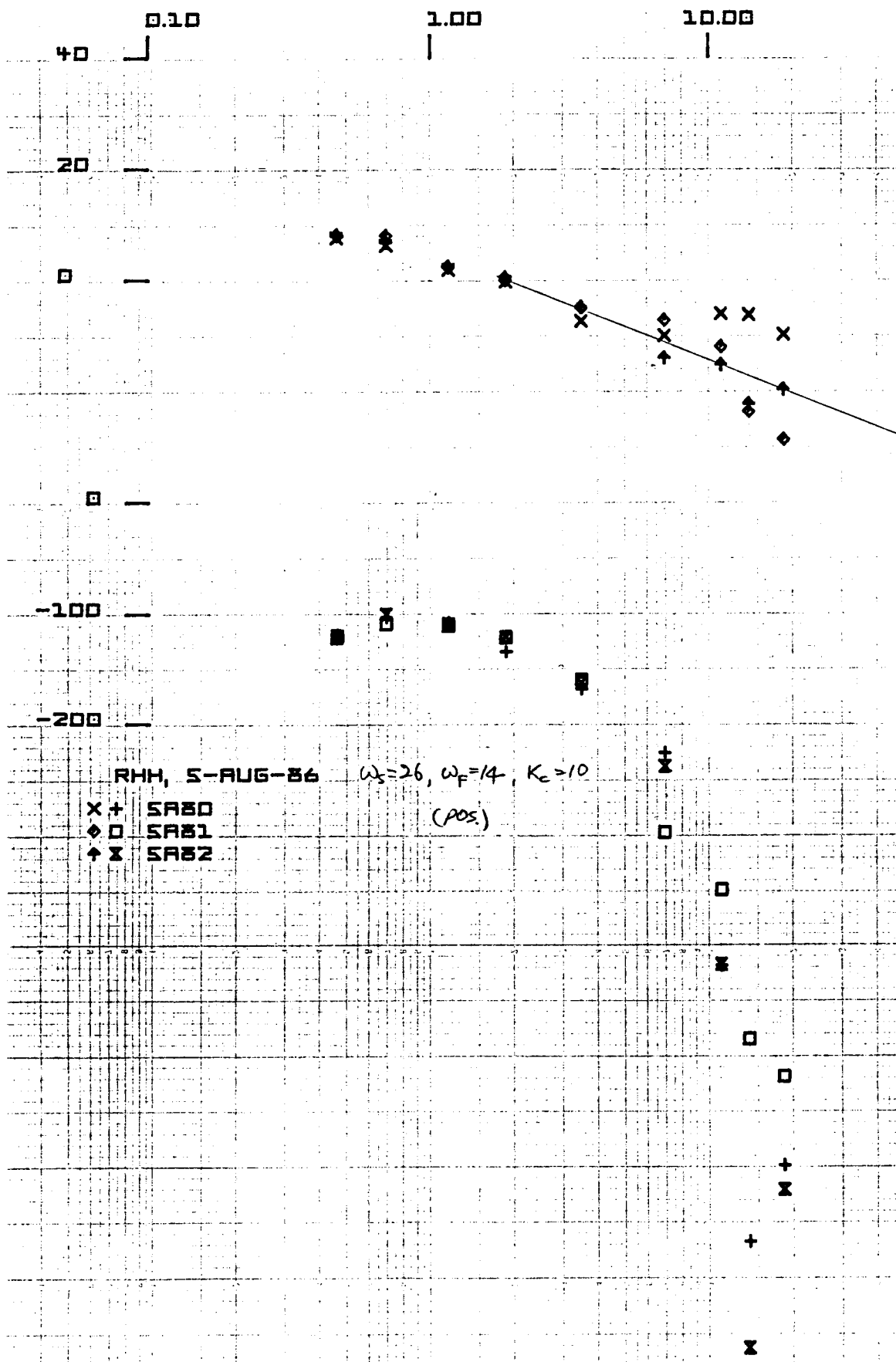


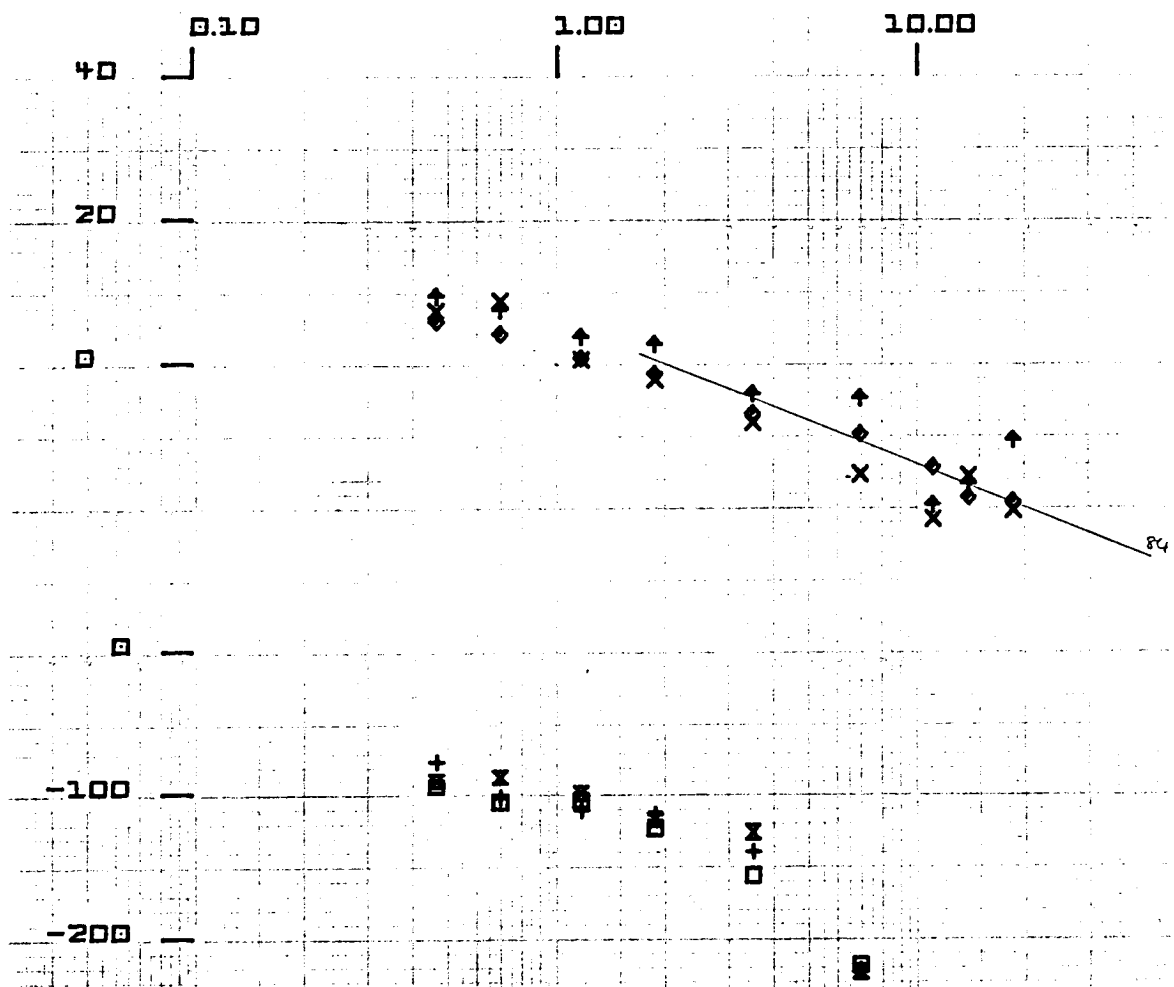






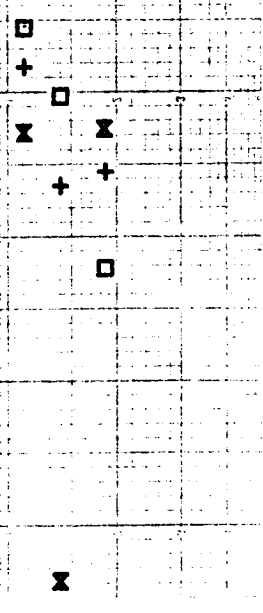


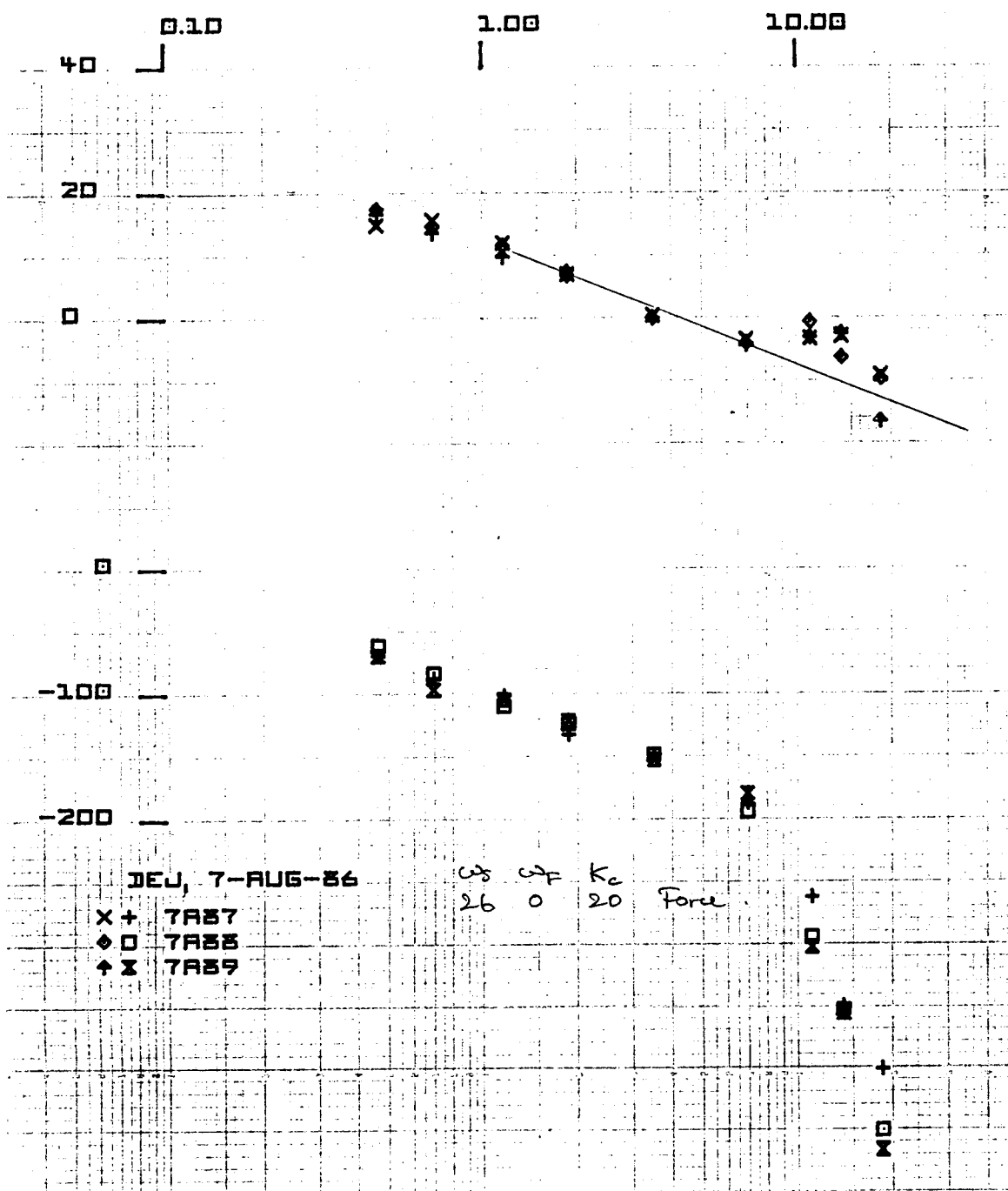


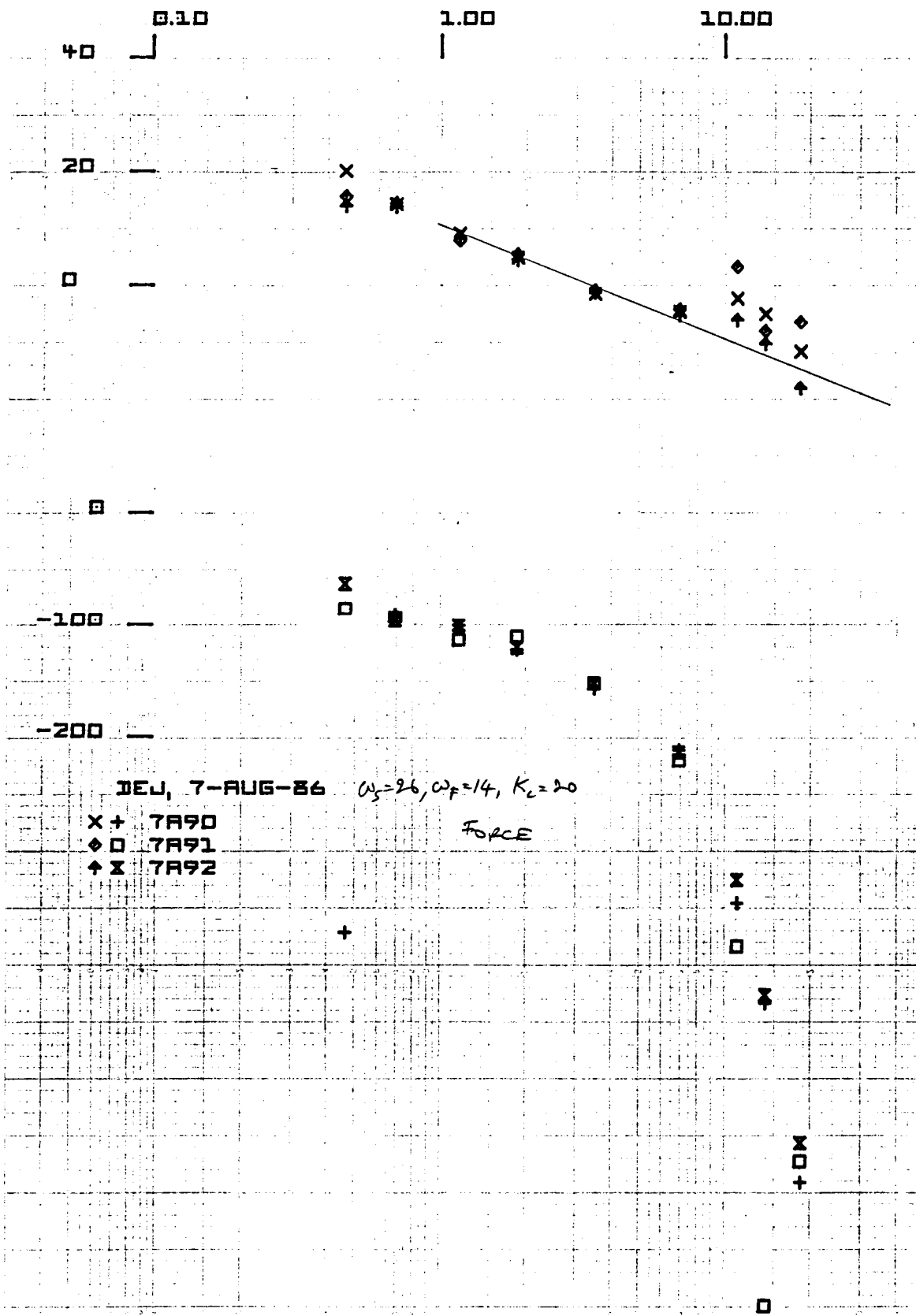


RHH, 5-AUG-86       $\omega_s$     $\omega_F$     $K_L$    Pos.  
 26      0      10

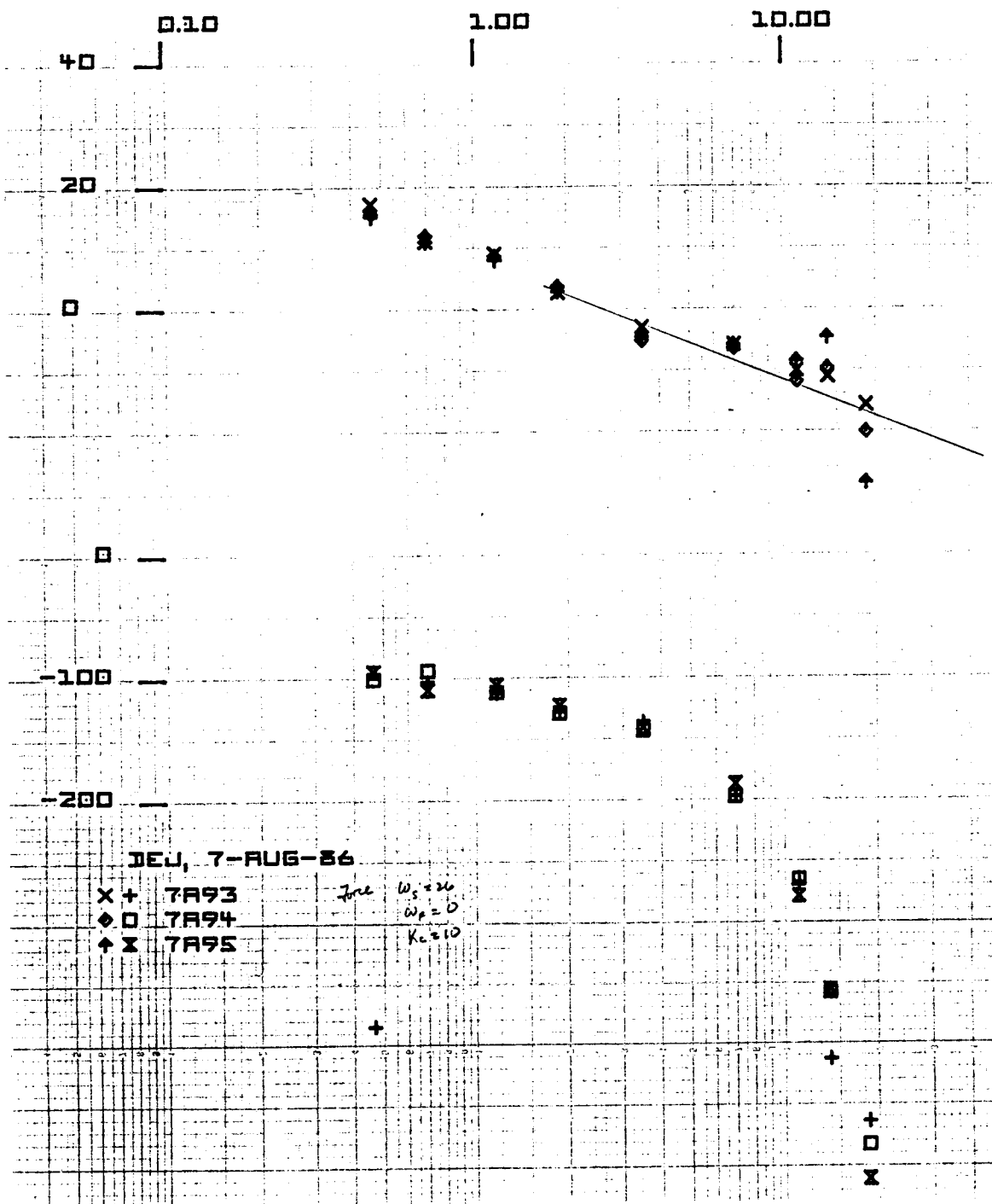
X +    SAB3  
 ◇    SAB4  
 + X    SAB5

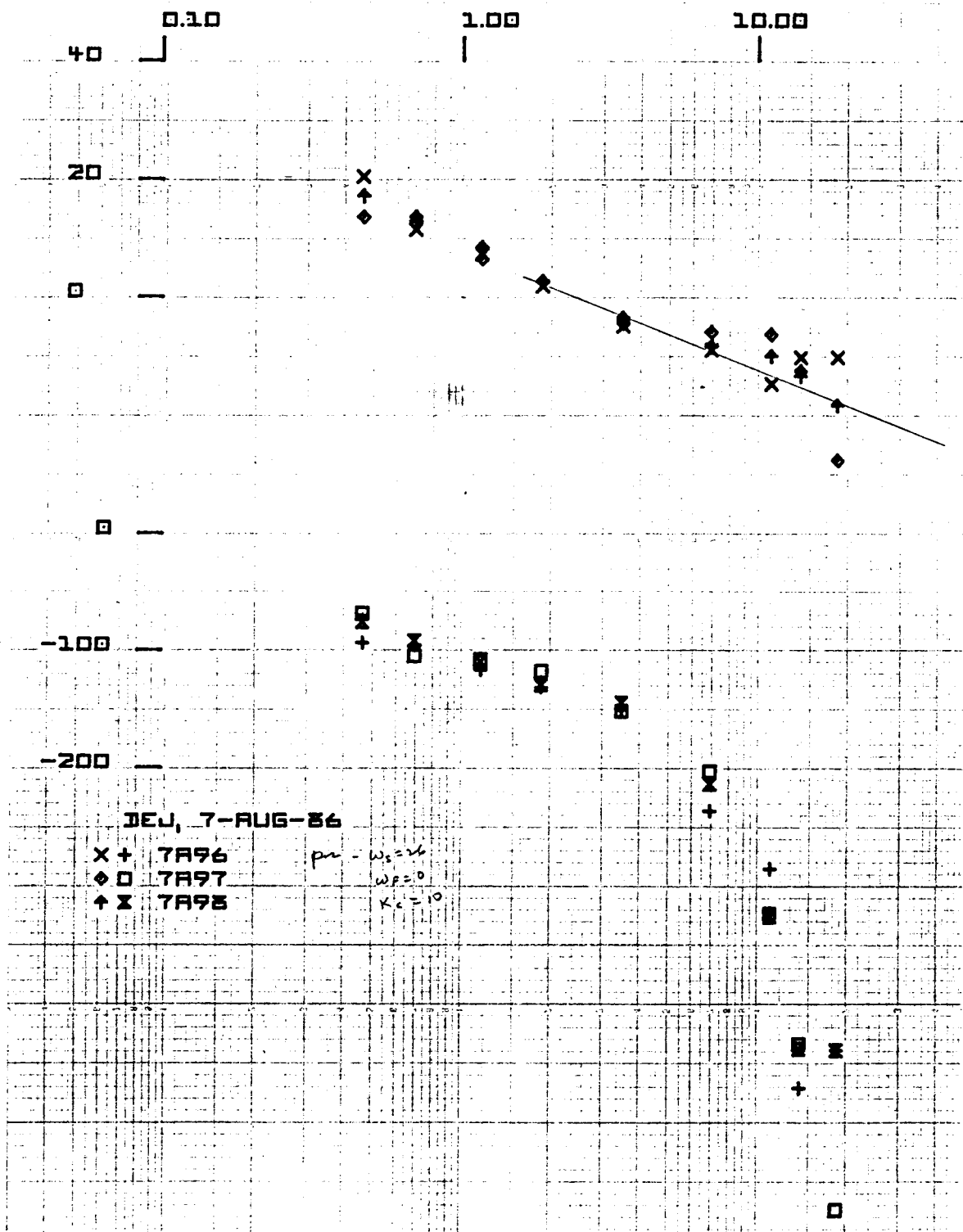


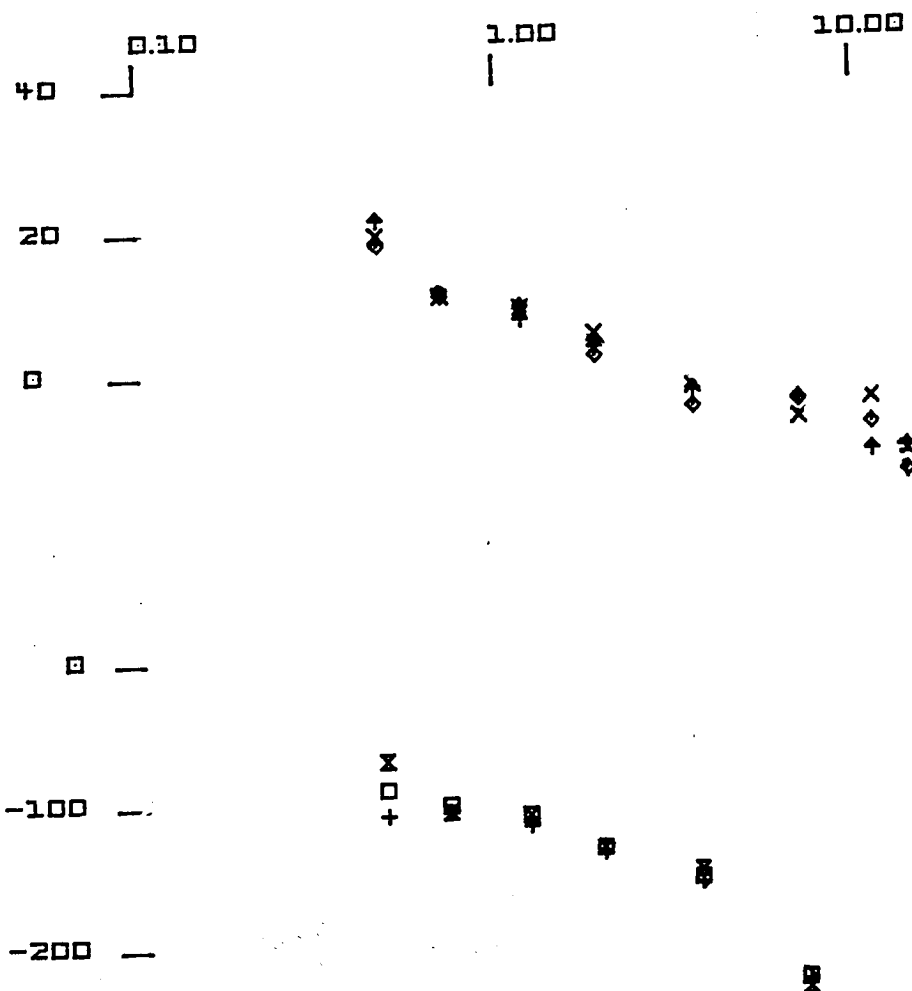












DEJ, 7-AUG-86

X+ 7A99  
 diamond 7A100  
 + X 7A101

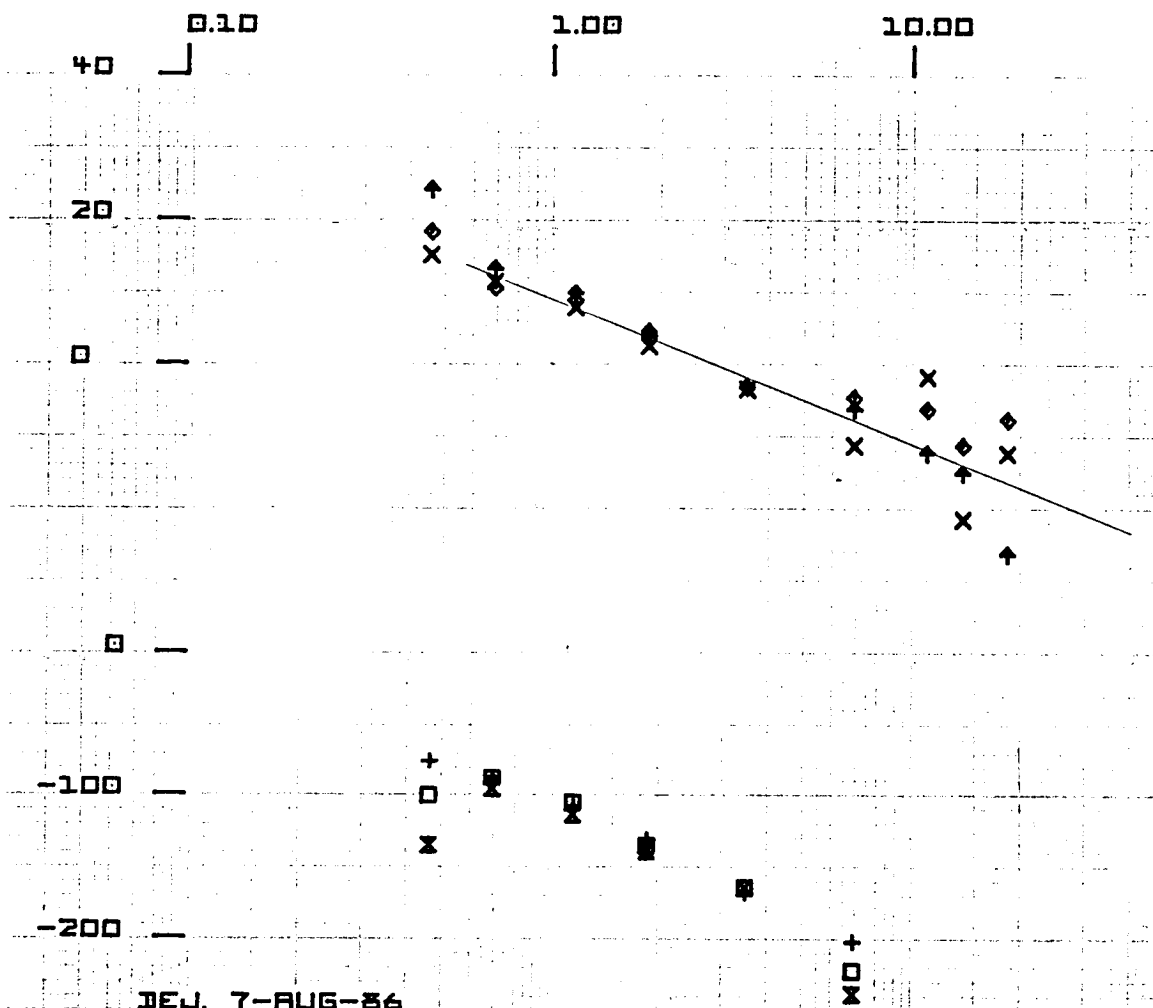
X  
 diamond  
 +

+

diamond

+

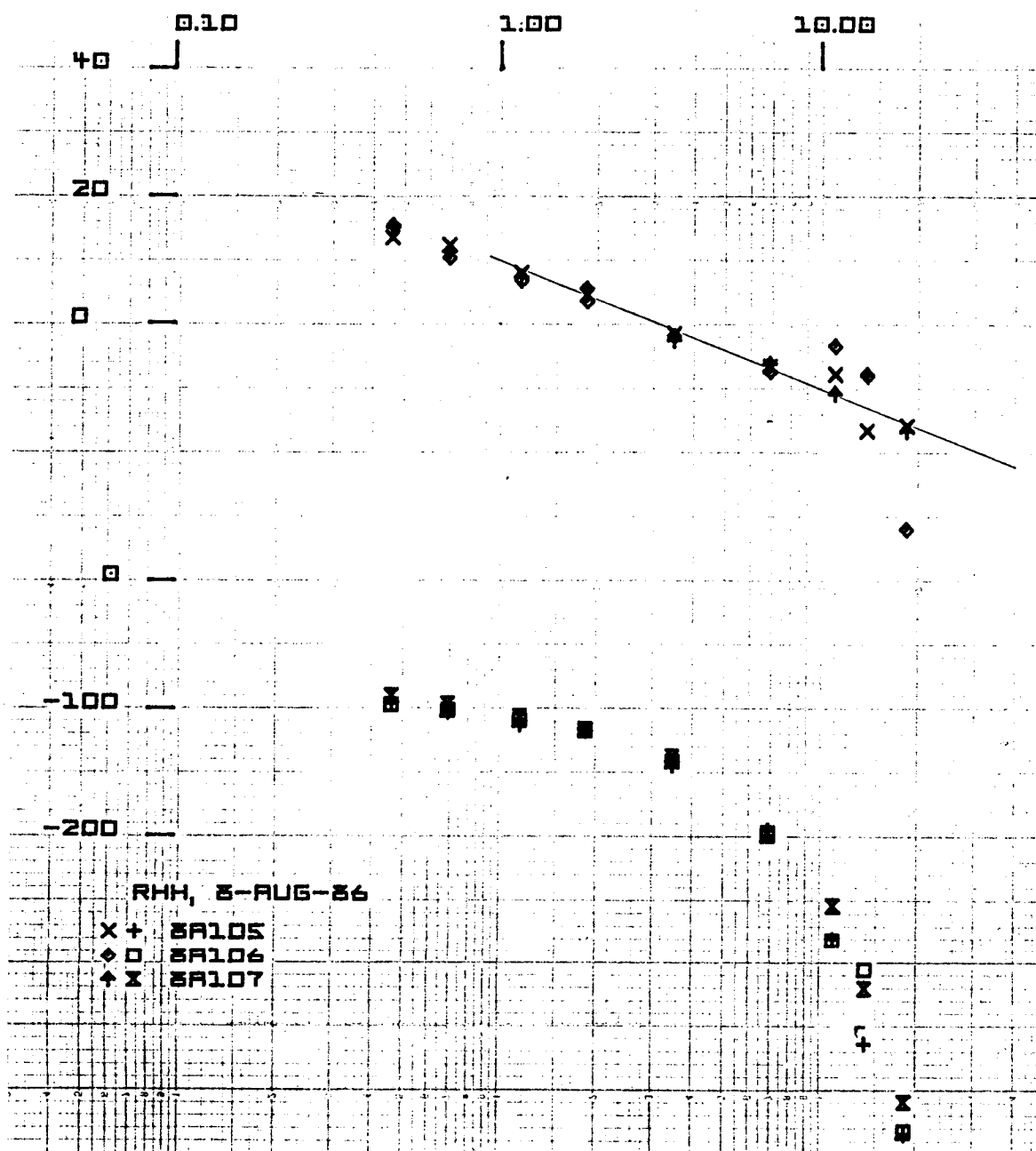
X

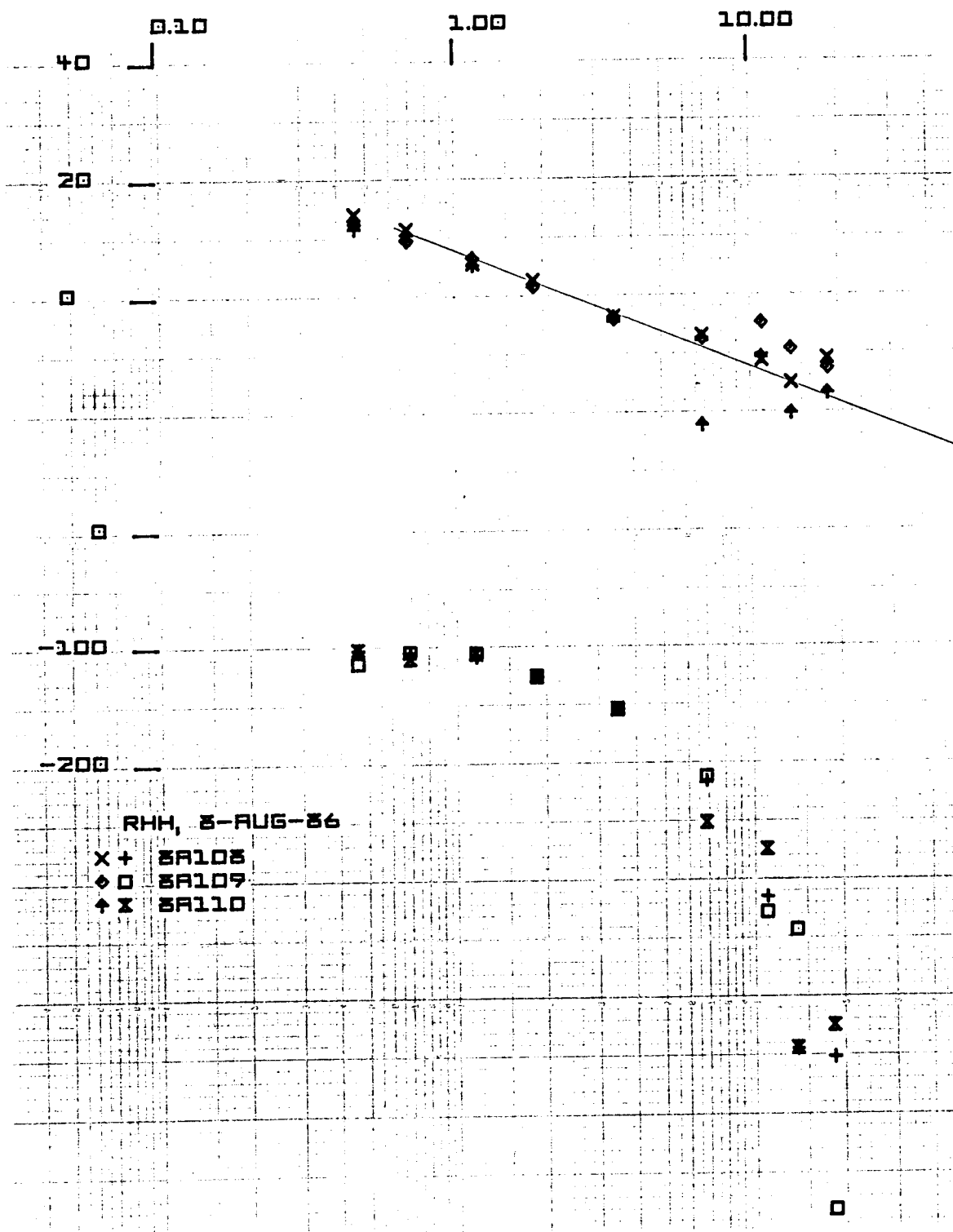


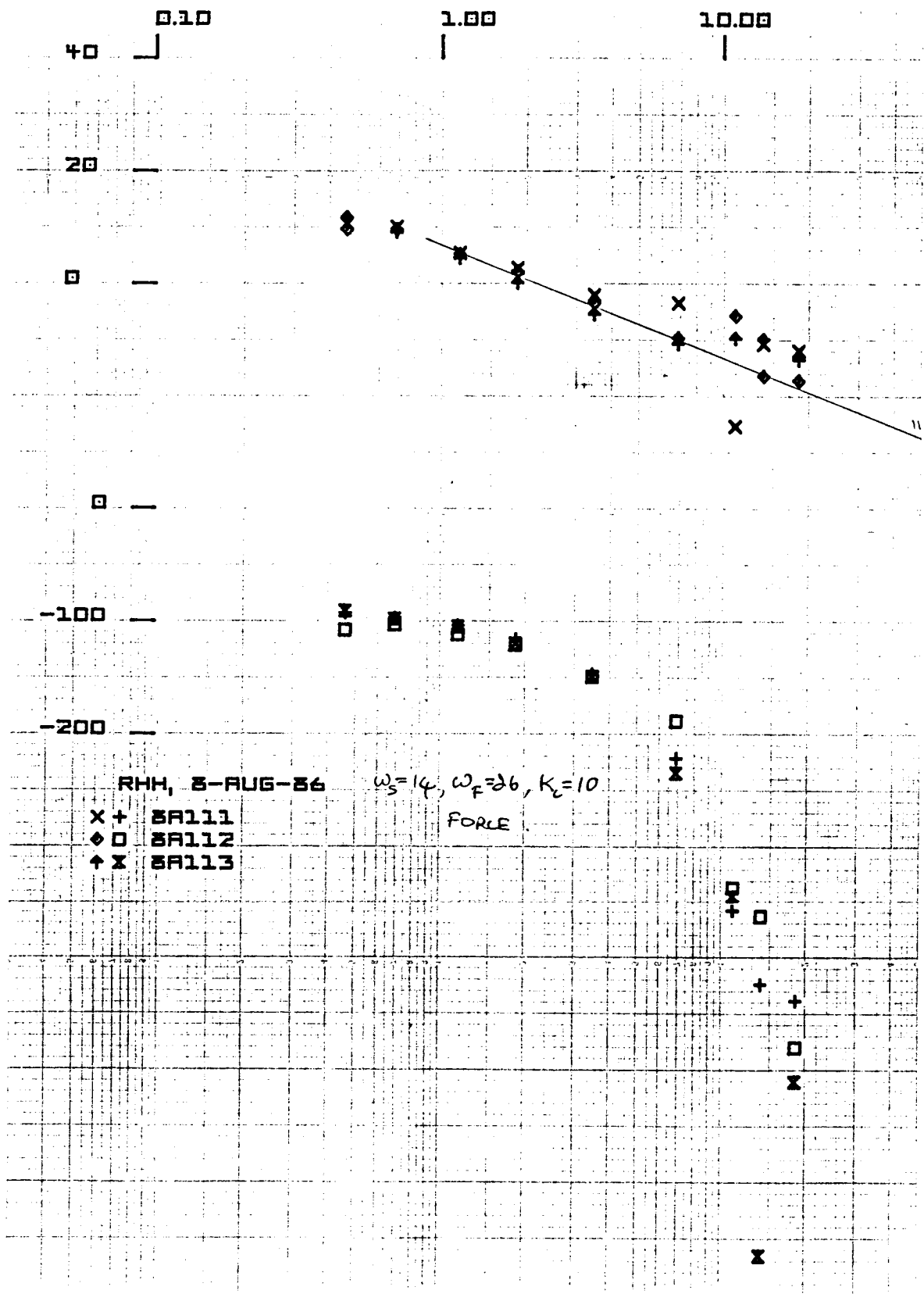
DEJ, 7-AUG-86

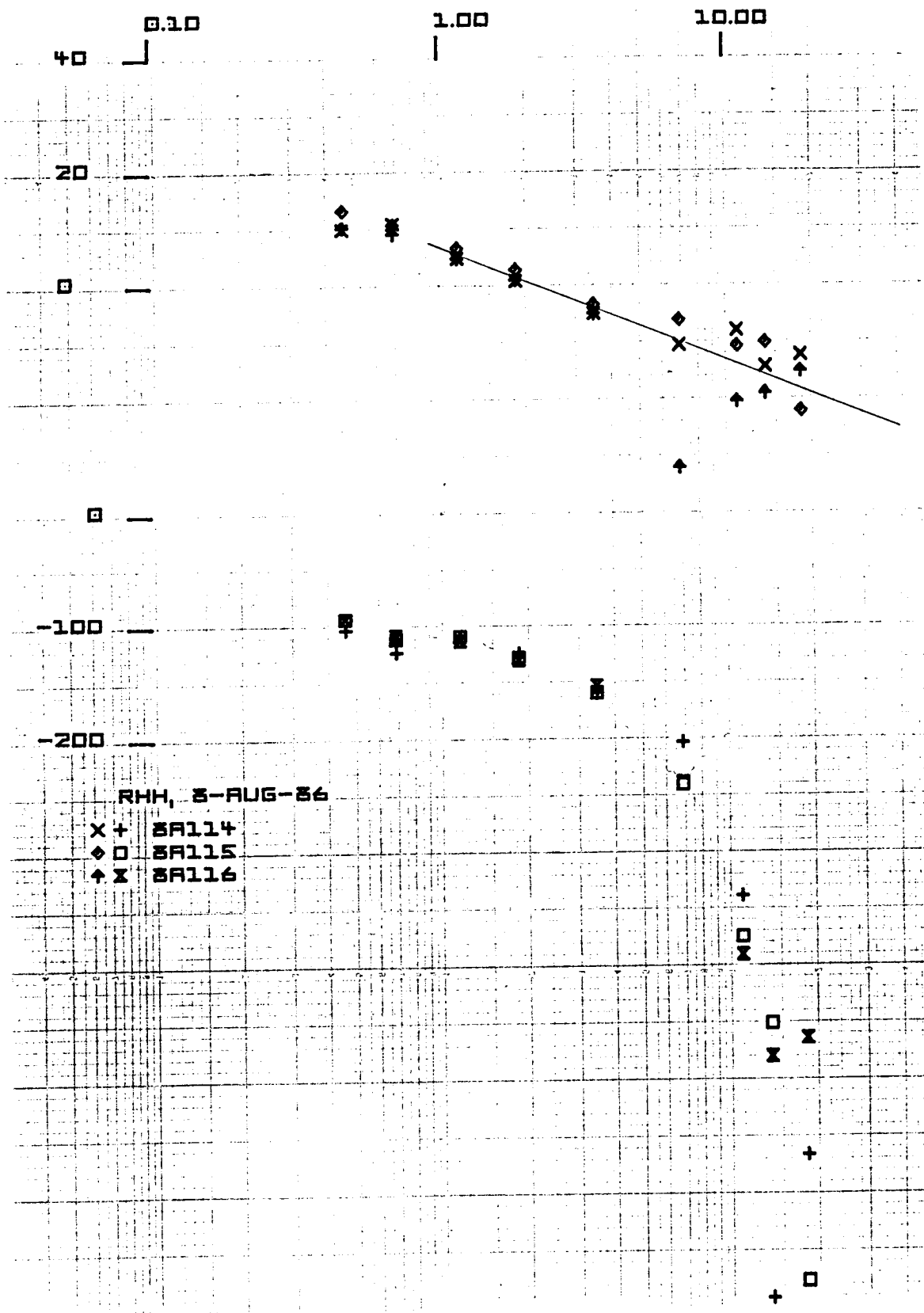
X+ 7A102  
 ◇ 7A103  
 + 7A104

Pos,  $\omega_F = 14$ ;  $\omega_S = 26$ ;  $K_c = 10$

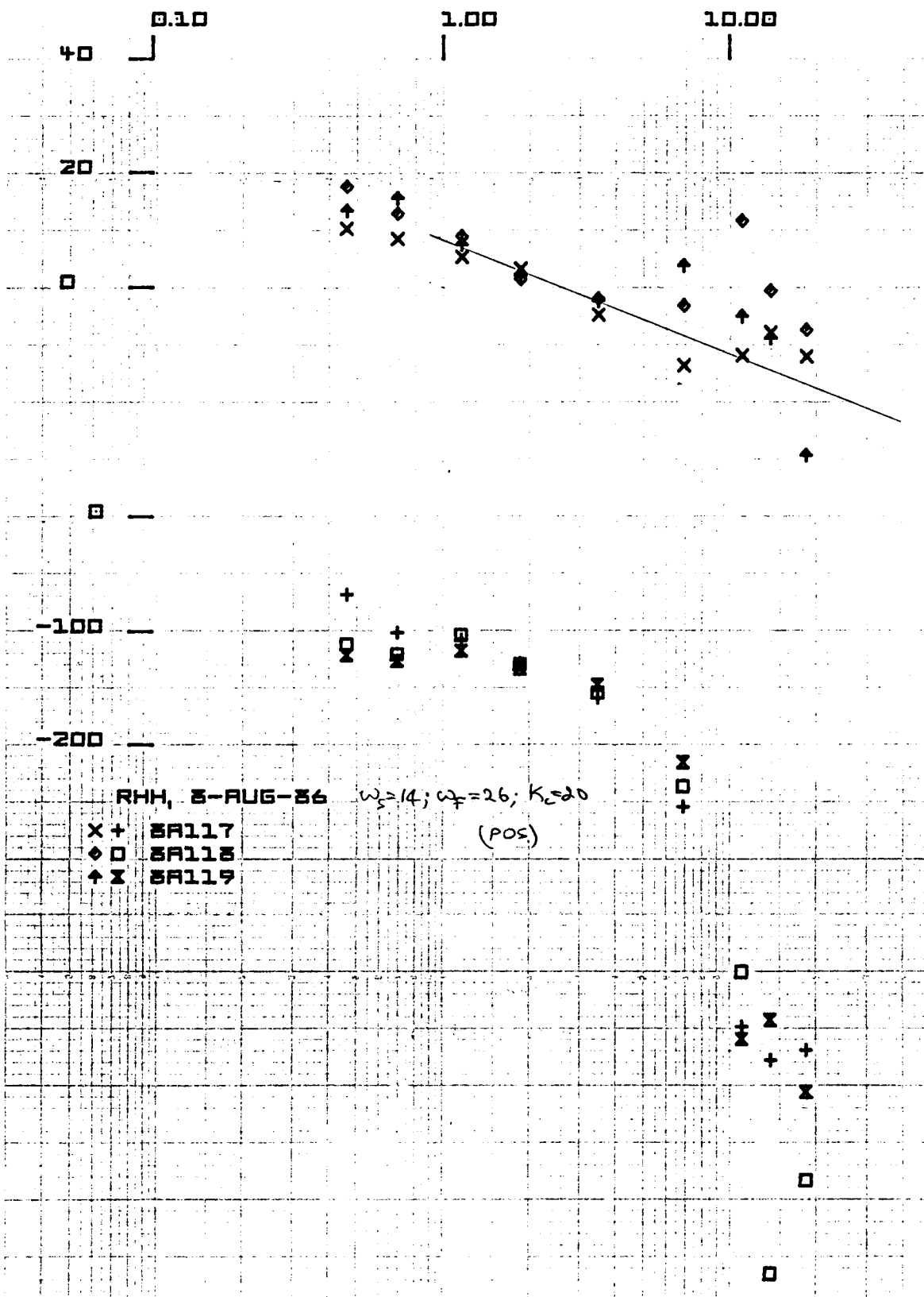


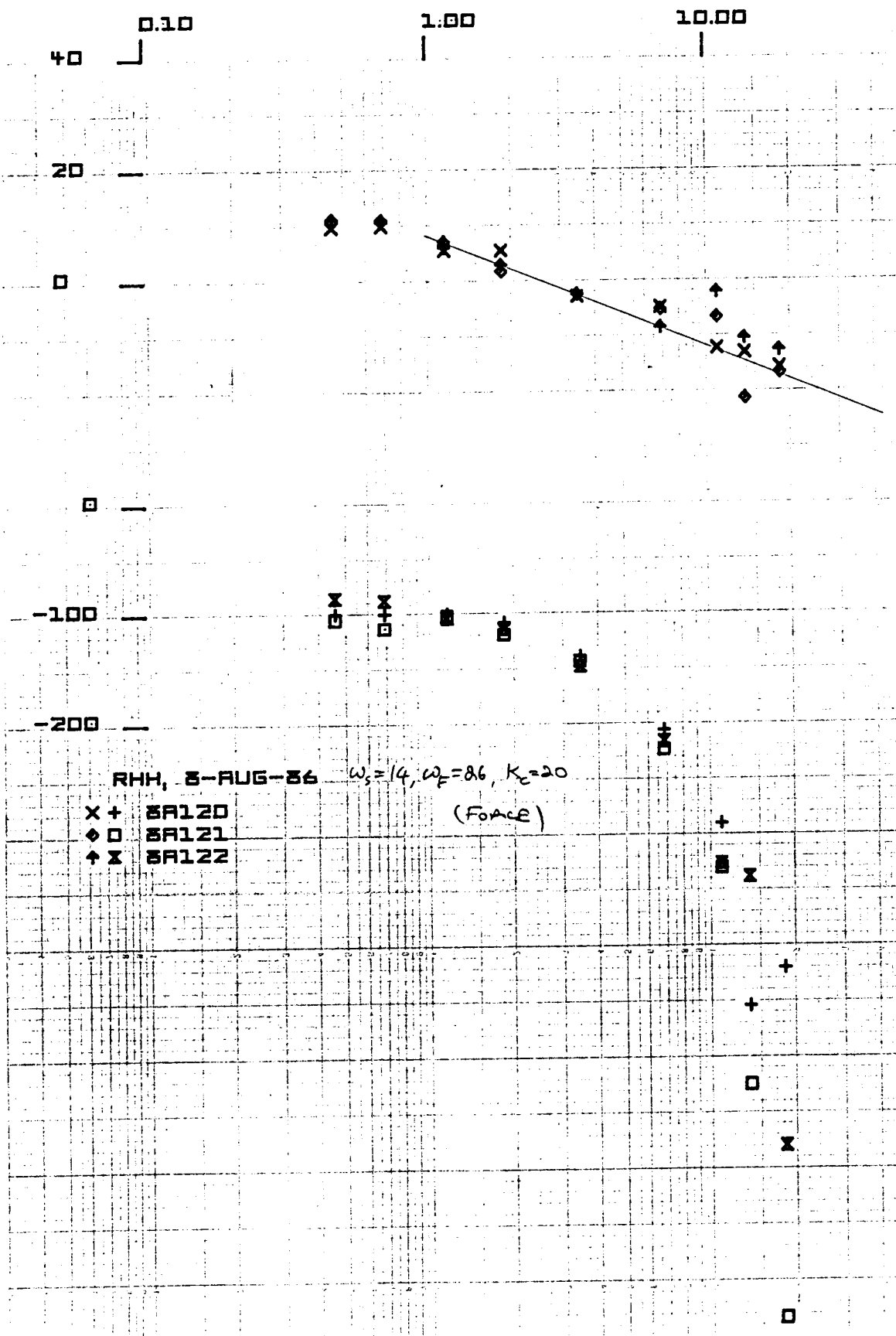


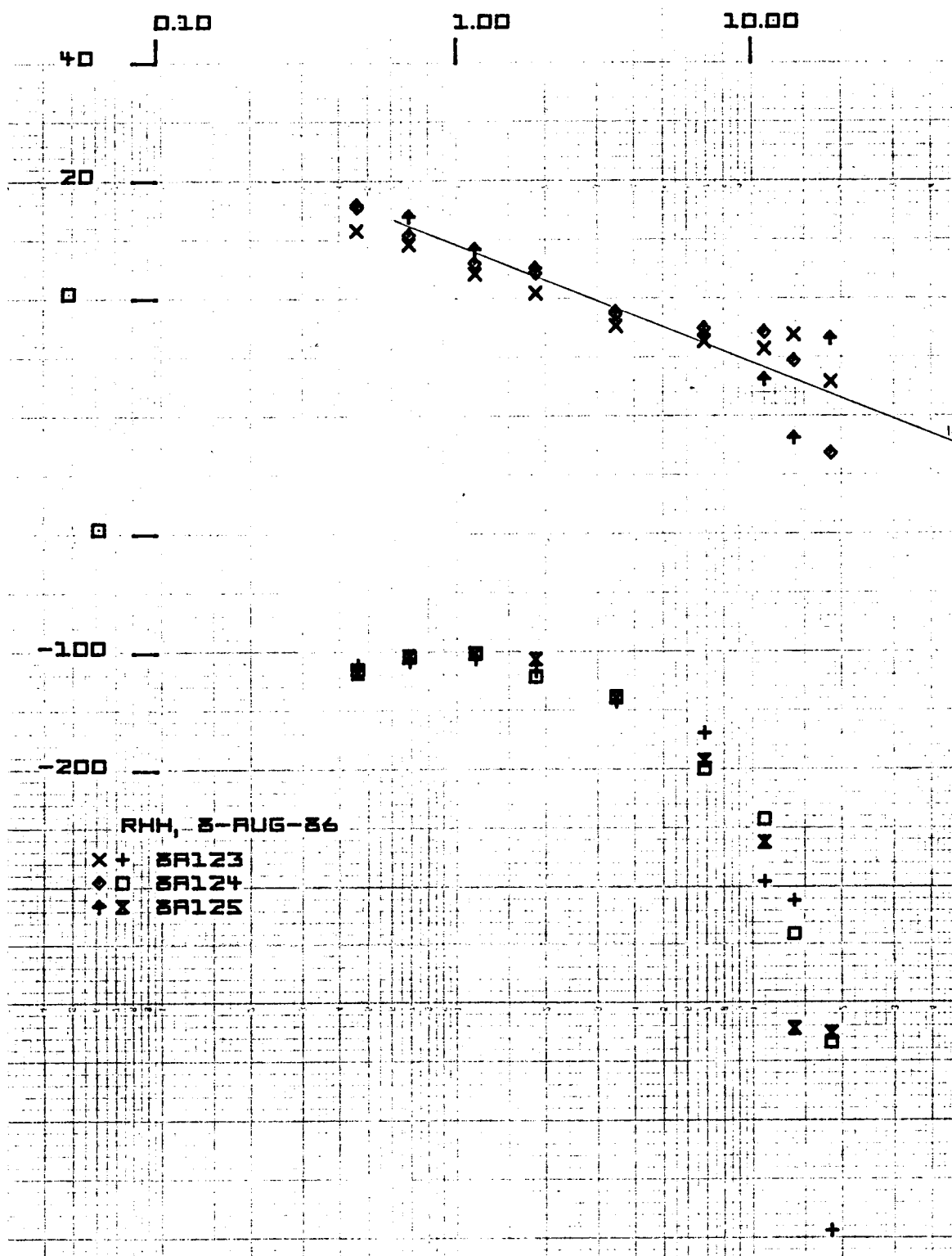


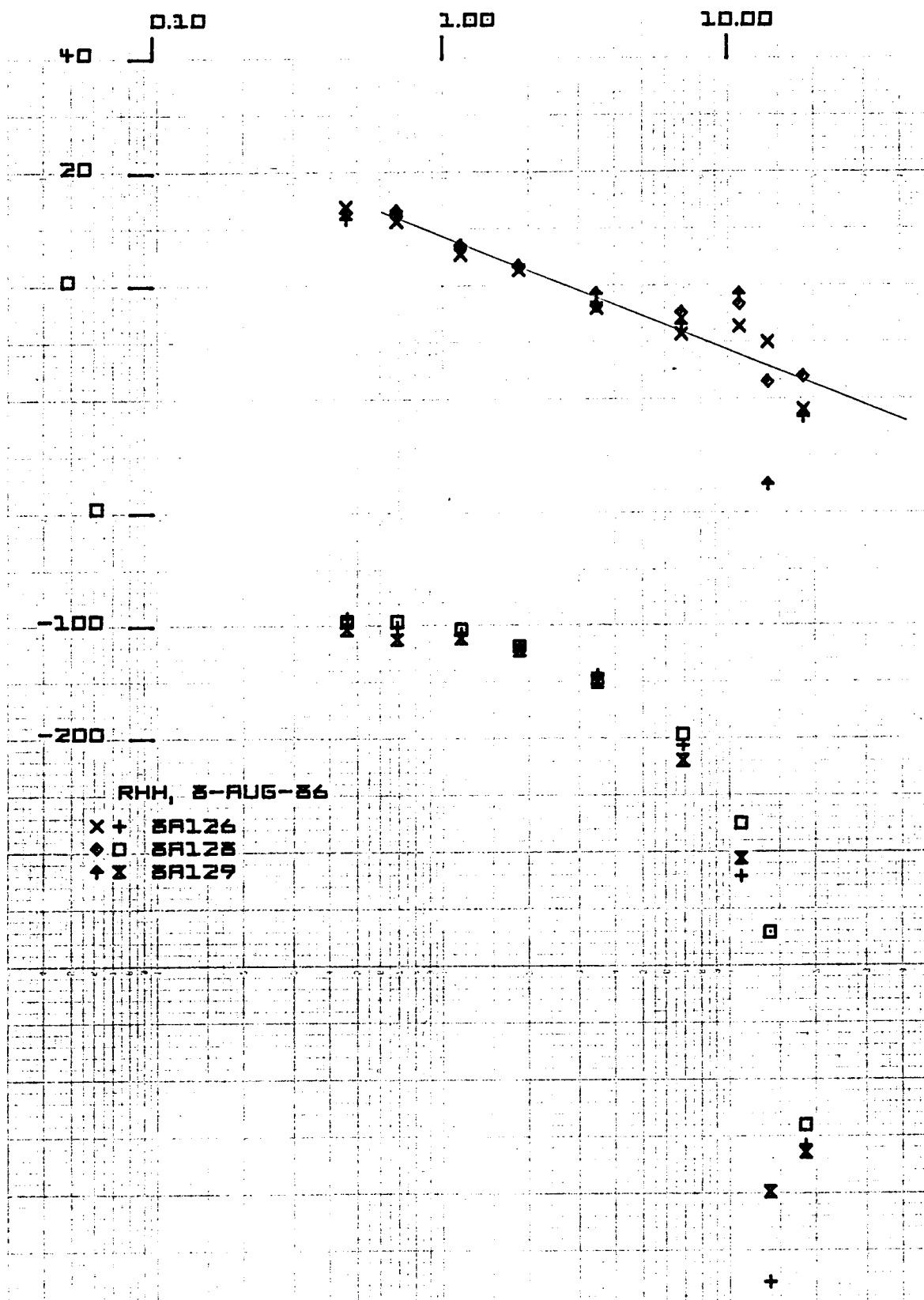


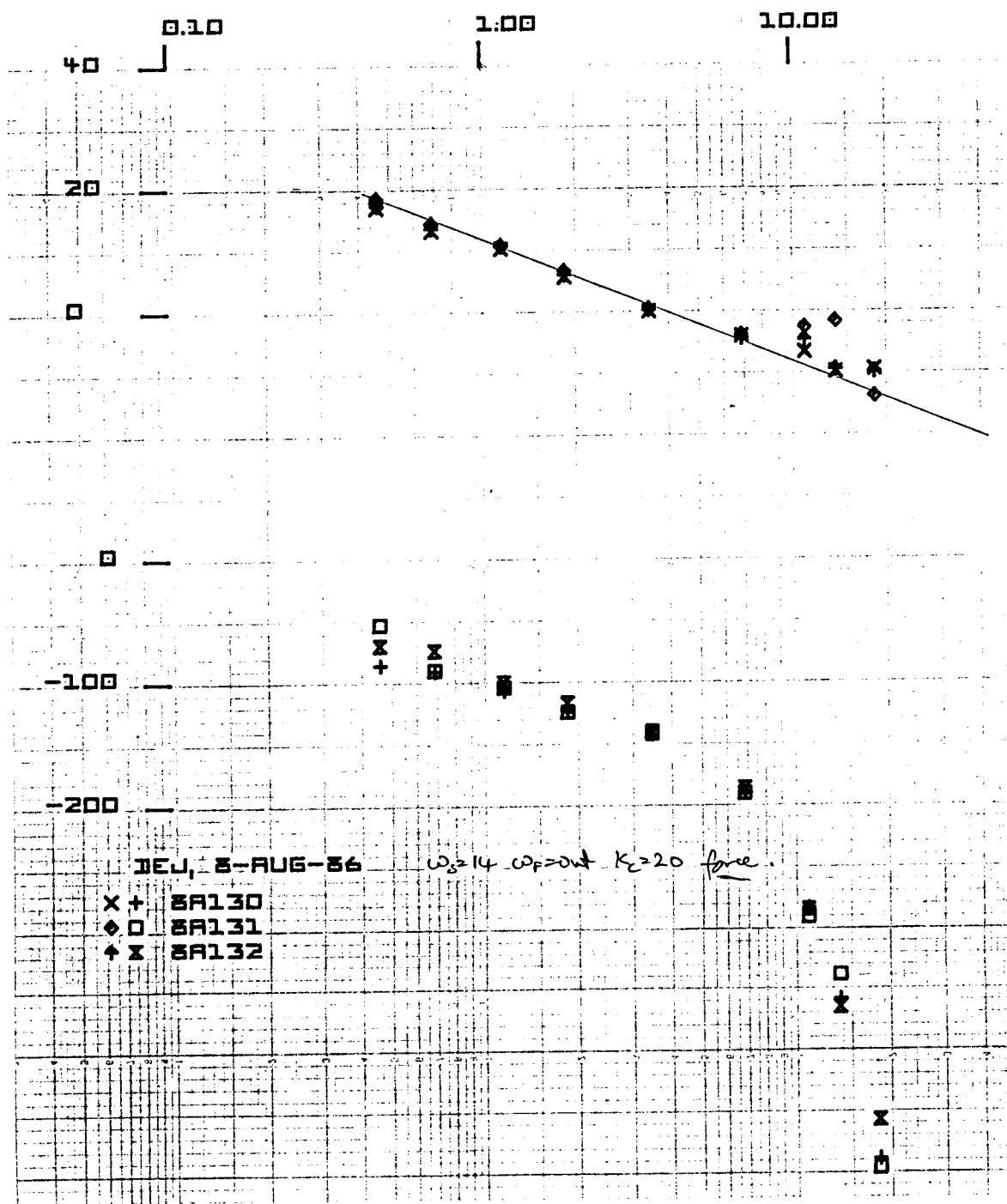


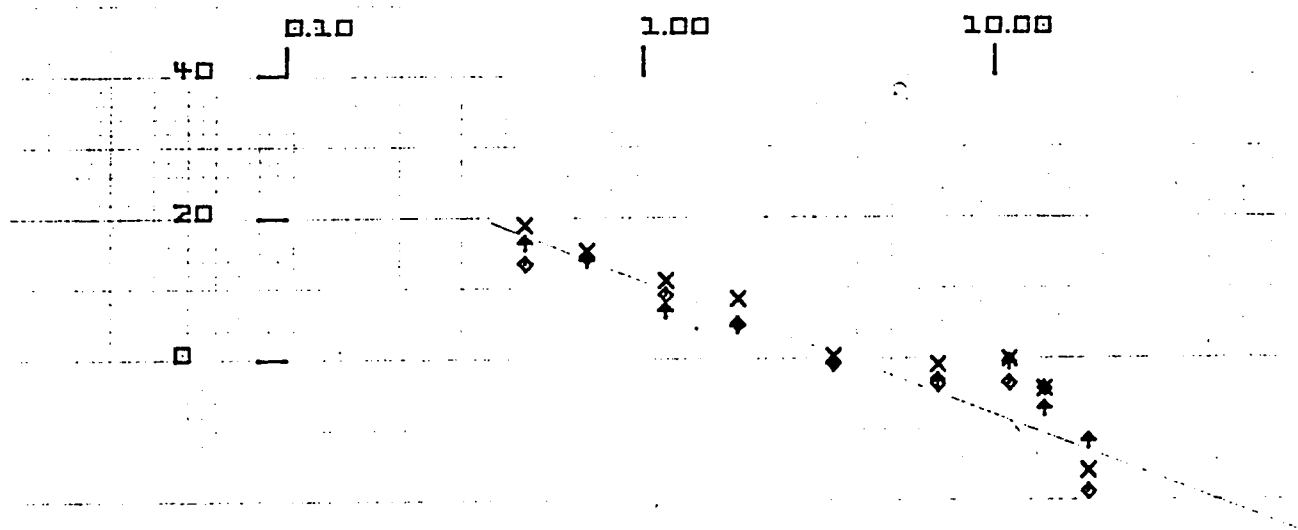












□ —

-100 —

-200 —

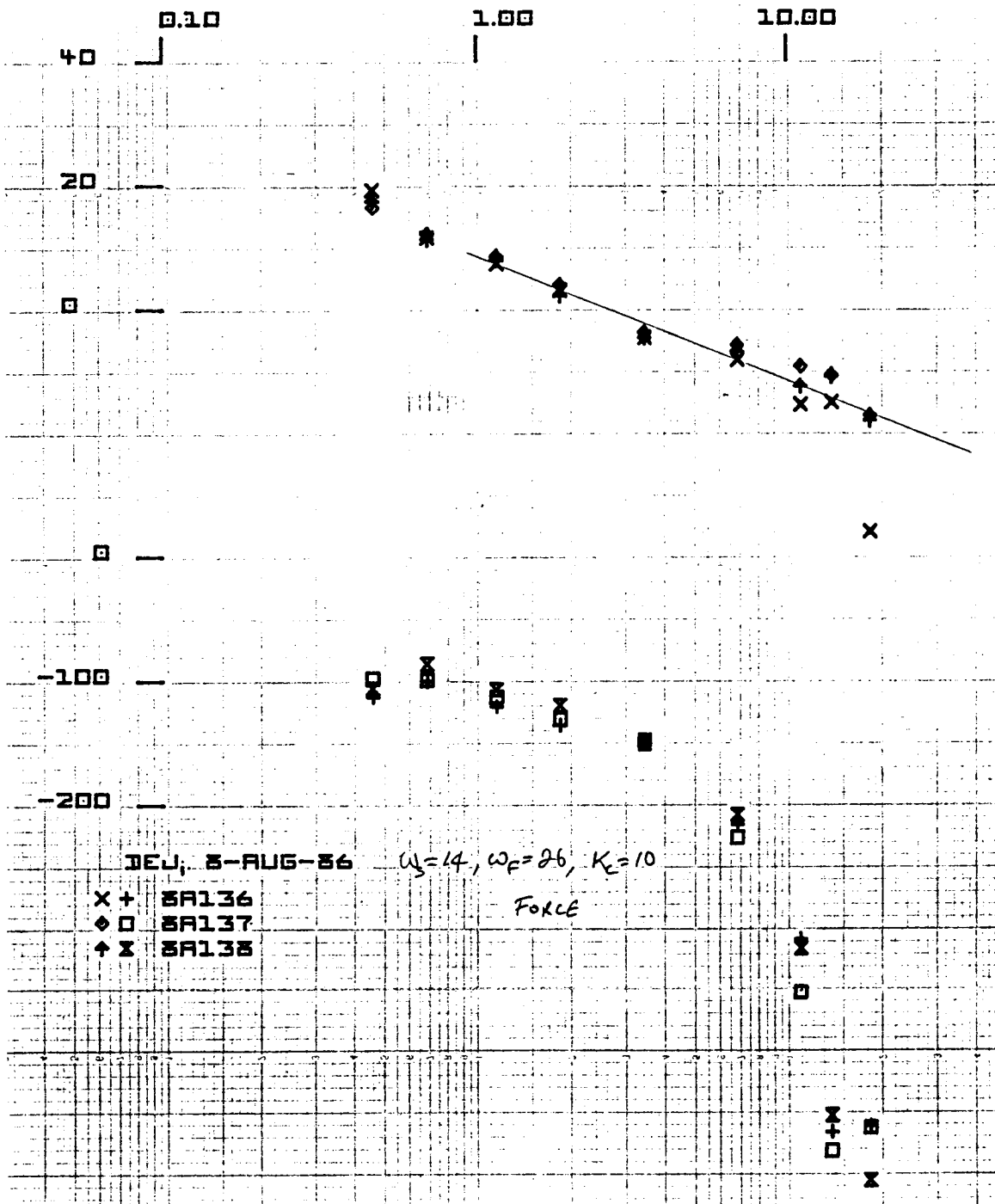
DEU; 8-AUG-86  $\omega_s=14, \omega_F=26, K_c=20$

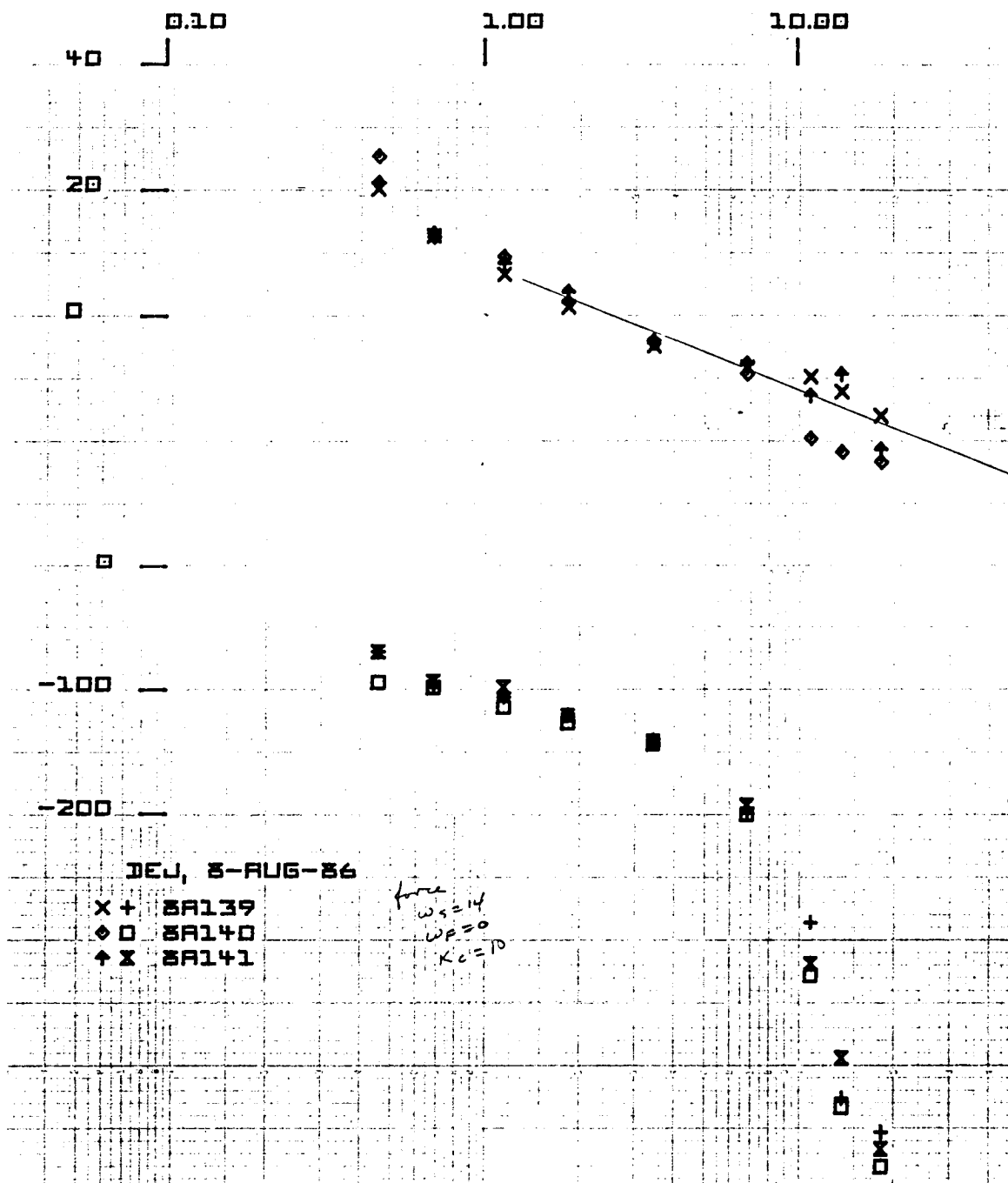
x + BA133

o BA134

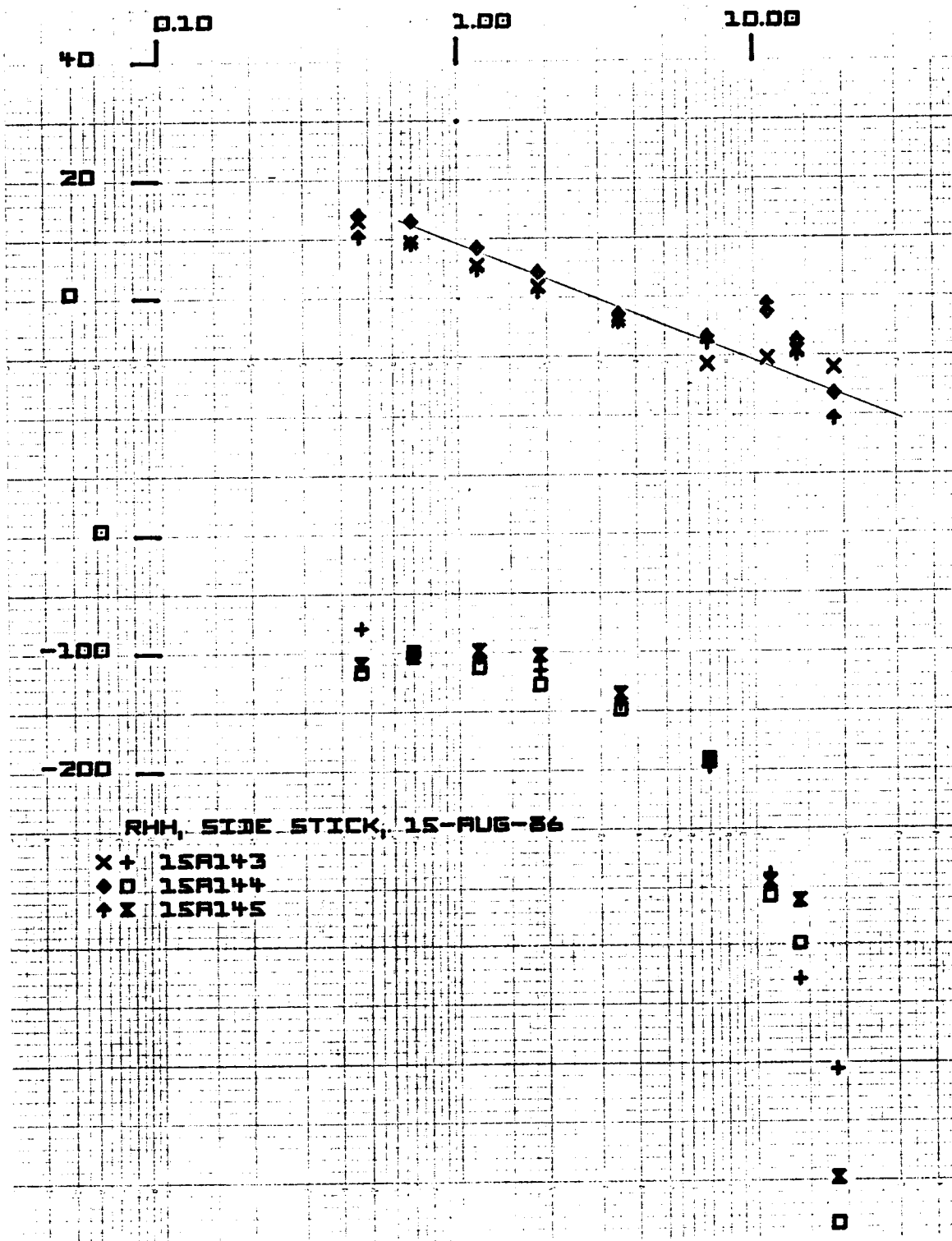
+ BA135

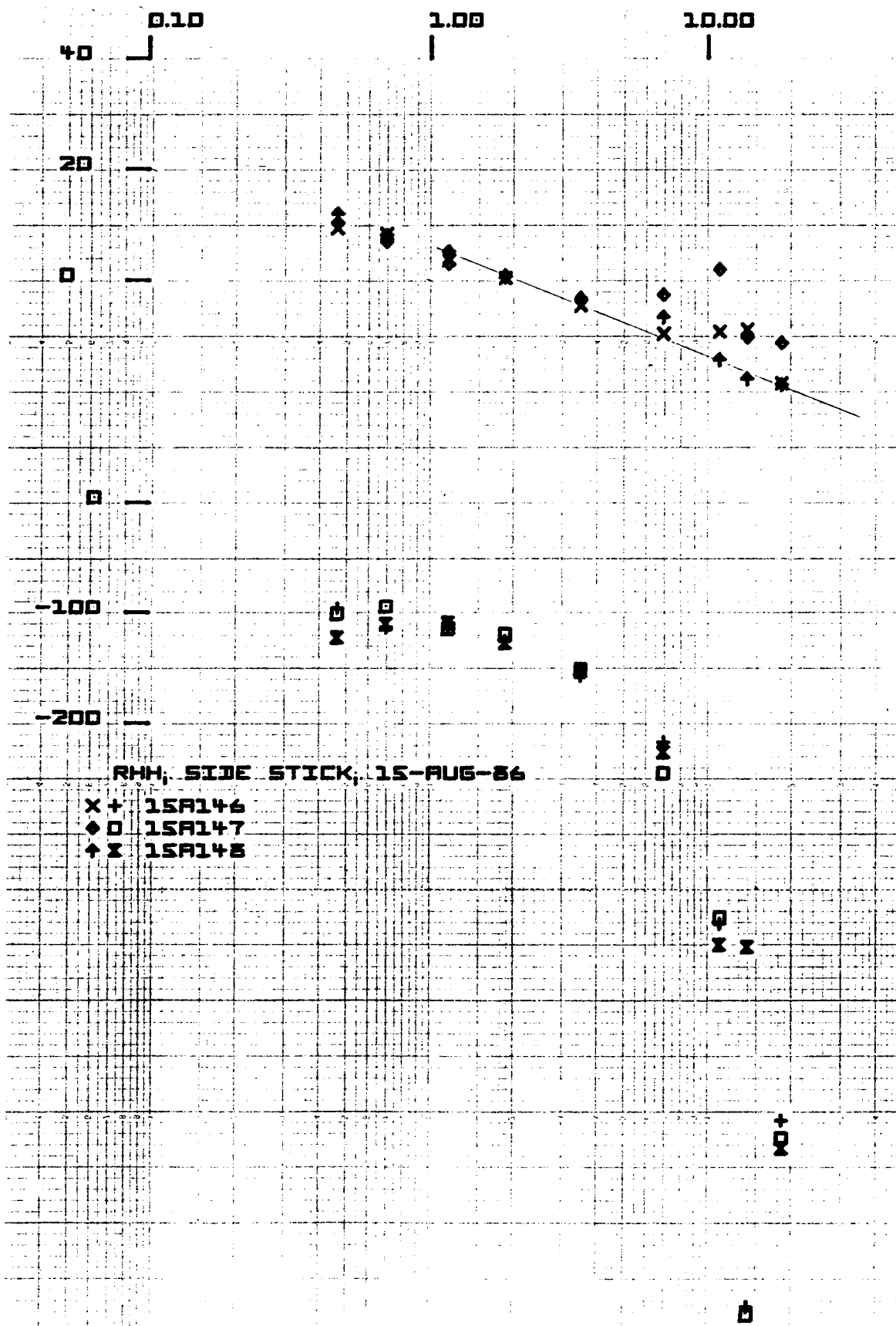
(Force)

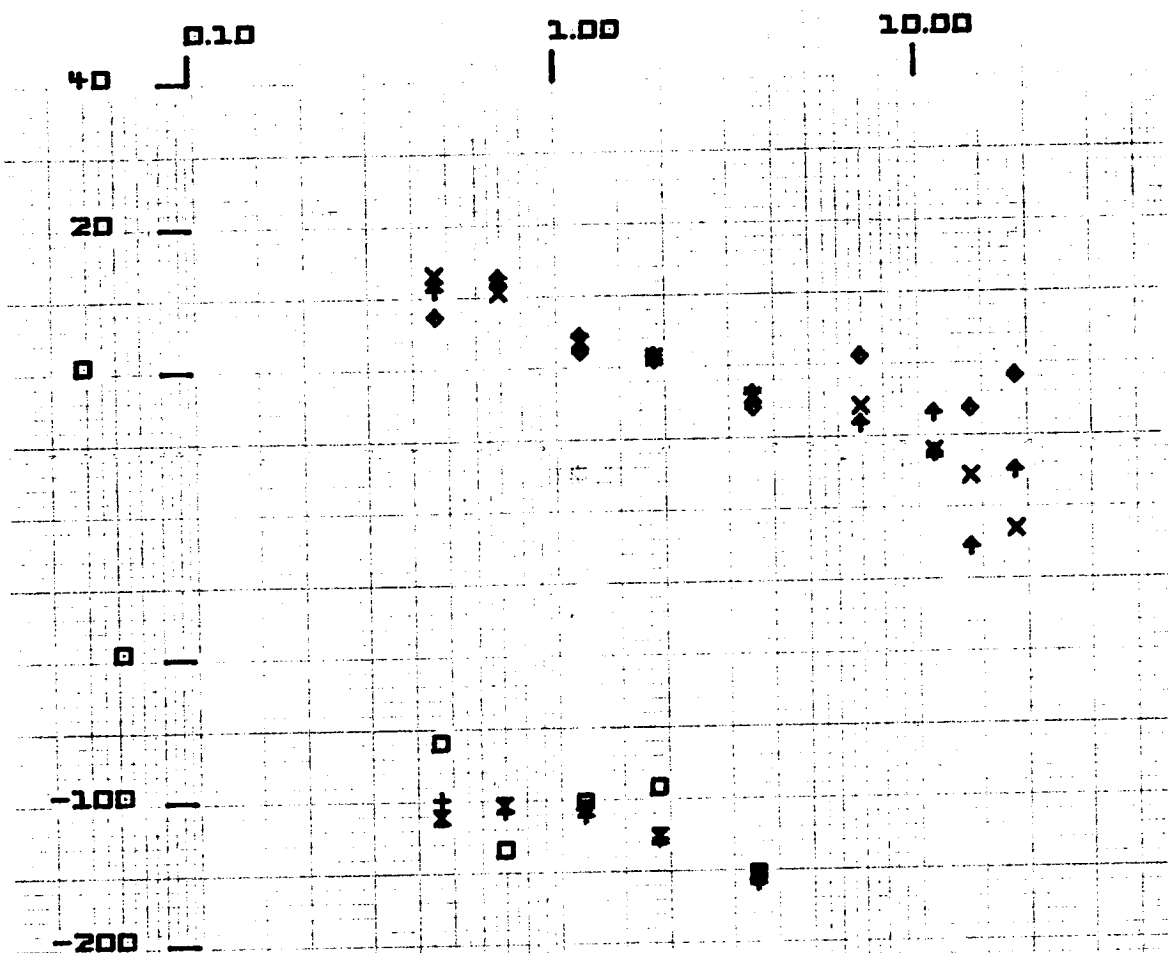








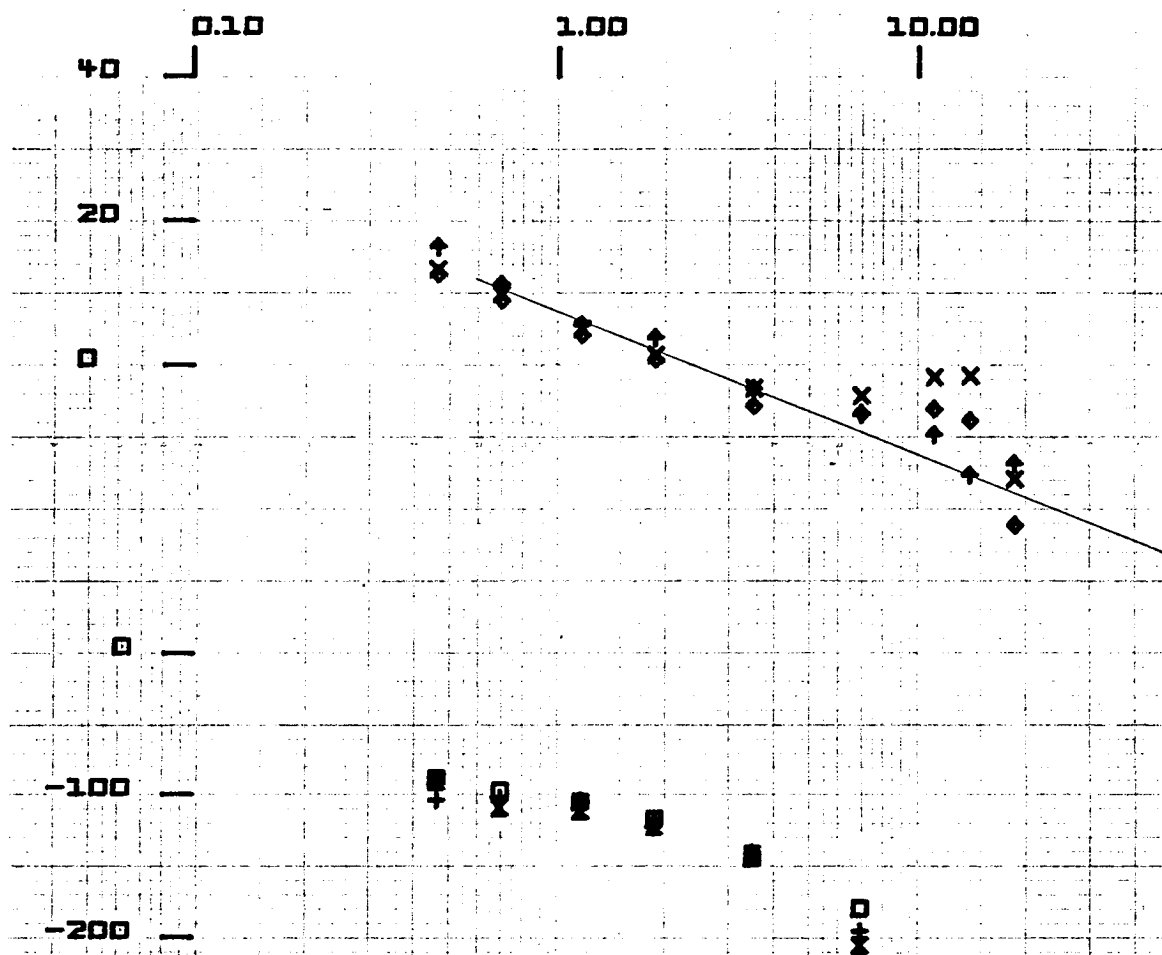




RHH, SIDE STICK, 15-AUG-86

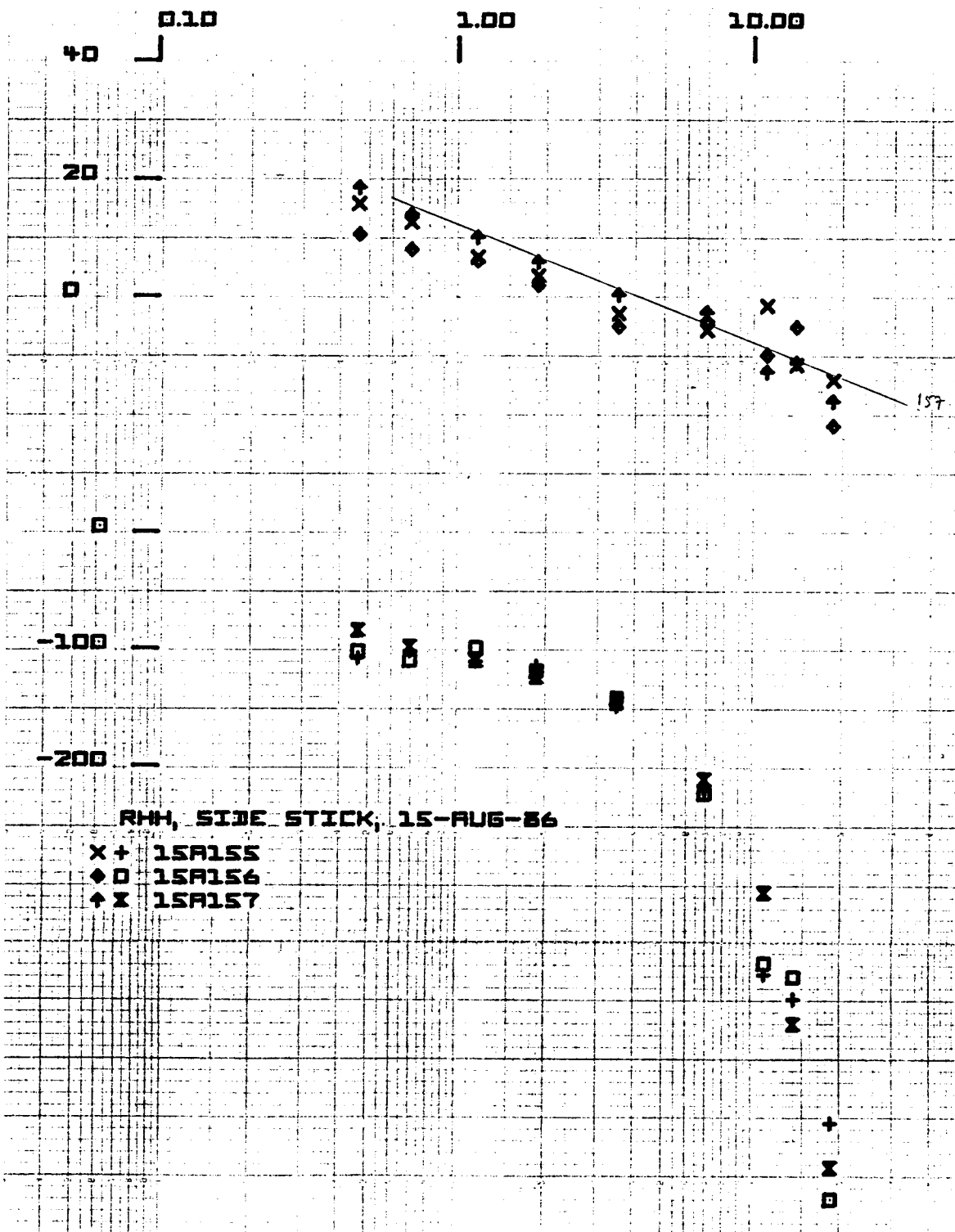
X + 15A149  
 ♦ 15A150  
 + X 15A151

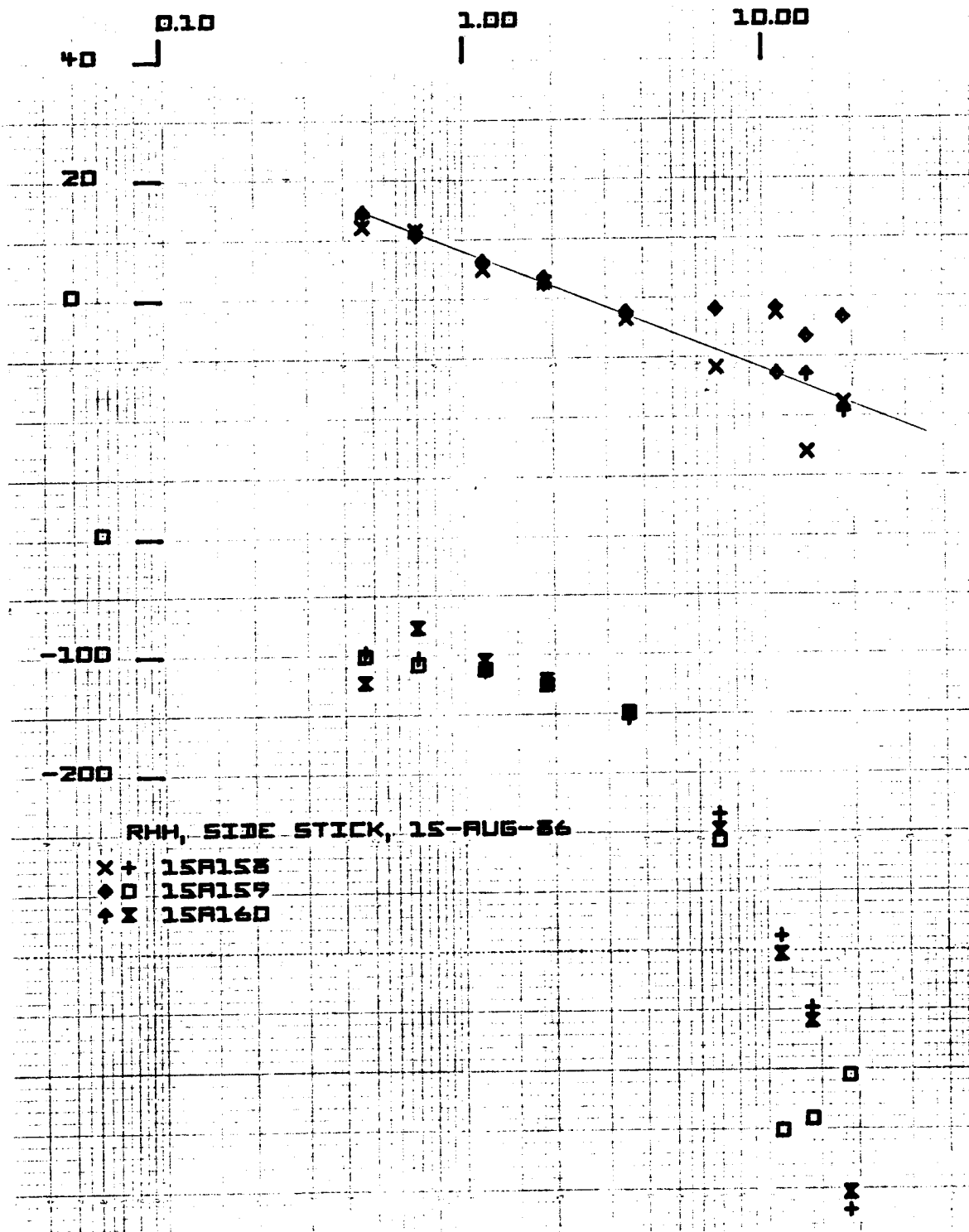
X  
 +  
 ♦  
 +  
 X

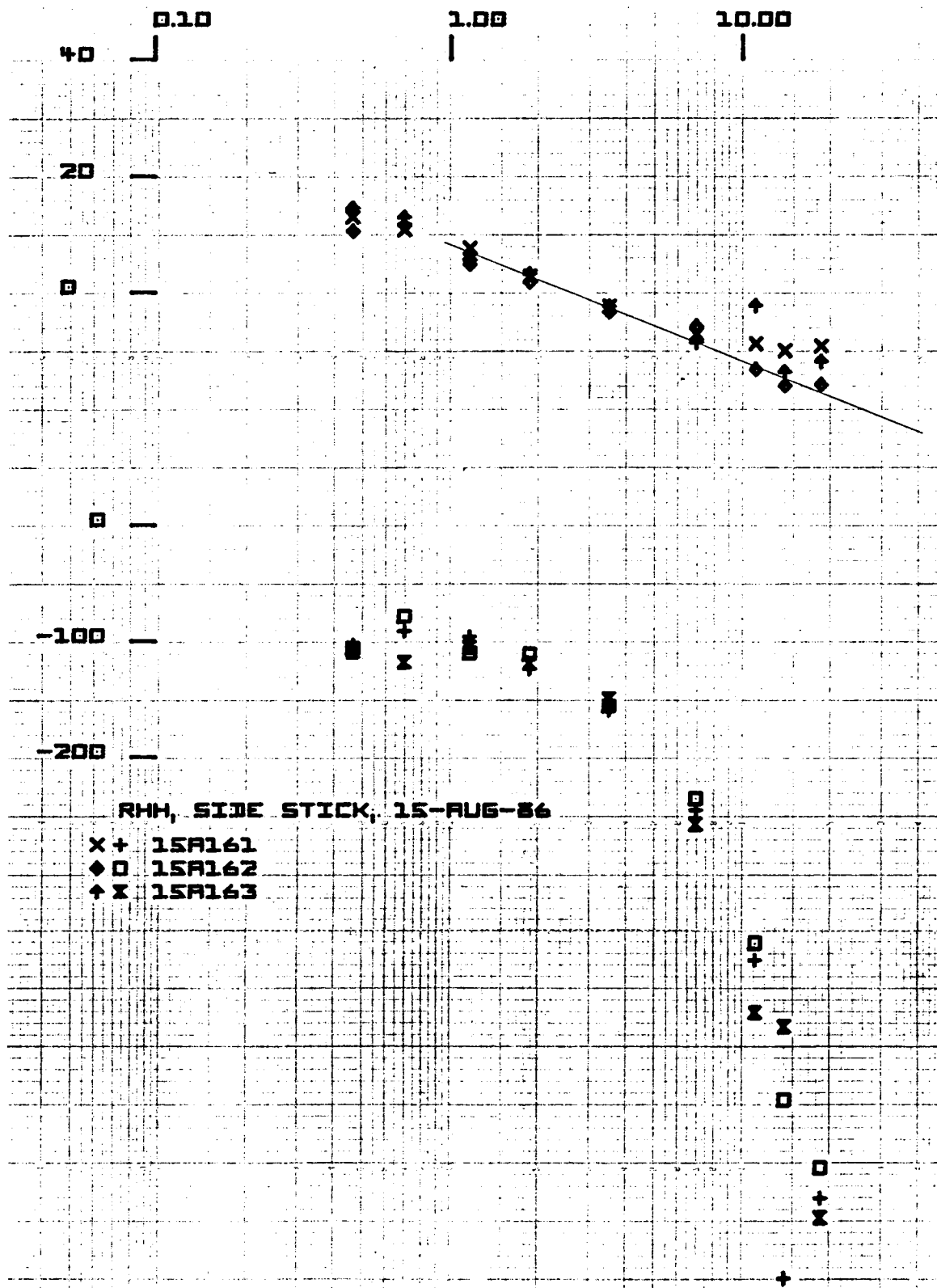


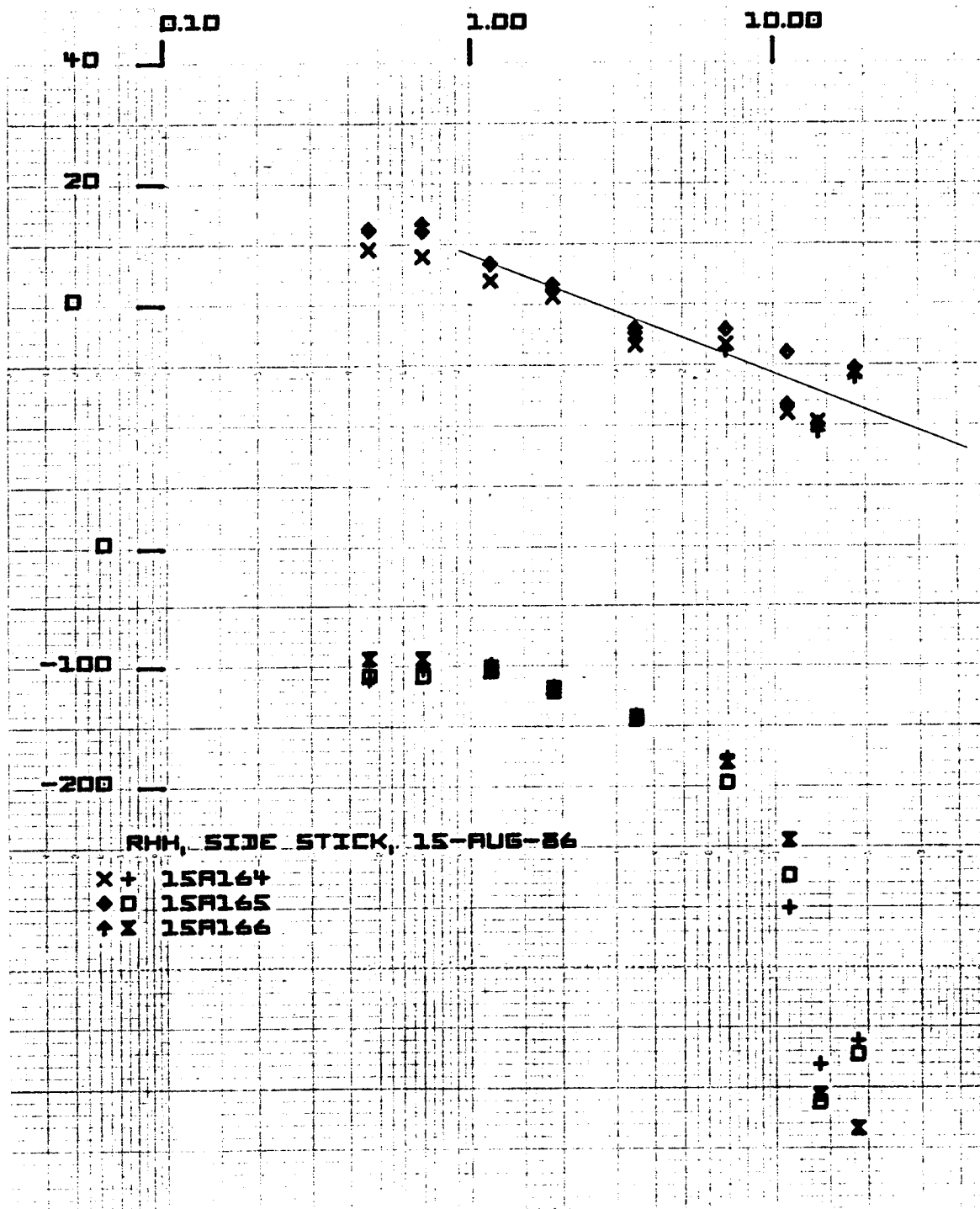
RHH, SIDE STICK, 15-AUG-86

x+ 15A152  
 o 15A153  
 + 15A154

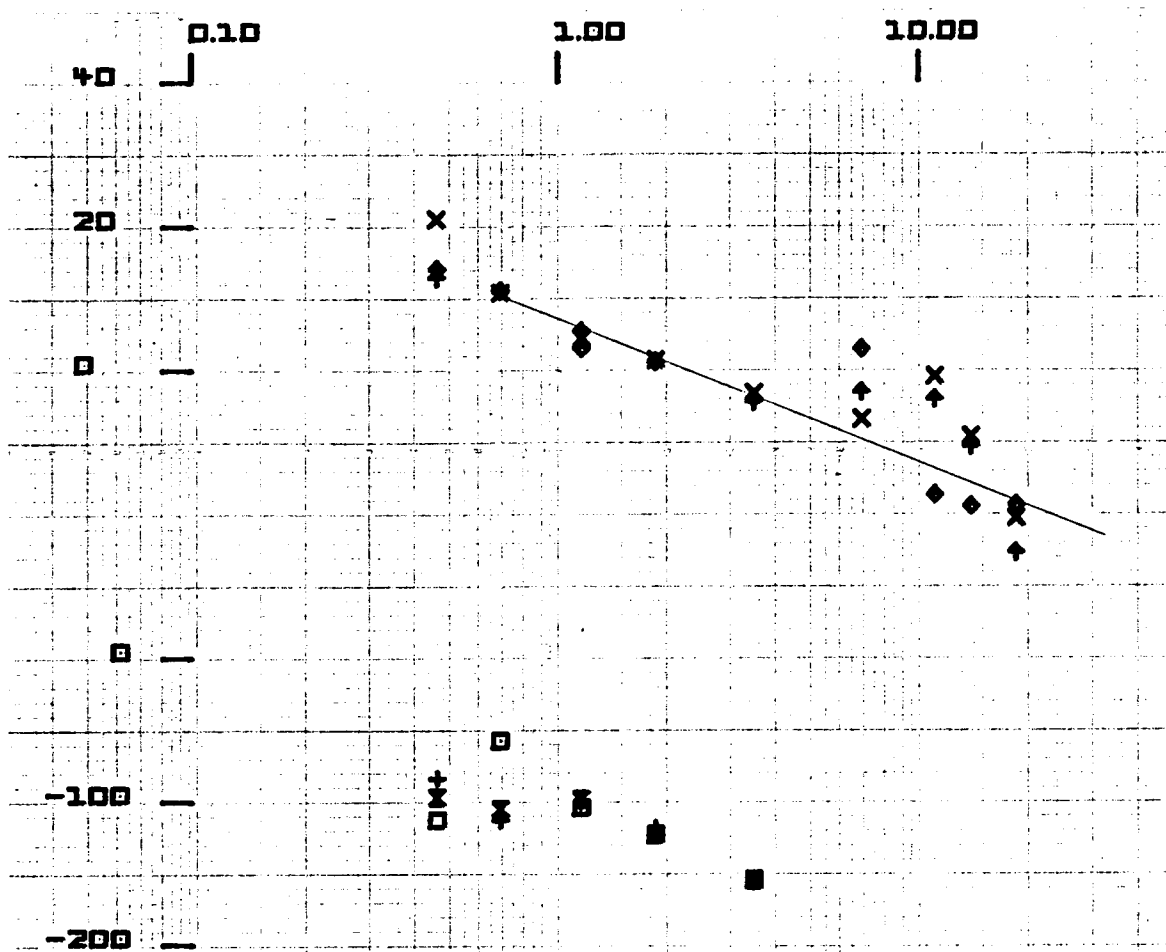










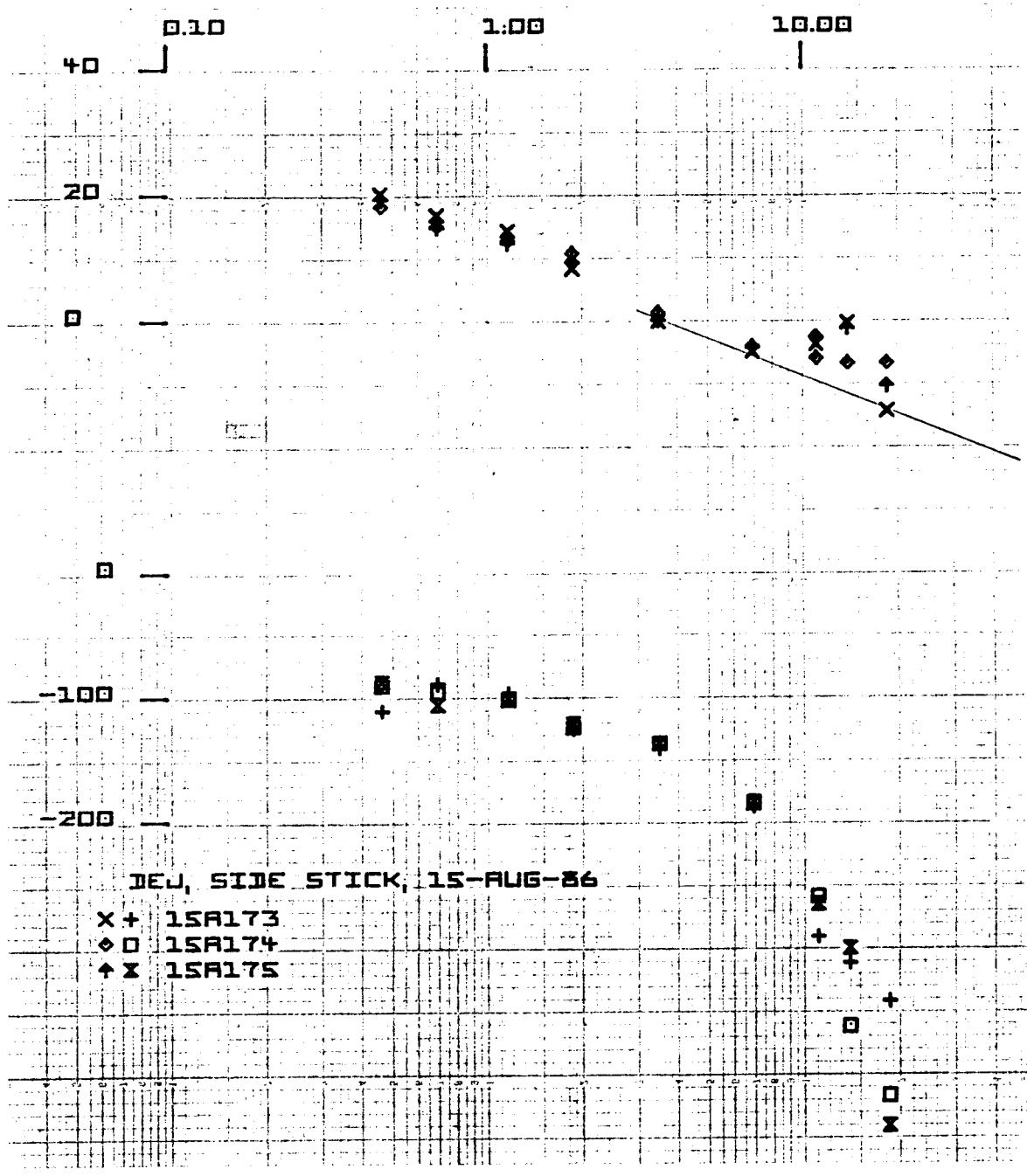


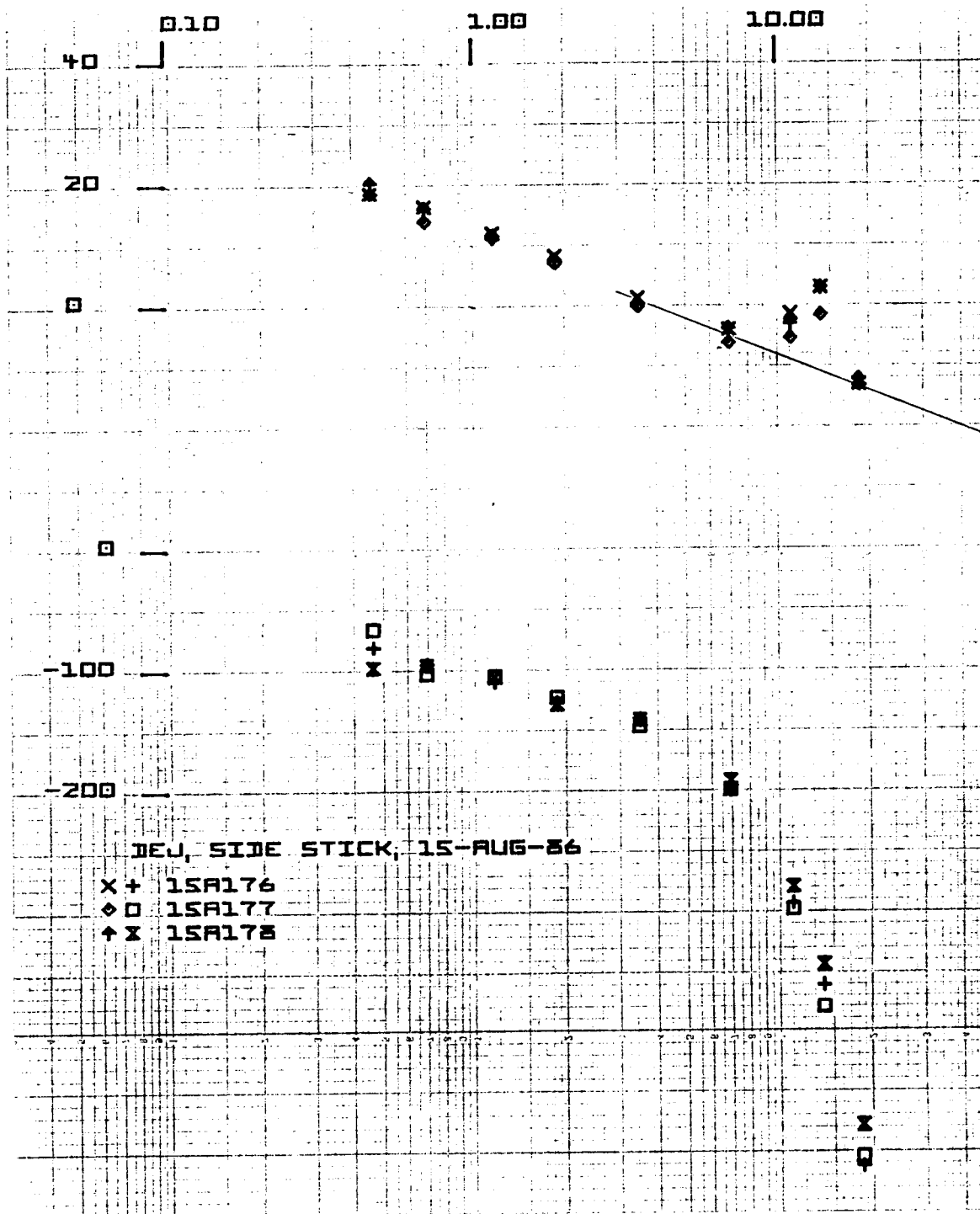
RHH, SIDE STICK, 15-AUG-86

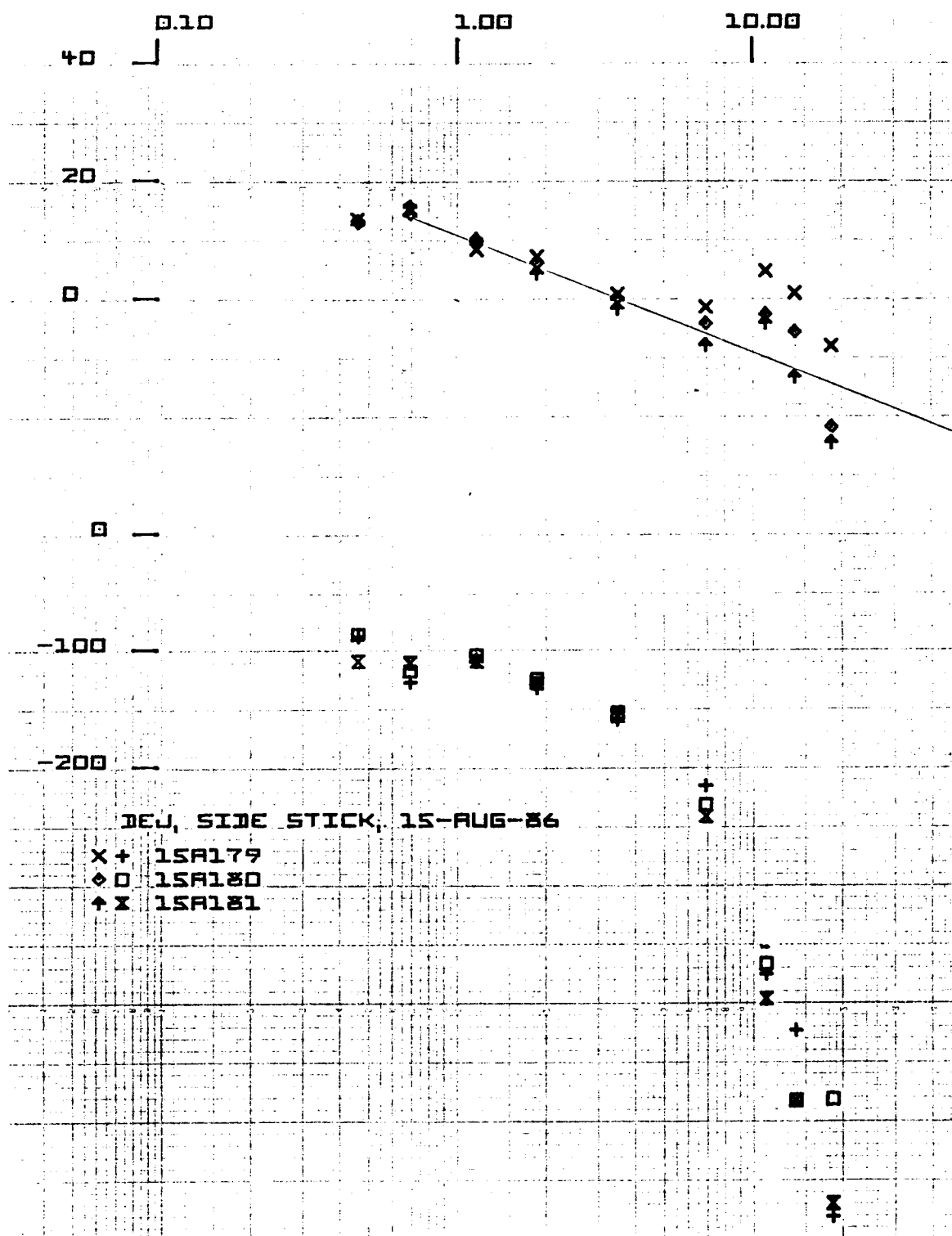
x + 15A167  
 o 15A168  
 + 15A170

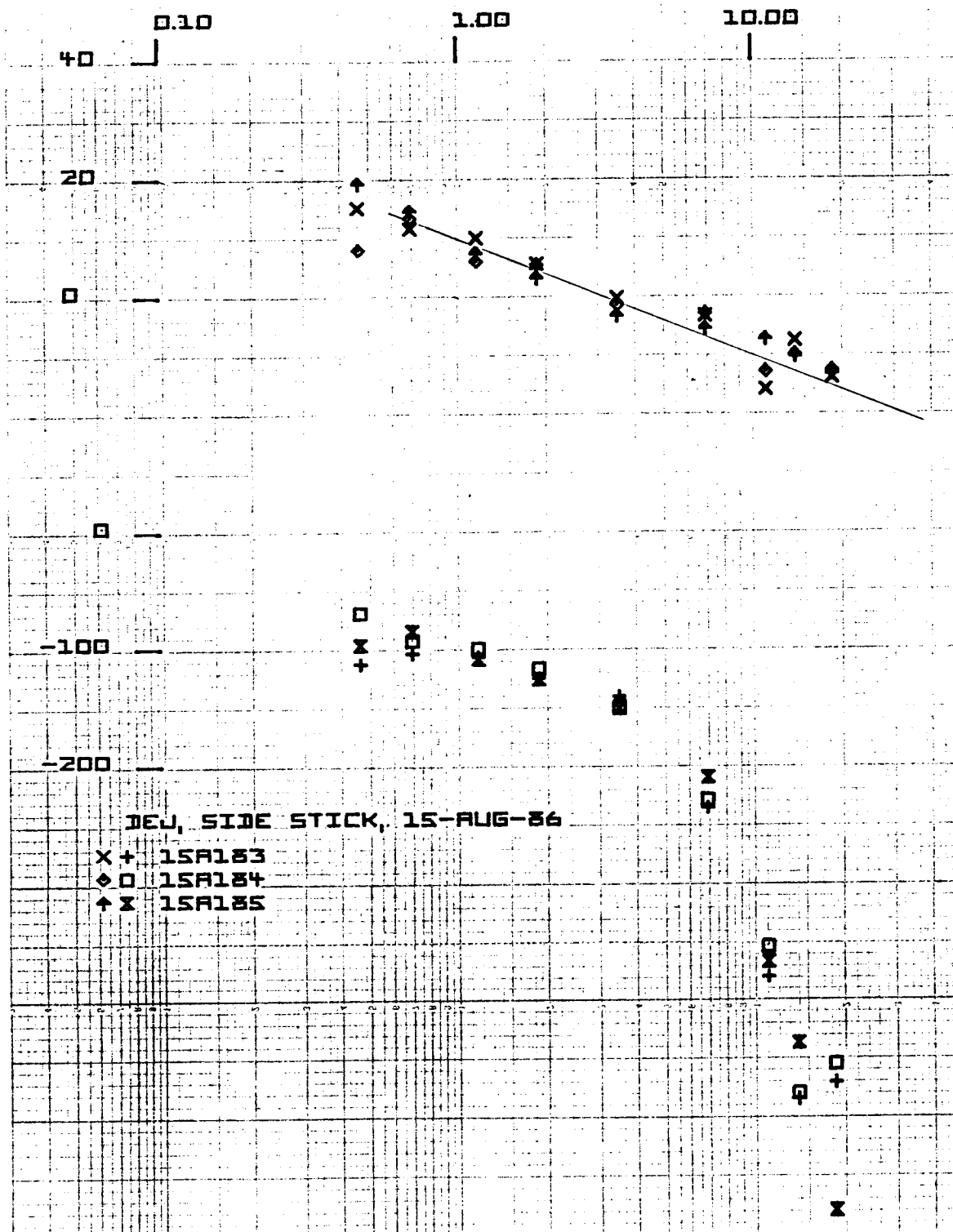
8  
 0

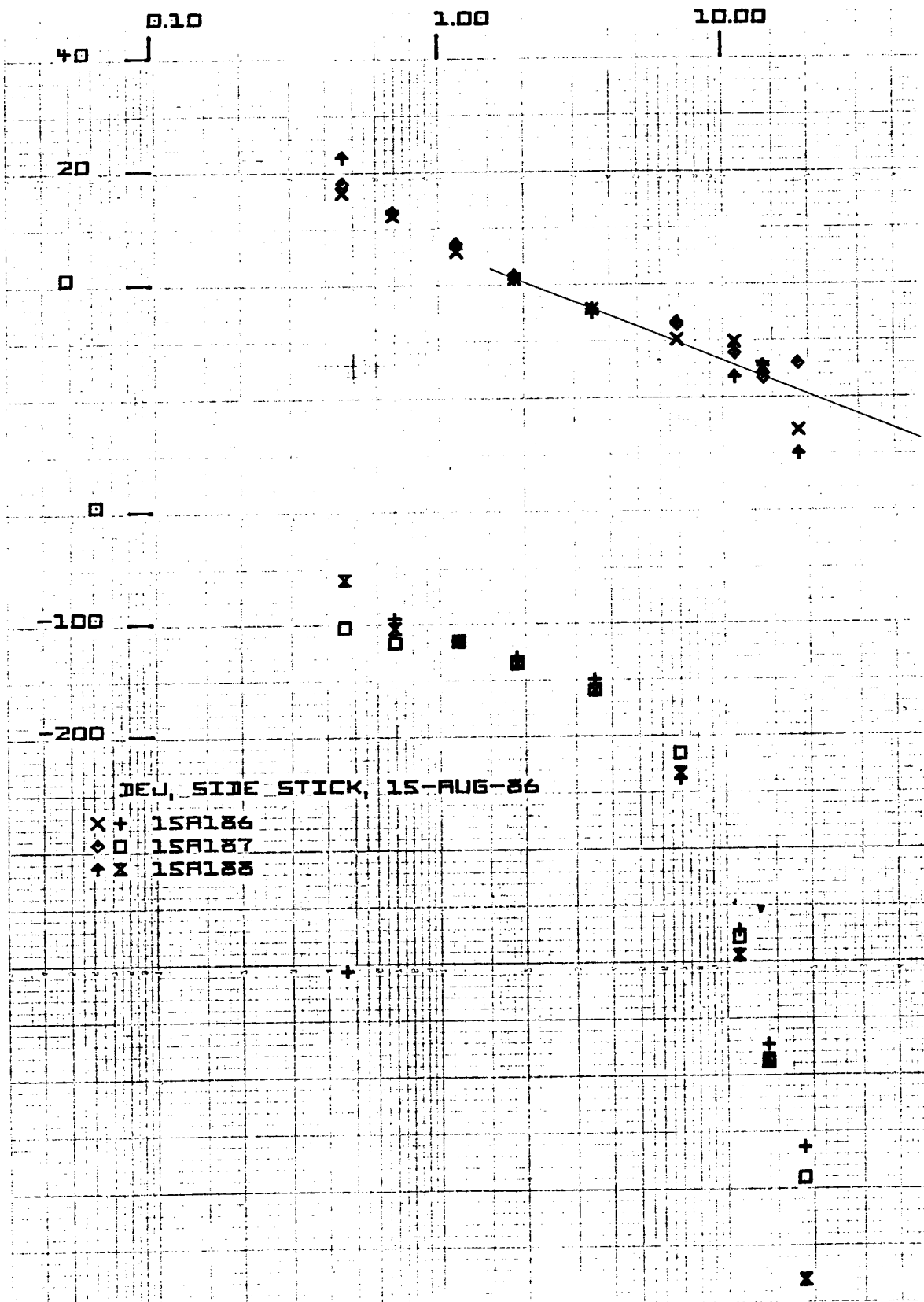
+  
 +  
 x  
 x  
 o  
 o  
 o  
 +  
 x

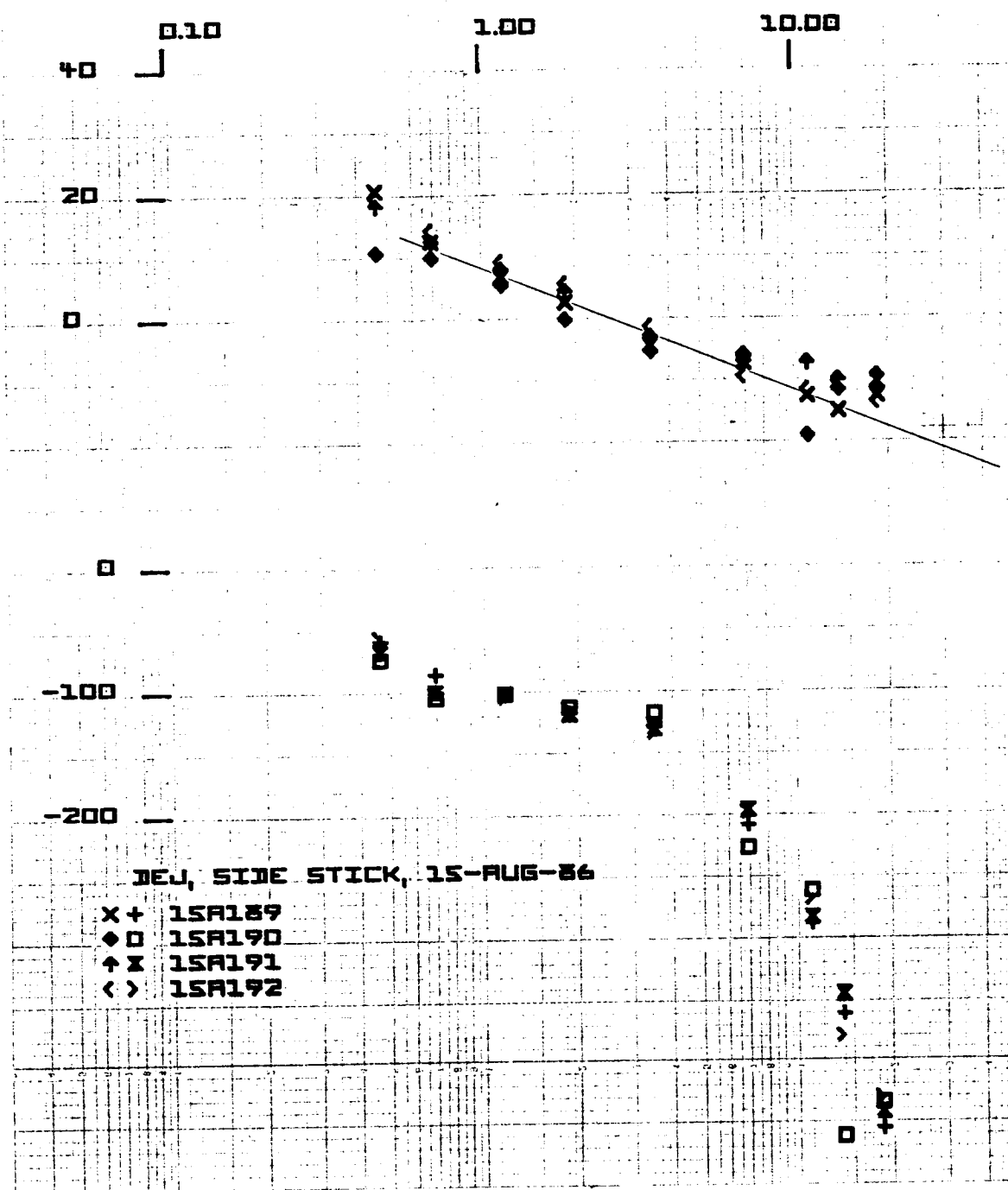


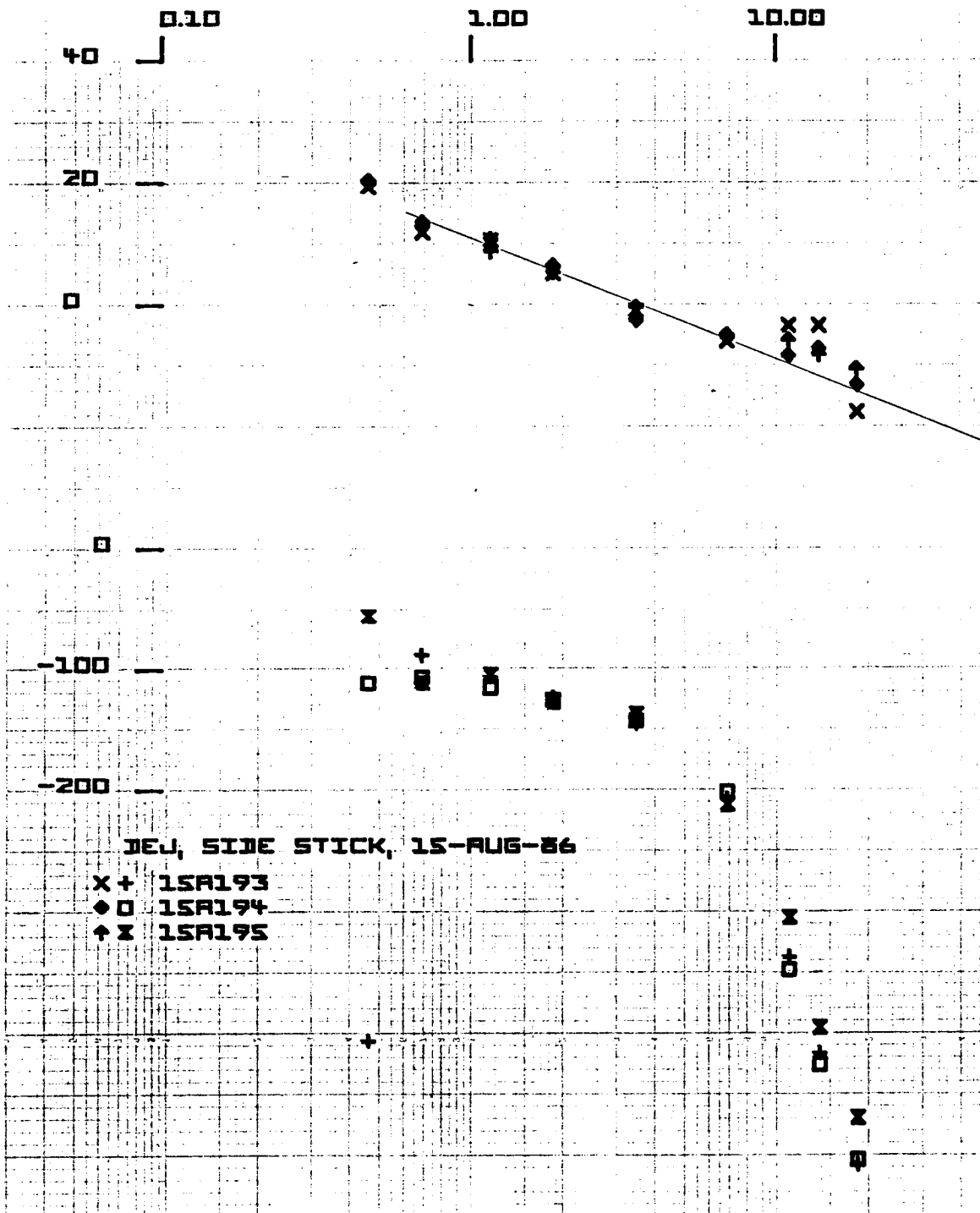




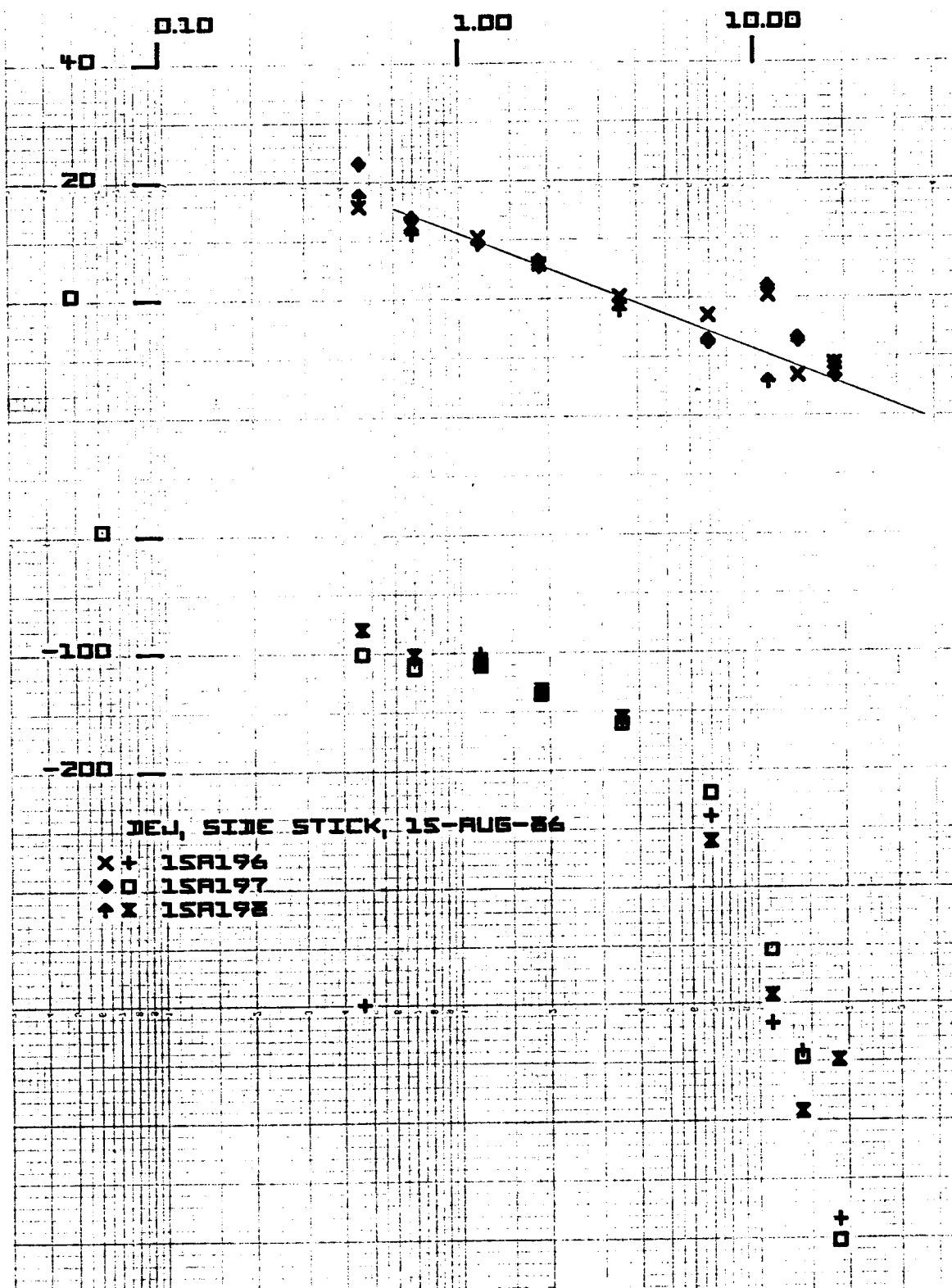


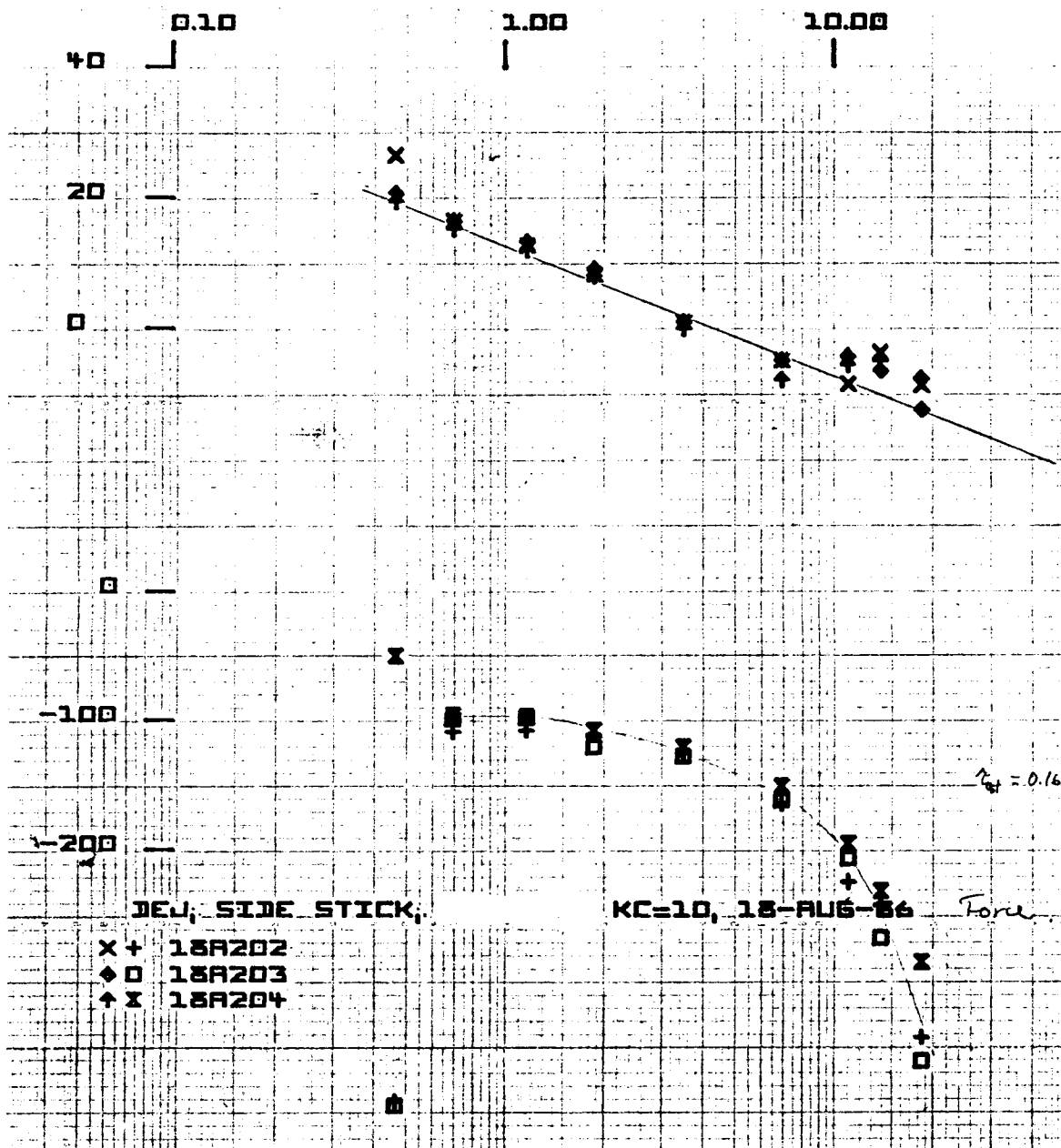


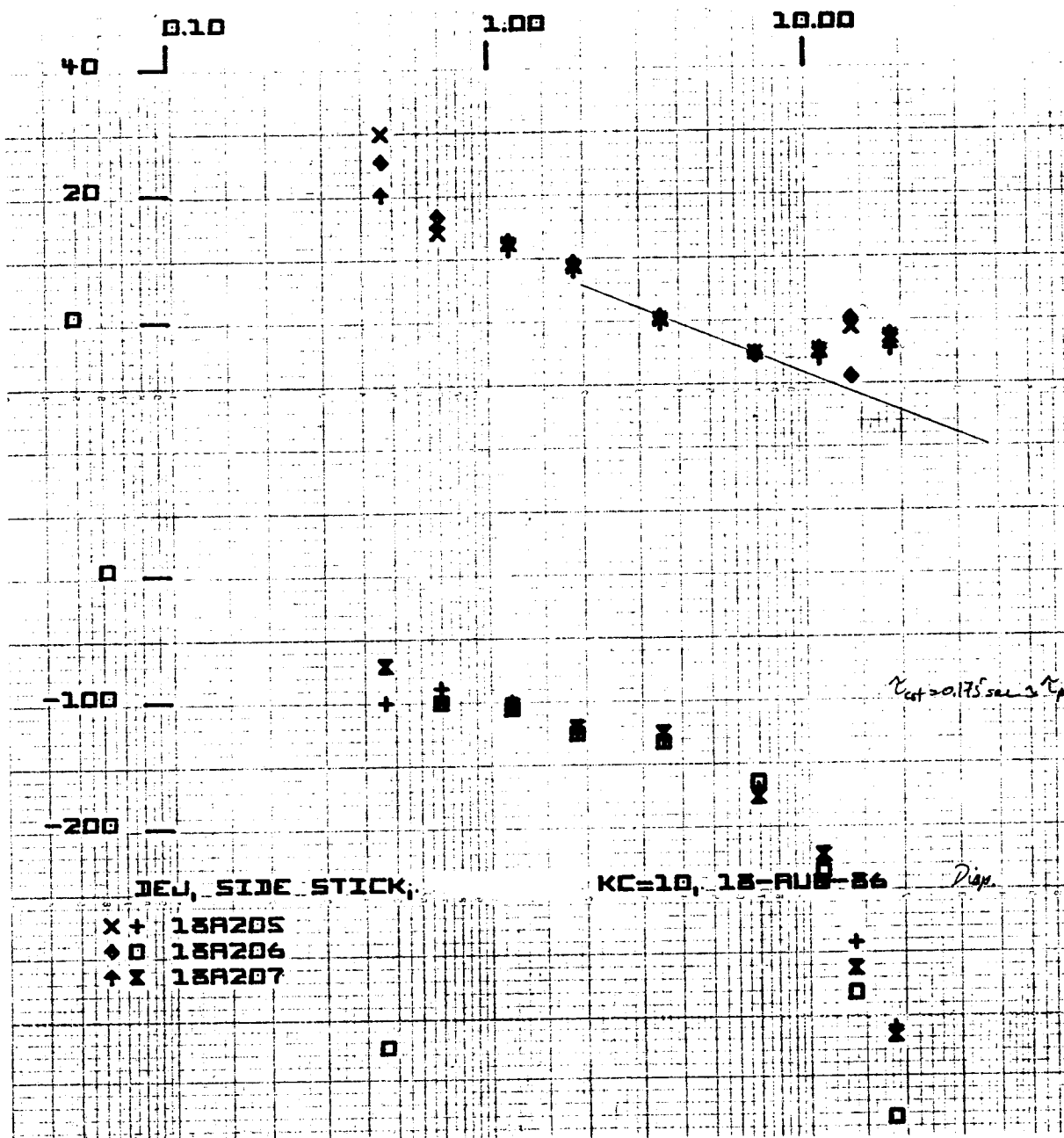


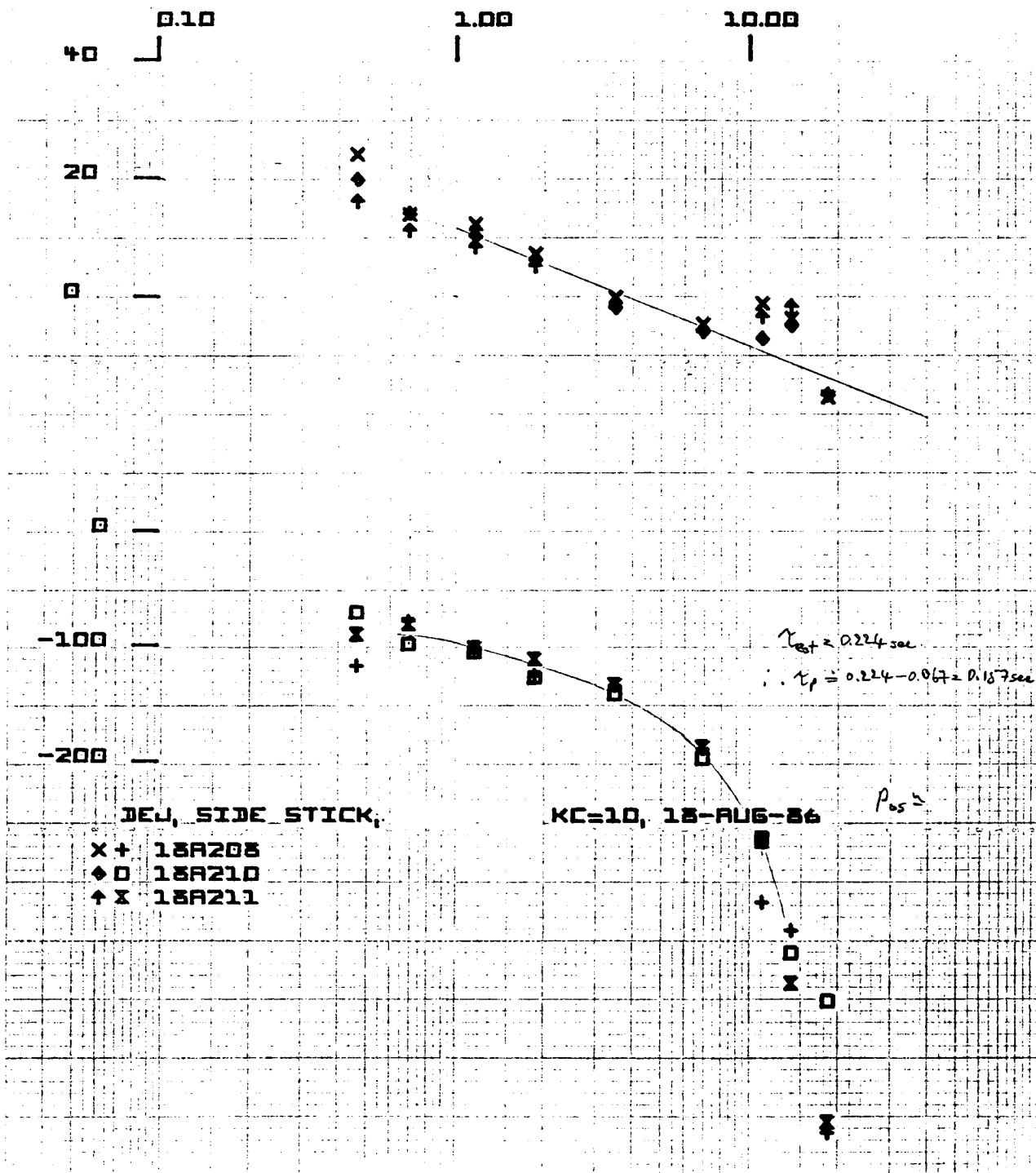


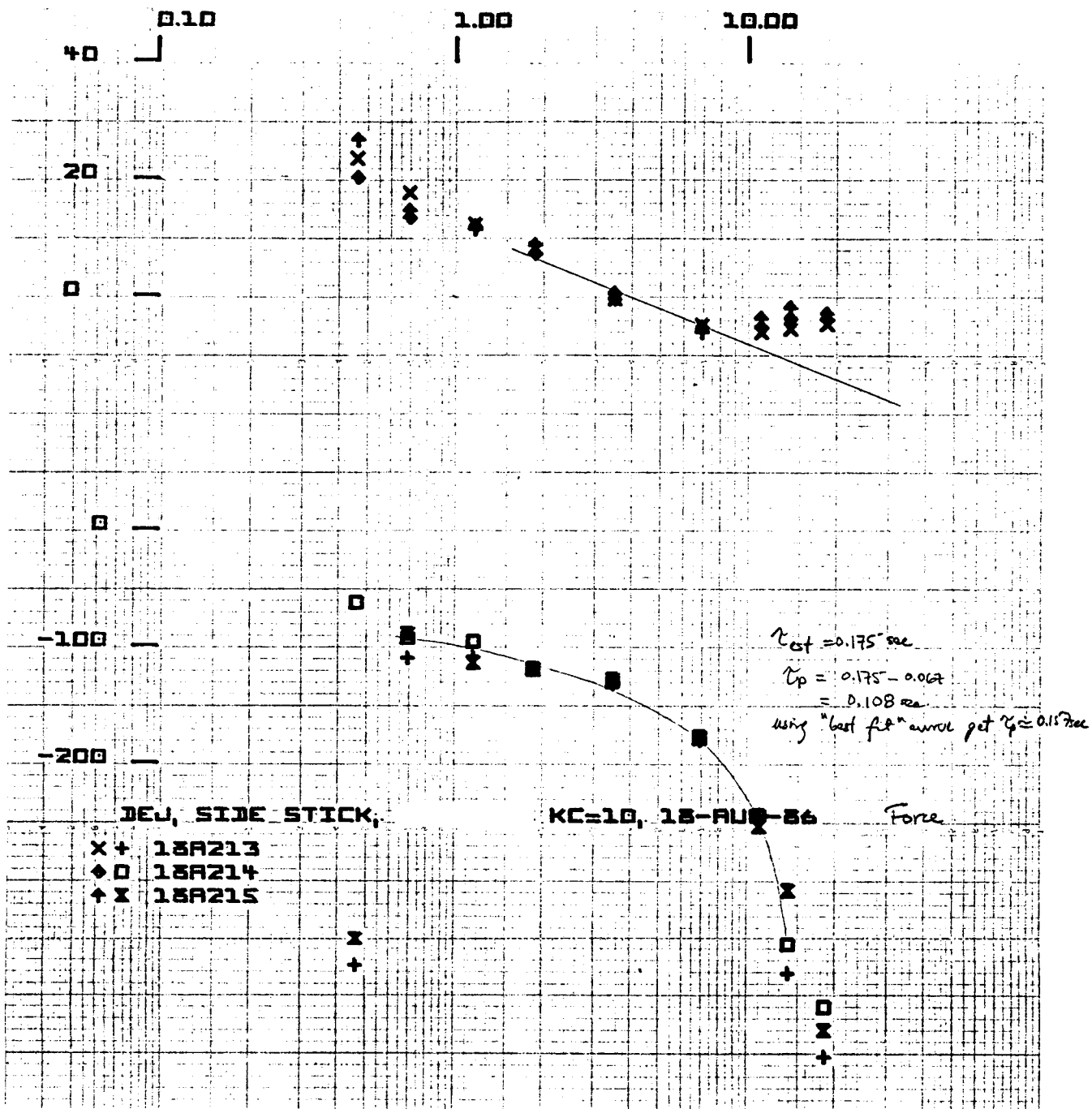


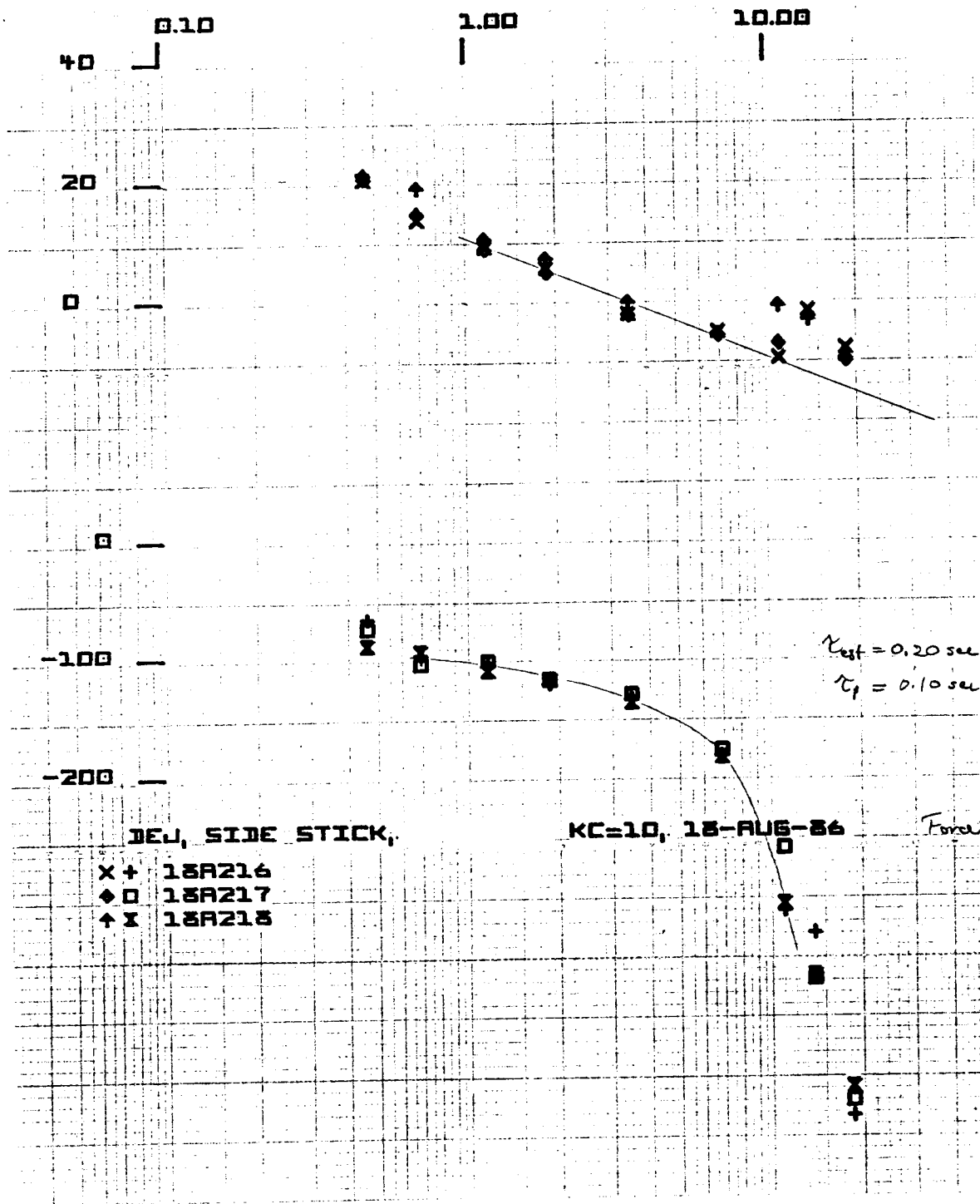


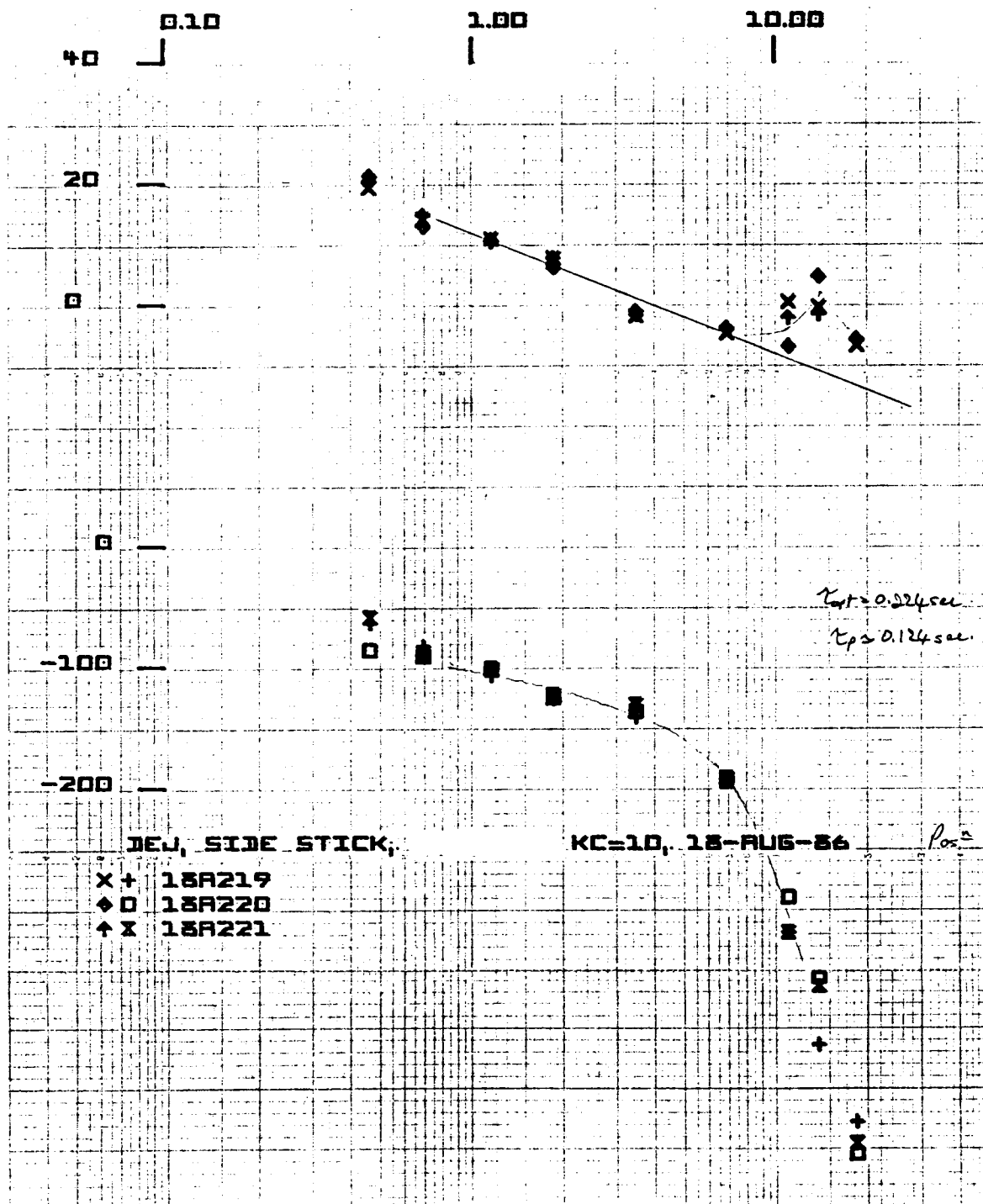


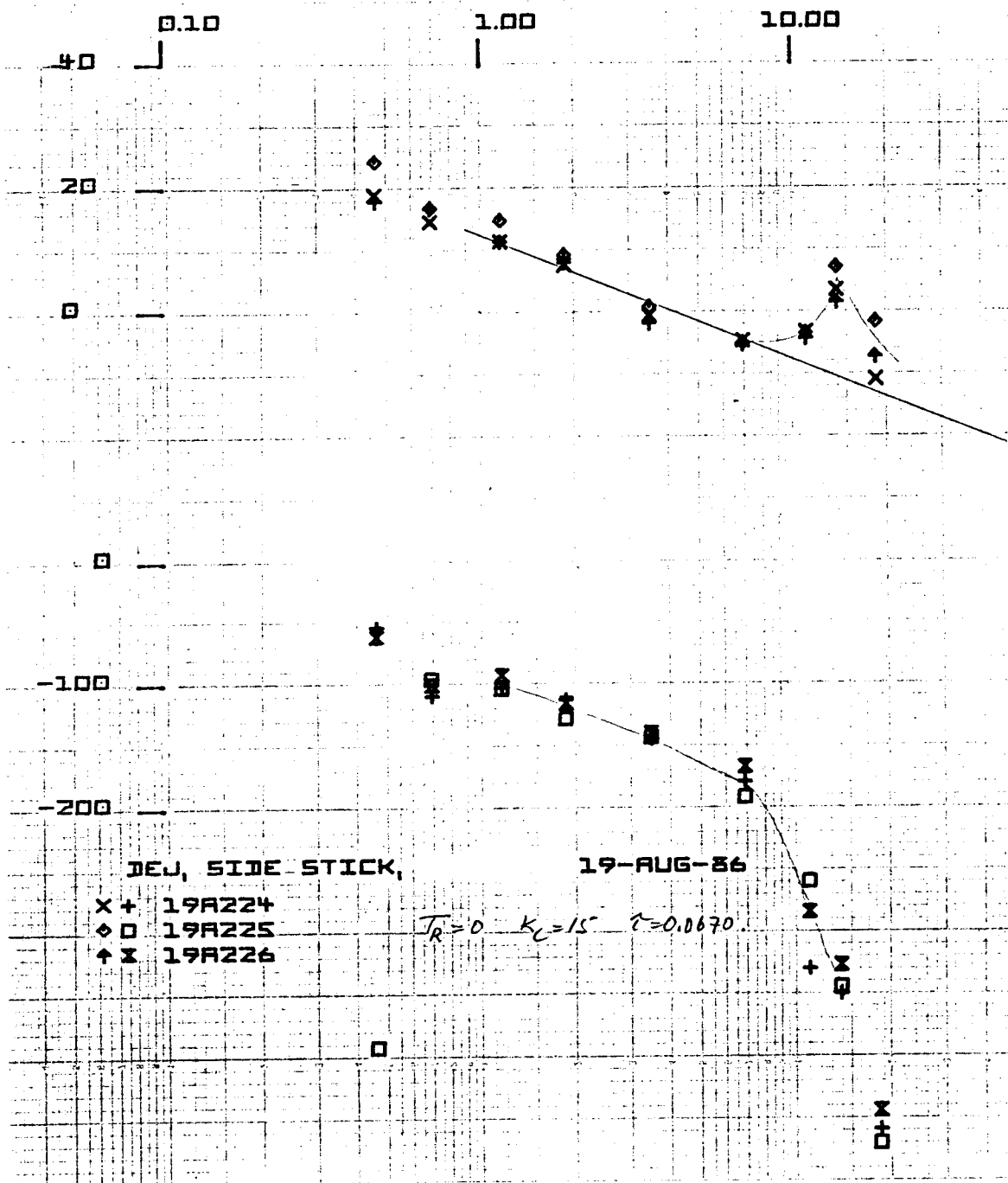




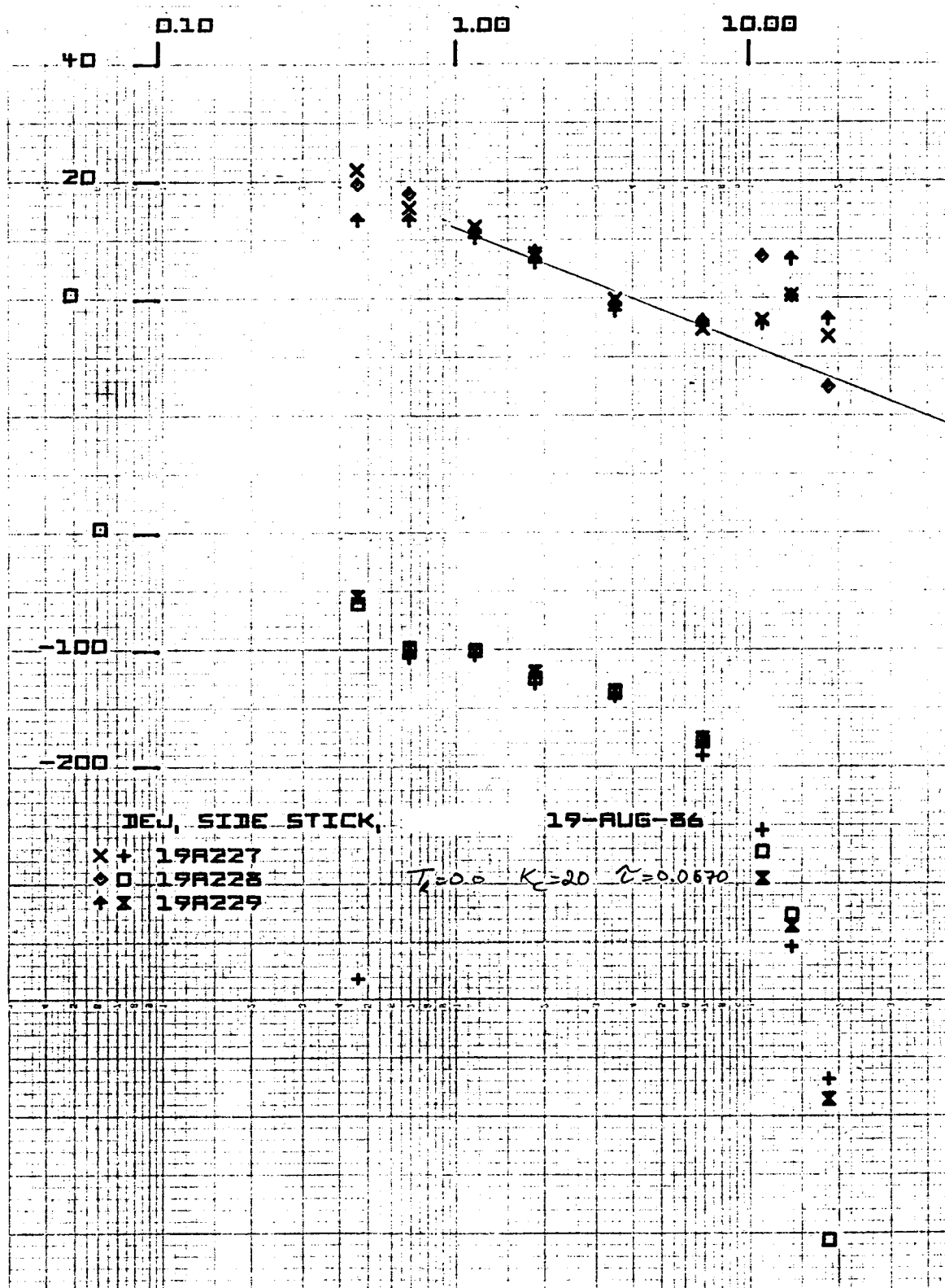


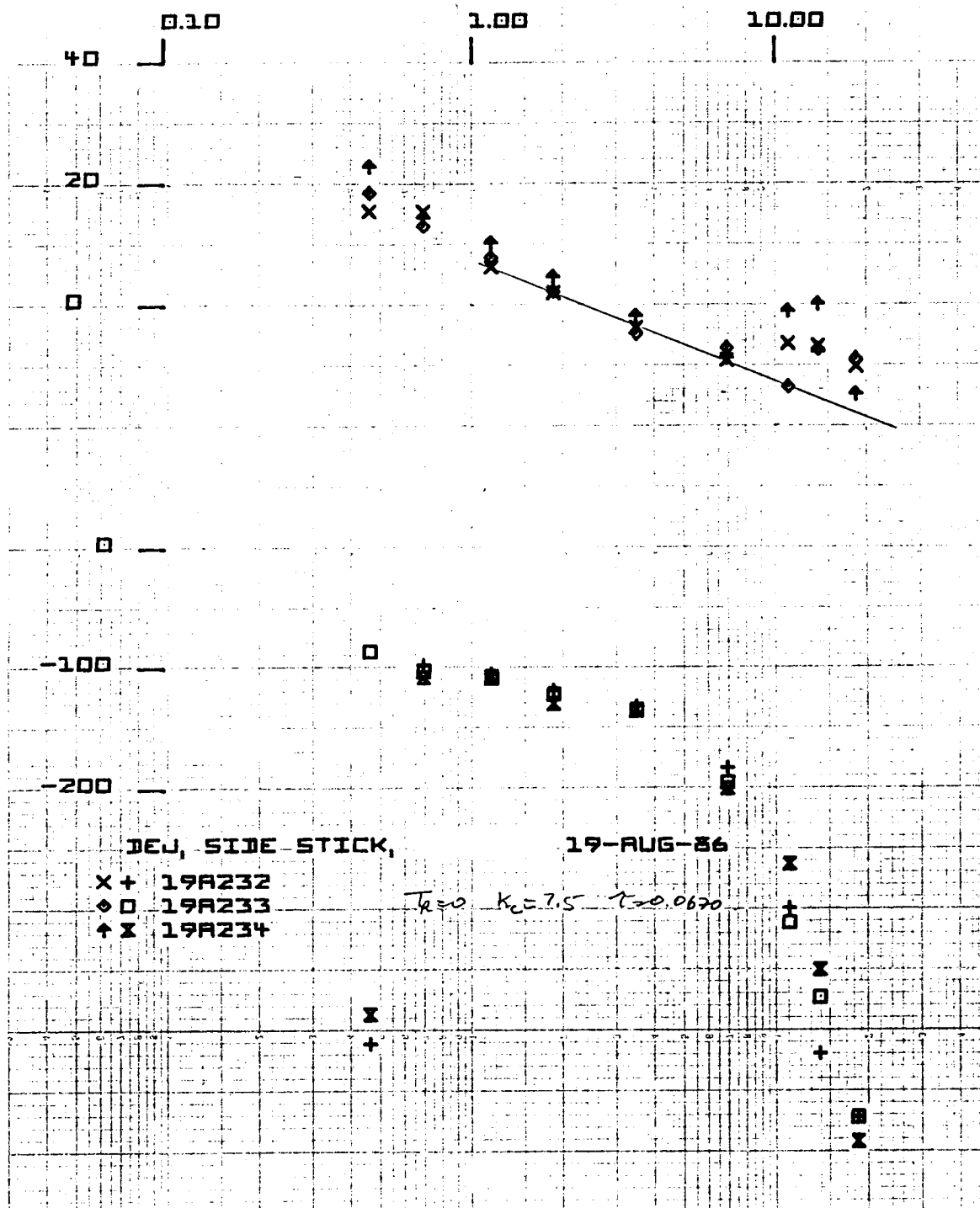


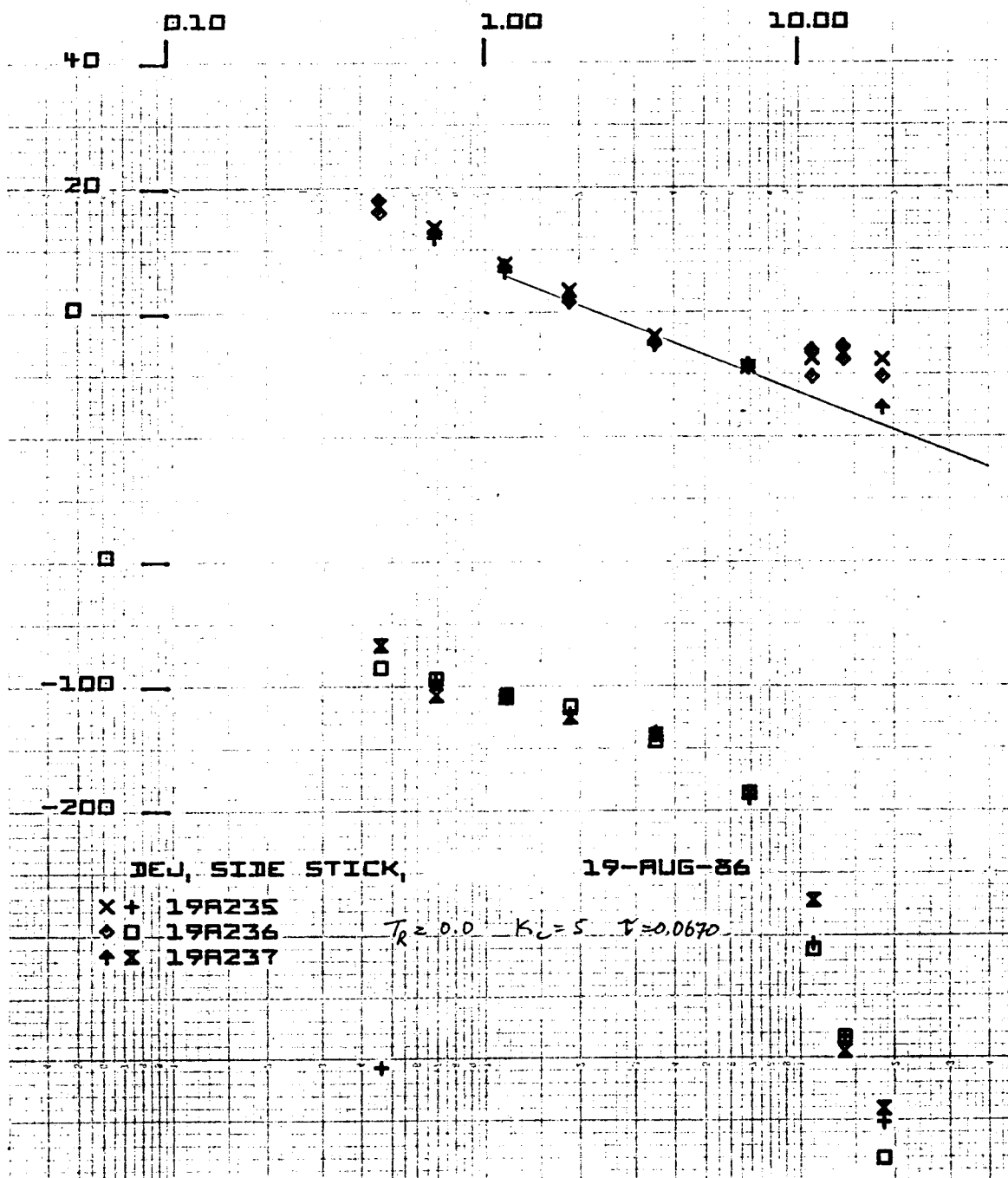


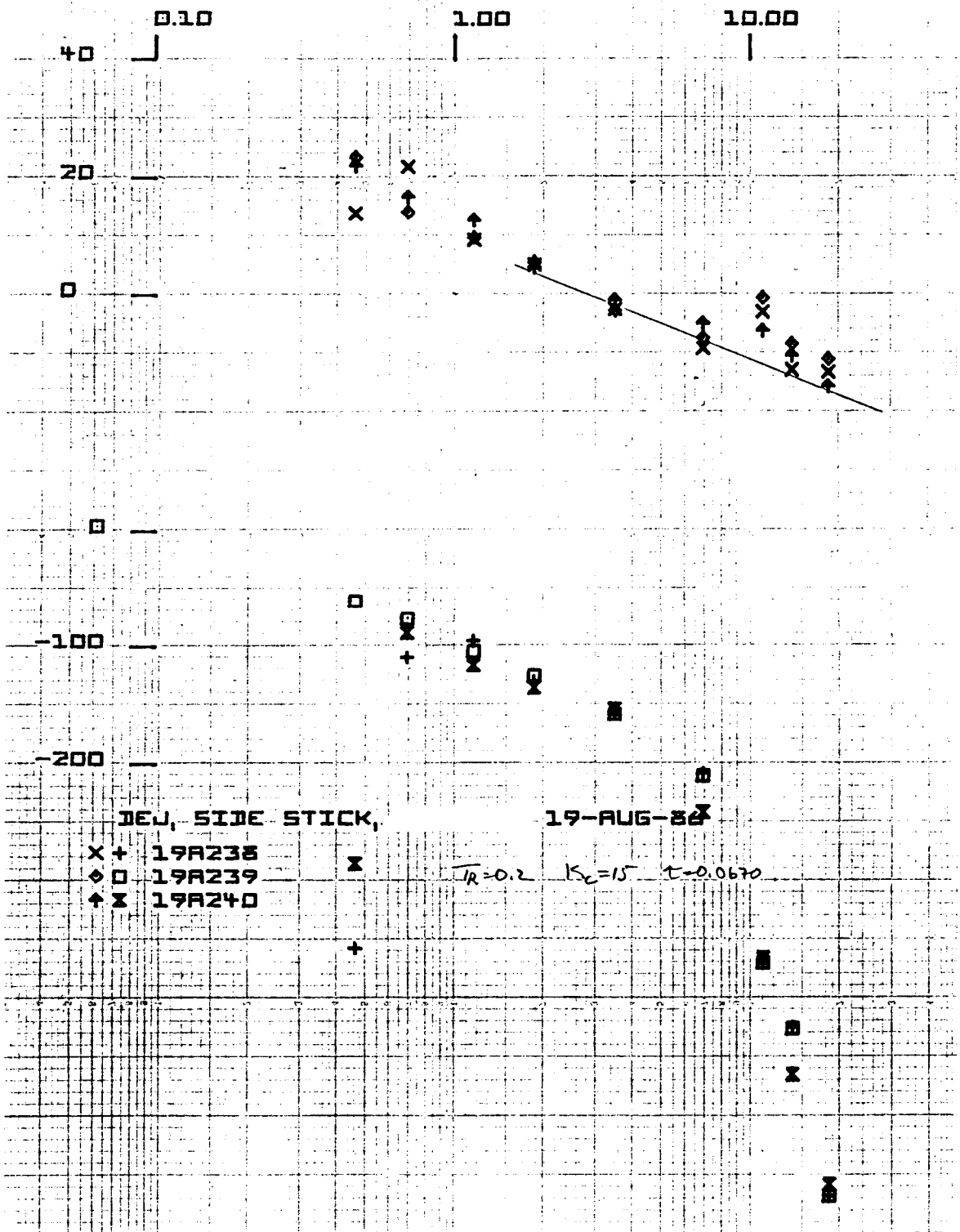


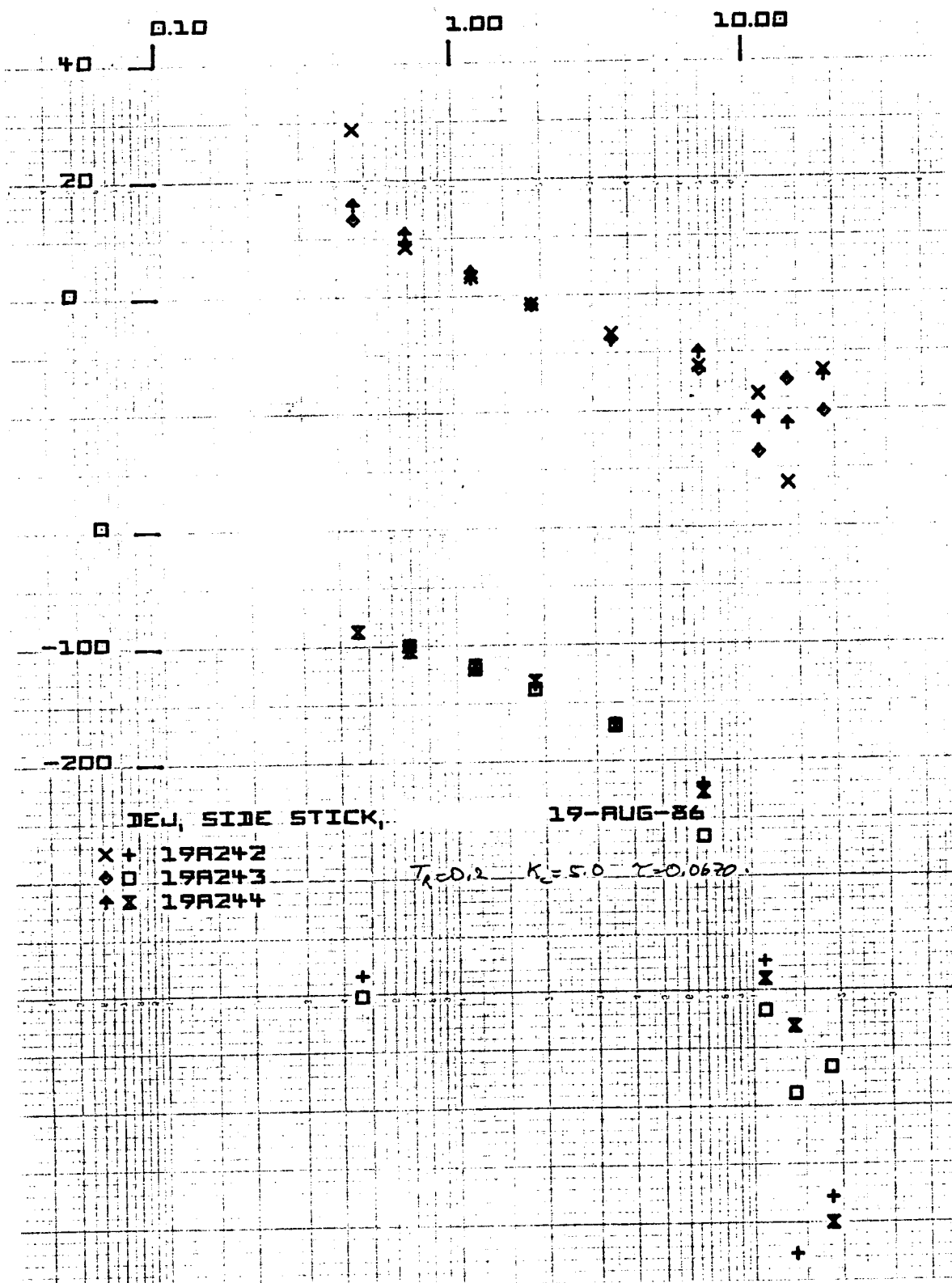


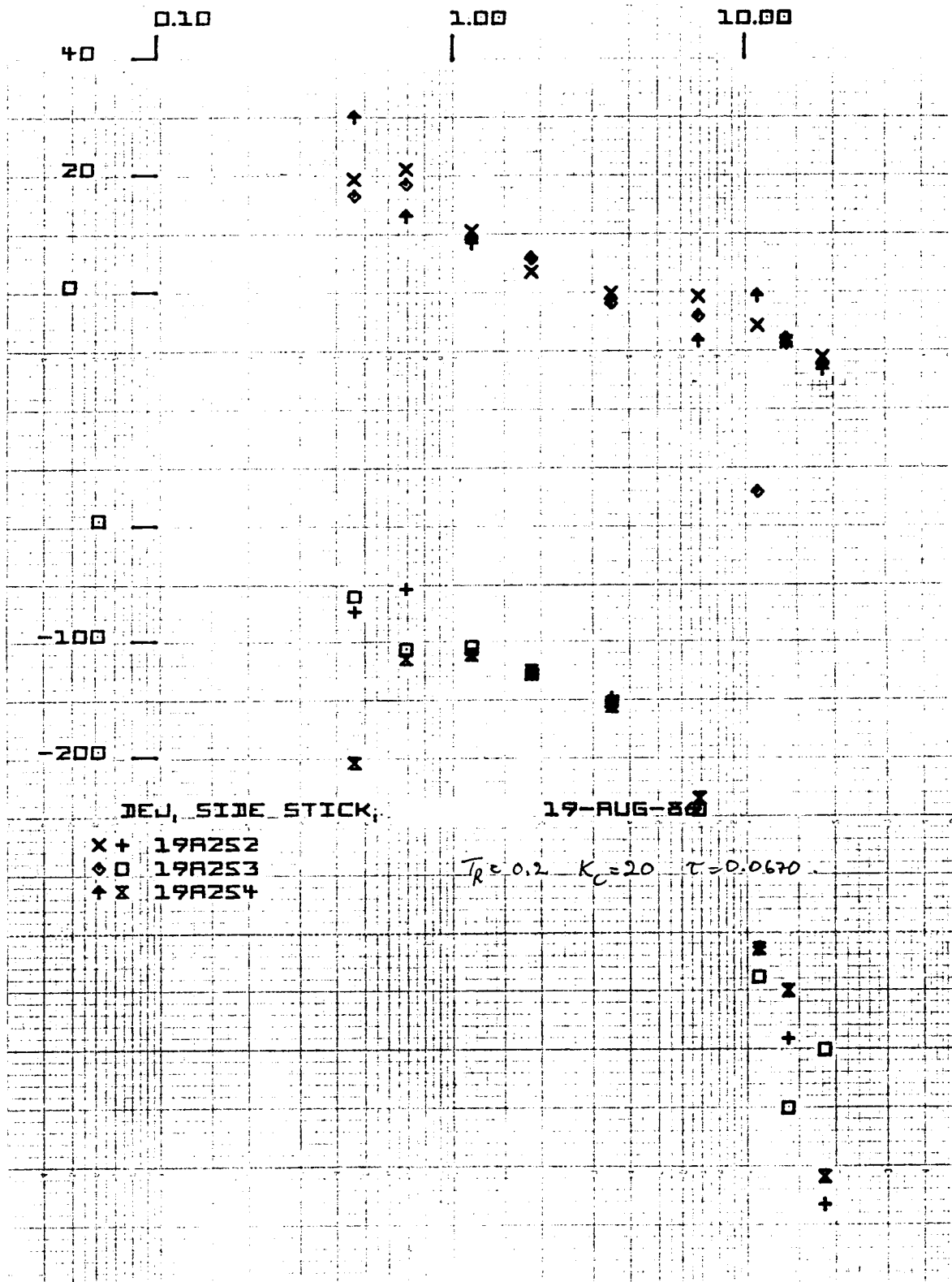


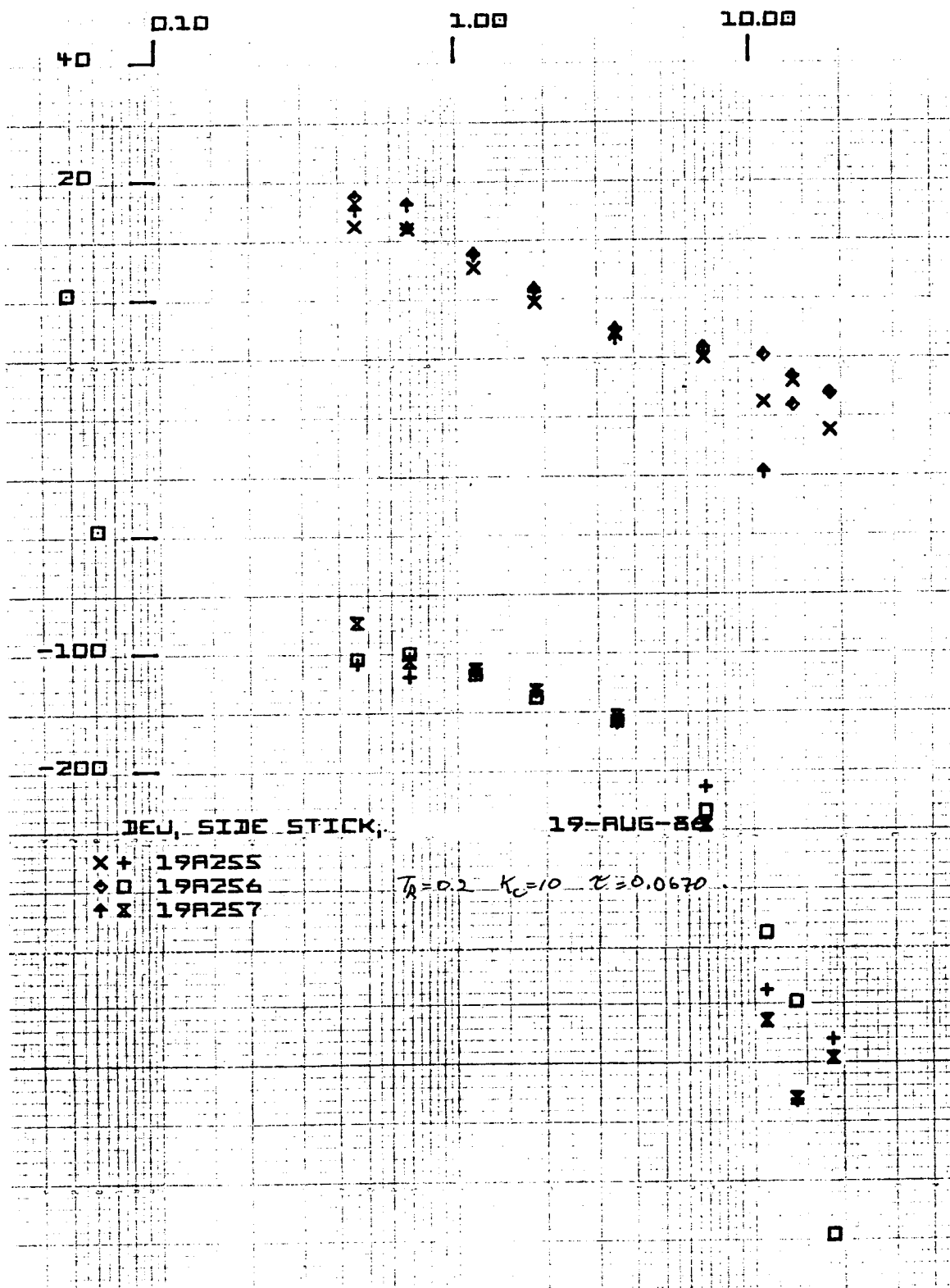


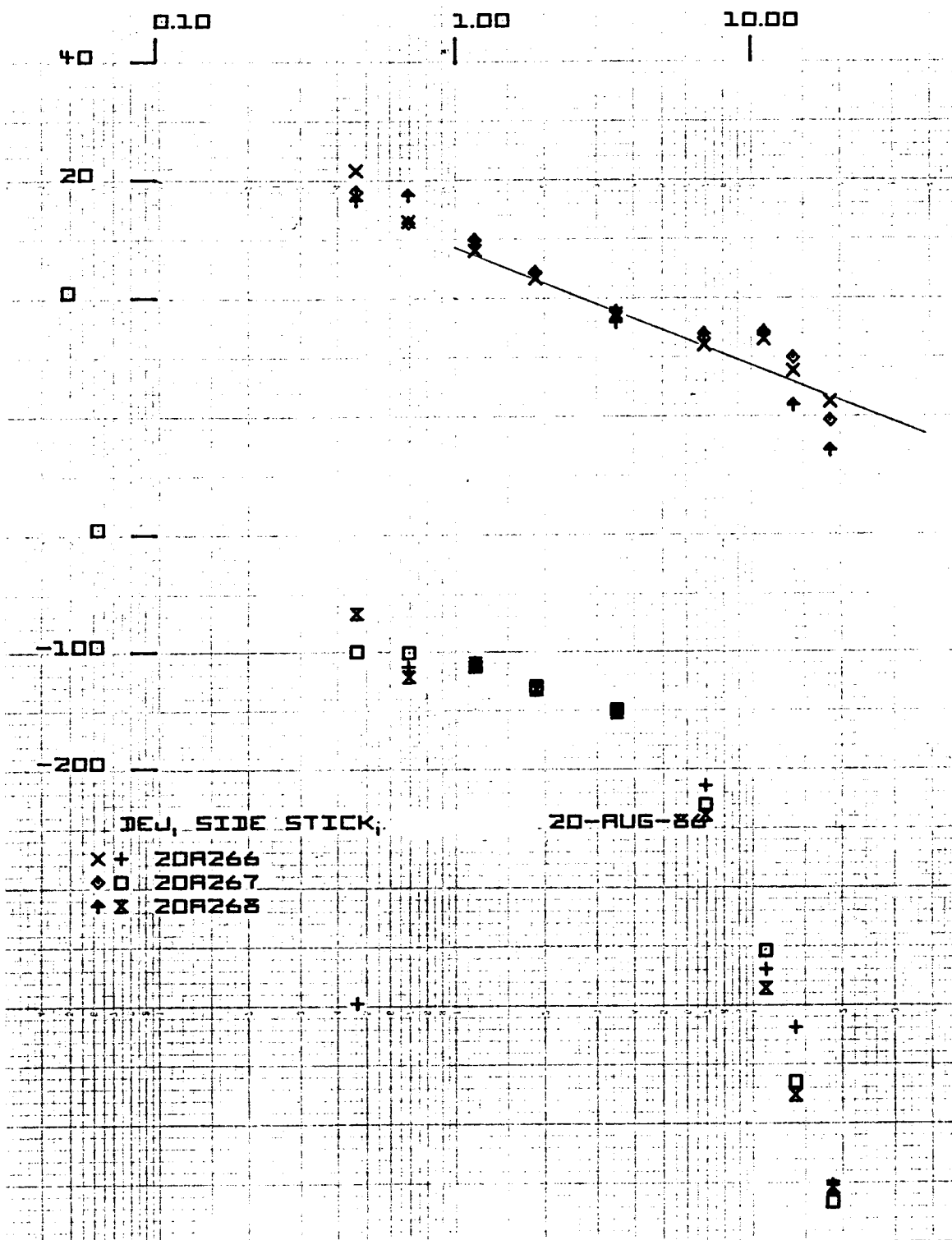




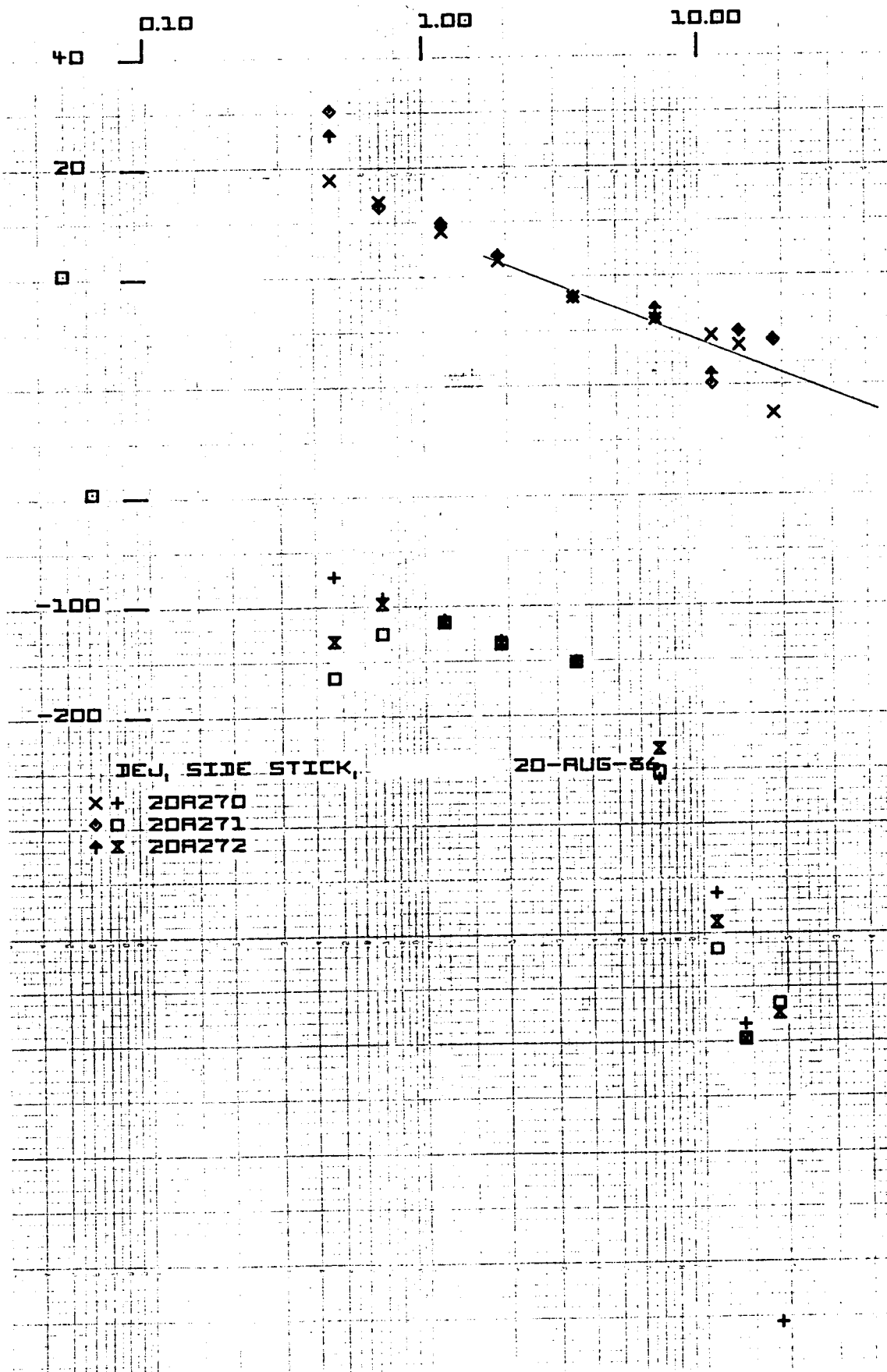


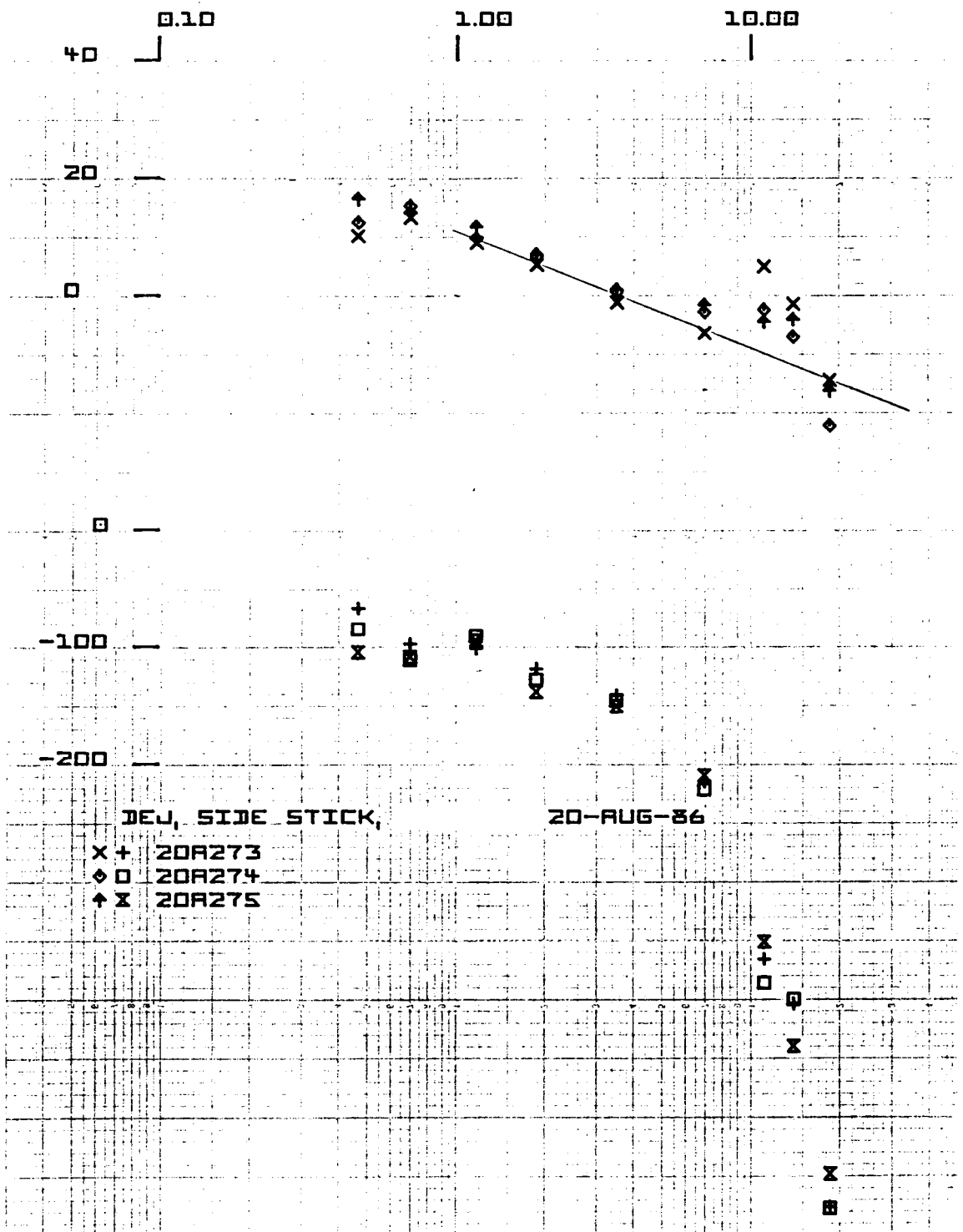


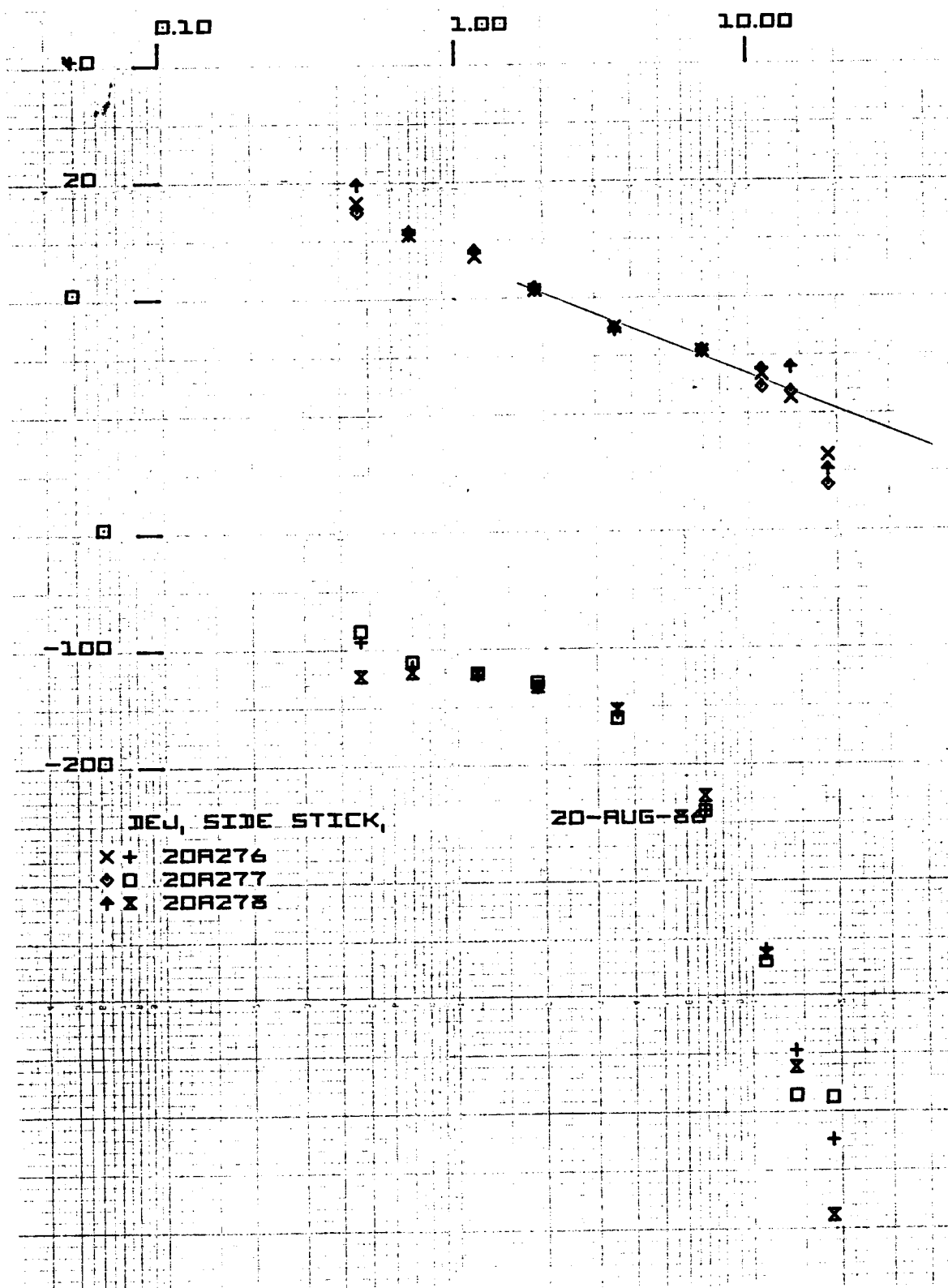




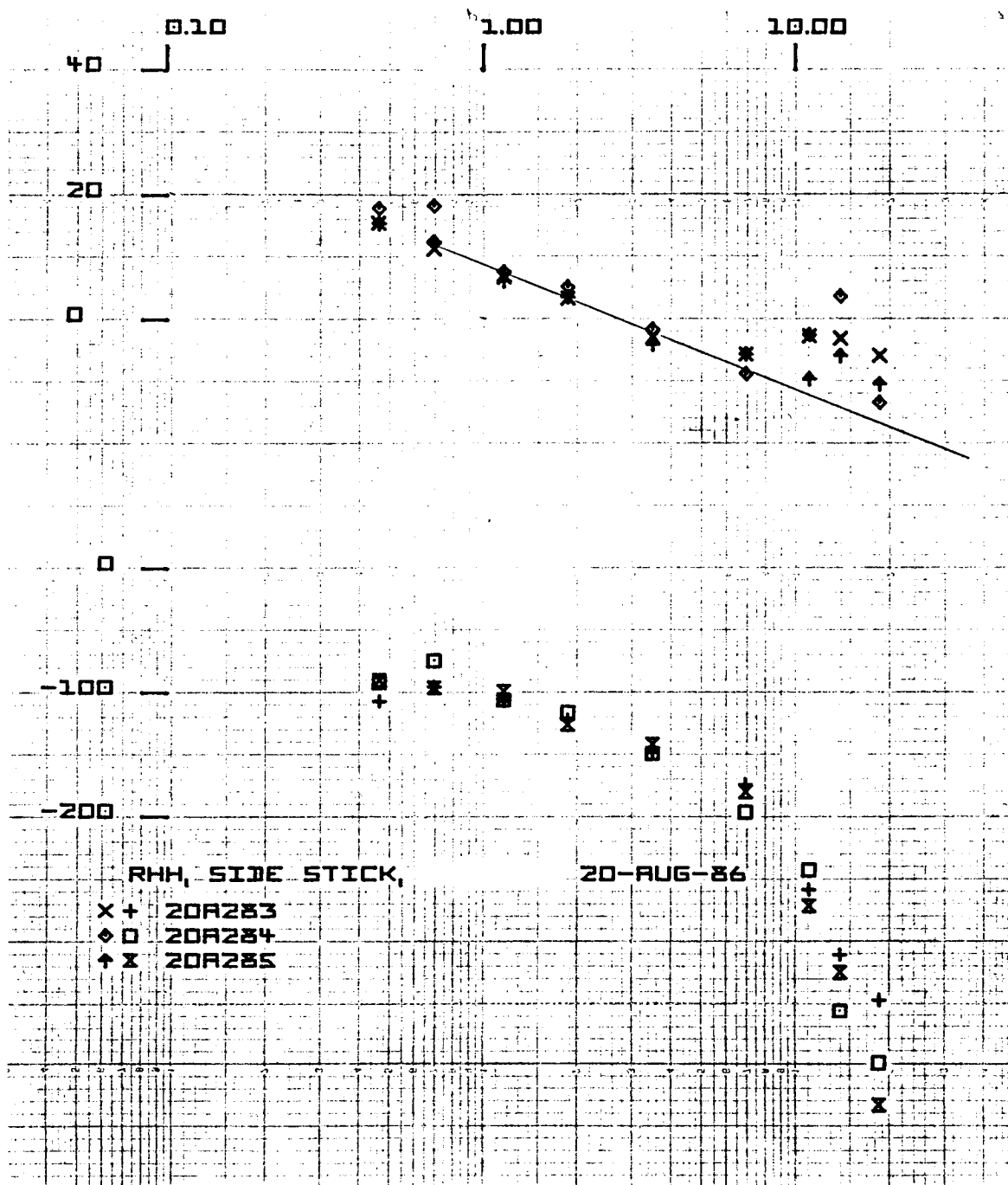


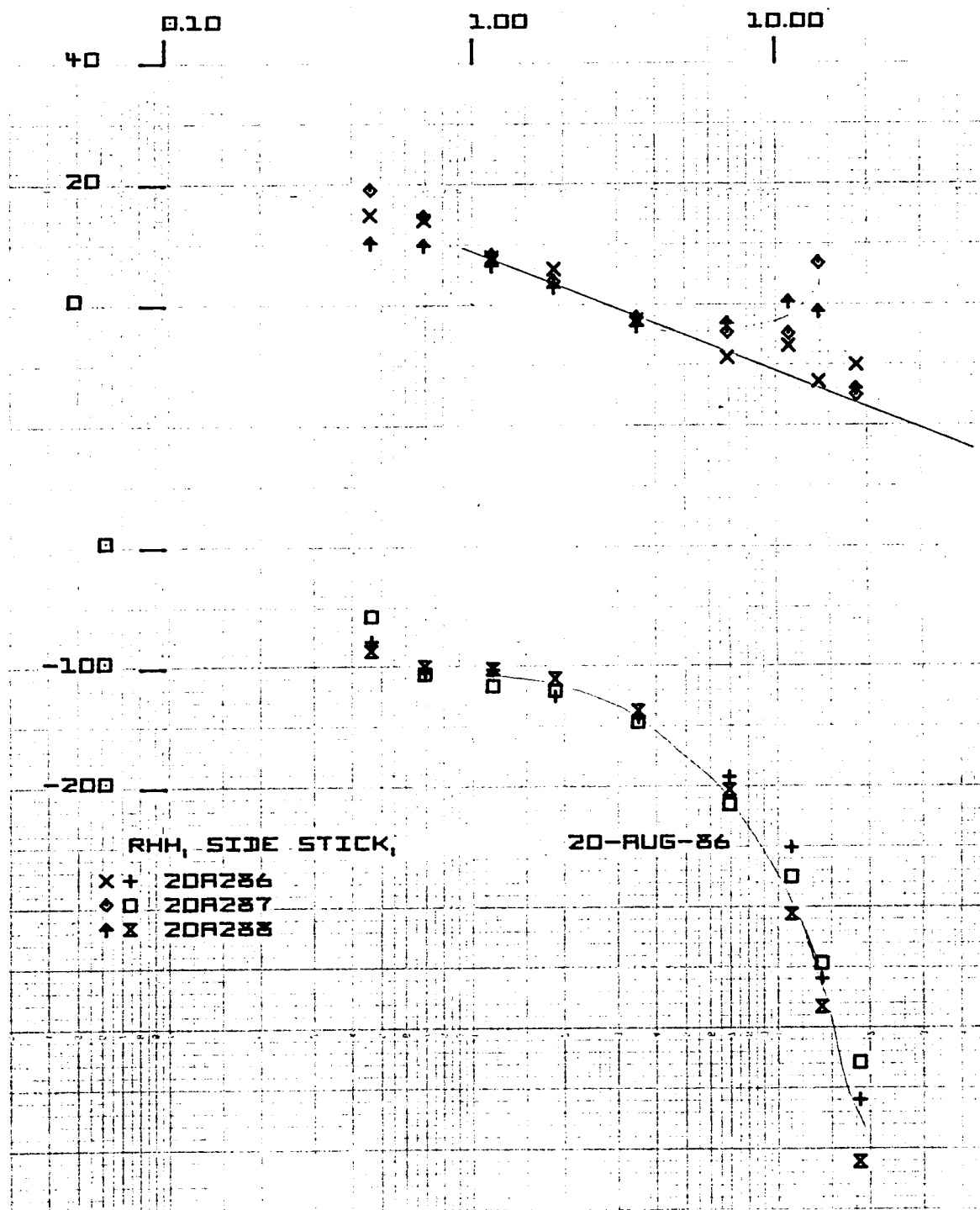


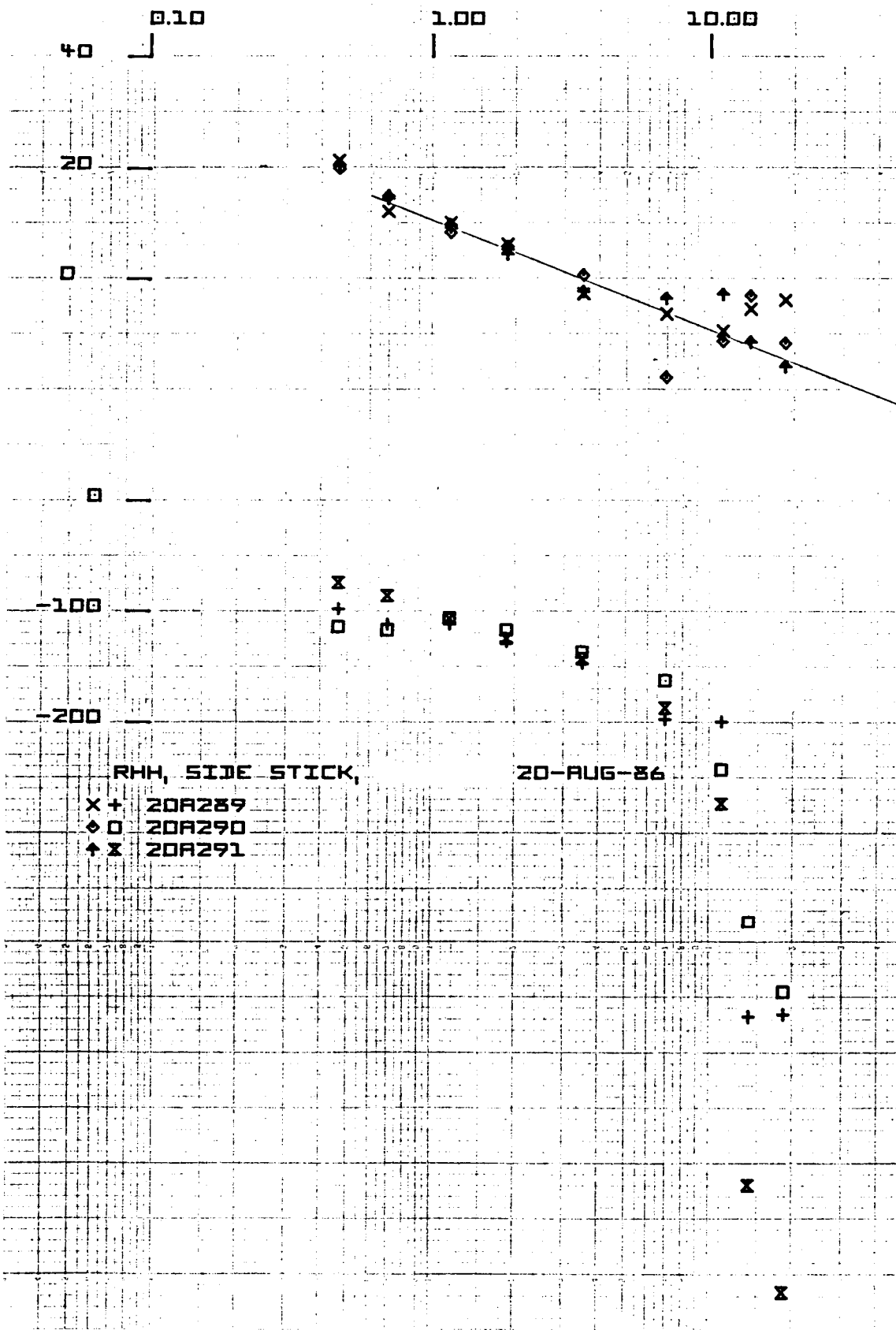


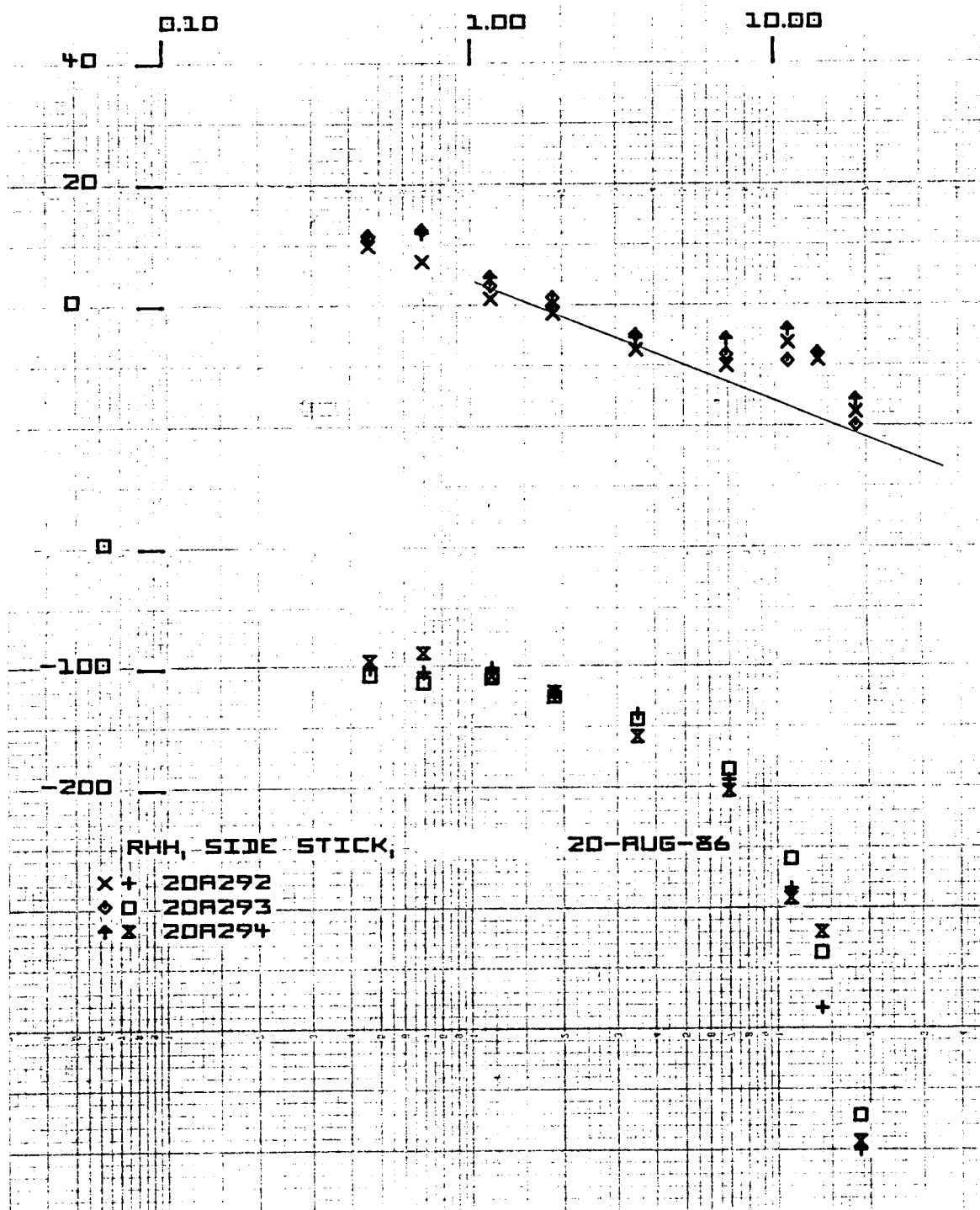




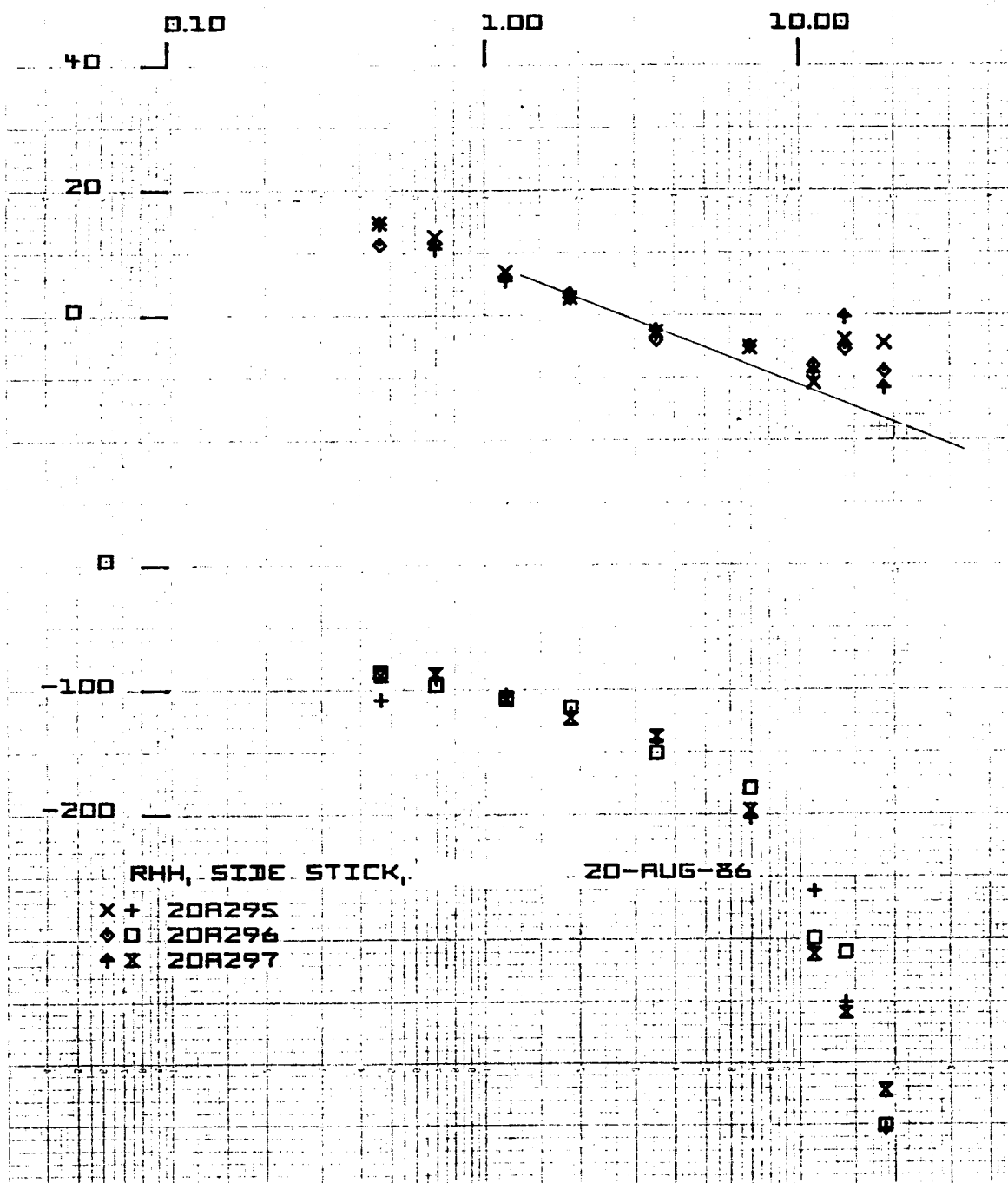


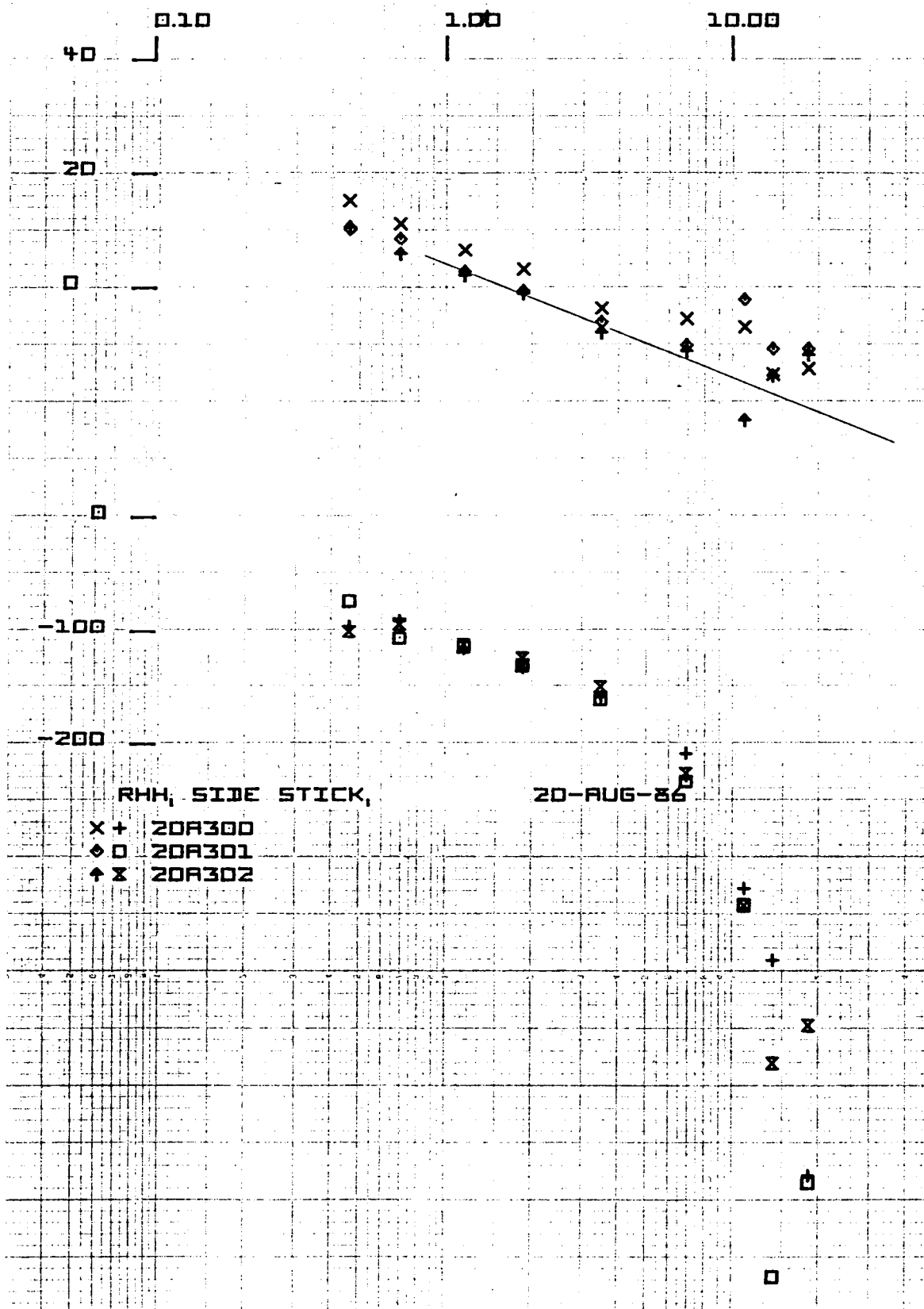


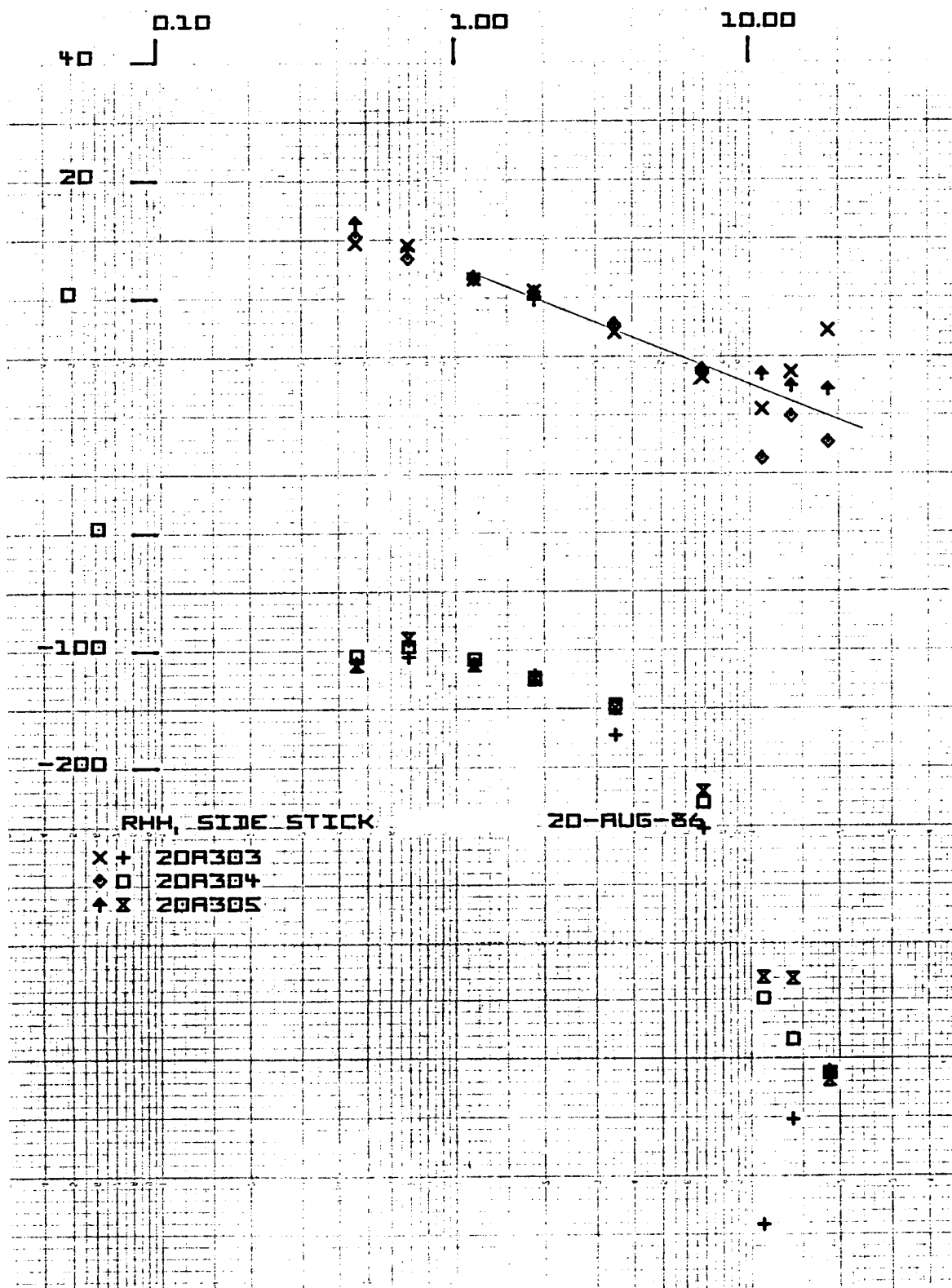


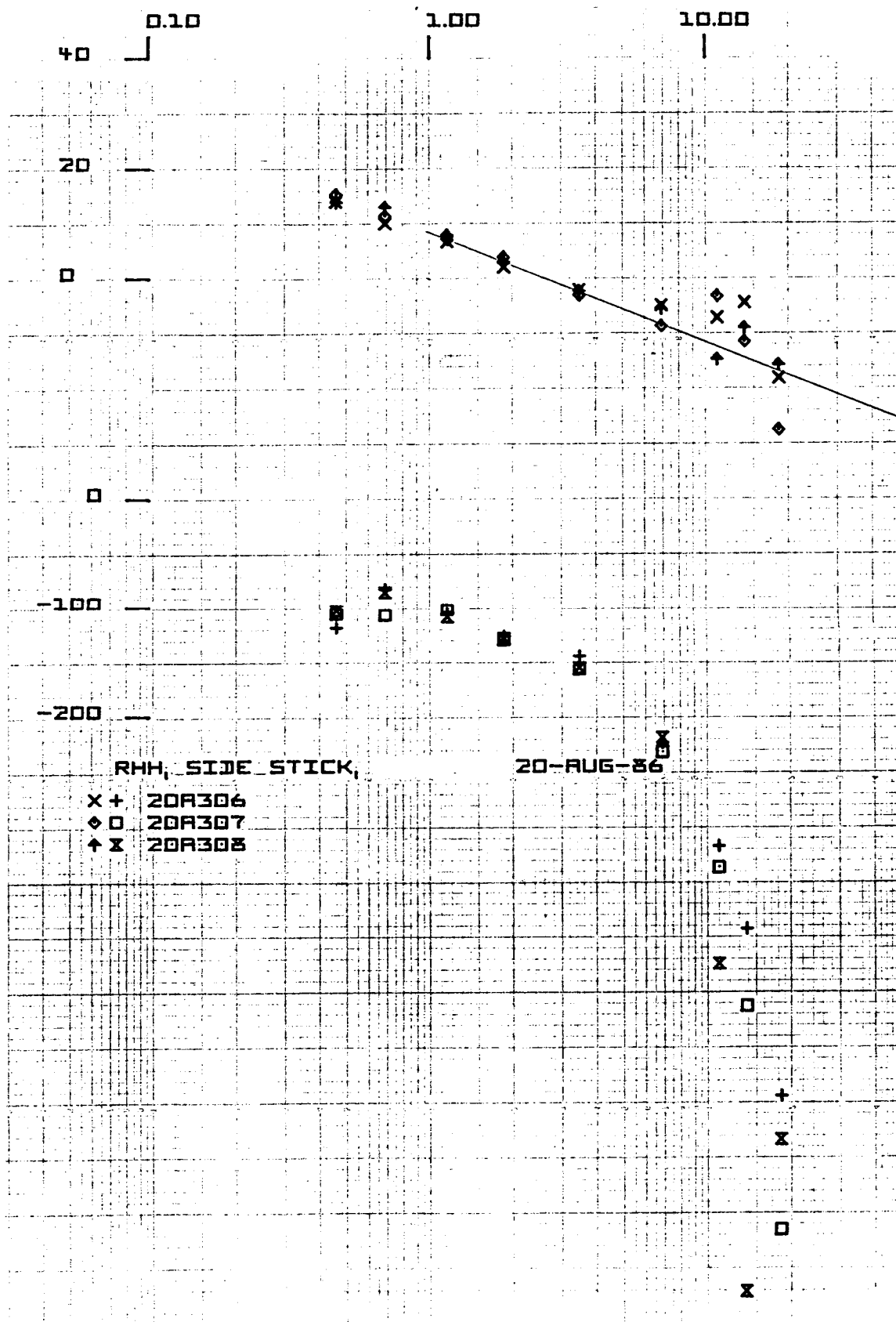


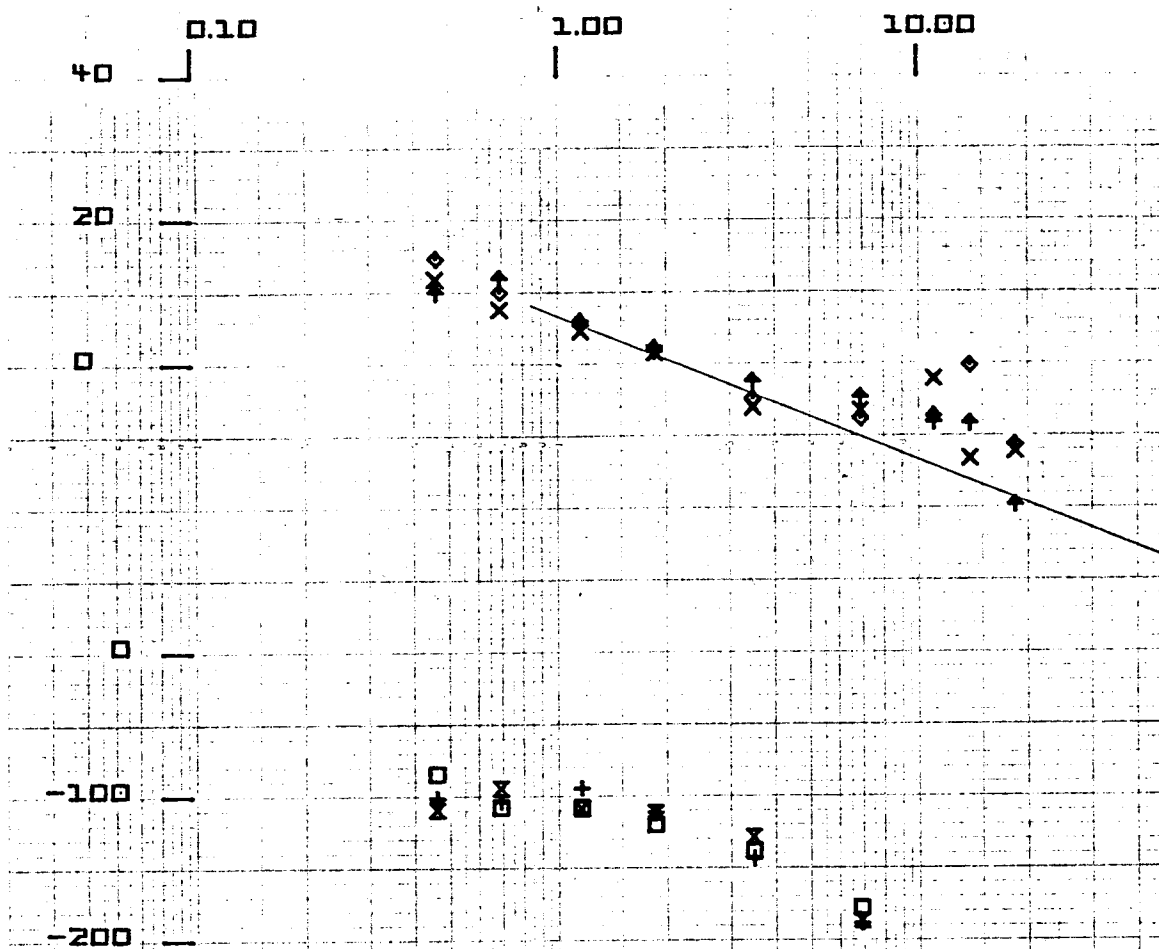


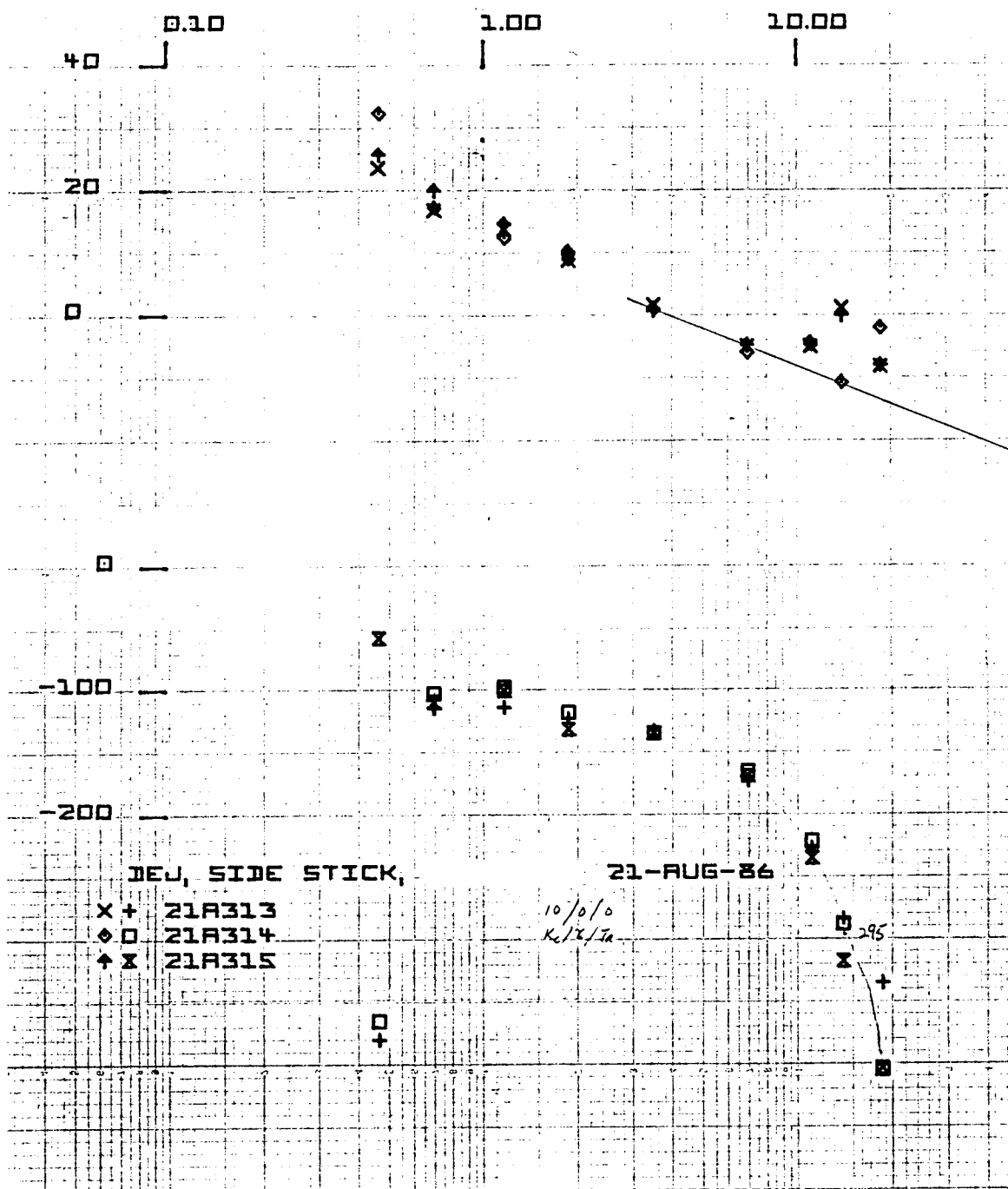


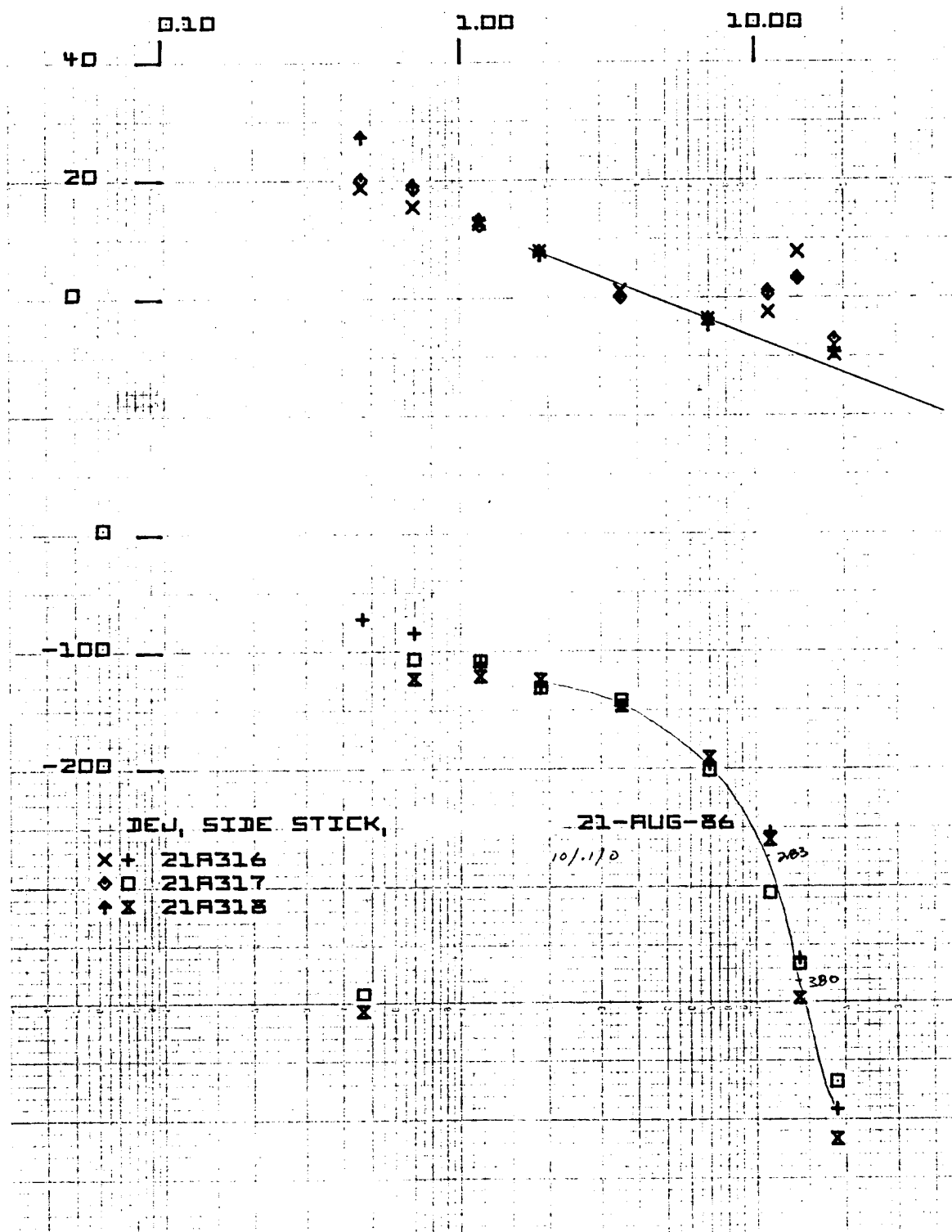


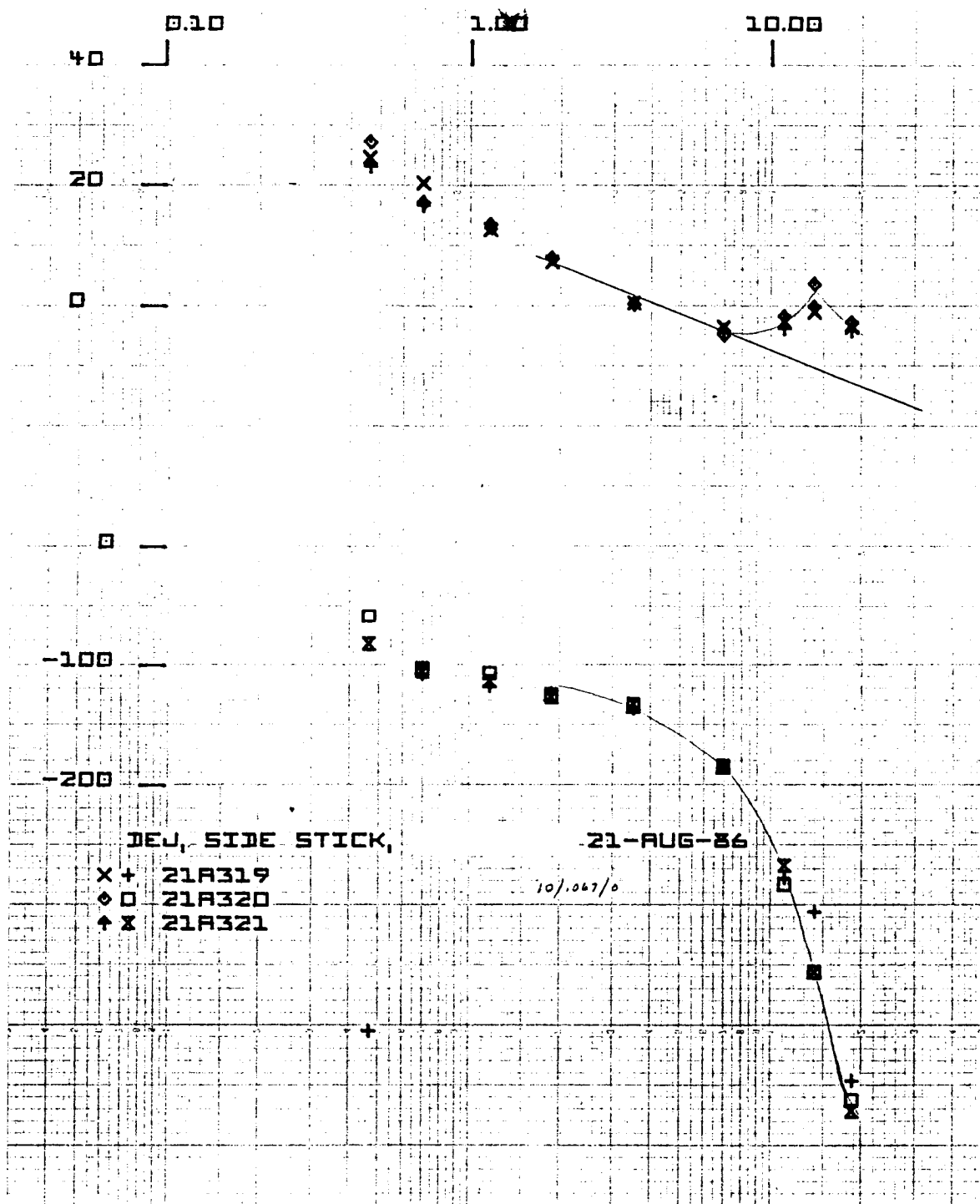




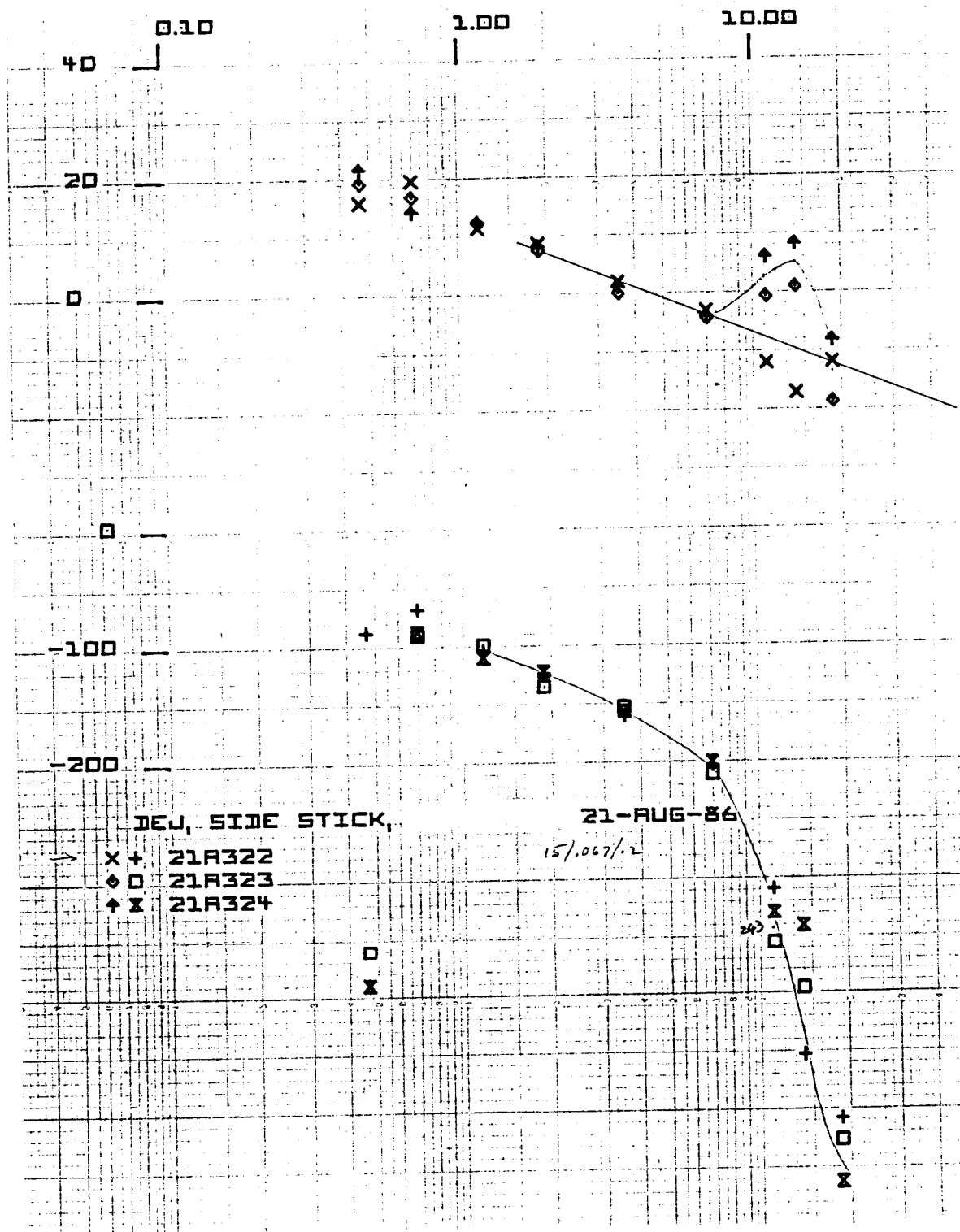


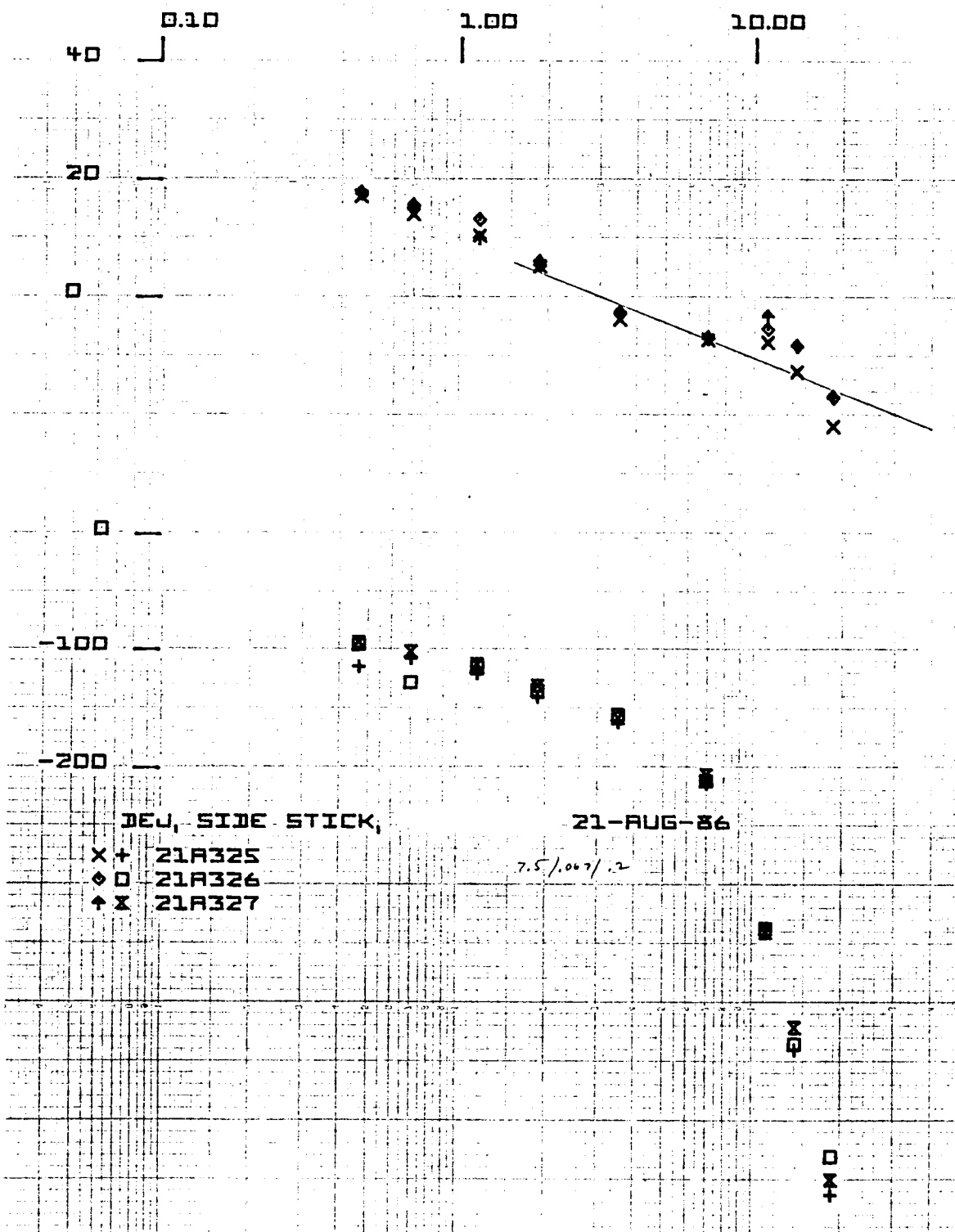


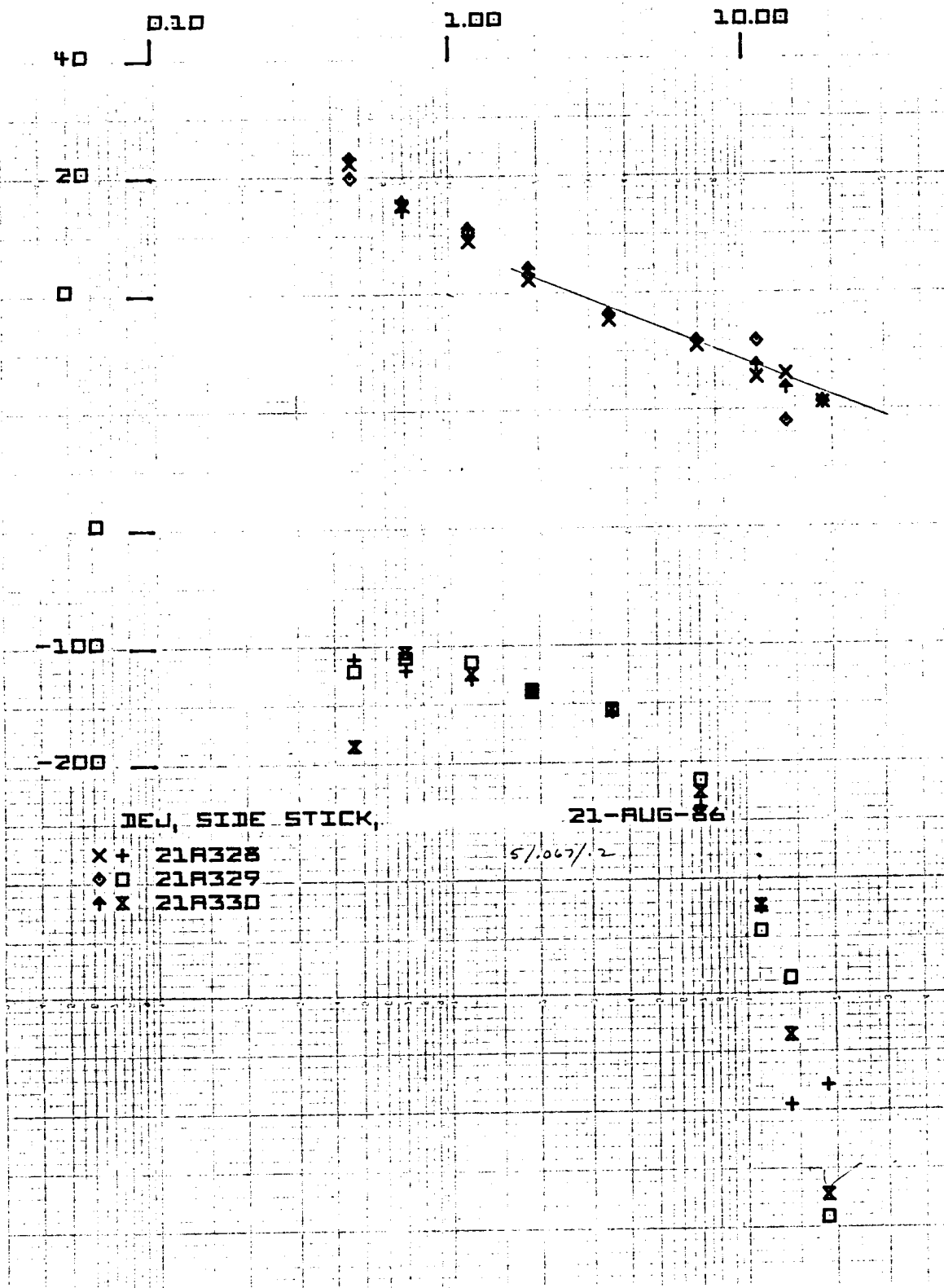


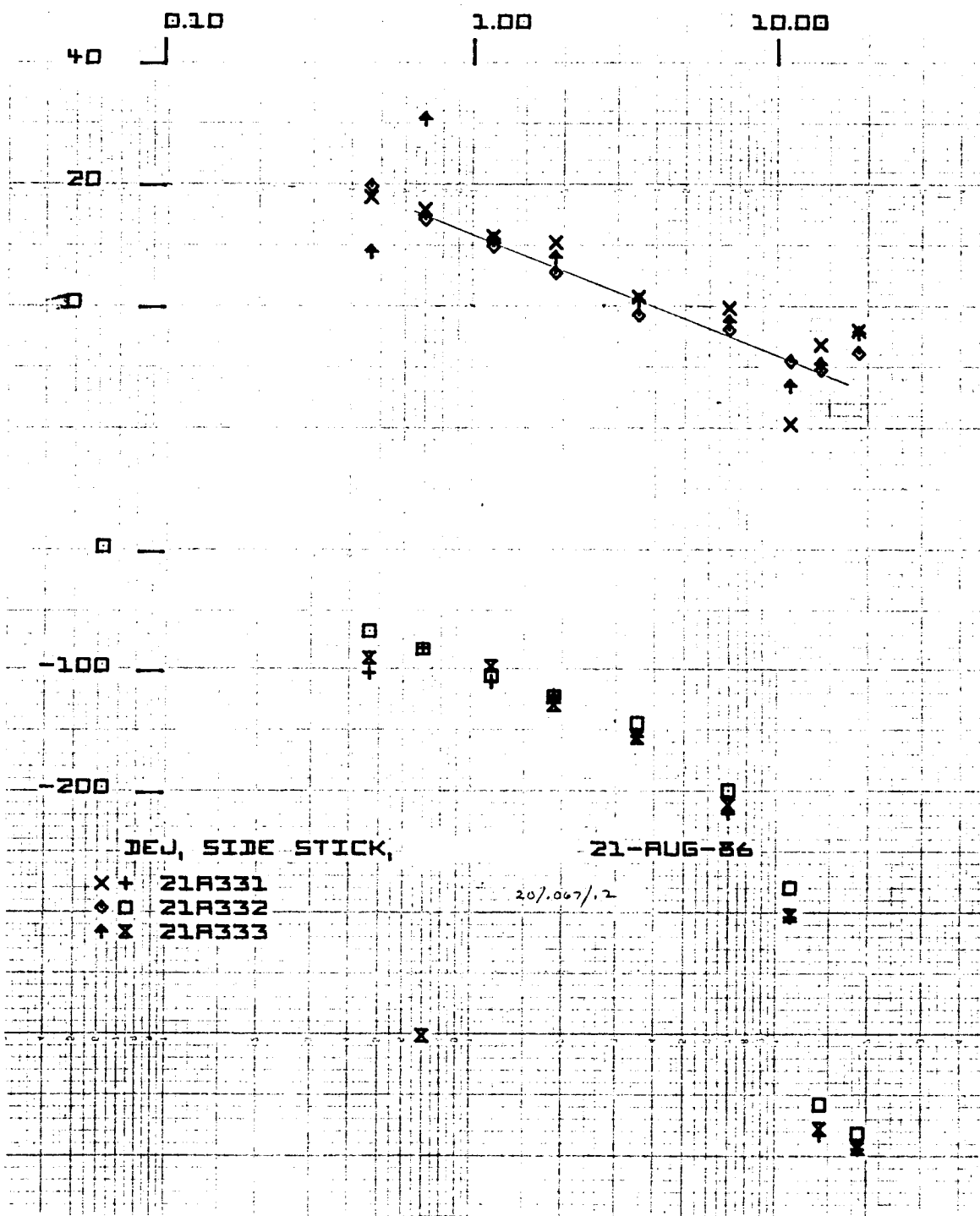


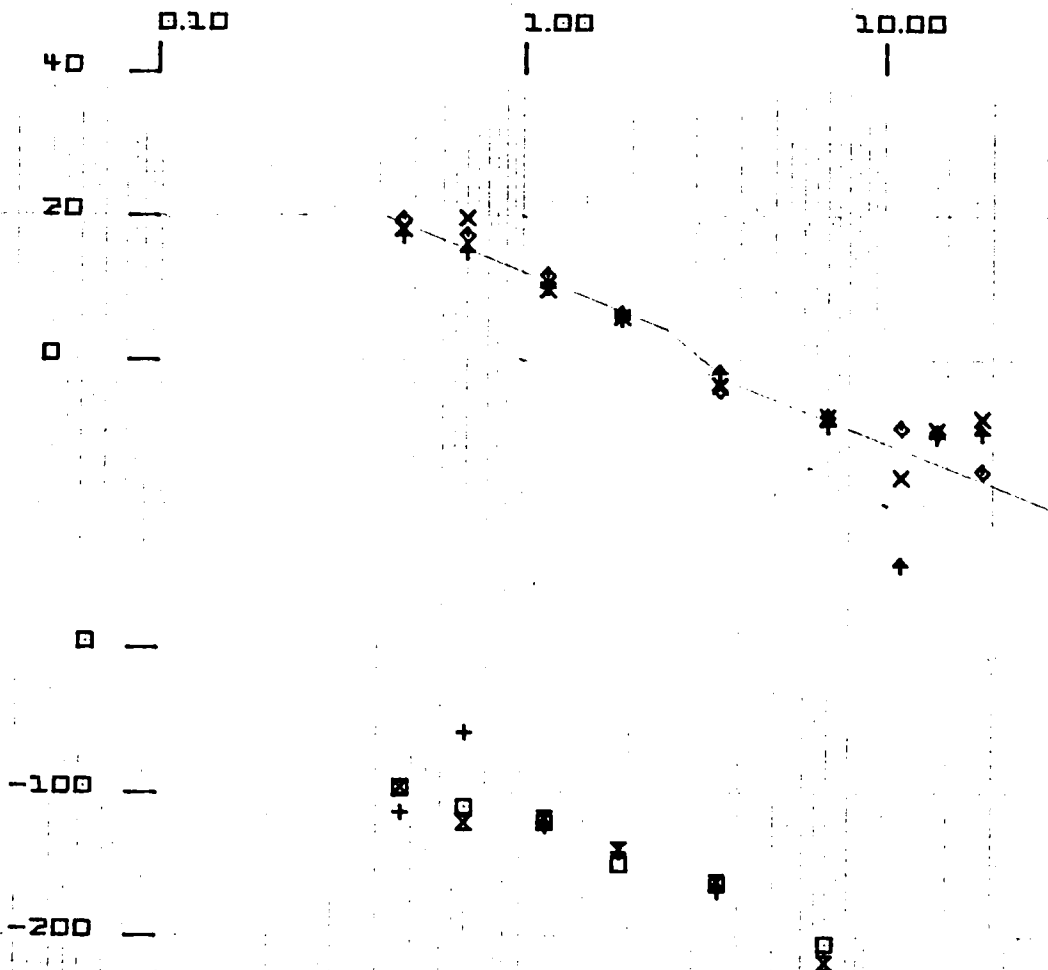


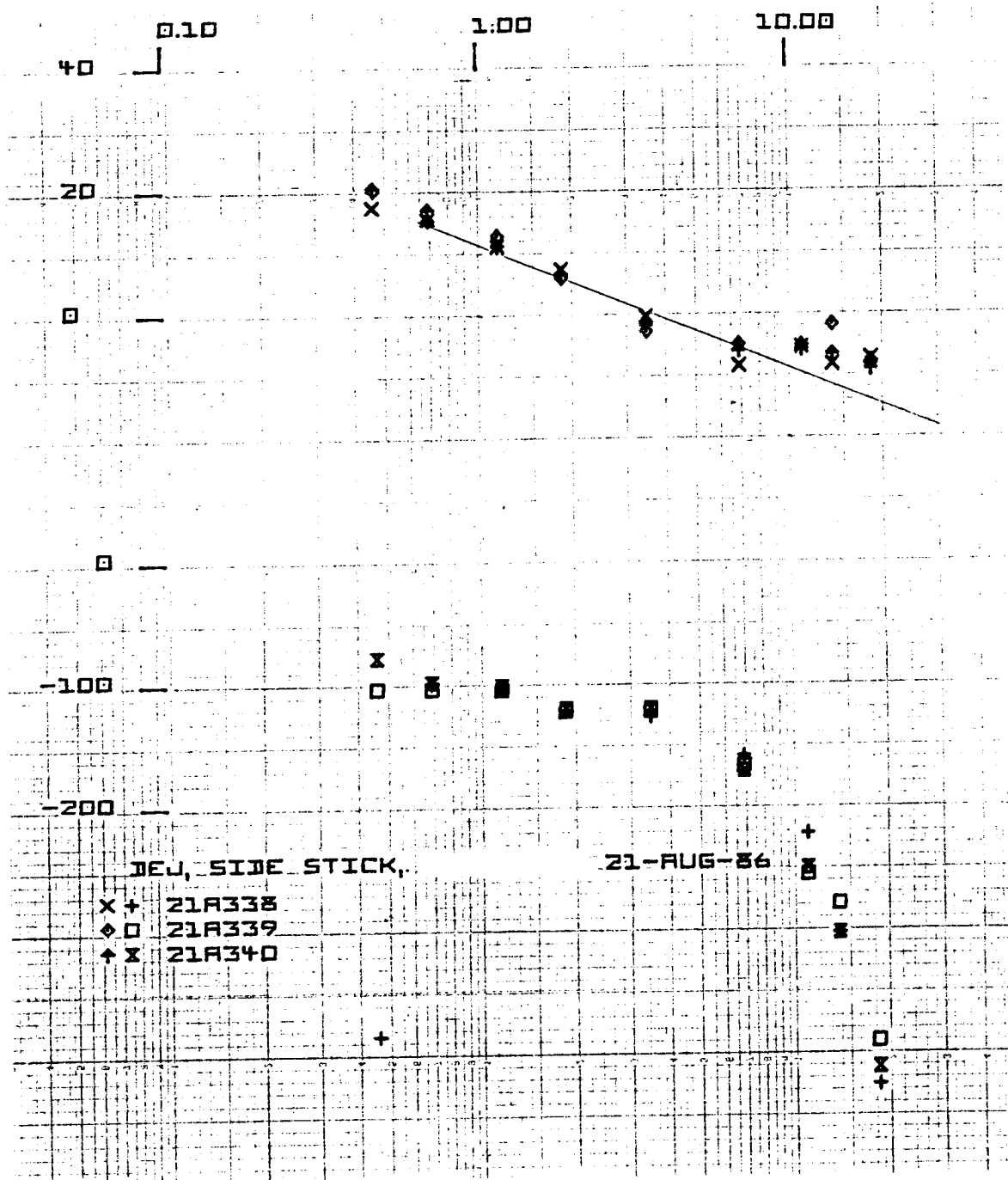


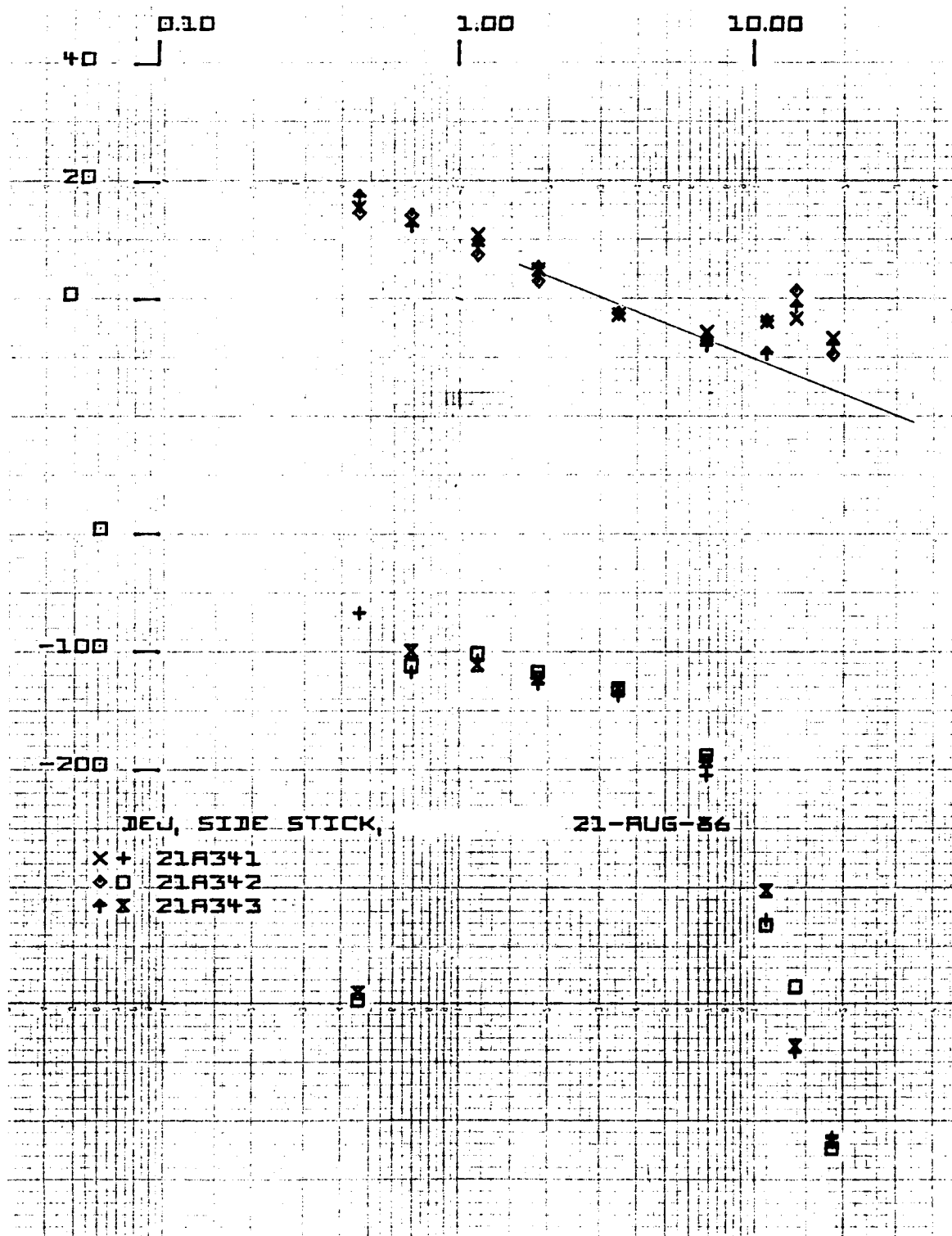


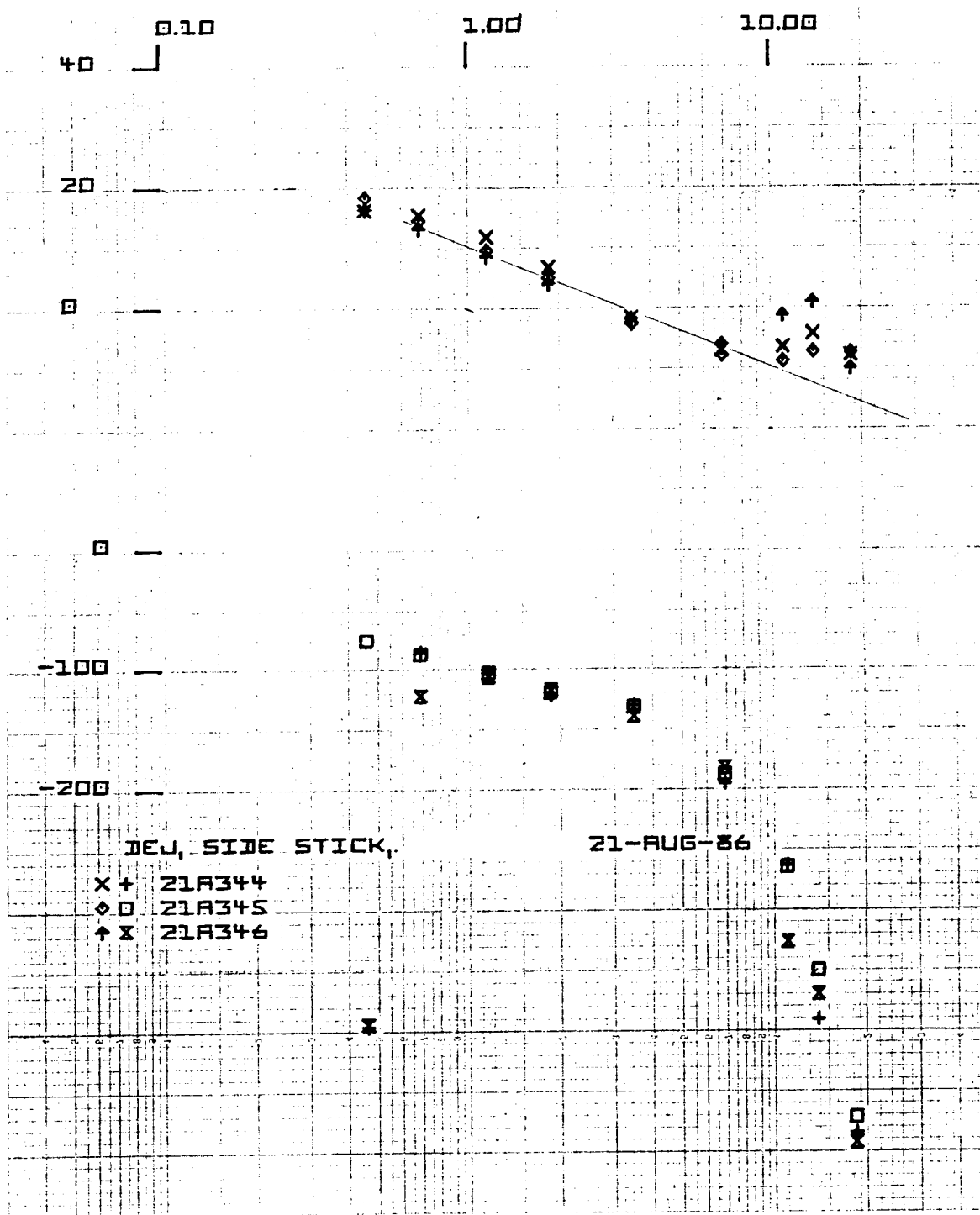




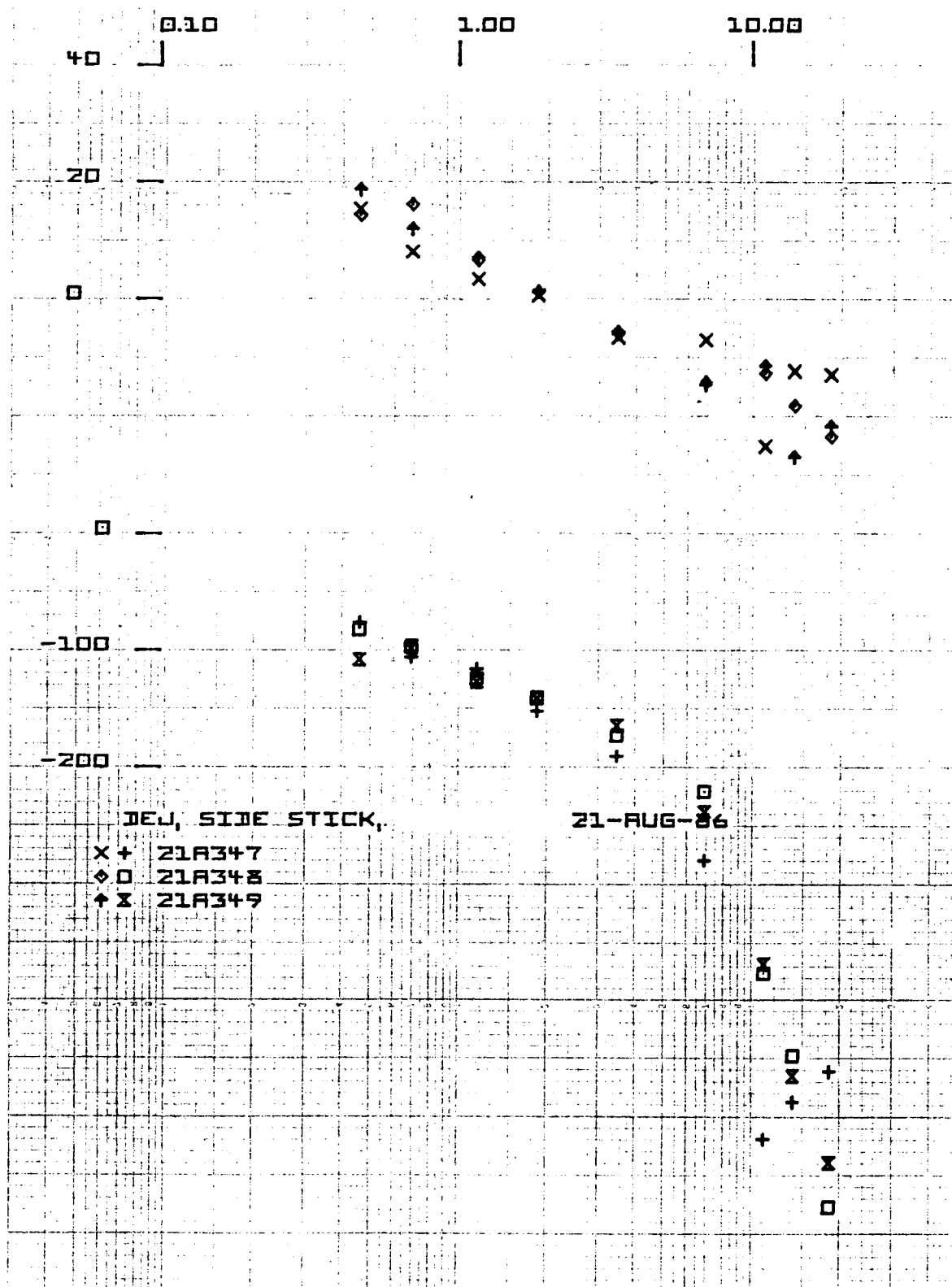


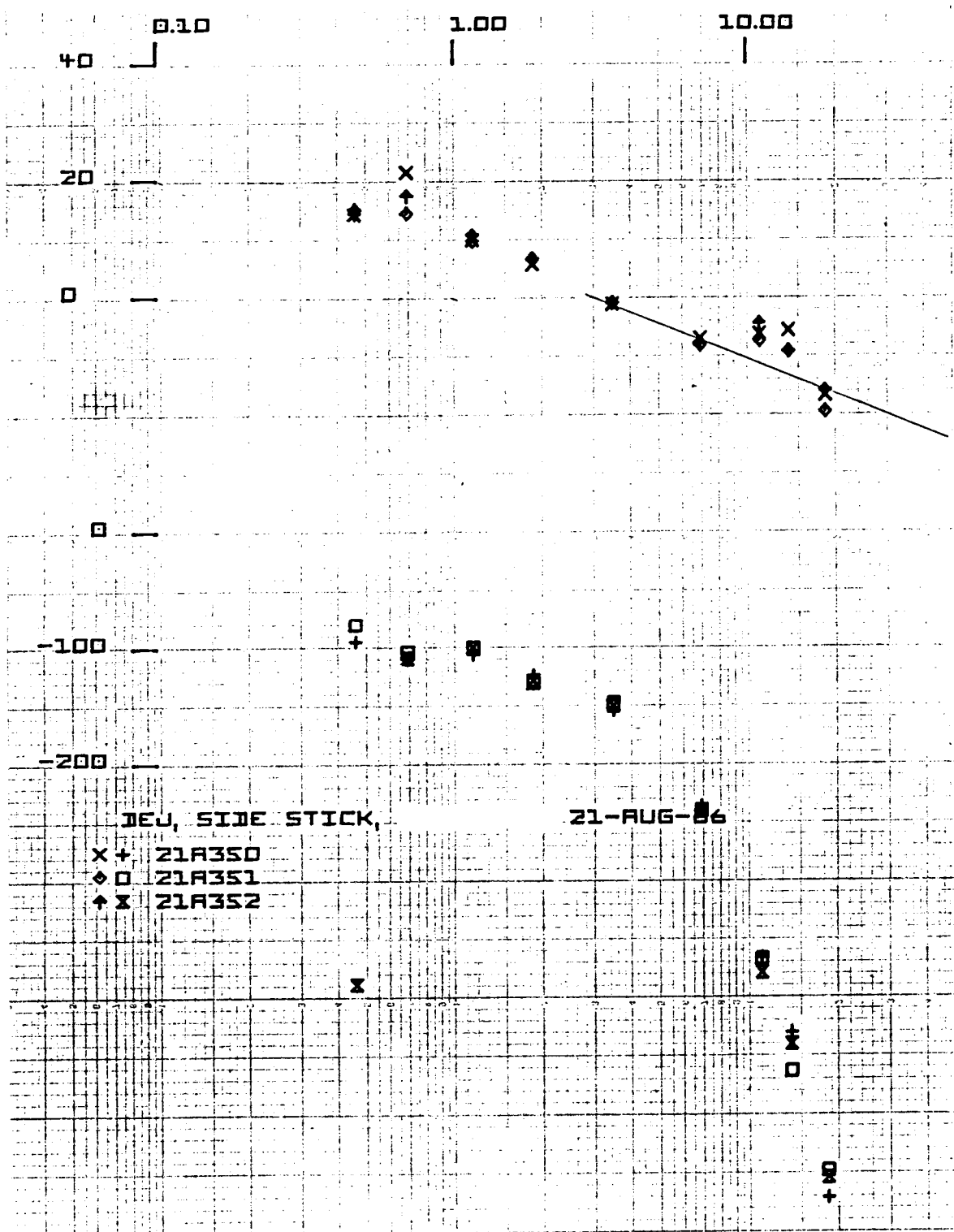


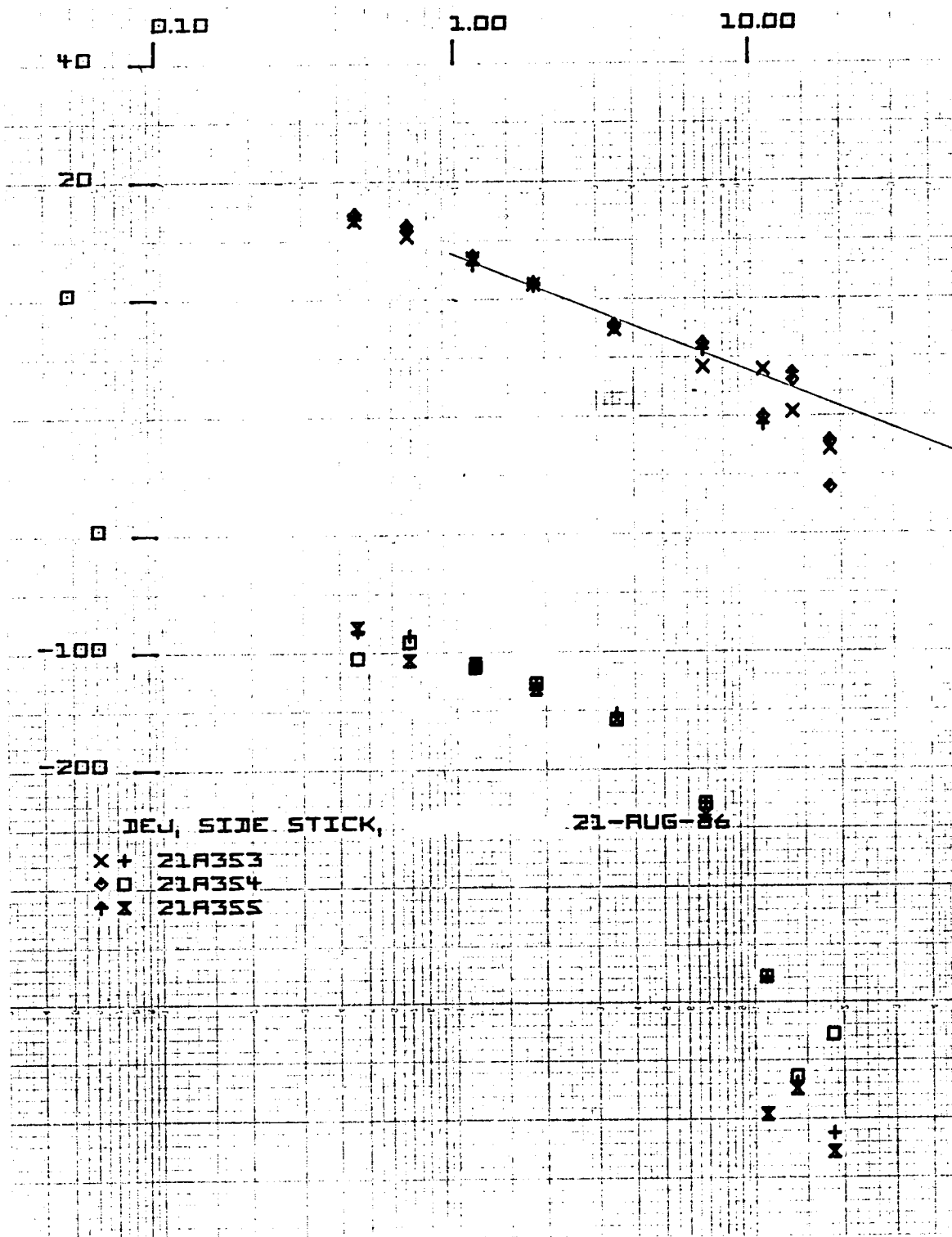


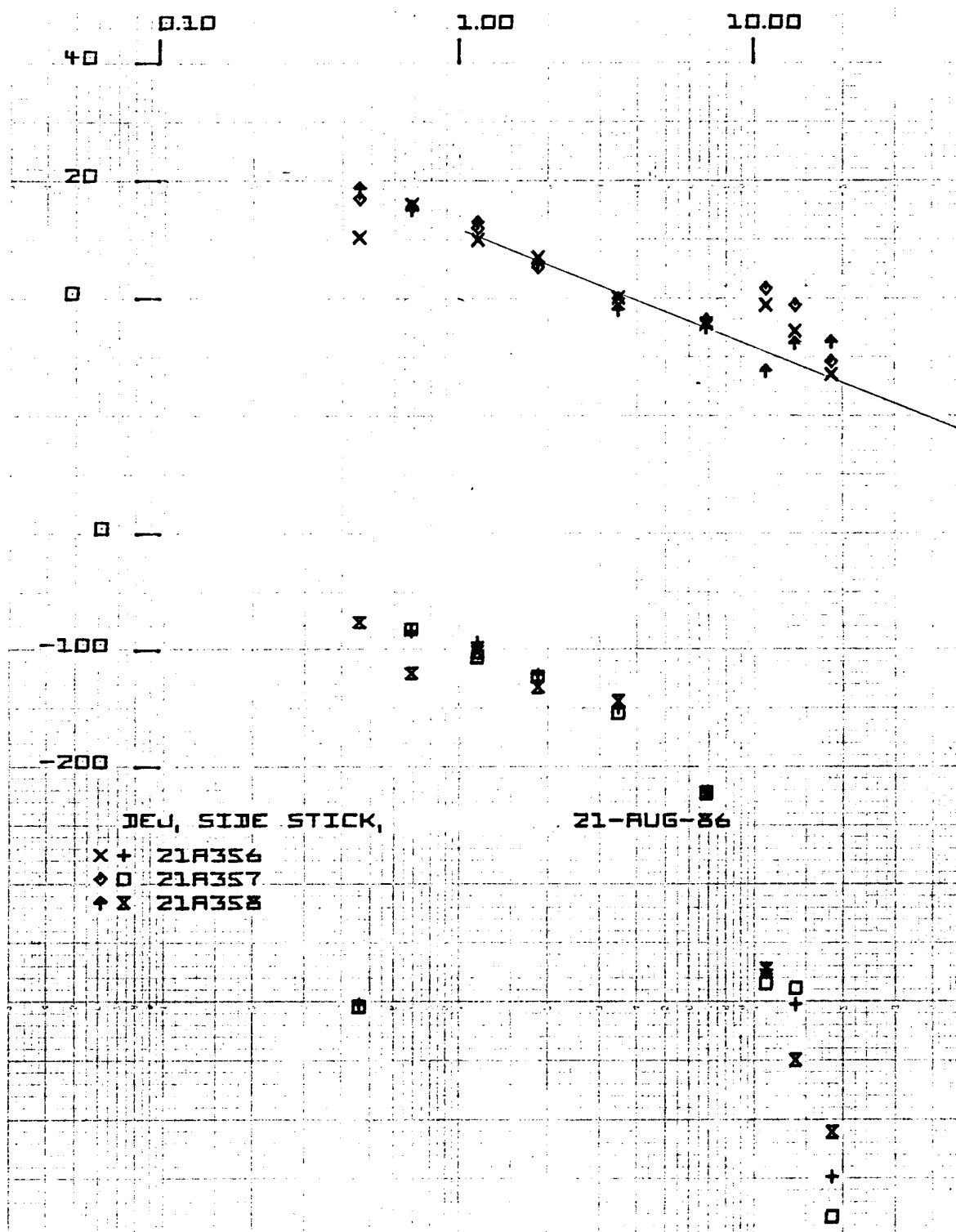


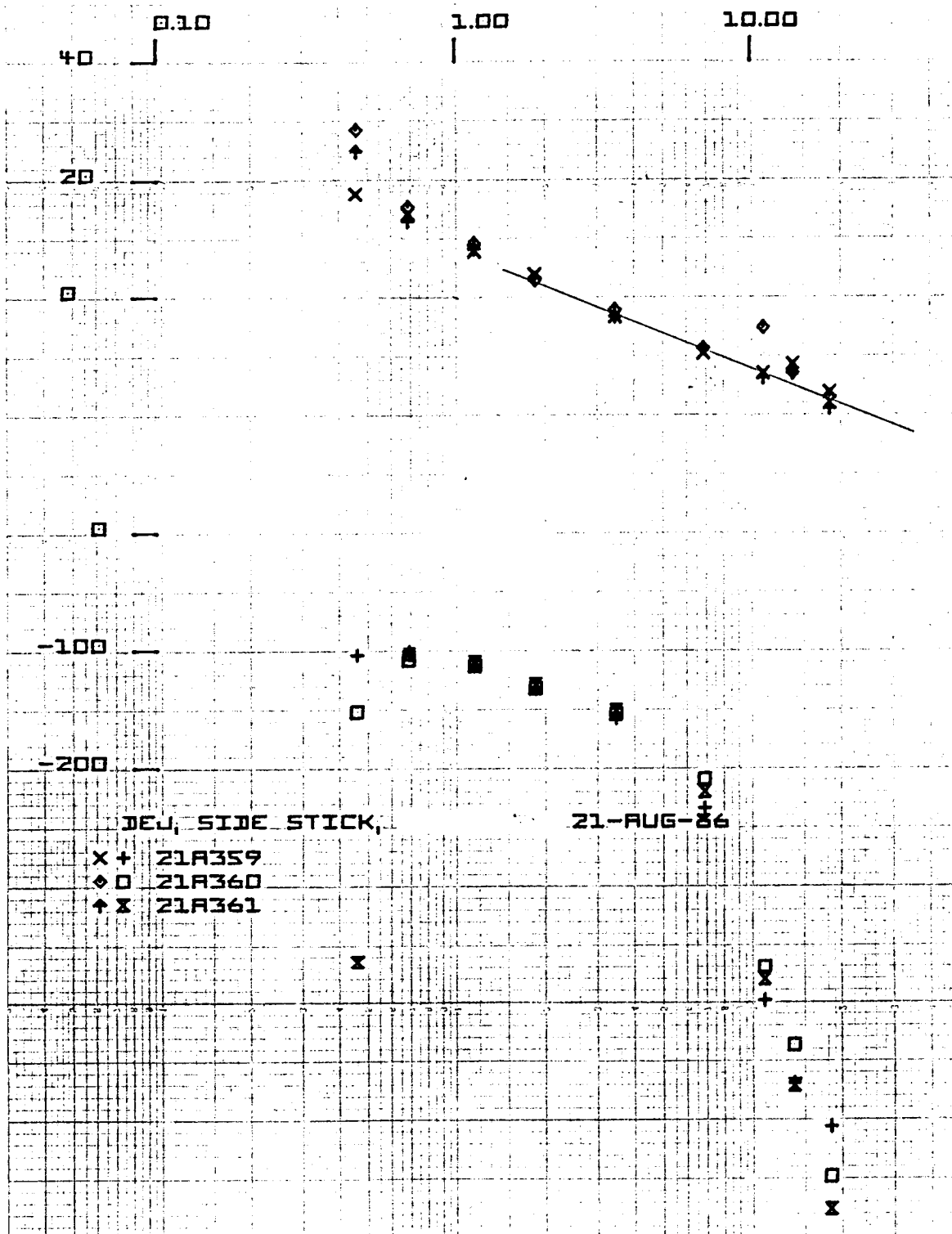


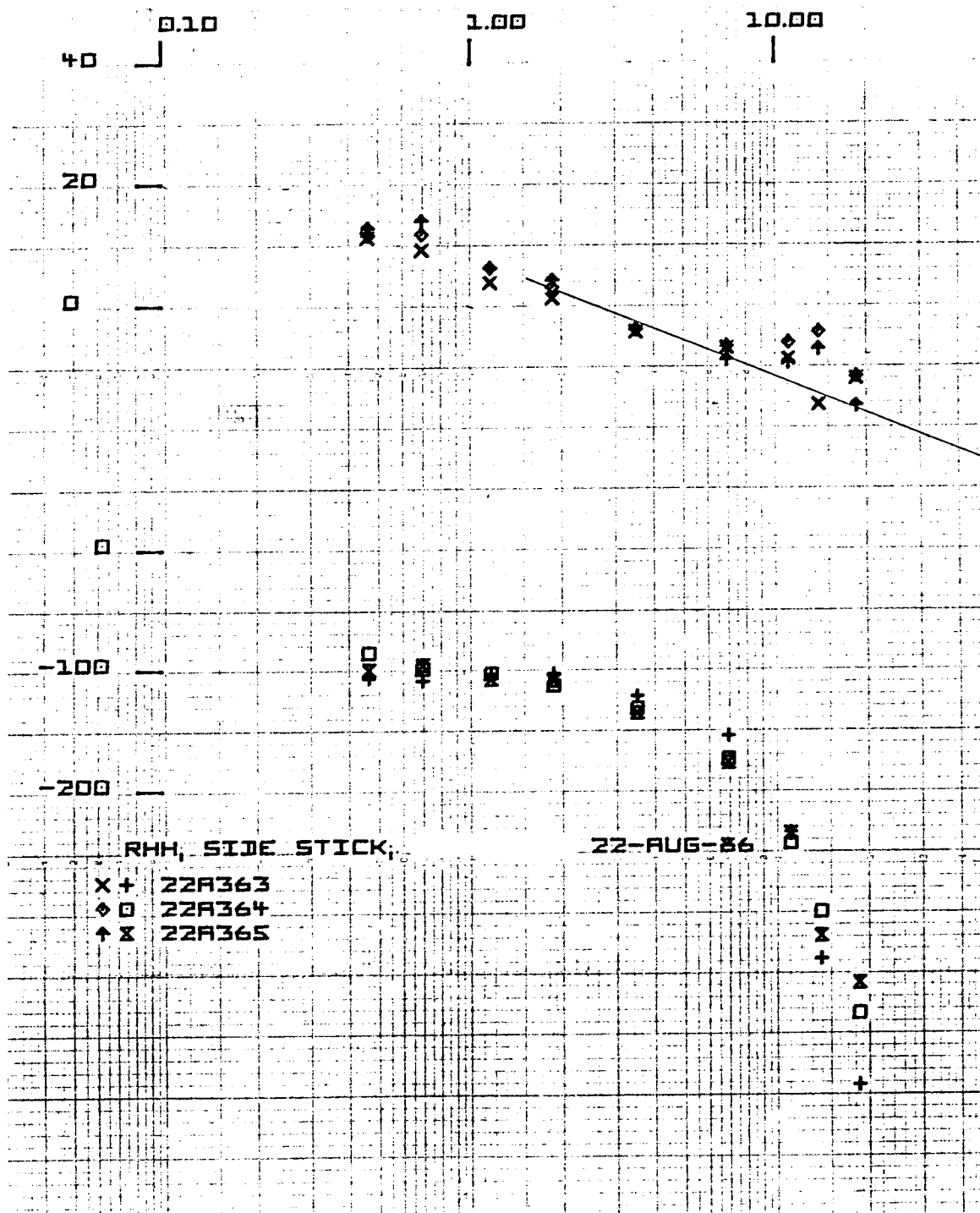


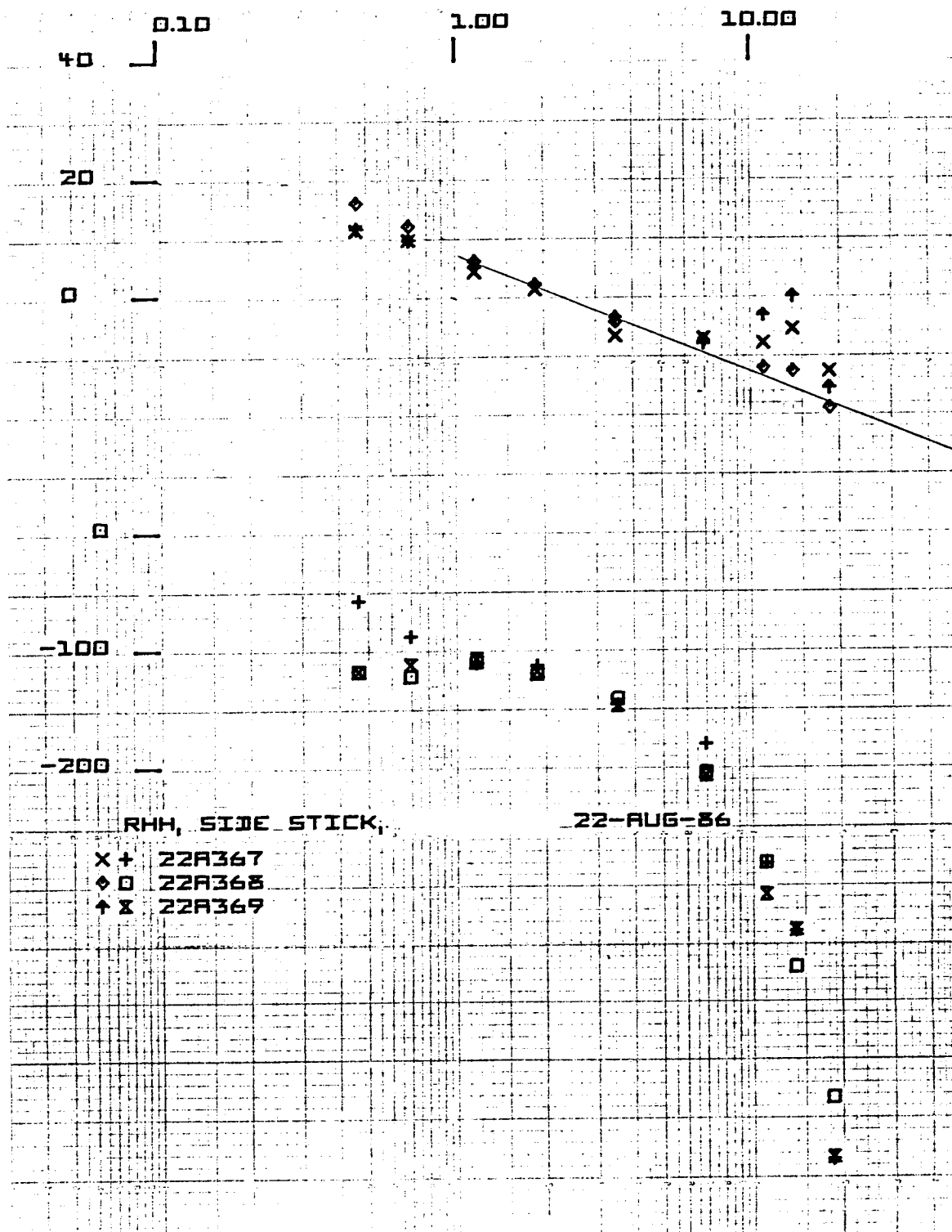


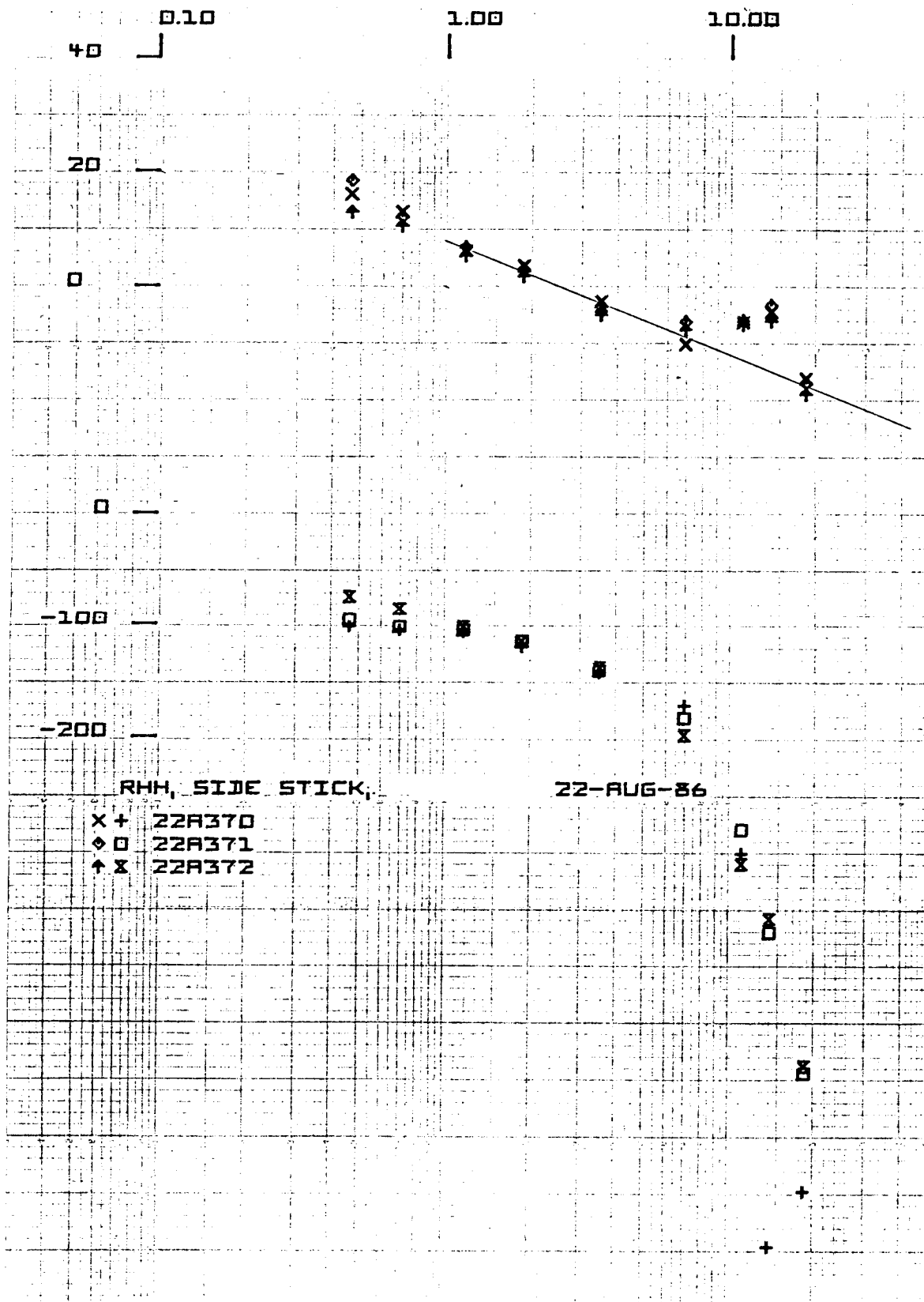




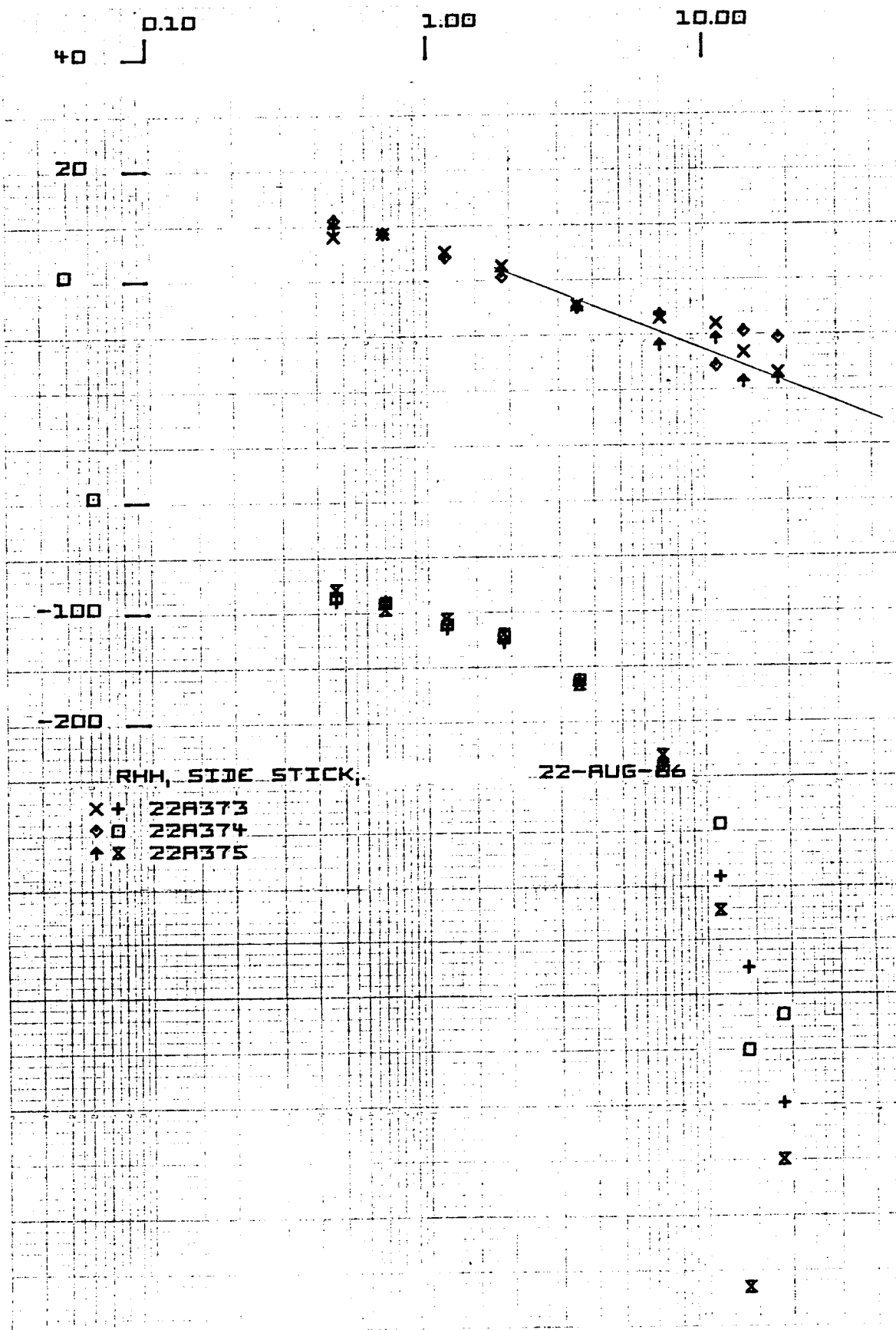


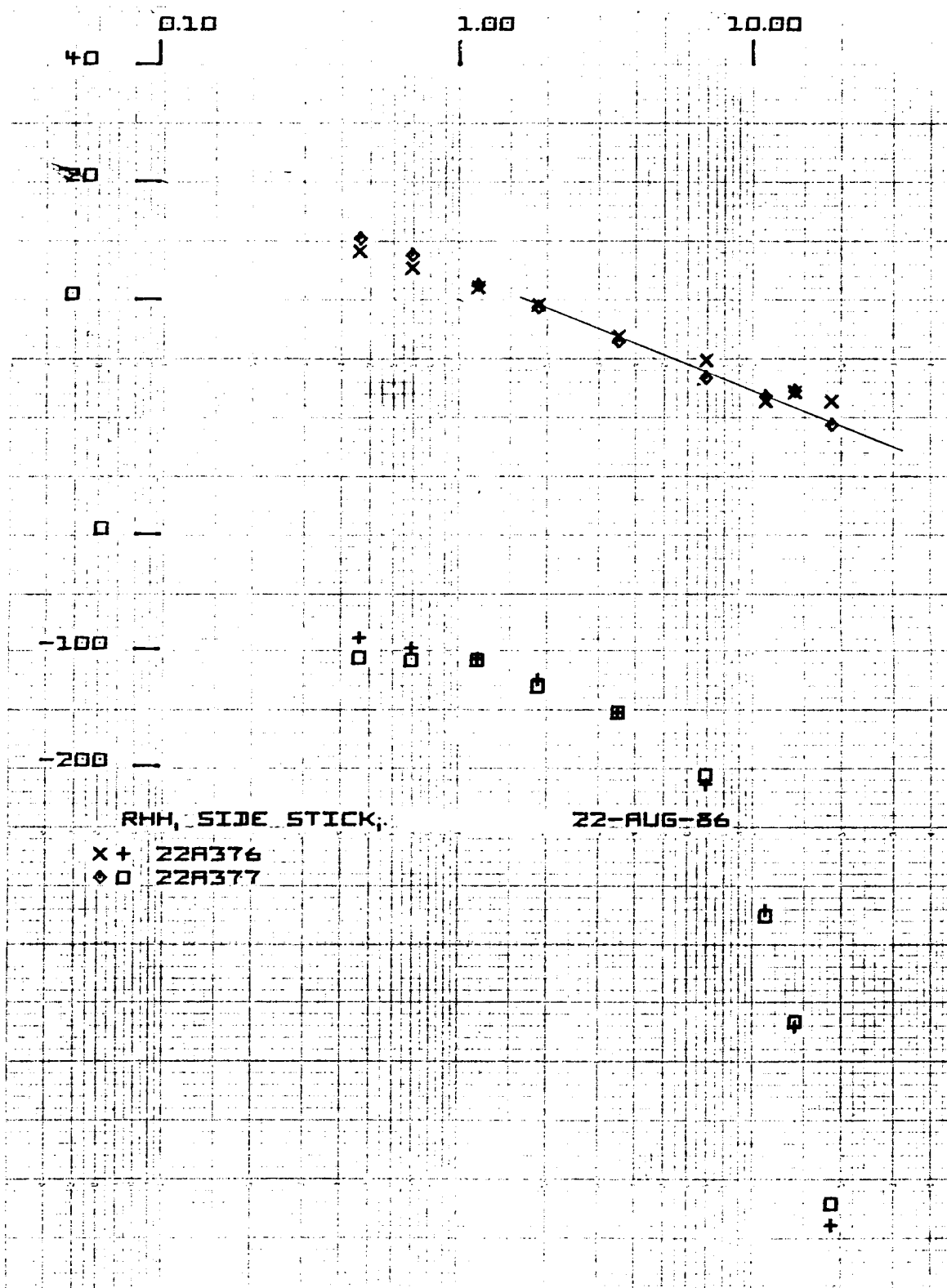


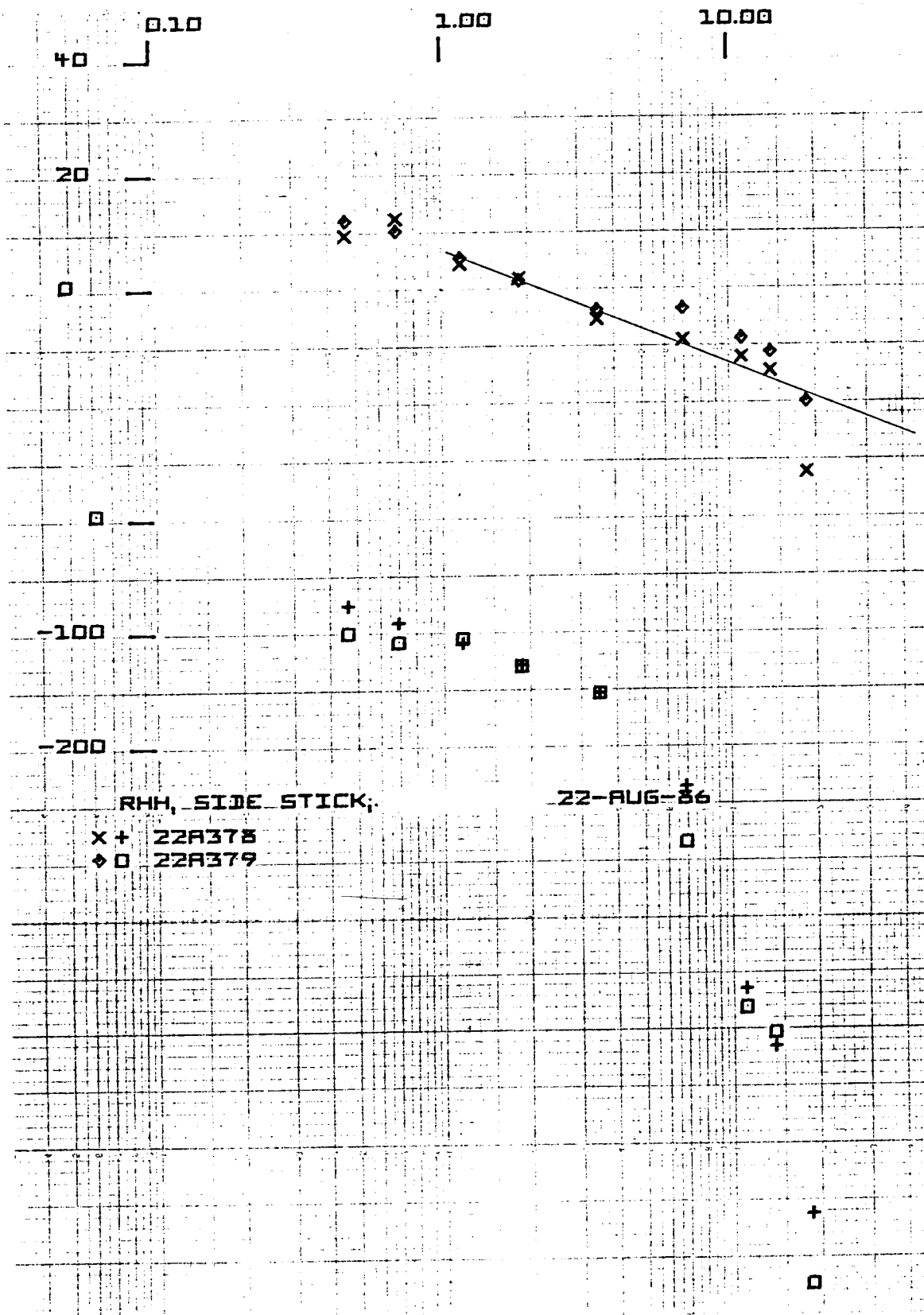












1. Report No. NASA CR- 4111		2. Government Accession No.		3. Recipient's Catalog No.	
4. Title and Subtitle  DESIGN CONSIDERATIONS OF MANIPULATOR AND FEEL SYSTEM CHARACTERISTICS IN ROLL TRACKING				5. Report Date February 1988	
				6. Performing Organization Code	
7. Author(s) Donald E. Johnston and Bimal L. Aponso				8. Performing Organization Report No. H-1438	
9. Performing Organization Name and Address  Systems Technology, Inc. 13766 South Hawthorne Blvd. Hawthorne, California				10. Work Unit No. RTOP 505-67-01	
				11. Contract or Grant No. NAS 2-12221	
				13. Type of Report and Period Covered Contractor Report - Final	
12. Sponsoring Agency Name and Address  National Aeronautics and Space Administration Washington, DC 20546				14. Sponsoring Agency Code	
15. Supplementary Notes  NASA Technical Monitor: Donald T. Berry, Ames Research Center, Dryden Flight Research Facility, Edwards, California 93523-5000					
16. Abstract  A fixed-base simulation was performed to identify and quantify interactions between the pilot's hand/arm neuromuscular subsystem and such control system features of typical modern fighter aircraft roll rate command mechanizations as: (1) force versus displacement sensing side-stick type manipulator, (2) feel force/displacement gradient, (3) feel system versus command prefilter dynamic lag, and (4) flight control system effective time delay.  The experiment encompassed some 48 manipulator/filter/aircraft configurations summarized in Sections IV and VI. Section IV concentrates on the displacement side-stick experiment results and compares these with the previous force sidestick experiment results. Attention is focused on control bandwidth, excitement (peaking) of the neuromuscular mode, feel force/displacement gradient effects, time delay effects, etc. Section V is devoted to experiments with a center-stick in which force versus displacement sensing, feel system lag, and command prefilter lag influences on tracking performance and pilot preference are investigated. Results in these two sections are summarized in numerous plots which are intended to serve as guides in the design of future control systems. Section VI concentrates on extraction of dynamic models for the pilot and closed-loop arm/manipulator/feel systems from the describing function data obtained in the Section V experiments. Parameters suitable for detailed models and for the simple crossover model are derived. Details concerning the manipulators, feel gradients, etc. along with run logs and data summaries are presented in the several appendixes.					
17. Key Words (Suggested by Author(s))  Flying qualities Limb-manipulator dynamics Neuromuscular system Roll control			18. Distribution Statement  Unclassified - Unlimited  Subject category 08		
19. Security Classif. (of this report)  Unclassified		20. Security Classif. (of this page)  Unclassified		22. Price* A11	
				21. No. of Pages 238	

\*For sale by the National Technical Information Service, Springfield, Virginia 22161.

NASA-Langley, 1988